THE POTENTIAL EFFECTS AND MECHANISMS OF CHINESE TRADITIONAL MEDICINE ON BONE HOMEOSTASIS AND REMODELING, 2nd Edition

EDITED BY: Jun Liu, Bo Liu, Xiaoqin Wu and Qi Wang

PUBLISHED IN: Frontiers in Endocrinology

frontiers Research Topics

ISSN 1664-8714
ISBN 978-2-8325-3530-1
DOI 10.3389/978-2-8325-3530-1

About Frontiers

Frontiers is more than just an open-access publisher of scholarly articles: it is a pioneering approach to the world of academia, radically improving the way scholarly research is managed. The grand vision of Frontiers is a world where all people have an equal opportunity to seek, share and generate knowledge. Frontiers provides immediate and permanent online open access to all its publications, but this alone is not enough to realize our grand goals.

Frontiers Journal Series

The Frontiers Journal Series is a multi-tier and interdisciplinary set of open-access, online journals, promising a paradigm shift from the current review, selection and dissemination processes in academic publishing. All Frontiers journals are driven by researchers for researchers; therefore, they constitute a service to the scholarly community. At the same time, the Frontiers Journal Series operates on a revolutionary invention, the tiered publishing system, initially addressing specific communities of scholars, and gradually climbing up to broader public understanding, thus serving the interests of the lay society, too.

Dedication to Quality

Each Frontiers article is a landmark of the highest quality, thanks to genuinely collaborative interactions between authors and review editors, who include some of the world's best academicians. Research must be certified by peers before entering a stream of knowledge that may eventually reach the public - and shape society; therefore, Frontiers only applies the most rigorous and unbiased reviews.
Frontiers revolutionizes research publishing by freely delivering the most outstanding research, evaluated with no bias from both the academic and social point of view. By applying the most advanced information technologies, Frontiers is catapulting scholarly publishing into a new generation.

What are Frontiers Research Topics?

Frontiers Research Topics are very popular trademarks of the Frontiers Journals Series: they are collections of at least ten articles, all centered on a particular subject. With their unique mix of varied contributions from Original Research to Review Articles, Frontiers Research Topics unify the most influential researchers, the latest key findings and historical advances in a hot research area! Find out more on how to host your own Frontiers Research Topic or contribute to one as an author by contacting the Frontiers Editorial Office: frontiersin.org/about/contact

THE POTENTIAL EFFECTS AND MECHANISMS OF CHINESE TRADITIONAL MEDICINE ON BONE HOMEOSTASIS AND REMODELING, 2nd Edition

Topic Editors:
Jun Liu, Guangdong Provincial Academy of Chinese Medical Sciences, China
Bo Liu, Chinese Medicine Active Substance Chemistry Research and Structure Optimization Team, Guangdong Provincial Hospital of Chinese Medicine, China
Xiaoqin Wu, Cleveland Clinic, United States
Qi Wang, Guangzhou University of Chinese Medicine, China

Publisher's note: In this 2nd edition, the cover copy has been updated.

Citation: Liu, J., Liu, B., Wu, X., Wang, Q., eds. (2023). The Potential Effects and Mechanisms of Chinese Traditional Medicine on Bone Homeostasis and Remodeling, 2nd Edition. Lausanne: Frontiers Media SA.
doi: 10.3389/978-2-8325-3530-1

Table of Contents

05 ***Editorial: The Potential Effects and Mechanisms of Traditional Chinese Medicine on Bone Homeostasis and Remodeling***
Jun Liu

08 ***Exploration of the Molecular Mechanism of Polygonati Rhizoma in the Treatment of Osteoporosis Based on Network Pharmacology and Molecular Docking***
Jinlong Zhao, Fangzheng Lin, Guihong Liang, Yanhong Han, Nanjun Xu, Jianke Pan, Minghui Luo, Weiyi Yang and Lingfeng Zeng

17 ***Quantitative Proteomics Revealed the Pharmacodynamic Network of Bugu Shengsui Decoction Promoting Osteoblast Proliferation***
Xu Wei, Baoyu Qi, Ruyun Ma, Yili Zhang, Ning Liu, Shengjie Fang, Yanning Zhu, Yanming Xie, Jianye Dai and Liguo Zhu

30 ***Integration of Network Pharmacology and Experimental Validation to Explore the Pharmacological Mechanisms of Zhuanggu Busui Formula Against Osteoporosis***
Huihao Zhang, Chengcong Zhou, Zhiguo Zhang, Sai Yao, Yishan Bian, Fangda Fu, Huan Luo, Yan Li, Shuxin Yan, Yuying Ge, Yuying Chen, Kunyu Zhan, Ming Yue, Weibin Du, Kun Tian, Hongting Jin, Xiaofeng Li, Peijian Tong, Hongfeng Ruan and Chengliang Wu

44 ***Comparative Efficacy of Xianling Gubao Capsules in Improving Bone Mineral Density in Postmenopausal Osteoporosis: A Network Meta-Analysis***
Ming-hui Luo, Jin-long Zhao, Nan-jun Xu, Xiao Xiao, Wen-xuan Feng, Zi-ping Li and Ling-feng Zeng

55 ***Mechanism and Experimental Verification of* Luteolin *for the Treatment of Osteoporosis Based on Network Pharmacology***
Guihong Liang, Jinlong Zhao, Yaoxing Dou, Yuan Yang, Di Zhao, Zhanpeng Zhou, Rui Zhang, Weiyi Yang and Lingfeng Zeng

68 ***Effects of Icariin on Modulating Gut Microbiota and Regulating Metabolite Alterations to Prevent Bone Loss in Ovariectomized Rat Model***
Shanshan Wang, Shengjie Wang, Xiaoning Wang, Yunteng Xu, Xin Zhang, Yidan Han, Hui Yan, Linglong Liu, Lili Wang, Hongzhi Ye and Xihai Li

88 ***Network Pharmacological Study on Mechanism of the Therapeutic Effect of Modified Duhuo Jisheng Decoction in Osteoporosis***
Xudong Huang, Zhou Zhou, Yingyi Zheng, Guoshuai Fan, Baihe Ni, Meichen Liu, Minghua Zhao, Lingfeng Zeng and Weiguo Wang

101 ***Chinese Proprietary Medicine Xianling Gubao Capsule for Osteoporosis: A Systematic Review and Meta-Analysis of Randomized Clinical Trials***
Bai-Ru Cheng, Rou-Yan Wu, Qin-Yang Gao, Kai-Xin Jiang, Shuang-Sang Li, Shi-Hao Qi, Ming-Yi Yuan and Jian-Ping Liu

112 ***Quercetin Attenuates Osteoporosis in Orchiectomy Mice by Regulating Glucose and Lipid Metabolism* via *the GPRC6A/AMPK/mTOR Signaling Pathway***
Jie Sun, Yalan Pan, Xiaofeng Li, Lining Wang, Mengmin Liu, Pengcheng Tu, Chengjie Wu, Jirimutu Xiao, Qiuge Han, Weiwei Da, Yong Ma and Yang Guo

125 ***Zuo-Gui-Wan Aqueous Extract Ameliorates Glucocorticoid-Induced Spinal Osteoporosis of Rats by Regulating let-7f and Autophagy***
Gengyang Shen, Qi Shang, Zhida Zhang, Wenhua Zhao, Honglin Chen, Ibrayinjan Mijiti, Guifeng Chen, Xiang Yu, Fuyong Yu, Peng Zhang, Jiahui He, Xuelai Zhang, Jingjing Tang, Jianchao Cui, De Liang, Lingfeng Zeng, Hui Ren and Xiaobing Jiang

137 ***Evolving Roles of Natural Terpenoids From Traditional Chinese Medicine in the Treatment of Osteoporosis***
Yue Zhuo, Meng Li, Qiyao Jiang, Hanzhong Ke, Qingchun Liang, Ling-Feng Zeng and Jiansong Fang

frontiers | Frontiers in Endocrinology

EDITORIAL
published: 07 July 2022
doi: 10.3389/fendo.2022.969729

Editorial: The Potential Effects and Mechanisms of Traditional Chinese Medicine on Bone Homeostasis and Remodeling

Jun Liu[1,2]*

[1] Bone and Joint Research Team of Degeneration and Injury, Guangdong Provincial Academy of Chinese Medical Sciences, Guangzhou, China, [2] Guangdong Second Traditional Chinese Medicine Hospital (Guangdong Province Enginering Technology Research Institute of Traditional Chinese Medicine), Guangzhou, China

Keywords: Chinese traditional medicine, Bone homeostasis, Bone Remodeling, effectiveness, mechanisms

Editorial on the Research Topic:

The Potential Effects and Mechanisms of Chinese Traditional Medicine on Bone Homeostasis and Remodeling

Traditional Chinese medicine (TCM) has a long history in the treatment of clinical diseases, but research efforts are needed to understand its mechanisms. Osteoporosis (OP) and its complications, such as osteoporotic fractures and pain, significantly reduce the quality of life and increase the economic burden for patients (1). The intervention measures commonly used in the treatment of OP include exercise therapy, calcium, vitamins, bisphosphates, etc., but these treatments have limitations or contraindications (2). Clinical applications of additional therapies (including drug therapy) are conducive to providing more choices for the treatment of OP. Although TCM, especially Chinese herbal medicine, has potential efficacy in the treatment of OP (3), it is necessary and urgent to clarify its mechanisms. Therefore, this topic presents the current research results focusing on the mechanisms of TCM in bone homeostasis balance and bone reconstruction to further reveal the specific mechanisms of TCM. This topic has been widely studied in the field of TCM and has led to excellent achievements in clinical and basic research. Based on the collected research results, this editorial further summarizes the role of TCM in bone homeostasis and remodeling.

OPEN ACCESS

Edited and reviewed by:
Jonathan H Tobias,
University of Bristol, United Kingdom

***Correspondence:**
Jun Liu
liujungdtcm@163.com

Specialty section:
This article was submitted to Bone Research, a section of the journal Frontiers in Endocrinology

Received: *15 June 2022*
Accepted: *23 June 2022*
Published: *07 July 2022*

Citation:
Liu J (2022) Editorial: The Potential Effects and Mechanisms of Traditional Chinese Medicine on Bone Homeostasis and Remodeling. Front. Endocrinol. 13:969729. doi: 10.3389/fendo.2022.969729

CLINICAL EVIDENCE-BASED RESULTS

Quantitative systematic evaluation is an objective method for clinical workers to evaluate the effects of different therapies. Xianling Gubao capsule (XLGB) is often used to treat OP and is considered to have good clinical efficacy. Luo et al. evaluated the effect of XLGB and its combination therapy on bone mineral density (BMD) in a postmenopausal osteoporosis population by network meta-analysis. Their results showed that the combined application of XLGB effectively improved BMD in patients with postmenopausal osteoporosis compared with oral calcium, vitamin D or bisphosphates alone. The results of a study by Cheng et al. suggested that the oral administration

of XLGB alone or combined with other conventional anti-osteoporosis drugs improved patients' quality of life and reduced pain. Although the above two studies provide objective data for the clinical application of XLGB, future clinical research needs stricter design criteria regarding specific details such as the drug dose and course of treatment. The source papers included in Luo and Cheng's study are all Chinese literature, which may produce evidence bias and reduce the credibility of the evidence. Furthermore, the above two studies used some inappropriate outcome indicators to evaluate the anti-osteoporosis efficacy of XLGB, such as pain, ALP and BGP levels, which should be avoided in future research protocols, and appropriate and standard evaluation indicators should be selected.

HERBAL MONOMERS

Exploring the efficacy of Chinese herbal medicine monomers in the treatment of disease models through animal or cell experiments is conducive to further promoting the development and utilization of drugs. This topic includes the results of three research teams on the interventions of *luteolin*, *quercetin* and *icariin* in the model of OP. Liang et al. found that *luteolin* reduced bone loss in ovariectomized rats, and further mechanistic studies have suggested that *luteolin* regulates the activity of the PI3K-Akt signaling pathway and promotes osteogenic differentiation of bone marrow stromal cells (BMSCs). Sun et al. discussed the effect and mechanism of *quercetin* on bone mass in mice with OP induced by androgen deprivation therapy. Their results showed that *quercetin* increased bone mass, enhanced bone strength and improved bone microstructure in mice, and its mechanism is regulating glucose and lipid metabolism through the GPRC6A/AMPK/mTOR signaling pathway. The mechanism of *icariin* in the treatment of OP is a hot spot in TCM research. Wang et al. evaluated the effect of *icariin* on the bone mass of ovariectomized rats by observing intestinal flora and metabolites. It was suggested that *icariin* can improve the bone mass of ovariectomized rats, and the results of a metabolomic analysis showed that amino acid and fatty acid metabolism play important roles. These studies explored the role of herbal monomers in the maintenance of bone homeostasis from the perspectives of glucose and lipid metabolism, intestinal flora and metabolomics, giving us a new perspective. In addition, these studies reflect the great potential of herbal monomers in the treatment of OP.

SINGLE HERBAL MEDICINE

With the development of TCM, a large number of Chinese herbal medicines are used in clinical practice. A single herbal medicine contains multiple compounds or monomers, which creates an extensive resource bank for new drug development. Therefore, it is an important research direction to study the efficacy of a single herbal medicine in the treatment of OP. Zhao et al. used network pharmacology and molecular docking technology to find that there are 12 active components that may become drugs in Polygonati Rhizoma, and these 12 components can directly act on 84 targets related to OP. It has been concluded that Polygonati Rhizoma plays an anti-osteoporosis role by regulating the target genes JUN, TP53, AKT1, ESR1 and CASP3. However, Zhao et al's discovery is only a preliminary theoretical derivation, and further experimental validation is required to support the reliability of the prediction results. Natural terpenoids commonly exist in Chinese herbal medicine and have been widely studied because they play a key role in physiological and pathological processes such as osteogenesis and bone resorption. Zhou et al. reviewed the source, molecular structure, and research progress of known terpenoids of Chinese herbal medicine and the mechanism of these compounds in the treatment of OP. To the best of my knowledge, this is the most comprehensive review on this topic, which provides a usable basis and clear direction for basic experiments and clinical drug development.

TRADITIONAL CHINESE MEDICINE COMPOUNDS

Traditional Chinese medicine compounds are combinations of two or more Chinese herbal medicines according to the theory of TCM and the principle of prescription, which plays an important role in the field of TCM. It is undeniable that due to the complex composition of traditional Chinese medicine compounds, research on the mechanism of TCM treatment has always been difficult. Zhang et al. screened the key targets and pathways of Zhuanggu Busui Formula (ZGBSF) through network pharmacology technology and verified them through strictly designed animal experiments. Their study showed that ZGBSF promotes osteogenesis by inhibiting osteoblast apoptosis and activating the PI3K-Akt signaling pathway, thereby reducing bone loss. Huang et al. showed that modified Duhuo Jisheng Decoction prevents bone loss by inhibiting the inflammatory response and downregulating the expression levels of TNF-α, IL-6 and CASP3. Proteomics is also a promising direction in the study of OP. Through quantitative proteomics, Wei et al. confirmed that Bugu Shengsui Decoction plays an anti-osteoporosis role by regulating the PI3K-Akt signaling pathway. Shen et al. investigated the effects of Zuo-Gui-Wan Aqueous Extract on glucocorticoid-induced rat vertebral bone microstructure, autophagy corpuscles, let-7f and autophagy-related genes through *in vivo* and *in vitro* experiments and concluded that Zuo-Gui-Wan can promote the osteogenic differentiation of BMSCs by activating let-7f and inhibiting autophagy. *Yushen Hezhi* is another important direction in the treatment of OP. Traditional Chinese medicine compounds for the treatment of OP, such as *Yushen Hezhi Formula*, should be studied further. Traditional Chinese medicine compounds are an indispensable part of the

theoretical system of TCM, which is considered to play a multicomponent and multitarget therapeutic role and regulate the biochemical network of the body as a whole. The above four studies have examined the treatment of OP with TCM from the perspectives of network pharmacology, quantitative proteomics, autophagy and metabolomics. Due to the complex composition of traditional Chinese medicine compounds, methodological exploration and improvement, multidisciplinary cooperation and the application of new technology in traditional Chinese medicine compound research in the future are key.

CONCLUSION

The 11 research results in this special issue are representative of the depth of content and the application of methodology, which has attracted the increasing attention of researchers and confirmed the great potential of TCM in the treatment of OP. Although the content of this topic is limited, these research results also give us great encouragement and confidence. Due to the particularity of TCM, in addition to learning from the existing research technologies and methods, it remains necessary to innovate the research methodology, technology and theory of TCM in the treatment of OP in the future.

REFERENCES

1. Anam AK, Insogna K. Update on Osteoporosis Screening and Management. *Med Clin North Am* (2021) 105(6):1117–34. doi: 10.1016/j.mcna.2021.05.016
2. Li SS, He SH, Xie PY, Li W, Zhang XX, Li TF, et al. Recent Progresses in the Treatment of Osteoporosis. *Front Pharmacol* (2021) 12:717065. doi: 10.3389/fphar.2021.717065
3. Liu Y, Liu JP, Xia Y. Chinese Herbal Medicines for Treating Osteoporosis. *Cochrane Database Syst Rev* (2014) 2014(3):CD005467. doi: 10.1002/14651858.CD005467.pub2

Conflict of Interest: The author declares that the research was conducted in the absence of any commercial or financial relationships that could be construed as a potential conflict of interest.

AUTHOR CONTRIBUTIONS

The author confirms being the sole contributor of this work and has approved it for publication.

FUNDING

This research was funded by grants from National key research and development program (2021YFC1712804), the Science and Technology Research Project of Guangdong Provincial Hospital of Chinese Medicine (No.YN2019ML08), Research Fund for Bajian Talents of Guangdong Provincial Hospital of Chinese Medicine (No.BJ2022KY01) andProject of Philosophy and Social Science Planning of Guangzhou in 2022 (No.2022GZQN42).

ACKNOWLEDGMENTS

We would like to thank all the authors and reviewers who contributed to the success of this Research Topic with their high-quality research or crucial comments. Thanks are due to other guest editors (Prof. Qi Wang, Dr. Bo Liu and Dr. Xiaoqin Wu) of this collection. This collection would not be realized without their input and dedication.

frontiers in Endocrinology

ORIGINAL RESEARCH
published: 05 January 2022
doi: 10.3389/fendo.2021.815891

Exploration of the Molecular Mechanism of Polygonati Rhizoma in the Treatment of Osteoporosis Based on Network Pharmacology and Molecular Docking

Jinlong Zhao[1†‡], Fangzheng Lin[1†], Guihong Liang[2†‡], Yanhong Han[2‡], Nanjun Xu[1], Jianke Pan[2‡], Minghui Luo[2‡], Weiyi Yang[2‡] and Lingfeng Zeng[1,2*‡]*

[1] The Second Clinical Medical College of Guangzhou University of Chinese Medicine, Guangzhou, China, [2] The 2nd Affiliated Hospital of Guangzhou University of Chinese Medicine, Guangzhou, China

Objective: To explore the effective components and mechanism of Polygonati Rhizoma (PR) in the treatment of osteoporosis (OP) based on network pharmacology and molecular docking methods.

Methods: The effective components and predicted targets of PR were obtained through the Traditional Chinese Medicine Systems Pharmacology and Analysis Platform (TCMSP) database. The disease database was used to screen the disease targets of OP. The obtained key targets were uploaded to the Search Tool for the Retrieval of Interacting Genes/Proteins (STRING) database for protein-protein interaction (PPI) network analysis. The Database for Annotation, Visualization, and Integrated Discovery (DAVID) was used for Gene Ontology (GO) and Kyoto Encyclopedia of Genes and Genomes (KEGG) pathway enrichment analyses of key targets. Analysis and docking verification of chemical effective drug components and key targets were performed with IGEMDOCK software.

Results: A total of 12 chemically active components, 84 drug target proteins and 84 common targets related to drugs and OP were obtained. Key targets such as JUN, TP53, AKT1, ESR1, MAPK14, AR and CASP3 were identified through PPI network analysis. The results of enrichment analysis showed that the potential core drug components regulate the HIF-1 signaling pathway, PI3K-Akt signaling pathway, estrogen signaling pathway and other pathways by intervening in biological processes such as cell proliferation and apoptosis and estrogen response regulation, with an anti-OP pharmacological role. The results of molecular docking showed that the key targets in the regulatory network have high binding activity to related active components.

Conclusions: PR may regulate OP by regulating core target genes, such as JUN, TP53, AKT1, ESR1, AR and CASP3, and acting on multiple key pathways, such as the HIF-1 signaling pathway, PI3K-Akt signaling pathway, and estrogen signaling pathway.

Keywords: Polygonati Rhizoma, potential therapeutic targets, signaling pathways, molecular mechanism, network pharmacology, molecular docking

OPEN ACCESS

Edited by:
Bo Liu,
Guangdong Provincial Hospital of Chinese Medicine, China

Reviewed by:
Zji Zhang,
The First Affiliated Hospital of Sun Yat-sen University, China
Minshan Feng,
China Academy of Chinese Medical Sciences, China
Junyuan Chen,
First Affiliated Hospital of Jinan University, China

***Correspondence:**
Weiyi Yang
czyangwy@163.com
Lingfeng Zeng
1347301175@qq.com

[†]These authors have contributed equally to this work

[‡]ORCID:
Jinlong Zhao
orcid.org/0000-0001-7079-1336
Guihong Liang
orcid.org/0000-0002-7599-2628
Yanhong Han
orcid.org/0000-0002-3474-5591
Jianke Pan
orcid.org/0000-0002-4596-6111
Minghui Luo
orcid.org/0000-0001-6831-6317
Weiyi Yang
orcid.org/0000-0001-8657-2269
Lingfeng Zeng
orcid.org/0000-0001-8149-242X

Specialty section:
This article was submitted to Bone Research, a section of the journal Frontiers in Endocrinology

Received: *16 November 2021*
Accepted: *13 December 2021*
Published: *05 January 2022*

INTRODUCTION

Osteoporosis (OP) is a systemic metabolic bone disease characterized by bone loss, bone tissue microstructure damage, bone pain and brittle fracture (1). The incidence of OP is closely related to age, and with the ageing of the population, OP has become an important factor affecting the quality of life of middle-aged individuals and elderly individuals. Research data show that 40% of postmenopausal women and 30% of men in the world will develop OP (2). In addition, OP may induce other diseases, which causes a heavy economic burden to the patient's family and society (3). At present, most of the drugs for the treatment of OP are chemical drugs that regulate bone metabolism, but there are adverse reactions such as kidney injury and joint pain (4, 5). In recent years, many scholars have studied the efficacy of traditional Chinese medicine in the treatment of OP from the perspective of molecular biology and have made remarkable progress, further proving the positive role of traditional Chinese medicine in the treatment of OP (6, 7).

OP belongs to the category of "*Guwei*" in traditional Chinese medicine. It is recorded in *Su Wen* that "If the kidney *Qi* is hot, the waist and spine will not lift, the bone will wither and the marrow decreases, it will develop into *Guwei*". The basic principles of traditional Chinese medicine treatment are tonifying the kidney and essence, promoting blood circulation and removing blood stasis (8, 9). The relevant molecular mechanism of traditional Chinese medicine in the treatment of OP has not been fully clarified, which restricts the further transformation of relevant traditional Chinese medicine theories into clinical practice. In the context of traditional Chinese medicine, it is believed that Polygonati Rhizoma (PR) has effects of tonifying the kidney, tonifying *Qi* and nourishing *Yin*, strengthening the spleen and moistening the lung, which is the theoretical basis for its anti-OP effects (10). Modern pharmacological studies have shown that PR has anti-OP, bone protection, neuroprotection and immune enhancement effects (10, 11). According to experimental studies, *Polygonatum sibiricum* polysaccharide, one of the main active components of PR, can effectively promote osteogenic differentiation of bone marrow stromal cells in mice and inhibit the formation of osteoclasts (12). *Polygonatum sibiricum* polysaccharide can also prevent and treat OP mainly by improving bone microstructure, reducing bone turnover, increasing OPG protein and reducing RANKL protein expression (13, 14). Network pharmacology systematically studies the potential targets and pharmacological effects of traditional Chinese medicine components on multiple genes, multiple targets and multiple ways, which provides a new idea for research on the modernization of traditional Chinese medicine (15). Molecular docking is a theoretical simulation method to predict a drug's binding mode and affinity through the interaction between receptor and drug molecules (16). We aimed to use network pharmacological methods and molecular docking technology to preliminarily explore the potential targets and pathways of PR in the treatment of OP to provide a basis for further clarifying the molecular mechanism of PR in the treatment of OP.

MATERIALS AND METHODS

Active Components and Action Targets of PR

The active components of PR were extracted from the Traditional Chinese Medicine Systems Pharmacology Database and Analysis Platform (TCMSP) (http://lsp.nwu.edu.cn/tcmsp.php) (15, 17). The compounds were screened according to oral bioavailability (OB) and drug likeness (DL). The screening conditions are OB ≥ 30% and DL ≥ 0.18 (18). The screened compounds are the core active components. The proteins corresponding to the above targets were transformed into species human genes through the UniProt database (https://www.UniProt.org/), and a database of PR compounds and their action target genes was constructed.

Acquisition of OP Disease Targets

In the Comparative Toxicogenomics Database (CTD) (http://ctdbase.org/), Genecards (https://www.genecards.org/) and DisGeNET databases (http://www.disgenet.org/web/DisGeNET/menu/home), "osteoporosis" was used as the search term to collect disease targets related to OP. Finally, duplicates from the three databases were removed to obtain the final OP-related targets.

Common Targets

The targets related to OP and the targets related to the active components of PR overlapped. The intersecting genes and Venn diagram of PR and OP targets were obtained through the online Venn map platform (http://bioinfogp.cnb.csic.es/tools/venny/index.html), and finally, OP-related targets of the drug active ingredients were obtained for subsequent analysis.

Construction of the Compound-Target Network

Information on the active ingredients and common targets was imported into Cytoscape_v3.7.1 software to construct a compound-target interaction network to show the interaction relationships between active components and targets. The software calculates the network topology parameters, degree and betweenness centrality (BC) and screens the main candidate targets and monomer components.

Protein-Protein Interaction Network

PPIs are the basis of cell function and play an important role in regulating physiological and pathological states. In the PPI network, network nodes represent proteins, network connecting lines represent PPIs, and node size, colour, connection length and thickness represent the topology parameters of the node network (19). To further understand the synergistic mechanism of the PR compound potential target and OP target at the protein level, the common target protein was passed through the Search Tool for the Retrieval of Interacting Genes/Proteins (STRING) 11.0 (https://string-db.org). The PPI relationship is obtained, and then the core gene is obtained according to the number of node connections.

Among them, the species selection was "*Homo sapiens*", and high confidence = 0.9 was set as the lowest interaction score.

Gene Ontology and Kyoto Encyclopedia of Genes and Genomes Enrichment Analysis

We imported the obtained potential targets of PR for the treatment of OP (the common target obtained in 1.1.3) into the target gene name list through Database for Annotation, Visualization, and Integrated Discovery (DAVID) (https://david.ncifcrf.gov/home.jsp) and limited the species to human. GO enrichment analysis and KEGG pathway annotation analysis were performed on the potential targets of PR for the treatment of OP to screen the important signaling pathway of PR in OP treatment.

Molecular Docking

The target proteins and ligand molecules were docked by IGEMDOCK docking software (http://gemdock.life.nctu.edu.tw/). The three-dimensional structure of the protein encoded by the top 15 core target genes from the Protein Data Bank (PDB) database (https://www.rcsb.org/) was downloaded as the protein receptor. The two-dimensional structure of the core active compound of PR was downloaded from the TCMSP database. The binding energy can be obtained by introducing them into IGEMDOCK. The binding ability of ligands and receptors is evaluated by the binding energy. If the binding energy is less than 0, it means that ligand and receptor can spontaneously bind, and the smaller the value, the higher the binding activity.

RESULTS

Active Ingredients of PR

Thirty-eight chemical constituents of PR were retrieved from the TCMSP database. After screening with the parameters OB ≥ 30% and DL ≥ 0.18, 12 active components of PR were obtained. Since the corresponding targets were not selected for the three compounds (MOL003889, MOL009760 and MOL009766), subsequent analysis was not carried out. There were 84 corresponding targets of active components (excluding repeated targets). See **Table 1** for specific information on the screened active ingredients. A summary of putative targets of PR is provided in **Supplement Table 1**.

OP-Related Genes

With "osteoporosis" as the search term, 36180 related disease genes were retrieved from the CTD, 2916 were retrieved from the Genecards database, and 1098 were retrieved from the DisGeNET database. After merging the results from the three databases and removing duplicates, a total of 23530 genes related to OP were obtained. The relevant disease genes of the above three databases can be found in **Supplement Table 2**.

Common Targets

The results for drug active ingredient targets and disease targets were intersected, and 84 drug active ingredient targets related to OP were obtained for subsequent analysis (**Figure 1**).

Construction and Analysis of the Compound-Target Network

Cytoscape 3.7.1 software was used to construct the active component target interaction network of 9 PR active monomers and 84 overlapping target genes. The green node represents the active component of PR, and the red node is the action target of the active component, with a total of 272 edges, representing the interaction between the target and the chemical component, reflecting the multicomponent and multitarget characteristics of PR (**Figure 2**). For network topology analysis, the network concentration was 0.367, the network density was 0.032, and the network heterogeneity was 1.891. The average degree value of nodes was 2.92, and there were 21 nodes with above average degree values. According to the topological properties of network nodes, such as degree value and BC, the core nodes were selected for analysis. The nodes with more connecting compounds or targets play a key role in the whole network and may be key compounds or targets. **Table 2** lists the 20 key nodes with above average value and their topological parameters in the compound-target network.

PPI Network

The 84 intersecting genes obtained in "2.3" were imported into STRING 11.0 for analysis. The PPI results are shown in **Figure 3**.

TABLE 1 | Information on active ingredients of PR.

Molecule ID	Molecule Name	OB (%)	DL
MOL001792	DFV	32.76	0.18
MOL002714	baicalein	33.52	0.21
MOL002959	3'-Methoxydaidzein	48.57	0.24
MOL000358	beta-sitosterol	36.91	0.75
MOL000359	sitosterol	36.91	0.75
MOL003889	methylprotodioscin_qt	35.12	0.86
MOL004941	(2R)-7-hydroxy-2-(4-hydroxyphenyl)chroman-4-one	71.12	0.18
MOL000546	diosgenin	80.88	0.81
MOL006331	4',5-Dihydroxyflavone	48.55	0.19
MOL009760	sibiricoside A_qt	35.26	0.86
MOL009763	(+)-Syringaresinol-O-beta-D-glucoside	43.35	0.77
MOL009766	zhonghualiaoine 1	34.72	0.78

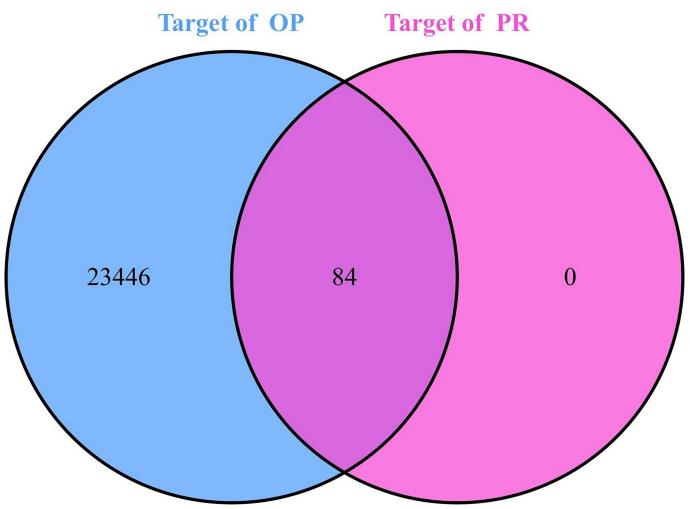

FIGURE 1 | Venn diagram of OP targets and PR targets.

The PPI results included 70 nodes and 346 edges, in which the nodes represented proteins and each edge represented a PPI relationship, with an average degree of 4.94. **Figure 4** is a bar chart of the top 15 target genes, which are considered to be the key targets of PR for the treatment of OP.

GO Enrichment Analysis

By GO enrichment analysis of 84 target genes intersecting PR and OP, 881 GO items were obtained, including 356 biological process (BP), 46 cellular component (CC) and 79 molecular function (MF) terms. According to the *p* value and the number of enriched genes, the top 10 enriched BPs, CCs and MFs were selected for visualization, and a bubble diagram was generated (**Figure 5**). The BPs were mainly related to the response to drug, positive regulation of transcription from RNA polymerase II promoter, response to estradiol, cellular response to hypoxia, etc.; the CCs were mainly related to the nucleoplasm, cytosol, nucleus and postsynaptic membrane; and the MFs were mostly related to enzyme binding, drug binding and steroid hormone receptor activity.

KEGG Pathway Enrichment Analysis

KEGG analysis of the intersecting target genes of PR and OP showed that the key target genes were enriched in 94 biological signaling pathways. Using the Benjamin correction method, the top 15 noncancer disease pathways were analysed after ranking the *p* value, and the KEGG functional enrichment bubble diagram was drawn (**Figure 6**). The main biological pathways involved included the p53 signaling pathway, HIF-1 signaling pathway, VEGF signaling pathway, TNF signaling pathway, estrogen signaling pathway and other signaling pathways.

Molecular Docking Results

The key targets in the PPI network were selected, and the relevant components were searched reversely according to the PPI network for molecular docking. The lower the binding

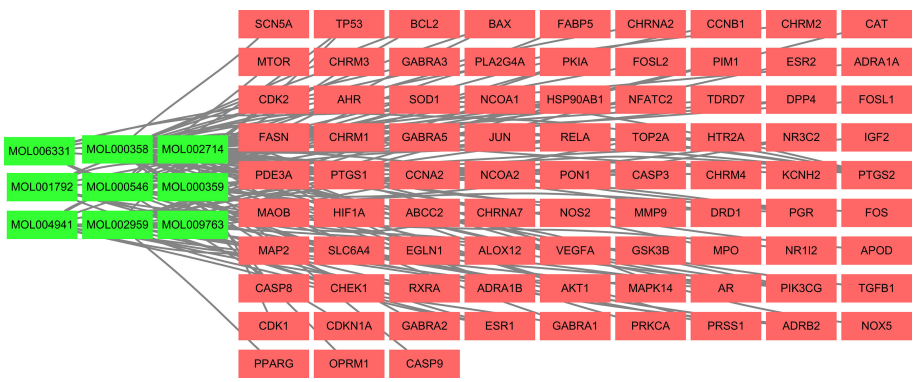

FIGURE 2 | The gene target network of the effective components of PR.

TABLE 2 | Key node of the compound-target network and table of its topological features.

Node	Node type	Degree	BC	Node	Node type	Degree	BC
MOL000358	Monomer	36	0.49952593	PIK3CG	Target	5	0.03609123
MOL002714	Monomer	34	0.45840389	SLC6A4	Target	3	0.00550579
MOL002959	Monomer	17	0.21181913	RXRA	Target	3	0.00374525
MOL000546	Monomer	16	0.20289903	PGR	Target	3	0.0443633
MOL004941	Monomer	12	0.05237295	PDE3A	Target	3	0.02399951
MOL001792	Monomer	10	0.03656977	NCOA2	Target	3	0.03311465
PTGS2	Target	7	0.17893754	MOL000359	Monomer	3	0.00567139
MOL006331	Monomer	7	0.0153846	MAOB	Target	3	0.00062739
PTGS1	Target	6	0.077882	ESR1	Target	3	0.00374525
HSP90AB1	Target	6	0.077882	AR	Target	3	0.01422897

energy between ligand and receptor was, the more stable the binding conformation and the greater the possibility of interaction. The molecular docking results showed that the binding energy between the effective chemical active ingredient and the key target protein was less than -50 kcal/mol (**Figure 7**), suggesting that the binding activity between the effective core ingredient and the core target protein is stable.

DISCUSSION

With the acceleration of the ageing process worldwide, OP has become the third most common chronic disease, and it is a frequently occurring disease (20). The treatments for OP in modern medicine mainly include calcium, vitamin supplements and estrogen replacement therapy. However, the long-term use of estrogen can increase the incidence of breast cancer and coronary heart disease, and other chemical synthetic drugs used in the clinic have noneligible adverse reactions (1, 21). In the context of traditional Chinese medicine, deficiency of kidney essence is believed to be the main pathogenesis of OP. PR has the effect of tonifying the kidney, and modern pharmacological studies indicate that PR has an anti-OP effect, but its mechanism is still unclear. Using network pharmacology and molecular docking technology, this study clarified the molecular mechanism of PR in the treatment of OP from a micro-level perspective to provide a theoretical basis for the treatment of OP with traditional Chinese medicine.

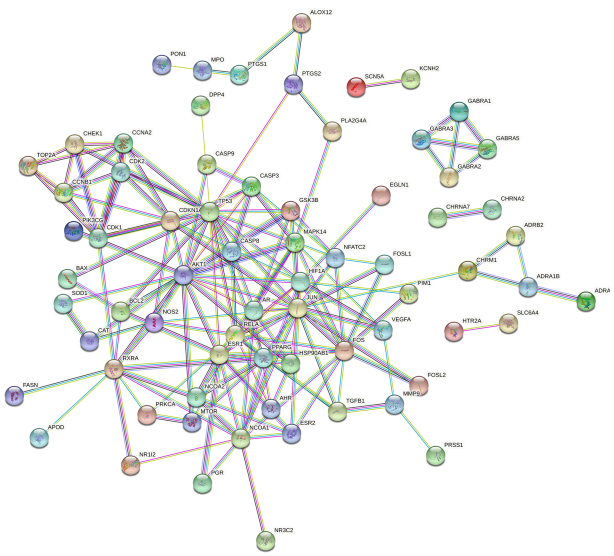

FIGURE 3 | PPI network diagram of target proteins.

The study shows that PR may act on key targets such as JUN, TP53, AKT1, ESR1, MAPK14, AR and CASP3 through a variety of chemical components, such as baicalein, beta-sitosterol, diosgenin and 3'-methoxydaidzein, and regulate biological processes, such as estrogen regulatory response, cell antioxidant and antiaging signaling, cell proliferation and apoptosis, to further exert its multicomponent, multitarget and multinetwork anti-OP effect by regulating the p53 signaling pathway, HIF-1 signaling pathway, TNF signaling pathway, PI3K Akt signaling pathway and estrogen signaling pathway. A previous study suggested that *Polygonatum* polysaccharide may increase the contents of GPR48, BMP-2 and bone metabolic factors in bone tissue, improving the biomechanical properties and bone mineral density of osteoporotic fracture rats and delaying OP progression (11). Considering these findings and our research results, further experimental and clinical studies should explore the effect of PR on bone metabolism-related factors *via* intervention of JUN, TP53, AKT1, ESR1 and other proteins, which is very important for assessing PR in future drug development.

The active components with high degree values in the component-target network included beta-sitosterol, baicalein and other chemically active components. Beta-sitosterol widely exists in a variety of traditional Chinese medicine components and has physiological effects such as anti-inflammatory, antioxidant and anti-androgen activities (22). Studies have shown that beta-sitosterol can inhibit cell proliferation in transplanted tumours in mice by inhibiting the expression of IL-6, TNF and VEGF (23). TNF-α and IL-6 can induce RANKL expression and promote osteoclast differentiation. Therefore, beta-sitosterol may have potential pharmacological effects on inhibiting osteoclast activity (24). The GO BP enrichment results reflect that the treatment process is highly correlated with the regulatory response of estrogen, cell antioxidant and anti-ageing processes, cell proliferation and apoptosis. The estrogen level is closely related to the activities of osteoblasts and osteoclasts. In the estradiol response, when estrogen is insufficient, RANKL is activated,

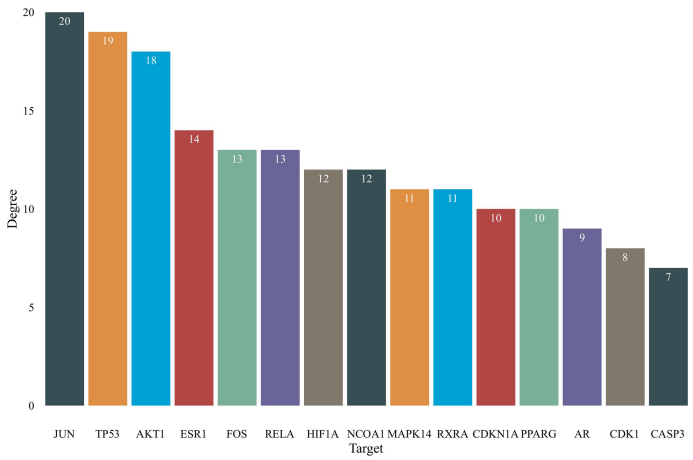

FIGURE 4 | Core targets of PR in the treatment of OP (top 15).

inhibits osteoclast apoptosis and accelerates the osteoclast process. Osteoblasts can increase their activity and enhance the process of osteogenesis by combining with estrogen. The key components of PR and the biological process of pharmacological action are strongly related to the dysregulation of bone remodeling in OP. The molecular docking results showed that the binding energy of potential core active components and key targets of PR were less than -50 kcal/mol, suggesting that the potential active components of PR have good binding activity with key targets, which indicates that they may be potential active components and targets for the treatment of OP.

The PPI and KEGG pathway enrichment results suggest that the effective components of PR mainly act on JUN, TP53, AKT1, ESR1, MAPK14, AR, CASP3 and other targets to play an anti-OP role, and these targets are mainly mapped to key pathways such as the HIF-1 signaling pathway, PI3K-Akt signaling pathway and estrogen signaling pathway. The HIF-1 signaling pathway is a classic multifunctional signaling pathway that plays an important role in bone formation and absorption. It can regulate the regeneration process of bone and blood vessels through osteogenic and angiogenic coupling (25, 26). In a hypoxic cell environment, it can widely participate in biological processes such as energy metabolism, angiogenesis and the cell cycle and can effectively strengthen the osteogenic and angiogenic differentiation ability of bone marrow mesenchymal stem cells (27). The PI3K-Akt signaling pathway

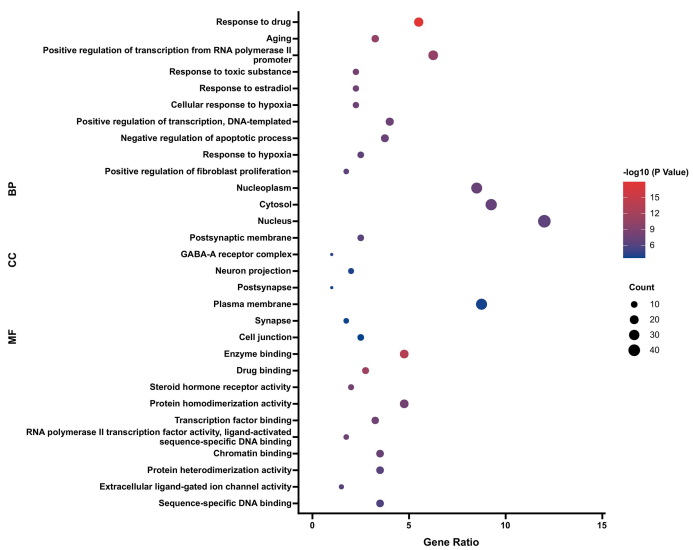

FIGURE 5 | GO enrichment analysis of PR targets in the OP treatment (top 10).

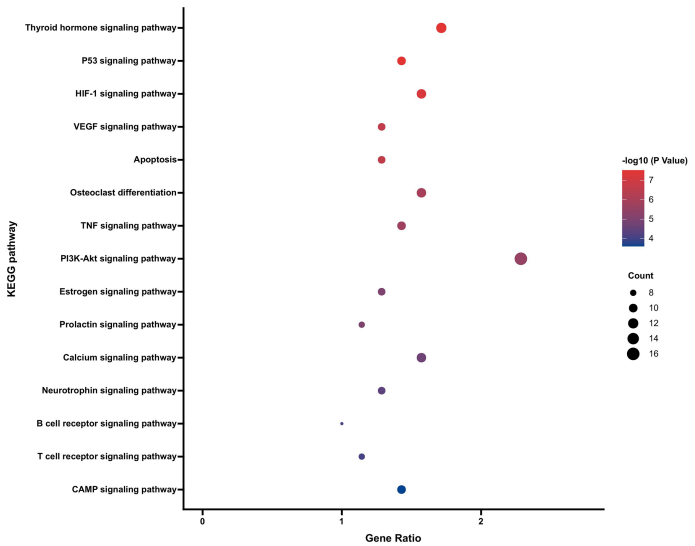

FIGURE 6 | KEGG pathway enrichment analysis of PR targets in the treatment of OP (top 15).

mainly regulates cell proliferation, differentiation and apoptosis *in vivo*. After PI3K is activated, it recruits the downstream signaling molecule AKT, promotes mTOR activation to affect osteoblast differentiation and inhibit apoptosis, which has important guiding significance for the treatment of OP (28, 29). Estrogen can not only participate in the physiological processes of osteoclasts and osteoblasts but can also maintain the dynamic and stable balance of the abilities of the two cells and then affect the proliferation and differentiation of mesenchymal stem cells in the direction of osteogenesis (30, 31). Estrogen deficiency can cause in imbalance in osteoclast levels and osteogenesis, leading to OP (31). The PPI results in this study suggest that estrogen-related targets such as ESR1 and AR are the key anti-OP targets of PR. Therefore, the estrogen signaling pathway may be an important way for PR to exert its anti-OP effect.

This study also has some limitations. First, research methods based on network pharmacology have the disadvantages of being unable to predict up-regulation and down-regulation of targets, which is not conducive to an accurate understanding of the mechanism of chemical components acting on disease targets. Second, due to the limitation of screening conditions, only the main compounds in PR were analysed, restricting the results to a certain extent. Third, although a large number of targets and pathways can be screened through network pharmacology technology, the findings need to be confirmed through basic research and clinical trials, which is the focus of our next study.

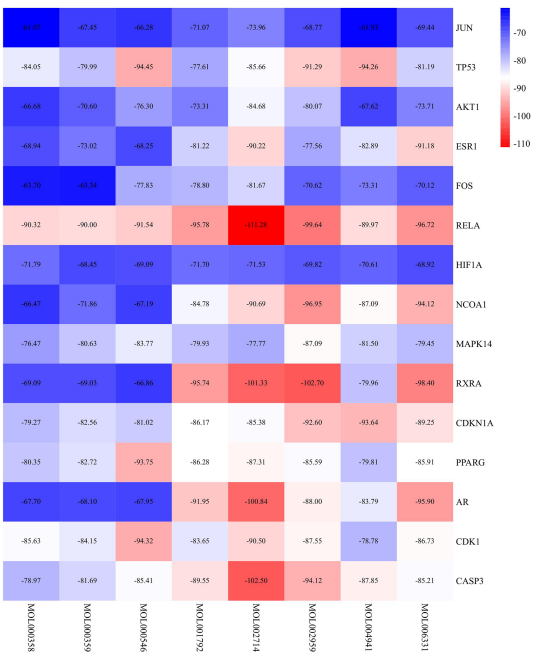

FIGURE 7 | Molecular docking heatmap of the main compounds and key targets (Kcal/mol).

CONCLUSION

Based on the methodology of network pharmacology, through the evaluation of pharmacokinetic parameters of PR and the enrichment analysis of biological functional pathways, this study further verified that PR has multicomponent, multitarget and multipathway pharmacological characteristics in the treatment of OP. The interaction mode between chemically active components and OP disease targets was preliminarily verified by molecular docking, which provided an experimental basis for further biological experiments *in vivo* and *in vitro*.

DATA AVAILABILITY STATEMENT

The data sets presented in this study can be found in online repositories. The names of the repository/repositories and accession number(s) can be found in the article/ **Supplementary Material**.

AUTHOR CONTRIBUTIONS

WY and LZ conceived this project. JZ, FL, and GL designed the study. ML and YH searched the literature data. NX and YH extracted the data. JZ, WY, and GL, ML, and JP drafted the manuscript. All authors contributed to the article and approved the submitted version.

FUNDING

This work was supported by the National Natural Science Foundation of China (82004383, 81974574), the National key research and development program (2021YFC1712804), the Science and Technology Research Project of Guangdong Provincial Hospital of Chinese Medicine (YN2019ML08), China Postdoctoral Science Foundation (No. 2018M633036) and Medical Scientific Research Foundation of Guangdong Province (No. B2019091).

SUPPLEMENTARY MATERIAL

The Supplementary Material for this article can be found online at: https://www.frontiersin.org/articles/10.3389/fendo.2021.815891/full#supplementary-material

REFERENCES

1. Fuggle NR, Curtis B, Clynes M, Zhang J, Ward K, Javaid MK, et al. The Treatment Gap: The Missed Opportunities for Osteoporosis Therapy. *Bone* (2021) 144:115833. doi: 10.1016/j.bone.2020.115833
2. Wright NC, Looker AC, Saag KG, Curtis JR, Delzell ES, Randall S, et al. The Recent Prevalence of Osteoporosis and Low Bone Mass in the United States Based on Bone Mineral Density at the Femoral Neck or Lumbar Spine. *J Bone Miner Res* (2014) 29(11):2520–6. doi: 10.1002/jbmr.2269
3. Noh J, Yang Y, Jung H. Molecular Mechanisms and Emerging Therapeutics for Osteoporosis. *Int J Mol Sci* (2020) 21(20):7623. doi: 10.3390/ijms21207623
4. Foger-Samwald U, Dovjak P, Azizi-Semrad U, Kerschan-Schindl K, Pietschmann P. Osteoporosis: Pathophysiology and Therapeutic Options. *EXCLI J* (2020) 19:1017–37. doi: 10.17179/excli2020-2591
5. Martiniakova M, Babikova M, Omelka R. Pharmacological Agents and Natural Compounds: Available Treatments for Osteoporosis. *J Physiol Pharmacol* (2020) 71(3):307–20. doi: 10.26402/jpp.2020.3.01
6. Zhao J, Zeng L, Wu M, Huang H, Liang G, Yang W, et al. Efficacy of Chinese Patent Medicine for Primary Osteoporosis: A Network Meta-Analysis. *Complement Ther Clin* (2021) 44:101419. doi: 10.1016/j.ctcp.2021.101419
7. Yang A, Yu C, You F, He C, Li Z. Mechanisms of Zuogui Pill in Treating Osteoporosis: Perspective From Bone Marrow Mesenchymal Stem Cells. *Evid-Based Compl Alt* (2018) 2018:3717391. doi: 10.1155/2018/3717391
8. Wang SJ, Yue W, Rahman K, Xin HL, Zhang QY, Qin LP, et al. Mechanism of Treatment of Kidney Deficiency and Osteoporosis is Similar by Traditional Chinese Medicine. *Curr Pharm Des* (2016) 22(3):312–20. doi: 10.2174/1381612822666151112150346
9. Zhang N, Han T, Huang B, Rahman K, Jiang Y, Xu H, et al. Traditional Chinese Medicine Formulas for the Treatment of Osteoporosis: Implication for Antiosteoporotic Drug Discovery. *J Ethnopharmacol* (2016) 189:61–80. doi: 10.1016/j.jep.2016.05.025
10. Chen Y, Zhou Y, Li D, Peng C. Research Progress on Modern Pharmacological Action of Polygonati Rhizoma. *J Chin Med Mater* (2021) 44(01):240–4. doi: 10.13863/j.issn1001-4454.2021.01.046
11. Ren H, Deng Y, Zhang J, Ye X, Xia L, Liu M, et al. Research Progress on Processing History Evolution, Chemical Components and Pharmacological Effects of Polygonati Rhizoma. *China J Chin Mater Med* (2020) 45(17):4163–82. doi: 10.19540/j.cnki.cjcmm.20200522.601
12. Du L, Nong MN, Zhao JM, Peng XM, Zong SH, Zeng GF. Polygonatum Sibiricum Polysaccharide Inhibits Osteoporosis by Promoting Osteoblast Formation and Blocking Osteoclastogenesis Through Wnt/β-Catenin Signalling Pathway. *Sci Rep* (2016) 6:32261. doi: 10.1038/srep32261
13. Yan F, Zeng G, Zong S, Peng X, Wu P, Zhang L, et al. The Effect of Polygonatum Sibiricum Polysaccharide on the Expression of OPG and RANKL in the Rat Model of Ovariectomy-Induced Osteoporosis. *J Pract Med* (2017) 33(08):1243–6. doi: 10.3969/j.issn.1006-5725.2017.08.013
14. Zhang L, Zeng G, Zong S, Wu P, He J, Wu Y, et al. Molecular Mechanism of Polygonatum Sibiricum Polysaccharide in the Prevention and Treatment of Postmenopausal Osteoporosis. *Chin J Tissue Eng Res* (2018) 22(04):493–8. doi: 10.3969/j.issn.2095-4344.0079
15. Wang X, Wang Z, Zheng J, Li S. TCM Network Pharmacology: A New Trend Towards Combining Computational, Experimental and Clinical Approaches. *Chin J Nat Med* (2021) 19(1):1–11. doi: 10.1016/S1875-5364(21)60001-8
16. Abdelsattar AS, Dawoud A, Helal MA. Interaction of Nanoparticles With Biological Macromolecules: A Review of Molecular Docking Studies. *Nanotoxicology* (2021) 15(1):66–95. doi: 10.1080/17435390.2020.1842537
17. Ru J, Li P, Wang J, Zhou W, Li B, Huang C, et al. TCMSP: A Database of Systems Pharmacology for Drug Discovery From Herbal Medicines. *J Cheminformat* (2014) 6(1):1–6. doi: 10.1186/1758-2946-6-13
18. Xu J, Stevenson J. Drug-Like Index: A New Approach To Measure Drug-Like Compounds and Their Diversity. *J Chem Inf Comput Sci* (2000) 40(5):1177–87. doi: 10.1021/ci000026+
19. Gfeller D, Grosdidier A, Wirth M, Daina A, Michielin O, Zoete V. SwissTargetPrediction: A Web Server for Target Prediction of Bioactive Small Molecules. *Nucleic Acids Res* (2014) 42(W1):W32–8. doi: 10.1093/nar/gku293
20. Kim K, Lee Y, Han I. The Role of Epigenomics in Osteoporosis and Osteoporotic Vertebral Fracture. *Int J Mol Sci* (2020) 21(24):9455. doi: 10.3390/ijms21249455
21. Zhao H, Zhao N, Zheng P, Xu X, Liu M, Luo D, et al. Prevention and Treatment of Osteoporosis Using Chinese Medicinal Plants: Special Emphasis on Mechanisms of Immune Modulation. *J Immunol Res* (2018) 2018:6345857. doi: 10.1155/2018/6345857
22. Su F, Liu D, Chen J, Yu S, Chiu W, Hsu C, et al. Development and Validation of an Osteoporosis Self-Assessment Tool for Taiwan (OSTAi) Postmenopausal Women-A Sub-Study of the Taiwan OsteoPorosis Survey (TOPS). *PLoS One* (2015) 10(6):e130716. doi: 10.1371/journal.pone.0130716
23. Lin M, Zhao Y, Cai E, Zhu H, Gao Y, He Z, et al. Anti-Tumor Effect of β-Sitosterol in H_{22} Tumor-Bearing Mice. *Chin J Public Health* (2017) 33(12):1797–800. doi: 10.11847/zgggws2017-33-12-31
24. Zhang F, Liu Z, He X, Li Z, Shi B, Cai F. β-Sitosterol-Loaded Solid Lipid Nanoparticles Ameliorate Complete Freund's Adjuvant-Induced Arthritis in Rats: Involvement of NF-Kb and HO-1/Nrf-2 Pathway. *Drug Deliv* (2020) 27(1):1329–41. doi: 10.1080/10717544.2020.1818883
25. Zhu J, Tang Y, Wu Q, Ji YC, Feng ZF, Kang FW. HIF-1α Facilitates Osteocyte-Mediated Osteoclastogenesis by Activating JAK2/STAT3 Pathway. *Vitro J Cell Physiol* (2019) 234(11):21182–92. doi: 10.1002/jcp.28721
26. Wang Y, Wan C, Deng L, Liu X, Cao X, Gilbert SR, et al. : The Hypoxia-Inducible Factor α Pathway Couples Angiogenesis to Osteogenesis During Skeletal Development. *J Clin Invest* (2007) 117(6):1616–26. doi: 10.1172/JCI31581
27. Fernández-Torres J, Martínez-Nava GA, Gutiérrez-Ruíz MC, Gómez-Quiroz LE, Gutiérrez M. Role of HIF-1α Signaling Pathway in Osteoarthritis: A

Systematic Review. *Rev Bras Reumatol (English Ed)* (2017) 57(2):162–73. doi: 10.1016/j.rbre.2016.07.008
28. Liu H, Li X, Lin J, Lin M. Morroniside Promotes the Osteogenesis by Activating PI3K/Akt/mTOR Signaling. *Biosci Biotechnol Biochem* (2021) 85 (2):332–9. doi: 10.1093/bbb/zbaa010
29. Zhou H, Jiao G, Dong M, Chi H, Wang H, Wu W, et al. Orthosilicic Acid Accelerates Bone Formation in Human Osteoblast-Like Cells Through the PI3K–Akt–mTOR Pathway. *Biol Trace Elem Res* (2019) 190(2):327–35. doi: 10.1007/s12011-018-1574-9
30. Li X, Jie Q, Zhang H, Zhao Y, Lin Y, Du J, et al. Disturbed MEK/ERK Signaling Increases Osteoclast Activity *via* the Hedgehog-Gli Pathway in Postmenopausal Osteoporosis. *Prog Biophys Mol Biol* (2016) 122(2):101–11. doi: 10.1016/j.pbiomolbio.2016.05.008
31. Ikeda K, Horie-Inoue K, Inoue S. Functions of Estrogen and Estrogen Receptor Signaling on Skeletal Muscle. *J Steroid Biochem Mol Biol* (2019) 191:105375. doi: 10.1016/j.jsbmb.2019.105375

Conflict of Interest: The authors declare that the research was conducted in the absence of any commercial or financial relationships that could be construed as a potential conflict of interest.

Publisher's Note: All claims expressed in this article are solely those of the authors and do not necessarily represent those of their affiliated organizations, or those of the publisher, the editors and the reviewers. Any product that may be evaluated in this article, or claim that may be made by its manufacturer, is not guaranteed or endorsed by the publisher.

Citation: *Zhao J, Lin F, Liang G, Han Y, Xu N, Pan J, Luo M, Yang W and Zeng L (2022) Exploration of the Molecular Mechanism of Polygonati Rhizoma in the Treatment of Osteoporosis Based on Network Pharmacology and Molecular Docking.*
Front. Endocrinol. 12:815891. doi: 10.3389/fendo.2021.815891

frontiers in Endocrinology

ORIGINAL RESEARCH
published: 25 January 2022
doi: 10.3389/fendo.2021.833474

Quantitative Proteomics Revealed the Pharmacodynamic Network of Bugu Shengsui Decoction Promoting Osteoblast Proliferation

Xu Wei[1†], Baoyu Qi[1†], Ruyun Ma[2†], Yili Zhang[3], Ning Liu[1], Shengjie Fang[1], Yanning Zhu[2], Yanming Xie[4], Jianye Dai[2,5*] and Liguo Zhu[1*]*

[1] Wangjing Hospital, China Academy of Chinese Medical Sciences, Beijing, China, [2] School of Pharmacy, Lanzhou University, Lanzhou, China, [3] School of Traditional Chinese Medicine & School of Integrated Chinese and Western Medicine, Nanjing University of Chinese Medicine, Nanjing, China, [4] Institute of Basic Research in Clinical Medicine, China Academy of Chinese Medical Sciences, Beijing, China, [5] Collaborative Innovation Center for Northwestern Chinese Medicine, Lanzhou University, Lanzhou, China

Background and Objective: With high morbidity and disability, osteoporosis is a worldwide bone metabolism disease, regulated by complex pathological processes. Insufficient osteogenesis is greatly essential to osteoporosis. Traditional Chinese Medicine, a complex natural herbal medicine system, has increasingly attracted attention all over the world. Bugu Shengsui Decoction, a compound formula for osteoporosis, has significant clinical effects in the treatment of osteoporosis. Yet the detailed mechanisms are unclear. Thus, we investigated the effects and mechanism of Bugu Shengsui Decoction on osteoporotic rats and osteoblasts *in vitro*.

Methods: In this study, we evaluated the effect of Bugu Shengsui Decoction in an animal model of orchiectomy. Multi-pharmacology indexes revealed that Bugu Shengsui Decoction obviously improved bone metabolism, bone mineral density, bone morphology, and biomechanics in the castrated rats. Then, serum pharmacology was employed to unveil that Bugu Shengsui Decoction promoted the proliferation and differentiation of osteoblasts. Moreover, quantitative proteomics combined with RNA interference assay was used to analyze and verify the pathway and key targets in pro-proliferation of MC3T3-E1 cells.

Results: Bugu Shengsui Decoction obviously improved the worse parameters of bone metabolism, bone mineral density, bone morphology, and biomechanics in a castrated rat model. *In vitro*, Bugu Shengsui Decoction exerted proliferation- and differentiation-promoting effects of osteoblasts induced by serum starvation. Moreover, quantitative proteomics analysis combined with RNA interfere assay illustrated that Bugu Shengsui Decoction promoted osteogenesis *via* the PI3K-AKT pathway.

OPEN ACCESS

Edited by:
Jun Liu,
Guangdong Provincial Academy of Chinese Medical Sciences, China

Reviewed by:
Xiang Rong Wu,
Shenyang Pharmaceutical University, China
Haiyang Yu,
Tianjin University of Traditional Chinese Medicine, China
Lili Sheng,
Shanghai University of Traditional Chinese Medicine, China

***Correspondence:**
Yanming Xie
ktzu2018@163.com
Jianye Dai
daijy@lzu.edu.cn
Liguo Zhu
tcmspine@163.com

[†]These authors have contributed equally to this work and share first authorship

Specialty section:
This article was submitted to Bone Research, a section of the journal Frontiers in Endocrinology

Received: *11 December 2021*
Accepted: *24 December 2021*
Published: *25 January 2022*

Citation:
Wei X, Qi B, Ma R, Zhang Y, Liu N, Fang S, Zhu Y, Xie Y, Dai J and Zhu L (2022) Quantitative Proteomics Revealed the Pharmacodynamic Network of Bugu Shengsui Decoction Promoting Osteoblast Proliferation. Front. Endocrinol. 12:833474. doi: 10.3389/fendo.2021.833474

Conclusion: Summarily, our discoveries certify that Bugu Shengsui Decoction is an effective treatment for osteoporosis *via* PI3K-AKT. This study is not only a beneficial attempt to explore the detailed mechanism of Traditional Chinese formula but also will provide inspiration for the treatment strategy of osteoporosis.

Keywords: Bugu Shengsui Decoction, PI3K-AKT pathway, osteoporosis, stable isotope dimethyl-labeled proteomics, bone formation

INTRODUCTION

Osteoporosis (OP), a common bone metabolic disease with high incidence, has become one of the urgent global major health problems (1, 2). It is caused by the imbalance of bone metabolism, including bone loss, destruction of bone tissue structure, and increased risk of bone fragility and fractures. It easily leads to disability and mortality, bringing heavy economic and medical burden to society (2). The pathogenesis of OP is complicated, yet more bone resorption than formation is the main pathological manifestation (3). Currently, the anti-osteoporosis strategies include using bone resorption inhibitors, calcium and vitamin supplements, diet adjustments, and increasing physical activities (2–4). Some researchers have demonstrated that the multilevel processes of bone formation are essential for maintaining bone mass (5). Under the regulation of cytokines, ossification centers are formed *via* osteoblasts' proliferation, differentiation, and migration. It is essential to the formation of bones (6). Therefore, it is beneficial to promote the proliferation, differentiation, and migration of bone cells for the prevention and treatment of OP.

Recently, Traditional Chinese medicine shows obvious curative effects on OP, which significantly increases bone density, reduces the incidence of fragility fractures, and plays anti-inflammatory and analgesic roles in OP patients (7–9). Especially, Bugu Shengsui Decoction (BGSSD), a traditional Chinese medicine compound formula, is applied to treat OP in clinical practice. It can effectively increase bone mineral density (BMD), serum calcitonin, luteinizing hormone, and calcium in OP patients, with total 82% efficiency (10). BGSSD can also improve blood circulation disorders in osteoporotic model rats (11) regulating the expression of related proteins in the Smad/ERK signaling pathway (12). Further, the active ingredients in BGSSD are capable of improving blood circulation in osteoporotic rats, performing anti-inflammatory and analgesic effects, increasing BMD, and regulating gene expressions (13–16). However, the detailed anti-osteoporotic mechanism of BGSSD is still unclear.

Therefore, we evaluated the anti-osteoporotic effect of BGSSD and explored the specific cellular phenotype (17). Then, a pharmacodynamic network was conducted to analyze the result of quantitative proteomics based on stable isotope dimethyl labeling (18–20). Finally, molecular biology was employed to verify the proposed mechanism of alleviating osteoporosis, relying on the PI3K-AKT pathway. The scheme of this work is as follows (**Figure 1**).

MATERIALS AND METHODS

Animal Experiment

Male Wistar rats (8 weeks old, average weight 244.5 g) were purchased from the Laboratory Animal Center of Lanzhou Veterinary Research Institute, Chinese Academy of Agricultural Sciences, with the license number of SCXK(Gan) 2020-0002, raised in the Animal Experiment Center of Lanzhou University, replenished with free food and water. Before modeling, they were fed to adapt to the environment for 7 days. The rats were randomly divided into 6 groups (8 rats in each group), which respectively were groups of control (Ctrl), model (Mod), positive control (P-Ctrl, alendronate sodium), low dose of BGSSD (BGSSD-L), medium dose of BGSSD (BGSSD-M), and high dose of BGSSD (BGSSD-H). A castrated rat model was established to evaluate the anti-osteoporotic effects. Intraperitoneal anesthesia was performed with ethyl ether, and an aseptic modeling operation was performed according to the method of removing testicles (21). Briefly, the midline skin and subcutaneous tissue of the rat scrotum were cut, the testis, epididymis, and surrounding tissues were separated, the testis and epididymis were excised, then the skin incision was sutured. The control group did not do the above operation. In the first 3 days after the operation, rats were injected with penicillin potassium at 50000U per 100g intramuscularly to prevent infection. One week after recovery, saline was given to the control group and model group, alendronate sodium solution (Savio Industrial S.R.L, Italy) was given to the positive control group at 0.88 $mg{\cdot}kg^{-1}{\cdot}d^{-1}$, and the low dose, medium dose, and high dose of BGSSD groups were respectively given at 2.94, 5.87, and 11.74 $g{\cdot}kg^{-1}{\cdot}day^{-1}$ intragastrically, once a day for 12 weeks. Chinese herbal medicine was purchased from Wangjing Hospital of China Academy of Chinese Medical Sciences. All administered dosages were converted according to the clinical effective dose. When all animals were euthanized, blood and femurs were collected. All animal experiments were conducted under the procedures and guidelines approved by Lanzhou University Institutional Animal Care and Use Committee and were approved by the Animal Experiments Ethics Committee of Lanzhou University.

Bone Metabolism Indicator Assay

Serum indicators of bone metabolism such as alkaline phosphatase (Alp), calcium, and phosphorus were assayed according to instructions of the commercial kit (Changchun Huili Biotech Co. Ltd., China). Alp was detected by a three-step reaction.

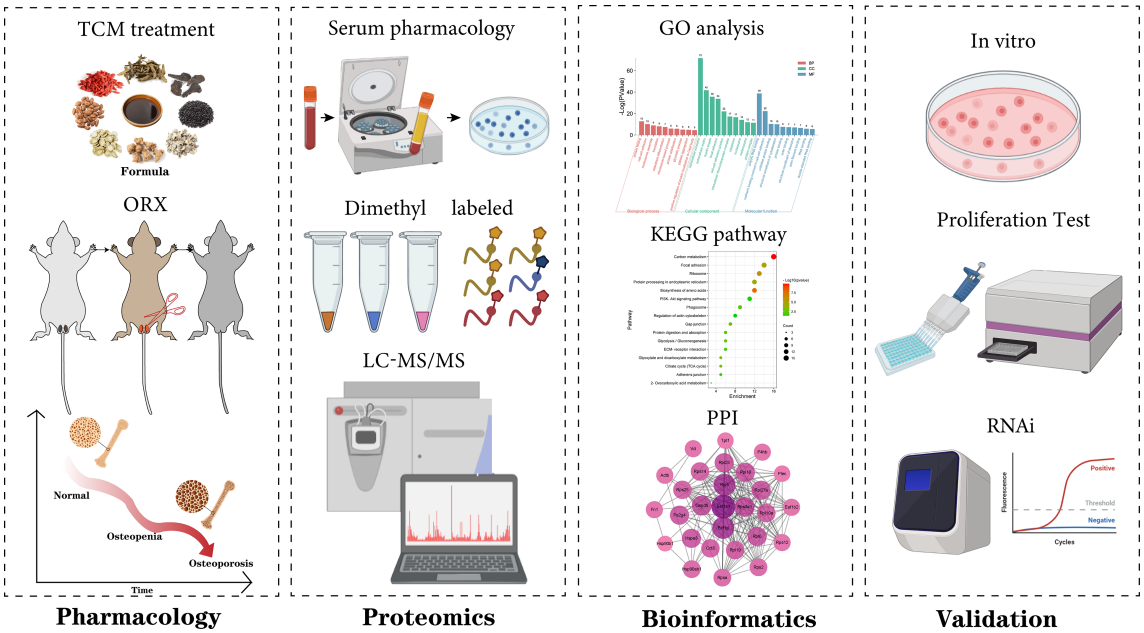

FIGURE 1 | The strategies of revealing the anti-osteoporosis mechanism of BGSSD.

Under alkaline conditions, phenyl disodium phosphate was decomposed into free phenol and phosphoric acid by Alp, which was then combined with aminoantipyrine and oxidized to form a red quinone structure. The quinone conjugate and Alp activity showed a linear relationship at 510 nm. Calcium-GBHA was measured at 520 nm to determine serum calcium concentration. The phosphomolybdic acid was measured at 660 nm to determine the concentration of serum inorganic phosphorus. Serum indicators of bone metabolism were quantitatively measured.

Bone Mineral Density Test

In order to detect the BMD of rats, the right femur of rats was stored at -80°C, and the whole bone was selected as the target region. A dual-energy X-ray scanner (Osteocore, Medilink, France) was used for scanning. Osteocore can automatically aim at the induction area and control quality and periosteum calibration. Cross-sectional images of the samples were collected, and the range of the femur was framed. Bone mineral mass and bone area were analyzed and calculated by Osteocore 3.7.0.0.5 software; finally, the BMD was calculated.

Bone Tissue Morphology Test

To analyze the morphological structure, the left femurs were fixed with a 3.7% neutral formalin solution for 24 h and scanned by microcomputed tomography (μ-CT, SkyScan 1174, Bruker, Belgium). Scanning conditions were 50 kV, 800 μA, scanning resolution of 12 μm, and 1,304 × 1,024 pixels of vision. The baseline was 1.0 mm below the growth plate on the knee side of the femur, 250 consecutive sections were taken, and the area with a thickness of 3 mm was selected as the ROI for 3D reconstruction. Three-dimensional (3D) image reconstructions were performed by N-RECON software, and the ratio of bone volume to tissue volume (BV/TV), trabecular thickness (Tb.Th), trabecular number (Tb.N), trabecular separation (Tb.Sp), and structural model index (SMI) were calculated by CT-AN software for 3D analysis.

Bone Tissue Biomechanical Test

To calculate the biomechanical parameters, the femurs were evaluated on a microcomputer-controlled electronic universal testing machine (RGWT-4005, Shenzhen Ragel, China). Detection conditions were 22°C, span was 20 mm, and running speed was 1 mm per min. The starting point was 2N (displacement clearance at the same time). The fracture sign was the force value less than 20% of the maximum. Bone biomechanical parameters such as maximum load, flexural strength, and elastic modulus of femurs were collected for analysis.

Preparation of Drug-Containing Serum

After the last intragastric administration, the blood of rats was collected and placed at 4°C for 1 h, then centrifuged for 10 min (4°C, 3,000 rpm). The supernatant was collected, and anhydrous ethanol of 4 times the volume of serum was added to precipitate proteins. The suspension was centrifuged for 10 min (4°C, 5,000 rpm) and the supernatant was dried in a vacuum centrifuge concentrator (45°C, 1,600 rpm, 300 min). The powder was stored separately at -80°C. To eliminate individual differences, the drug-containing serum of each group was premixed and concentrated.

Cell Culture

Osteoblastic progenitor cells (MC3T3-E1, from China Infrastructure of Cell Line Resource, China) were cultured in alpha-modified minimum essential medium eagle (α-MEM, L570KJ, Shanghai Basalmedia Technologies Co., Ltd., China) containing 10% fetal

bovine serum (FBS, 10099-141C, Gibco, USA) and 1% penicillin–streptomycin (15140-122, Gibco, USA) and incubated at 37°C and 5% CO_2. The medium was changed every 2 days.

MTS Assay

The cell viability was tested *via* an MTS kit (G3581, Promega, USA). MC3T3-E1 cells were inoculated into 96-well plates at $5*10^3$ per well and incubated overnight to adhere, including a control group and experimental groups. After 8 h, the cells were treated with different drug-containing sera. MTS reagent (10%, v/v) was added after 48 h of administration, and the optical density (OD) was detected at 492 nm to measure the cells' proliferation.

Western Blot Assay

The proteins were separated by electrophoresis in 10% sodium dodecyl sulfate-polyacrylamide gel (01413/60341, Cwbio, China), and then the separated proteins were transferred to the polyvinylidene fluoride (PVDF) membrane (A29643309, GE Healthcare, Germany). The PVDF membrane was combined with anti-Col-I antibody (PA5-95137, Sigma, USA), anti-Alp antibody (ET1601-21, HUABIO, China), anti-Runx2 antibody (ET1612-47, HUABIO, China), and anti-β-actin antibody (SA00001-1, Proteintech, USA) incubated overnight at 4°C, then shaken with secondary antibody at room temperature for 1 h. Exposure was taken in a TANON gel imager.

RNA Interference Assay

MC3T3-E1 cells were plated at $4.0*10^5$ in 6-well plates. The cells with nearly 60% confluency were transfected with siRNA of Fn1, Col1a1, Col1a2, Col6a1, Col6a2, Col6a3, Rac1, Hsp90ab1, Hsp90b1, Ywhaz, PI3K, AKT, BAD, and Bcl-2. Non-specific control (NC) of siRNA was also used. The sequences are shown in **Table 1**.

Quantitative Real-Time Polymerase Chain Reaction

Total RNA was extracted and purified according to the commercial kit (LS1040, Promega, USA) and used as a template for cDNA reverse transcription synthesis with the commercial kit (K1622, Thermo, USA). The conditions were as follows: 42°C 30 min and 85°C 10 min. By using UltraSYBR Mixture (Low ROX, CW2601, Cwbio, China), quantitative real-time polymerase chain reaction (qRT-PCR) was performed by Stratagene Mx3000P (Agilent, USA); reaction conditions were 95°C 3 min, 95°C 15 s, 55°C 30 s, 72°C 30 s, operated in 40 cycles. The primer gene sequences are listed in **Table 2**.

Stable Isotope Dimethyl Labeling

MC3T3-E1 cells were collected after being washed with PBS for 3 times and centrifuged at 4°C, 3,000 rpm for 3 min. The cells were lysed in 0.1% Triton X-100 (T8787, Sigma, USA)–100 mM TEAB (T7408, Sigma, USA) containing EDTA-free protease inhibitor

TABLE 1 | Sequences of siRNA used in RNA interference.

siRNA for RNA interference (5′–3′)		
Fn1	Sense	GCCCUAAAGAUUCCAUGAUTT
	Antisense	AUCAUGGAAUCUUUAGGGCTT
Col1a1	Sense	CCCGGAAGAAUACGUAUCATT
	Antisense	UGAUACGUAUUCUUCCGGGTT
Col1a2	Sense	GCCUAGCAACAUGCCAAUATT
	Antisense	UAUUGGCAUGUUGCUAGGCTT
Col6a1	Sense	GUCUGGAAGAUGCAGUAAATT
	Antisense	UUUACUGCAUCUUCCAGACTT
Col6a2	Sense	CCACCACUGAAAGGAACAATT
	Antisense	UUGUUCCUUUCAGUGGUGGTT
Col6a3	Sense	CGGCUGACAUAGUGUUUCUTT
	Antisense	AGAAACACUAUGUCAGCCGTT
Rac1	Sense	GGUGGGAGACGGAGCUGUUTT
	Antisense	AACAGCUCCGUCUCCCACCTT
Hsp90ab1	Sense	CUGGGAACCAUUGCUAAGUTT
	Antisense	ACUUAGCAAUGGUUCCCAGTT
Hsp90b1	Sense	GGUCGUGGAACAACAAUUATT
	Antisense	UAAUUGUUGUUCCACGACCTT
Ywhaz	Sense	CCUUCUCUCUGUUGCUUAUTT
	Antisense	AUAAGCAACAGAGAGAAGGTT
PI3K	Sense	GCAGGAUCAAGUUGUCAAATT
	Antisense	UUUGACAACUUGAUCCUGCTT
AKT	Sense	GGCCCAACACCUUUAUCAUTT
	Antisense	AUGAUAAAGGUGUUGGGCCTT
BAD	Sense	GGAGCAACAUUCAUCAGCATT
	Antisense	UGCUGAUGAAUGUUGCUCCTT
Bcl-2	Sense	GGGAGAUCGUGAUGAAGUATT
	Antisense	UACUUCAUCACGAUCUCCCTT
NC	Sense	UUCUCCGAACGUGUCACGUTT
	Antisense	ACGUGACACGUUCGGAGAATT

All sequences were designed, synthesized, and validated by GenePharma (Shanghai, China). The interference was performed based on the protocol of Lipofectamine® 3000 (2304349, Thermo, USA). The silencing efficiency was examined by qRT-PCR.

TABLE 2 | Sequences of primers used in qRT-PCR.

Primers for qRT-PCR (5′–3′)		
Fn1	F	CTTGCACGATGATATGGAGA
	R	AGCTGAACACTGGGTGCTAT
Col1a1	F	TCCGGCTCCTGCTCCTCTTA
	R	GTATGCAGCTGACTTCAGGGATGT
Col1a2	F	TCGTGCCTAGCAACATGCC
	R	TTTGTCAGAATACTGAGCAGCAA
Col6a1	F	GATGAGGGTGAAGTGGGAG
	R	CACTCACAGCAGGAGCACAT
Col6a2	F	GATGACATGGAAGACGTCCTTTG
	R	GCTCTGTTTGGCAGGGAAGTT
Col6a3	F	CCTAACCACATATGTTAGTGGAGGT
	R	GAATGTCTCGCTTGCTCTCTG
Rac1	F	CTGCCAATGTTATGGTAGATGG
	R	TTTCAAATGATGCAGGACTCAC
Hsp90ab1	F	TTGACATCATCCCCAACCCTC
	R	ACCAAACTGCCCAATCATGGA
Hsp90b1	F	TTCTGGAAGGAGTTCGGCAC
	R	TCCATGTTGCCAGACCATCC
Ywhaz	F	TAGGTCATCGTGGAGGGTCG
	R	GAAGCATTGGGGATCAAGAACTT
PI3K	F	GATTTGCCCCACCATGACGAGAAGA
	R	CTCCTTCAGGGAGCTGTACAGGTTGTAG
AKT	F	TGTATGAGAAGAAGCTGAGCCC
	R	TCACTGTCCACACACTCCATG
BAD	F	TGAGCCGAGTGAGCAGGAA
	R	GCCTCCATGATGACTGTTGGT
Bcl-2	F	AGTTCGGTGGGGTCATGTGTG
	R	CCAGGTATGCACCCAGAGTG
β-actin	F	TGGCTCCTAGCACCATGAAG
	R	AACGCAGCTCAGTAACAGTCC

All primers were designed and synthesized by SunBiotech (Tianjin, China). Cycle threshold (Ct) values were processed to evaluate the relative mRNA expression via the $2^{-\Delta\Delta Ct}$ method, and β-actin served as the internal control.

cocktail (04693132001, Sigma-Aldrich, Gemany) by complete ultrasonication on ice. The supernatant was collected, and protein content was detected by Pierce™ BCA Protein Assay Kit. 10-μl samples (3 mg/ml) were reacted with 30 μl 8 M urea and 2 μl 200 mM DTT at 65°C in darkness for 15 min. Then, 2 μl 400 mM iodoacetamide (IAA) was added for reaction for 30 min in darkness at 35°C. 2 μl 200 mM DTT was added to react with the leftover IAA for 15 min at 65°C. 100 μl 100 mM TEAB, 2 μl 0.2 μg/μl trypsin (V528A, Promega, USA), and 1.5 μl 100 mM calcium chloride were added to perform enzyme cutting at 37°C for no less than 14 h. Dimethyl labeling (18) was as follows: for the control ("light") group, the peptides were reacted with 6 μl 4% CH_2O (F1635, Sigma, USA) and 6 μl 0.6 M $NaBH_3CN$ (42077, Sigma, USA); for the modeling ("middle") group, the peptides were reacted with 6 μl 4% $^{13}CD_2O$ (596388, Sigma, USA) and 6 μl 0.6 M $NaBH_3CN$; and for the BGSSD ("heavy") group, the peptides were reacted with 6 μl 4% $^{13}CD_2O$ and 6 μl 0.6 M $NaBD_3CN$ (190020, Sigma, USA). The labeling reaction was incubated for 1 h at 22°C. It was quenched by 24 μl 1% ammonia hydroxide and 12 μl formic acid. Finally, the "light," "middle," and "heavy" samples were mixed and the desalting was performed with Pierce™ C18 Tips (87782, Thermo, USA).

LC-MS/MS Test and Data Analysis

All samples were analyzed by LC-MS/MS on Q Exactive Orbitrap mass spectrometers (Thermo, USA), coupled with an UltiMate 3000 LC system (22). In short, full-scan mass spectra were captured over the ratio of m/z from 350 to 1,800, using the analyzer with a mass resolution of 7,000 in positive-ion mode. MS/MS fragmentation was performed in a data-dependent mode, of which the TOP 20 intensity ions were selected for MS/MS analysis with a resolution of 17500, using the collision mode of HCD. Other important parameters were isolation window of 2.0-m/z units, default charge of 2+, normalized collision energy of 28%, maximum IT of 50 ms, and dynamic exclusion of 20.0 s. Then, data analysis was performed by ProLuCID. The different isotopic modifications (28.0313 and 34.0631 Da, respectively, for light and heavy labeling) were set as static modifications on the N-terminal of a peptide and lysine. The ratios of reductive dimethylation were quantified by the CIMAGE software. Proteins with an average ratio (light/heavy) of more than 1.5 were selected for further GO analysis.

Statistical Analysis

Statistical Product and Service Solutions (IBM SPSS 25.0) was used to check the data normality and homogeneity of variance by the Kolmogorov–Smirnov test and Levene's test, respectively. When three or more means were compared for statistical significance, one- or two-way ANOVA was conducted. The two-sided Student's t-test was conducted when two groups of measurements were examined for statistical significance. All data are presented as mean ± s.e.m.; p-value <0.05 is considered statistically significant.

RESULTS

BGSSD Can Prevent Osteoporosis in Castrated Rats

On the premise of clinical effectiveness, to further determine the therapeutic effects of BGSSD, we established a common orchiectomy-induced (ORX) rat model of OP (21). Littermate male rats received the same bilateral orchiectomy for 12 weeks, and a simultaneous administration was carried out. With the serum markers of bone metabolism detected, we found that the concentrations of Alp, calcium, and phosphorus in serum of ORX rats were significantly decreased. Alendronate as well as three doses of BGSSD could increase the contents of serum Alp, calcium, and phosphorus (**Figures 2A–C**). In order to better quantify and compare the changes of OP, we scanned the femurs *via* μ-CT (**Figure 2D**) and dual-energy X-ray absorptiometry (DXA). Then, we found that the BMD of osteoporotic model rats lessened, and BGSSD can prevent the loss of BMD effectively (**Figure 2E**). Moreover, the microstructure of μ-CT-scanned femurs was further analyzed to demonstrate that ORX rats had a lower percentage of bone volume versus tissue volume (BV/TV), trabecular number (Tb.N), trabecular thickness (Tb.Th), and larger trabecular separation (Tb.Sp) together with the structural model index (SMI) compared with control rats (**Figure 2F**). As expected, BGSSD could ameliorate the microstructural indicators by increasing the ratio of BV/TV, Tb.N, and Tb.Th and decreasing Tb.Sp (medium-dose) and SMI of the ORX rats (**Figure 2F**). In addition, the three-point bending test showed that worse elastic modulus and maximum load are presented in osteoporotic model rats (**Figure 2G** and **Supplementary Material, Figure S1B**), yet BGSSD played a positive role in strengthening elastic modulus (**Figure 2G**). All the above evidence supported that BGSSD is an effective Chinese medical formula for OP.

BGSSD Can Promote the Proliferation and Differentiation of MC3T3-E1 Cells in Serum-Deprivation-Induced Cell Model

As known, the osteoporotic lesion is in an ischemic and hypoxic environment under the pathological state, which causes the cells to produce a corresponding stress response (23, 24). To further identify the cell phenotype of BGSSD. We screened cell models with the methods of serum deprivation and oxygen deprivation (**Supplementary Material, Figures S3A, B**), and the serum-starved cell model was selected for pharmacodynamic experiments. Finally, we caught that drug-containing serum of BGSSD could obviously increase the viability of serum-deprived MC3T3-E1 cells (**Figure 3A**).

Furthermore, we found that BGGSD could also promote the differentiation of MC3T3-E1 cells. Quantification analysis of Western blots showed that lower expressions of Col-I, Alp, and Runx2 proteins in the Ctrl group and drug-containing serum of all doses of BGSSD could remarkably increase the expressions of Col-I, Alp, and Runx2 (**Figures 3B–D**). The above-listed confirmations indicated that BGSSD could effectively promote both proliferation and differentiation of MC3T3-E1 cells.

Quantitative Proteomics Revealed the Pharmacodynamic Network and Mechanism of BGSSD

According to the clinical and experimental effects, quantitative proteomics was conducted to elaborate the pharmacology network and mechanism of BGSSD. The proteomes of the control group, modeling group, and BGSSD-treated group were respectively collected. Then, stable isotope dimethyl labeling was performed to distinguish and simultaneously compare the changes of proteomic networks in three groups (**Figure 4A**).

After bioinformatics analysis (**Figures 4B–D**), GO and KEGG analyses revealed that the top five pathways named ribosome, focal adhesion, carbon metabolism, protein processing in the endoplasmic reticulum, and PI3K-AKT signaling pathway were most relevant to the anti-osteoporosis efficacy of BGSSD (**Figure 4E**). In further literature mining, PI3K-AKT signaling pathway attracted our attention (25), which was highly correlated with the regulation of both proliferation and differentiation of osteoblasts according to published reports (26, 27). Important pharmacodynamic-related proteins in the PI3K-AKT pathway are listed in **Figure 4G**. Fn1, Col1a1, Col1a2, Col6a1, Col6a2, Col6a3, Rac1, Hsp90ab1, Hsp90b1, Ywhaz, and Gnb2 were significantly intervened by BGSSD (**Figure 4F**). Compared with the Ctrl, all the abovementioned proteins were increased in the BGSSD group, which was the content we will focus on especially.

RNA Interference Verified That the PI3K-AKT Signaling Pathway Are Crucial for the Osteogenetic Effect of BGSSD

According to **Figure 5A**, BGSSD could significantly promote the proliferation of serum-deprived MC3T3-E1 cells. With the combination of proteomic analysis and literature mining (28), we found that the PI3K-AKT signaling pathway is closely related to BGSSD's pharmacological effects, in which the PI3K-AKT pathway played an important role in the process of bone metabolism, which can regulate the proliferation and differentiation of bone formation in the bone formation stage. After comprehensive consideration, Fn1, Col1a1, Col1a2, Col6a1, Col6a2, Col6a3, Rac1, Hsp90ab1, Hsp90b1, Ywhaz, PI3K, AKT, BAD, and Bcl-2 were selected to verify the osteogenetic effect of BGSSD. In this experiment, the solvent (Mock) and negative control (NC) of siRNA almost did not affect the viability of MC3T3-E1 cells (**Figure 5B**), and each of the genes Fn1, Col1a1, Col1a2, Col6a1, Col6a2, Col6a3, Rac1, Hsp90ab1, Hsp90b1, Ywhaz, PI3K, AKT, BAD, and Bcl-2 was effectively knocked down by siRNA (**Supplementary Material, Figures S5A, B**). However, when the above key proteins were knocked down, the pro-proliferation effect of BGSSD was suppressed, even showing an inhibiting effect (**Figures 5C–L**). Among them, the knockdown of Col6a3 and Ywhaz proteins had no significant effect on the

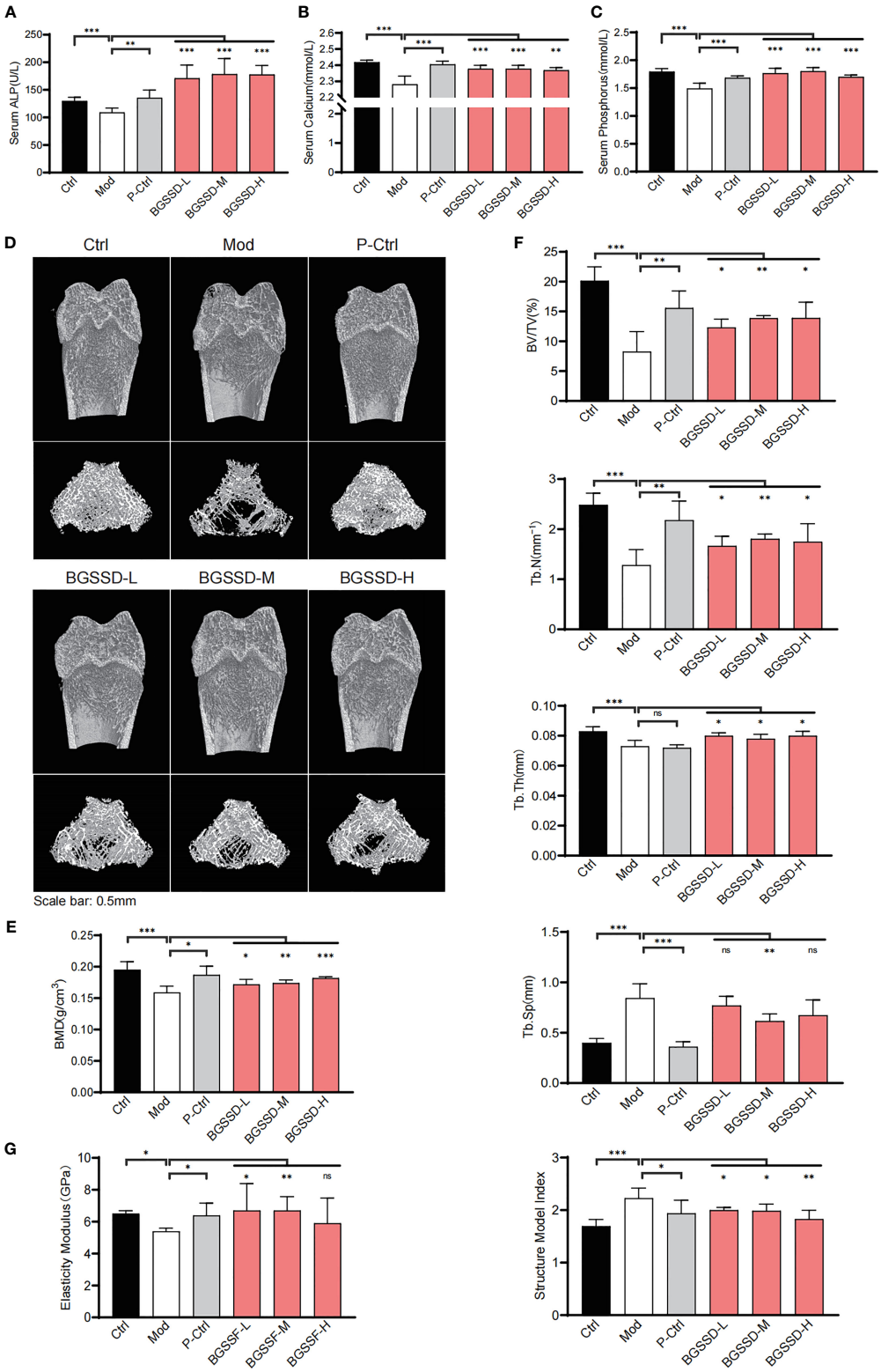

FIGURE 2 | The efficacy results of BGSSD in the treatment of osteoporotic rats. **(A–C)** The effects of different doses of BGSSD on serum Alp, calcium, and phosphorus. **(D)** Representative photomicrographs of distal femur sections by μ-CT. **(E)** Quantitative analysis of BMD (mg·ccm^{-1}) of femurs. **(F)** Quantitative analysis of the ratio of bone volume to tissue volume (BV/TV, %), trabecular number (Tb.N, mm^{-1}), trabecular thickness (Tb.Th, mm), trabecular separation (Tb.Sp, mm), and the structural model index (SMI) of the μ-CT-scanned distal femurs. **(G)** Quantitative analysis of the elastic modulus of femurs. The results are presented as the mean ± s. e.m., $^{*}p < 0.05$, $^{**}p < 0.01$, $^{***}p < 0.001$, n = 6 per group. NS, not statistically significant.

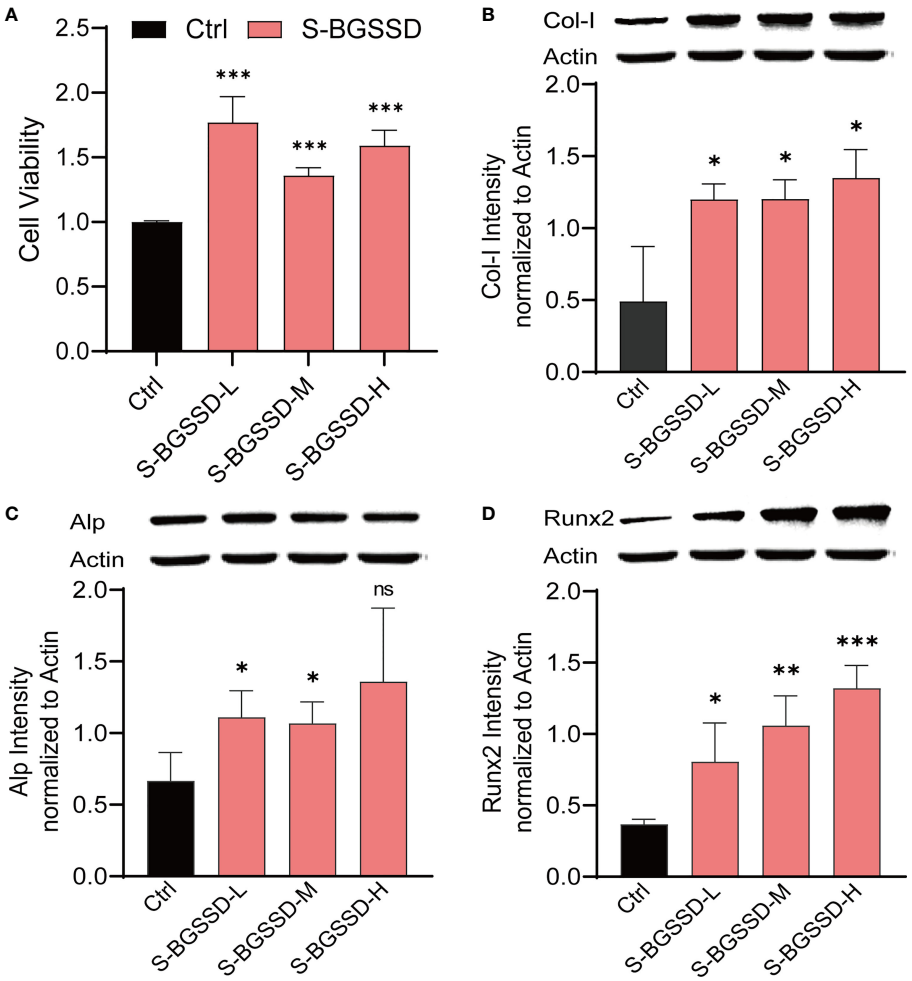

FIGURE 3 | The results of drug-containing serum of BGSSD intervening in the proliferation and differentiation of serum-deprivation-induced MC3T3-E1 cells. **(A)** MTS assay analysis of the viability of MC3T3-E1 cells dealt with the drug-containing serum of low, medium, and high doses of BGSSD (to eliminate the influence of rat serum on cells, all the Ctrl group was treated with the drug-free serum of rats). **(B)** Western blot and quantification (underneath the blots) of Col-I in MC3T3-E1. **(C)** Western blot and quantification (underneath the blots) of Alp in MC3T3-E1. **(D)** Western blot and quantificational analysis (underneath the blots) of Runx2 in MC3T3-E1. Asterisks denote the comparison to serum-starved cells treated with rats' blank serum (Ctrl). All intervening times of drug-containing serum of BGSSD were 48 h; β-actin served as the internal control in all Western blots. Data are presented as the mean ± s.e.m., $^{*}p < 0.05$, $^{**}p < 0.01$, $^{***}p < 0.001$, n = 3 per group. NS, not statistically significant.

proliferation-promoting effect of medium dose (**Figures 5H, L**). Otherwise, we further investigated the functions of other key proteins in PI3K-AKT and its downstream signaling pathway, such as PI3K, AKT, BAD, and Bcl-2, and ascertained that knockdown of the above 4 proteins also eliminated the pro-proliferation effect to a different extent of BGSSD (**Figures 5M–P**).

The outcomes indicate that the PI3K-AKT pathway is indispensable for the pro-proliferation effect of BGSSD.

DISCUSSION

Osteoporosis is a systemic bone metabolism disease with complex pathogenesis and serious clinical consequences (29). With the aggravation of population aging, the incidence of OP is on the rise. In recent years, extensive studies on the pathogenesis and treatment of OP have revealed that osteoporosis can be prevented by regulating bone metabolism (30–32). It is generally recognized that bone metabolism includes two important processes, which are bone formation mediated by osteoblasts and bone resorption mediated by osteoclasts (32). Previous studies mostly focused on bone resorption, and the clinical drugs approved by the FDA for the treatment of OP are mainly bone resorption inhibitors (2, 33, 34). Currently, only parathyroid hormone-like drugs are approved to promote bone formation, but long-term use of chemical drugs is accompanied by shortcomings of high cost and obvious side effects (2). Therefore, Chinese herbal medicines and compound formulas, used in treating OP for a long time, have received extensive attention and have good research value due to their precise curative effect and few side effects (8, 35).

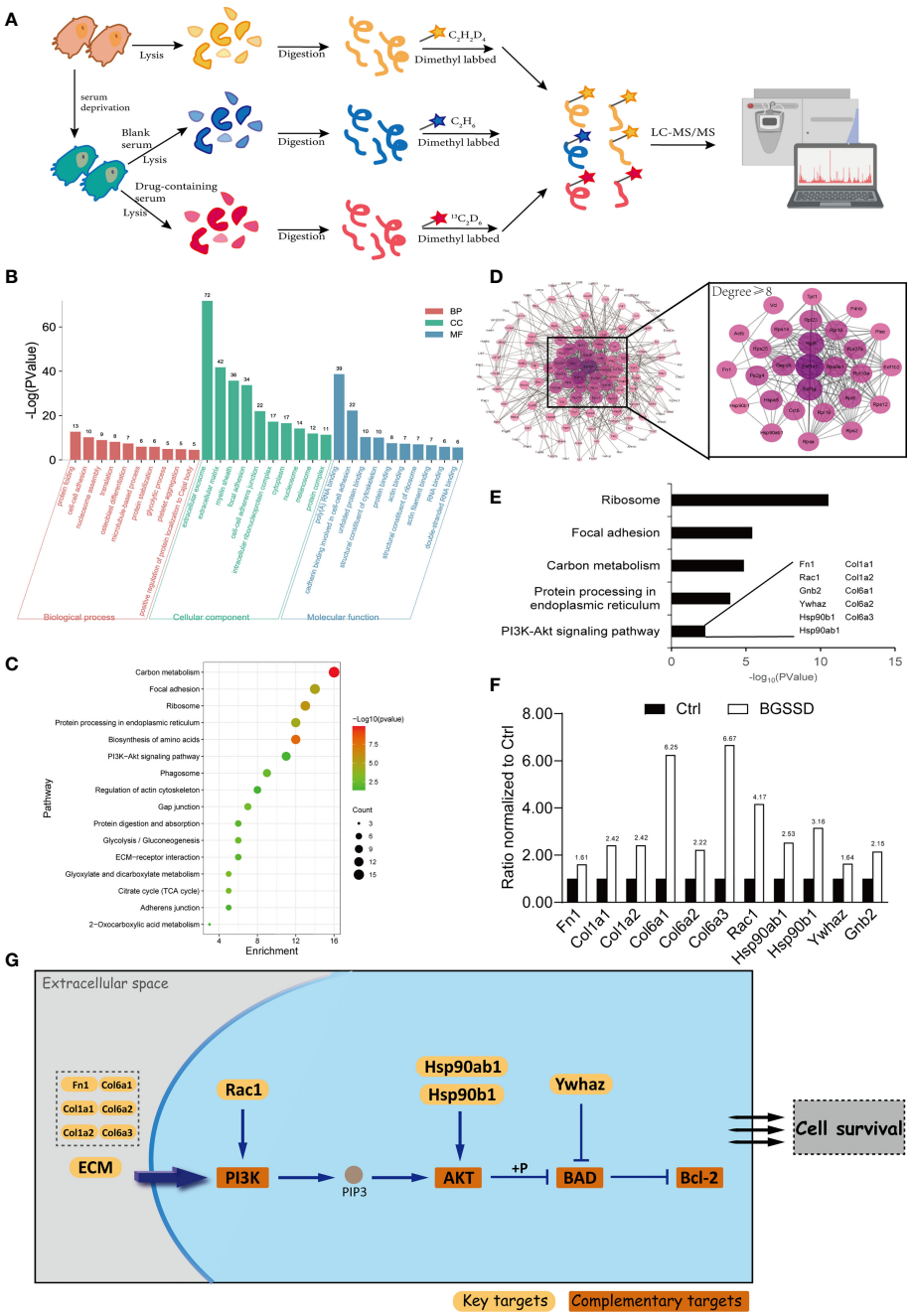

FIGURE 4 | Quantitative proteomics analysis for the pharmacodynamic network and mechanism of BGSSD. **(A)** Quantitative proteomics experimental scheme for detecting the differential expression of proteins. **(B)** Gene Ontology (GO) analysis of the upregulated targets of BGSSD, the top 10 biological processes (BP), cell component (CC), and molecular function (MF) is shown. **(C)** KEGG pathway analysis of the upregulated targets of BGSSD and the top 16 pathways is displayed. **(D)** Protein–protein interaction (PPI) networks of the upregulated targets. The proteins whose degrees are more than 8 were important and enlarged (the right part). **(E)** GO analysis of the important proteins identified by PPI revealed their association with the PI3K-AKT signaling pathway. The key proteins associated with the PI3K-AKT pathway were laid out. **(F)** The expression ratio of key proteins intervened by BGSSD compared to Ctrl. **(G)** The key proteins in the PI3K-AKT pathway.

BGSSD is an effective Chinese medical compound formula for treating OP. Preliminary studies have shown that its clinical efficacy rate is as high as 82%, and it can increase BMD, serum calcitonin, luteinizing hormone, and calcium content (10). Otherwise, Rhizoma Drynariae is the sovereign medicinal in BGSSD, which is a commonly used kidney-tonifying Chinese medicine for the treatment of OP. Among them, flavonoids have a good clinical effect on OP, which can

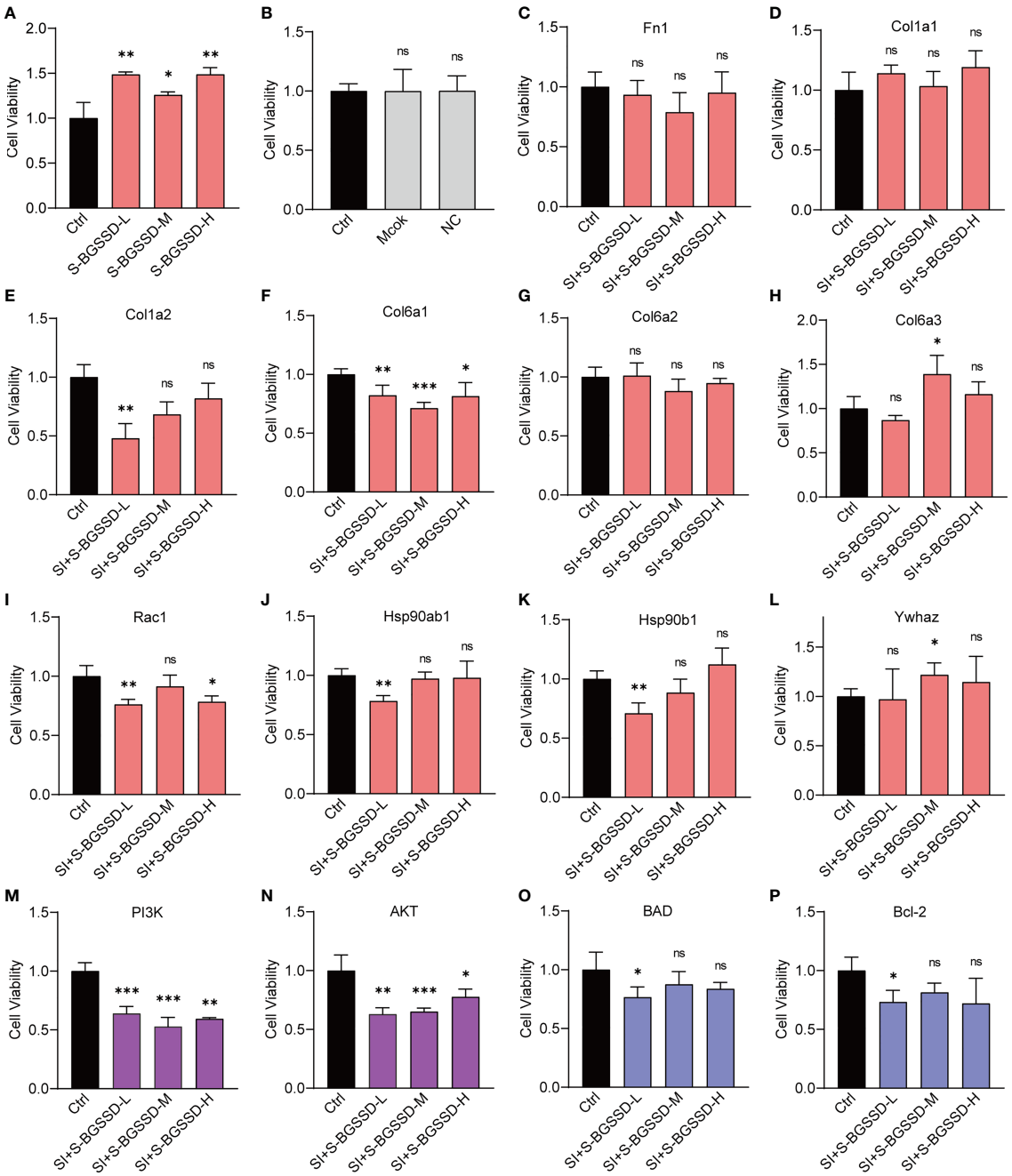

FIGURE 5 | RNA interference to verify the effects of targeting proteins of the PI3K-AKT pathway on the efficacy of BGSSD. **(A)** BGSSD could promote the proliferation of MC3T3-E1 cells. **(B)** The solvent (Mock) and negative control (NC) of siRNA almost had no effect on the viability of MC3T3-E1 cells. **(C–L)** Knockdown of each of the ten targeted proteins (Fn1, Col1a1, Col1a2, Col6a1, Col6a2, Col6a3, Rac1, Hsp90ab1, Hsp90b1, and Ywhaz, except the Col6a3 and Ywhaz in the S-BGSSD-M group) by siRNA abolished the proliferation-promoting effect to various extents of BGSSD in MC3T3-E1 cells. **(M–P)** Knockdown of the proteins of PI3K-AKT and its downstream pathway, named PI3K, AKT, BAD, and Bcl-2, revoked the pro-proliferation effect of BGSSD. The pink columns represent the outcomes of targets obtained by quantitative proteomics. The purple columns refer to the proteins in the PI3K-AKT signaling pathway. The blue are proteins in the downstream pathway. Asterisks denote the comparison to serum-starved cells treated with rats' blank serum (Ctrl). All intervening times were 48 h. All data are presented as the mean ± s.e.m., $^{*}p < 0.05$, $^{**}p < 0.01$, $^{***}p < 0.001$. NS, not statistically significant.

improve lumbar and femoral bone mass density, serum Alp, and other indicators.

Therefore, in order to illustrate the mechanism of BGSSD in treating OP, we designed experiments from multiple perspectives of "formula-herb-molecule." Firstly, we established a rat model of osteoporosis by removing the testicles and confirmed that BGSSD and Rhizoma Drynariae have similar therapeutic effects on OP, with no significant weight loss (**Supplementary Material, Figures S1A, S2A**). In terms of bone metabolism, Alp is an indicator of bone formation (36); calcium and phosphorus are the "raw materials" for bone formation (37, 38); and BGSSD could effectively increase serum Alp, calcium, and phosphorus concentrations, whereas Rhizoma Drynariae only increased the serum calcium and phosphorus contents distinctly, which indicated that BGSSD and Rhizoma Drynariae may regulate the bone formation process in summary. Furthermore, we found that BGSSD and Rhizoma Drynariae could increase BMD, bone volume to tissue volume (BV/TV), trabecular number (Tb.N), trabecular thickness (Tb.Th), and elastic modulus of femurs and reduce trabecular separation (Tb.Sp) and structural model index (SMI) (**Figures 2A–F**, **Supplementary Material, Figures S2B–G**). However, they have no significant effect on the bending strength and maximum load of the bone (**Supplementary Material, Figures S1B, C, S2H**).

After confirming the efficacy of BGSSD and Rhizoma Drynariae on the model rats, we further studied their effects on MC3T3-E1 cells. To begin, the serum pharmacological method was used to obtain the drug-containing serum with the effective ingredients of BGSSD and Rhizoma Drynariae. The serum-starved cell model was then intervened with drug-containing serum as a therapeutic agent. The results demonstrated that the active ingredients of BGSSD and Rhizoma Drynariae could promote the proliferation and differentiation of MC3T3-E1 cells (**Figure 3A**, **Supplementary Material, Figures S4A, B**).

Relevant studies have also provided some evidence that BGSSD and Rhizoma Drynariae can effectively improve the clinical symptoms related to OP (10, 39, 40). In addition, studies have shown that Rhizoma Drynariae can prevent OP by intervening in oxidative stress response and amino acid metabolism (41). Among them, naringin and naringenin have a two-way regulation of estrogen, which can promote the proliferation of osteoblasts and effectively prevent OP (42). These studies support our experimental results from the side.

Based on previous studies and the abovementioned experimental results, we speculate that BGSSD and the sovereign medicinal Rhizoma Drynariae may play an anti-osteoporotic effect by promoting bone formation. To further prove the speculation, quantitative proteomics strategy and bioinformatics methods were used to analyze the potential drug targets of BGSSD and Rhizoma Drynariae. The results indicated that BGSSD may exert anti-osteoporosis effects through upregulating the pathways of the ribosome, focal adhesion, protein processing in endoplasmic reticulum, carbon metabolism, PI3K-AKT, and so on, and the anti-osteoporosis mechanism of Rhizoma Drynariae may be related to the promotion of functions of ribosome, endoplasmic reticulum, and cell adhesion to a certain extent.

Furthermore, we conducted RNA interference experiments on the important proteins enriched in the PI3K-AKT signaling pathway. Under normal situations, BGSSD can promote the proliferation of MC3T3-E1 cells (**Figure 3A**). When proteins, such as Fn1, Col1a1, Col1a2, Col6a1, Col6a2, Col6a3, Rac1, Hsp90ab1, Hsp90b1, Ywhaz, PI3K, AKT, BAD, and Bcl-2, were knocked down, the effect of BGSSD in promoting the proliferation of MC3T3-E1 cells was suppressed, even showing an opposite effect (**Figures 5C–P**). This evidence indicates that the PI3K-AKT pathway is essential for the anti-osteoporosis of BGSSD, and its key proteins are critical targets for BGSSD to exert anti-osteoporosis effects.

CONCLUSION

In this study, we conducted a castrated rat model to evaluate the anti-osteoporotic effects of a traditional Chinese formula, Bugu Shengsui Decoction, which has been proven effective clinically. It is consistent with clinical manifestations that BGSSD presents significant effects in serum markers of bone metabolism, bone mineral density, and tissue morphology. Moreover, these results were derived from that BGSSD can promote the proliferation and differentiation of osteoblastic progenitor cells (MC3T3-E1 cell line). Furthermore, quantitative proteomics with stable isotope dimethyl labeling was employed to unveil the pharmacodynamic network and mechanism of BGSSD. Actually, the PI3K-AKT pathway had been proved to be crucial for the efficacy, of which key proteins' effects had been verified by RNAi experiments. With the combination of systemic-level, cellular-level, and molecular-level experiments, we could confirm the curative effect, cell phenotype, and molecular mechanism of BGSSD. This work may enlighten a new perspective for exploring the material basis of BGSSD and treatment strategy for osteoporosis *via* the PI3K-AKT pathway.

DATA AVAILABILITY STATEMENT

The original contributions presented in the study are publicly available. These data can be found here: PRIDE (PRoteomics IDEntifications Database), PXD030275.

ETHICS STATEMENT

The animal study was reviewed and approved by the Animal Ethics Committee, School of Pharmacy, Lanzhou University.

AUTHOR CONTRIBUTIONS

XW, YX, JD, and LZ designed and developed the experiments. XW and BQ prepared the draft of the manuscript. BQ, RM, YLZ, NL, SF, and YZ participated in all the experiments. XW, YX, JD,

and LZ provided the conditions of experiments. XW, BQ, and RM analyzed the data and drafted the manuscript. YX, JD, and LZ supervised all research and revised the manuscript. All authors contributed to the article and approved the submitted version.

FUNDING

This work was supported by the National Natural Science Foundation of China (NSFC) Youth Program (81704102), the Fundamental Research Funds for the Central Public Welfare Research Institutes (ZZ15-XY-CT-06, ZZ13-YQ-039), the Inheritance and Innovation Team Project of National Traditional Chinese Medicine (ZYYCXTD-C-202003), National Key Research and Development Program of China (2018YFC17063005), the Science and Technology Planning Project of Gansu Province (20JR10RA586), the Fundamental Research Funds for the Central Universities (lzujbky-2021-kb40), and the Project for Longyuan Youth Innovation and Entrepreneurship Talent.

SUPPLEMENTARY MATERIAL

The Supplementary Material for this article can be found online at: https://www.frontiersin.org/articles/10.3389/fendo.2021.833474/full#supplementary-material

REFERENCES

1. Lane N. Epidemiology, Etiology, and Diagnosis of Osteoporosis. *Am J Obstetrics Gynecol* (2006) 194:S3–11. doi: 10.1016/j.ajog.2005.08.047
2. Compston J, McClung M, Leslie W. Osteoporosis. *Lancet* (2019) 393 (10169):364–76. doi: 10.1016/s0140-6736(18)32112-3
3. Mediero A, Cronstein B. Adenosine and Bone Metabolism. *Trends Endocrinol Metab* (2013) 24(6):290–300. doi: 10.1016/j.tem.2013.02.001
4. Komm B, Morgenstern D A, Yamamoto L, Jenkins S. The Safety and Tolerability Profile of Therapies for the Prevention and Treatment of Osteoporosis in Postmenopausal Women. *Expert Rev Clin Pharmacol* (2015) 8(6):769–84. doi: 10.1586/17512433.2015.1099432
5. Canalis E, Deregowski V, Pereira R, Gazzerro E. Signals That Determine the Fate of Osteoblastic Cells. *J Endocrinol Invest* (2005) 28:3–7.
6. Rachner T, Khosla S, Hofbauer L. Osteoporosis: Now and the Future. *Lancet* (2011) 377(9773):1276–87. doi: 10.1016/s0140-6736(10)62349-5
7. Li J, Sun K, Qi B, Feng G, Wang W, Sun Q, et al. An Evaluation of the Effects and Safety of Zuogui Pill for Treating Osteoporosis: Current Evidence for an Ancient Chinese Herbal Formula. *Phytother Res* (2021) 35(4):1754–67. doi: 10.1002/ptr.6908
8. Liu Y, Liu J, Xia Y. Chinese Herbal Medicines for Treating Osteoporosis. *Cochrane Database Syst Rev* (2014) 3:CD005467. doi: 10.1002/14651858.CD005467.pub2
9. Zhang N, Han T, Huang B, Rahman K, Jiang Y, Xu H, et al. Traditional Chinese Medicine Formulas for the Treatment of Osteoporosis: Implication for Antiosteoporotic Drug Discovery. *J Ethnopharmacol* (2016) 189:61–80. doi: 10.1016/j.jep.2016.05.025
10. Xie Y, Zhang F, Zhou W. Clinical Study of Bugu Shengsui Capsule in Treating Primary Osteoporosis With Kidney-Yang Deficiency Syndrome. *Chin J Integr traditional West Med* (1997) 17(9):526–30.
11. Liu J, Xu X, Ji Y, Zhang F, Xie Y. Bugu Shengsui Capsule' Activating Blood Circulation and Removing Blood Stasis and its Influence on Experimental Microcirculation Disorders. *J Integr Traditional Chin West Med* (1997) 4(S1):255–7.
12. Sun K, Wei X, Xie Y, Zhang P, Wang Y, Zhang Y, et al. Effect of Bu Gu Shengsui Decoction on Smad/ERK Signal Pathway in Ovariectomized Rats With Osteoporosis. *Chin J Osteoporosis* (2019) 25(11):1556–61. doi: 10.3969/j.issn.1006-7108.2019.11.010
13. Liu J, Xie Y, Xu Z, Zhao J, Deng W. Effect of Assemble Flavone of Rhizome Drynaria on Experimental Osteoporosis and Microcirculation. *Chin J Osteoporosis* (2006) 4(01):46–9+24.
14. Xie Y, Ju D, Zhao J. Effect of Osteoporotic Total Flacone on Bone Mineral Density and Bone Histomorphometry in Ovariectomized Rats. *China J Chin Mater Med* (2004) 4(04):59–62.
15. Liu J, Xie Y, Zhao J, Deng W, Xu Z. Effects of Capsule Assemble Flavones of Fortune's Drynaria Rhizome on the Experimental Osteoporosis in Rat and Analgesia Action in Mouse. *Chin J Exp Traditional Med Formulae* (2004) 4 (05):31–4. doi: 10.13422/j.cnki.syfjx.2004.05.014
16. Xie Y, Zhang L, Wang Z, Tu R, Zhao J. Study the Effects of Flavonoids of Rhizoma Drynariae on Gene Level of Rats Without Ovaries by Technology of cDNA Array. *China J Chin Mater Med* (2005) 4(14):1092–5.
17. Iwama H, Amagaya S, Ogihara Y. Effect of Shosaikoto, a Japanese and Chinese Traditional Herbal Medicinal Mixture, on the Mitogenic Activity of Lipopolysaccharide: A New Pharmacological Testing Method. *J Ethnopharmacol* (1987) 21(1):45–53. doi: 10.1016/0378-8741(87)90093-6
18. Lau H, Suh H, Golkowski M, Ong S. Comparing SILAC- and Stable Isotope Dimethyl-Labeling Approaches for Quantitative Proteomics. *J Proteome Res* (2014) 13(9):4164–74. doi: 10.1021/pr500630a
19. Wu X, Han X, Li L, Fan S, Zhuang P, Yang Z, et al. iTRAQ-Based Quantitative Proteomics and Target-Fishing Strategies Reveal Molecular Signatures on Vasodilation of Compound Danshen Dripping Pills. *Chem-Biol Interact* (2020) 316:108923. doi: 10.1016/j.cbi.2019.108923
20. Wang J, Gao L, Lee Y, Kalesh K, Ong Y, Lim J, et al. Target Identification of Natural and Traditional Medicines With Quantitative Chemical Proteomics Approaches. *Pharmacol Ther* (2016) 162:10–22. doi: 10.1016/j.pharmthera.2016.01.010
21. Shao S, Cui Y, Chen Z, Zhang B, Huang S, Liu X. Androgen Deficit Changes the Response to Antidepressant Drugs in Tail Suspension Test in Mice. *Aging Male* (2020) 23(5):1259–65. doi: 10.1080/13685538.2020.1762074
22. Boersema P, Raijmakers R, Lemeer S, Mohammed S, Heck A. Multiplex Peptide Stable Isotope Dimethyl Labeling for Quantitative Proteomics. *Nat Protoc* (2009) 4(4):484–94. doi: 10.1038/nprot.2009.21
23. Luo C, Yang Q, Liu Y, Zhou S, Jiang J, Reiter R, et al. The Multiple Protective Roles and Molecular Mechanisms of Melatonin and its Precursor N-Acetylserotonin in Targeting Brain Injury and Liver Damage and in Maintaining Bone Health. *Free Radical Biol Med* (2019) 130:215–33. doi: 10.1016/j.freeradbiomed.2018.10.402
24. Chen Y, Zhou F, Liu H, Li J, Che H, Shen J, et al. SIRT1, a Promising Regulator of Bone Homeostasis. *Life Sci* (2021) 269:119041. doi: 10.1016/j.lfs.2021.119041
25. Marie P. Signaling Pathways Affecting Skeletal Health. *Curr Osteoporosis Rep* (2012) 10(3):190–8. doi: 10.1007/s11914-012-0109-0
26. Cheng Y, Dong J, Bian Q. Small Molecules for Mesenchymal Stem Cell Fate Determination. *World J Stem Cells* (2019) 11(12):1084–103. doi: 10.4252/wjsc.v11.i12.1084
27. Wang T, Zhang X, Bikle D. Osteogenic Differentiation of Periosteal Cells During Fracture Healing. *J Cell Physiol* (2017) 232(5):913–21. doi: 10.1002/jcp.25641
28. Iyer S, Margulies B, Kerr W. Role of SHIP1 in Bone Biology. *Ann New York Acad Sci* (2013) 1280:11–4. doi: 10.1111/nyas.12091
29. Lane J, Russell L, Khan S. Osteoporosis. *Clin Orthopaedics Relat Res* (2000) 372):139–50. doi: 10.1097/00003086-200003000-00016
30. Miller P. Management of Severe Osteoporosis. *Expert Opin pharmacother* (2016) 17(4):473–88. doi: 10.1517/14656566.2016.1124856
31. Khosla S, Hofbauer L. Osteoporosis Treatment: Recent Developments and Ongoing Challenges. *Lancet Diabetes Endocrinol* (2017) 5(11):898–907. doi: 10.1016/s2213-8587(17)30188-2
32. Hadjidakis D, Androulakis I. Bone Remodeling. *Ann New York Acad Sci* (2006) 1092:385–96. doi: 10.1196/annals.1365.035
33. Langdahl B. Treatment of Postmenopausal Osteoporosis With Bone-Forming and Antiresorptive Treatments: Combined and Sequential Approaches. *Bone* (2020) 139:115516. doi: 10.1016/j.bone.2020.115516

34. Banu J, Varela E, Fernandes G. Alternative Therapies for the Prevention and Treatment of Osteoporosis. *Nutr Rev* (2012) 70(1):22–40. doi: 10.1111/j.1753-4887.2011.00451.x
35. Li C, Li Q, Liu R, Niu Y, Pan Y, Zhai Y, et al. Medicinal Herbs in the Prevention and Treatment of Osteoporosis. *Am J Chin Med* (2014) 42(1):1–22. doi: 10.1142/s0192415x14500013
36. Li T, Jiang S, Lu C, Yang W, Yang Z, Hu W, et al. Melatonin: Another Avenue for Treating Osteoporosis? *J Pineal Res* (2019) 66(2):e12548. doi: 10.1111/jpi.12548
37. Black D, Rosen C. Clinical Practice. Postmenopausal Osteoporosis. *N Engl J Med* (2016) 374(3):254–62. doi: 10.1056/NEJMcp1513724
38. Ensrud K, Crandall C. Osteoporosis. *Ann Internal Med* (2017) 167(3):ITC17–32. doi: 10.7326/aitc201708010
39. Liao H, Yeh C, Lin C, Chen B, Yeh M, Chang K, et al. Prescription Patterns of Chinese Herbal Products for Patients With Fractures in Taiwan: A Nationwide Population-Based Study. *J Ethnopharmacol* (2015) 173:11–9. doi: 10.1016/j.jep.2015.07.014
40. Wei X, Xu A, Shen H, Xie Y. Qianggu Capsule for the Treatment of Primary Osteoporosis: Evidence From a Chinese Patent Medicine. *BMC Complementary Altern Med* (2017) 17(1):108. doi: 10.1186/s12906-017-1617-3
41. Liu X, Zhang S, Lu X, Zheng S, Li F, Xiong Z. Metabonomic Study on the Anti-Osteoporosis Effect of Rhizoma Drynariae and its Action Mechanism Using Ultra-Performance Liquid Chromatography-Tandem Mass Spectrometry. *J Ethnopharmacol* (2012) 139(1):311–7. doi: 10.1016/j.jep.2011.11.017
42. Guo D, Wang J, Wang X, Luo H, Zhang H, Cao D, et al. Double Directional Adjusting Estrogenic Effect of Naringin From Rhizoma Drynariae (Gusuibu). *J Ethnopharmacol* (2011) 138(2):451–7. doi: 10.1016/j.jep.2011.09.034

Conflict of Interest: The authors declare that the research was conducted in the absence of any commercial or financial relationships that could be construed as a potential conflict of interest.

frontiers in Endocrinology

ORIGINAL RESEARCH
published: 28 January 2022
doi: 10.3389/fendo.2021.841668

Integration of Network Pharmacology and Experimental Validation to Explore the Pharmacological Mechanisms of Zhuanggu Busui Formula Against Osteoporosis

Huihao Zhang[1†], Chengcong Zhou[1†], Zhiguo Zhang[1†], Sai Yao[1], Yishan Bian[1], Fangda Fu[1], Huan Luo[2], Yan Li[1], Shuxin Yan[1], Yuying Ge[1], Yuying Chen[3], Kunyu Zhan[4], Ming Yue[5], Weibin Du[1,6], Kun Tian[7], Hongting Jin[1], Xiaofeng Li[8], Peijian Tong[1]*, Hongfeng Ruan[1]* and Chengliang Wu[1]*

[1] Institute of Orthopaedics and Traumatology, The First Affiliated Hospital of Zhejiang Chinese Medical University, Hangzhou, China, [2] Department of Pharmacy, The Second Affiliated Hospital, School of Medicine, Zhejiang University, Hangzhou, China, [3] The Fourth Clinical Medical College, Zhejiang Chinese Medical University, Hangzhou, China, [4] The Second Clinical Medical College, Zhejiang Chinese Medical University, Hangzhou, China, [5] Department of Physiology, College of Basic Medical Sciences, Zhejiang Chinese Medical University, Hangzhou, China, [6] Research Institute of Orthopedics, The Affiliated Jiang Nan Hospital of Zhejiang Chinese Medical University, Hangzhou, China, [7] Department of Orthopedics, The First Affiliated Hospital of Zhejiang Chinese Medical University, Hangzhou, China, [8] Department of Orthopedics and Traumatology, Shanghai Municipal Hospital of Traditional Chinese Medicine, Shanghai University of Traditional Chinese Medicine, Shanghai, China

Osteoporosis (OP) is a common skeletal disease, characterized by decreased bone formation and increased bone resorption. As a novel Chinese medicine formula, Zhuanggu Busui formula (ZGBSF) has been proved to be an effective prescription for treating OP in clinic, however, the pharmacological mechanisms underlying the beneficial effects remain obscure. In this study, we explored the pharmacological mechanisms of ZGBSF against OP *via* network pharmacology analysis coupled with *in vivo* experimental validation. The results of the network pharmacology analysis showed that a total of 86 active ingredients and 164 targets of ZGBSF associated with OP were retrieved from the corresponding databases, forming an ingredient-target-disease network. The protein-protein interaction (PPI) network manifested that 22 core targets, including Caspase-3, BCL2L1, TP53, Akt1, *etc*, were hub targets. Moreover, functional enrichment analyses revealed that PI3K-Akt and apoptosis signalings were significantly enriched by multiple targets and served as the targets for *in vivo* experimental study validation. The results of animal experiments revealed that ZGBSF not only reversed the high expression of Caspase-3, Bax, Prap, and low expression of Bcl-2 in osteoblasts of the OP mouse model but also contributed to the phosphorylation of Akt1 and expression of PI3K, thereby promoting osteogenesis and ameliorating the progression of OP. In conclusion, this study systematically and intuitively illustrated that the possible pharmacological

OPEN ACCESS

Edited by:
Jun Liu,
Guangdong Provincial Academy of Chinese Medical Sciences, China

Reviewed by:
Xing Ji,
Children's Hospital of Philadelphia, United States
Yan Wu,
Zhejiang Provincial Key Laboratory of Diagnosis and Treatment of Sports System Diseases, China
Yong Ma,
Nanjing University of Chinese Medicine, China

***Correspondence:**
Hongfeng Ruan
rhf@zcmu.edu.cn
Peijian Tong
peijiantongzjtcm@163.com
Xiaofeng Li
lixiaofeng0409@163.com

[†]These authors have contributed equally to this work

Specialty section:
This article was submitted to Bone Research, a section of the journal Frontiers in Endocrinology

Received: 22 December 2021
Accepted: 30 December 2021
Published: 28 January 2022

Citation:
Zhang H, Zhou C, Zhang Z, Yao S, Bian Y, Fu F, Luo H, Li Y, Yan S, Ge Y, Chen Y, Zhan K, Yue M, Du W, Tian K, Jin H, Li X, Tong P, Ruan H and Wu C (2022) Integration of Network Pharmacology and Experimental Validation to Explore the Pharmacological Mechanisms of Zhuanggu Busui Formula Against Osteoporosis. Front. Endocrinol. 12:841668. doi: 10.3389/fendo.2021.841668

mechanisms of ZGBSF against OP through multiple ingredients, targets, and signalings, and especially the inhibition of the apoptosis and the activation of PI3K-Akt signaling.

Keywords: osteoporosis, Zhuanggu Busui formula, network pharmacology, pharmacological mechanisms, apoptosis, PI3K-Akt signalling

INTRODUCTION

Osteoporosis (OP), a common metabolic bone disease, is featured with decreased bone density and increased brittleness of bone, resulting in an increased risk of fracture (1, 2). It's estimated that approximately 200 million people worldwide are suffering from OP (10.4% for males, 31.2% for females) and the number is climbing, representing a major worldwide public health problem (3, 4). The homeostasis of bone mass during bone metabolism is dynamically regulated by the osteoblast-mediated bone formation and osteoclast-mediated bone resorption (5, 6), and OP is a pathological state in which bone resorption is greater than bone formation (7, 8). Current strategies for OP fall into two categories, including anti-resorptive drugs and osteogenic drugs (9). Although these drugs are available, some are limited by side effects, such as dizziness, heart palpitations, and nausea (10). Thus, it is of importance to find new alternative therapies for OP (11).

Traditional Chinese medicine (TCM) herb formulae have their advantages and characteristics in fewer side-effects and early intervention (12, 13). "Kidney dominating bone, generating marrow" is the theoretical basis of TCM in the treatment of OP, and the deficiency of kidney function leads to OP (14). Zhuanggu Busui formula (ZGBSF) is a novel TCM formula composed of *Epimedium* (Yin Yang Huo), *Dipsaci Radix* (Xu Duan), *Paeoniae Radix Alba* (Bai Shao), *Chuanxiong Rhizoma* (Chuan Xiong), *Hedysarum Multijugum Maxim.* (Huang Qi), *Rehmanniae Radix Praeparata* (Shu Di Huang), *Eucommiae Cortex* (Du Zhong), *Achyranthis Bidentatae Radix* (Niu Xi), *Carthami Flos* (Hong Hua), *Angelicae Sinensis Radix* (Dang Gui), which is used for tonifying kidney and strengthening bone. Clinical practice has confirmed that ZGBSF is an effective prescription for treating OP. Recent system pharmacology works have shown that *Eucommiae Cortex, Dipsaci Radix and Epimedium*, several main components in ZGBSF, could promote osteogenic differentiation and ameliorate bone loss due to their anti-inflammatory and antioxidant properties (15–17). However, the underlying integrated pharmacological mechanisms of ZGBSF on OP remain largely elusive.

Because of multiple components and targets of TCM formulae, it is a challenge to explore their pharmacological mechanisms using conventional pharmacological methods (18, 19). With the rapid development of computer technology and system biology theory, network pharmacology, an emerging interdisciplinary subject, has great advantages to decipher the pharmacologic mechanisms of TCM with multi-components, multi-targets, and multi-pathways. A study reported that 16 compounds and 28 targets in Luohua Zizhu granule associated with colorectal adenoma were screened by network pharmacology, which revealed the mechanism of Luohua Zizhu granule against colorectal adenoma (20). Our previous study in the mouse model showed that apoptosis screened by network pharmacology had been validated to be the key signaling pathway of Liuwei Dihuang Decoction against intervertebral disc degeneration (21). Therefore, all evidence illustrated that network pharmacology analysis may be a good way to explore pharmacological mechanisms of ZGBSF in the treatment of OP.

In this study, the active compounds of ZGBSF were firstly obtained according to the screening criteria (oral bioavailability (OB) ≥ 30% and drug-likeness (DL) ≥ 0.18) (22), and the core targets of ZGBSF associated with OP were screened by the PPI network. Next, the GO and KEGG functional enrichment analyses were utilized to screen the core signaling pathways of ZGBSF against OP. Finally, the core target proteins related to the predicted pathway were further verified in OVX mice treated with ZGBSF. A flowchart of this research was shown in **Figure 1**.

MATERIALS AND METHODS

Screening for Active Compounds of ZGBSF and Target Prediction

The active compounds of ZGBSF were retrieved from the Traditional Chinese Medicine Systems Pharmacology (TCMSP) Database and Analysis Platform (http://tcmspw.com/tcmsp.php) (23) by using 'Yin Yang Huo', 'Xu Duan', 'Bai Shao', 'Chuan Xiong', 'Huang Qi', 'Shu Di Huang', 'Du Zhong', 'Niu Xi', 'Hong Hua' and 'Dang Gui' as keywords to screen targets correlated with ZGBSF. All target names were standardized through the UniProt database (https://sparql.uniprot.org/) (24).

Screening of Potential Targets for OP

The potential targets related to OP were screened from DrugBank (https://go.drugbank.com/) (25), Genecards (https://www.genecards.org/) (26), Therapeutic Target Database (TTD, http://bidd.nus.edu.sg/group/ttd/ttd.asp) (27), PharmGkb (https://www.pharmgkb.org/) (28) and Online Mendelian Inheritance in Man (OMIM, https://www.genecards.org/) (29). After elimination of repetitive targets, the potential targets correlated with OP were obtained.

Drug-Target-Disease Network Construction

A drug-target-disease interaction network was constructed by inputting active compounds in ZGBSF and common targets of these active compounds and OP into Cytoscape 3.8 software. The degree was used to evaluate the importance of compounds and targets, which represented the total number of routes associated

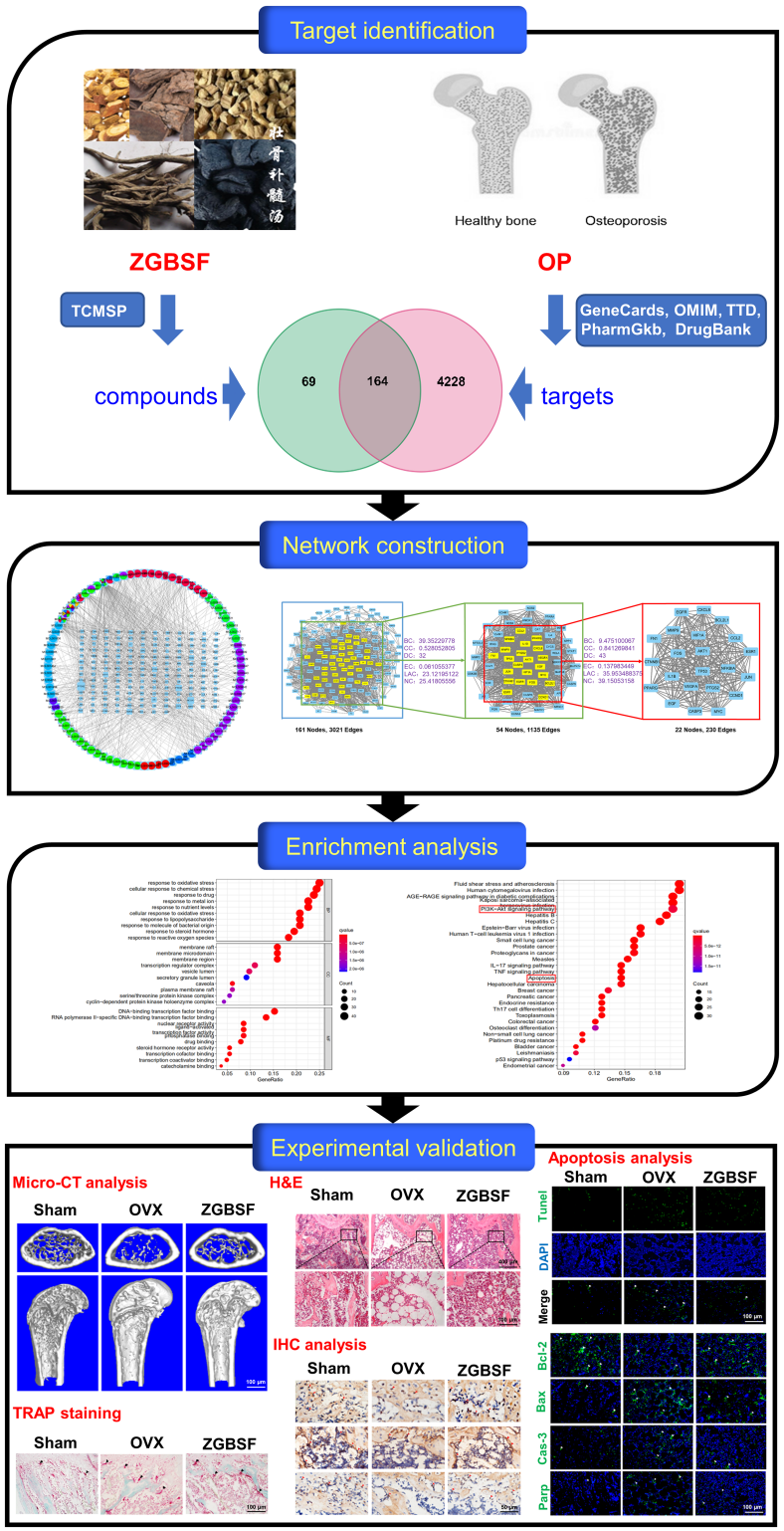

FIGURE 1 | A flowchart for explaining the mechanism of ZGBSF against OP through targets identification, network construction, enrichment analysis, and experimental validation.

with the node and other nodes. And the higher the degree, the more important it was (30).

Protein-Protein Interaction Network

To clarify the functional interactions among the screened potential proteins, they were all imported to the String database (https://string-db.org/) to construct Protein-Protein Interaction (PPI) network (31). Then the PPI network was inputted into Cytoscape 3.8 software, and key proteins were identified by CytoNCA software according to betweenness centrality (BC), closeness centrality (CC), degree centrality (DC), Eigenvector centrality (EC), local average connectivity-based method (LAC), and network centrality (NC), which were greater than or equal to the median value (32).

Functional Enrichment Analyses

The GO and KEGG functional enrichment analyses were performed through R software to obtain the core biological processes and signaling pathways. The top 10 items of GO analysis and 30 items of KEGG analysis were mapped as bubble plots. Finally, R software was utilized to generate the key signaling pathways related to OP (33).

Chemicals and Reagents

Primary antibodies against total (t)-Akt1, Bcl-2, Bax, Parp were purchased from Ruiying Biological Co. (Jiangsu, China). Primary antibodies against Caspase-3, p-Akt1(S473), PI3K were obtained from Hua'an Biological Co. (Hangzhou, China). Primary antibodies against alkaline phosphatase (Alp), Osterix (Osx) were from CUSABIO Biological Co. (Wuhan, China). And primary antibody against Runx2 was supplied by Abcam Company Ltd. (Cambridge, MA, USA). Alexa Fluor® 488 rabbit anti-goat IgG (H+L) secondary antibody (green) was obtained from Zhongshan Jinqiao Biotech Co. (Beijing, China). TUNEL Bright Green Apoptosis Detection Kit was supplied by Vazyme Biotech Co. (Nanjing, China). The remaining chemicals were from Sigma-Aldrich (St. Louis, Mo, USA) unless otherwise stated.

Preparation of ZGBSF

Ten raw herbs of ZGBSF were provided from the pharmacy department of the first affiliated hospital of Zhejiang Chinese Medical University (Hangzhou, China). A voucher of the specimen was stored at the first affiliated hospital of Zhejiang Chinese Medical University (**Table 1**). *Epimedium, Dipsaci Radix, Paeoniae Radix Alba, Chuanxiong Rhizoma, Hedysarum Multijugum Maxim., Rehmanniae Radix Praeparata, Eucommiae Cortex, Achyranthis Bidentatae Radix, Carthami Flos, Angelicae Sinensis Radix* were mixed as a proportion of 2:1.5:1.5:1:1.5:2:1.5:1.5:1:1.5 (w/w), and then soaked in 12 volumes of distilled water (v/m) for 1 h, decocted for 2 times, and 1.5 h each time. Finally, the water-based decoction was concentrated to 1 g/mL and stored at -20°C prior to use.

Animals and Experimental Grouping

Twenty-four C57BL/6J female mice (8-week-old, 20 ± 1 g) were provided by the animal center of Zhejiang Chinese Medical University (Hangzhou, China) and housed at the Animal Care Facility of Zhejiang Chinese Medical University according to the institutional guidelines for laboratory animals. All proposals concerning animals were approved by the Ethics Committee of Zhejiang Chinese Medical University (20211220–02), and all laboratory procedures were performed following the Regulations for the Administration of Affairs Concerning Experimental Animals approved by the State Council of the People's Republic of China.

OVX Modeling and Treatments

All mice were randomly divided into 3 groups: Sham group, Ovariectomy (OVX) group, ZGBSF group (n = 8 in each group). After anesthesia with 1.5% isoflurane (R510-22-16, RWD Life Science, Shenzhen, China) in 100% oxygen flowing at 1.0 L/min, two ovaries of OVX and ZGBSF mice were removed, while the ovaries of Sham mice were preserved, and only part of the fat tissue around the ovaries was removed. Two days after OVX surgery, mice in the ZGBSF group were orally administered with ZGBSF (0.2 mL/10 g body weight), once a day for 8 consecutive weeks. Mice in the other two groups were given the same dosage of normal saline. All mice were euthanized 8 weeks after intragastric administration, and the femurs were collected for further analysis.

Micro-CT Analysis

After fixation with paraformaldehyde, the femurs were scanned using micro-CT (μCT) equipment (Skyscan 1176, Bruker μCT N.V., Kontich, Belgium) at a voltage of 50 kV with a current of

TABLE 1 | Detailed information of Zhuanggu Busui formula (ZGBSF).

Chinese Name	Latin Name	Parts Used	Place of Origin	Voucher Specimen NO.
Yin Yang Huo	*Epimedium*	Stem Leaf	Shanxi, China	161100
Xu Duan	*Dipsaci Radix*	Root	Jiangxi, China	161101
Bai Shao	*Paeoniae Radix Alba*	Root	Guangxi, China	161102
Chuan Xiong	*Chuanxiong Rhizoma*	Root Stem	Sichuan, China	161103
Huang Qi	*Hedysarum Multijugum Maxim.*	Root	Shanxi, China	161104
Shu Di Huang	*Rehmanniae Radix Praeparata*	Root	Henan, China	161105
Du Zhong	*Eucommiae Cortex*	Bark	Guangxi, China	161106
Niu Xi	*Achyranthis Bidentatae Radix*	Root	Anhui, China	161107
Hong Hua	*Carthami Flos*	Flower	Henan, China	161108
Dang Gui	*Angelicae Sinensis Radix*	Root	Gansu, China	161109

500 μA and a resolution of 9 μm per pixel. The NRecon v1.6 and CTAn v1.15 software were utilized to reconstruct the three-dimensional (3D) structure of the distal femoral metaphysis as we previously described (34).

Histological, Immunohistochemistry, and Immunofluorescence Analyses

After μCT analysis, the femurs were decalcified with 14% EDTA (pH 7.4) for 3 weeks, then dehydrated, embedded in paraffin, and processed into 5-μm-thick coronal-oriented sections. Then sections were stained with hematoxylin-eosin (H&E) and tartrate-resistant acid phosphatase (TRAP) as we previously described (35, 36). For immunohistochemistry (IHC) or immunofluorescence (IF) analysis, sections were incubated with primary antibodies of Runx2 (diluted 1:300), Alp (diluted 1:200), Osx (diluted 1:300), t-Akt1 (diluted 1:300), p-Akt1(S473) (diluted 1:50), PI3K (diluted 1:50), Bcl-2 (diluted 1:300), Bax (diluted 1:300), Caspase-3 (diluted 1:300), Parp (diluted 1:300) at 4°C overnight. Secondary biotinylated goat anti-rabbit antibody (diluted 1:1000) (Invitrogen) was added for 30 min the following day, and a diaminobenzidine solution (Invitrogen) was used to detect IHC staining. For IF analysis, secondary goat anti-rabbit antibody conjugated with fluorescence (diluted 1:1000) was added for 30 min the next day. The quantification of positive cells was estimated in a blinded manner with Image-Pro Plus 6.0 (Media Cybernetics, Silver Spring, MD, USA).

TUNEL Assay

To further evaluate apoptosis of osteoblasts in femoral tissues, the DNA damage, another hallmark of aopotosis, was determined by the TUNEL Bright Green Apoptosis Detection Kit (Vazyme Biotech, Nanjing, China). All operations were performed according to the manufacturer's instructions. The Image-Pro Plus 6.0 (Media Cybernetics, Silver Spring, MD, USA) was used to calculate the number of positive cells by using three sections from each sample in three randomly selected fields of view with blind method. And the total number of cells was calculated by DAPI staining.

Statistical Analysis

All numerical data were expressed as mean ± standard error of mean (SEM). One-way analysis of variance (ANOVA) with a Student-Newman-Keuls (SNK) *post hoc* test was performed using GraphPad Prism 6.0 (GraphPad Software Inc., La Jolla, CA). When $P < 0.05$, the differences were considered to be statistically significant.

RESULTS

Active Compounds in ZGBSF and Targets Prediction

A total of 145 active compounds of ZGBSF were screened, including 23 from Yin Yang Huo, 8 from Xu Duan, 13 from Bai Shao, 7 from Chuan Xiong, 20 from Huang Qi, 2 from Shu Di Huang, 28 from Du Zhong, 20 from Niu Xi, 22 from Hong Hua, and 2 from Dang Gui. And 2729 related targets of ZGBSF were obtained from the TCMSP database, containing 511 types in Yin Yang Huo, 63 types in Xu Duan, 123 types in Bai Shao, 42 types in Chuan Xiong, 462 types in Huang Qi, and 34 types in Shu Di Huang, 532 types in Du Zhong, 444 types in Niu Xi, 449 types in Hong Hua, and 69 types in Dang Gui. After excluding duplicates, a total of 86 compounds and 233 targets were selected for the following research.

Potential Targets Prediction of OP

To identify potential targets of OP, we searched 5 databases for OP-related research reports. A total of 4725 targets of OP were screen out, of which 384 were from the DrugBank database, 4273 from the GeneCards database, 31 from the TTD database, 3 from the PharmGkb database, 34 from the OMIM database. After expurgating duplicate targets, 4392 targets related to OP were screened out (**Figure 2A**).

Drug-Target-Disease Network Construction

To obtain the intersection of ZGBSF target genes and OP target genes, the Venn diagram analysis was performed. The results showed that a total of 164 target genes were identified (**Figure 2B**), which matched with the related targets of 86 active compounds. Then, to clarify the relationship among active compounds, targets, and OP, a drug-target-disease network, including 250 nodes and 847 edges, was constructed by using Cytoscape 3.8 software (**Figure 2C**). The top 10 core compounds of ZGBSF against OP were listed in **Table 2**.

PPI Network Construction and Key Targets

To obtain the pivotal proteins of ZGBSF in treating OP, after removing 3 isolates, a PPI network with 161 nodes and 3021 edges was constructed by using a String database (**Figure 2D**). Then, the thresholds of BC, CC, DC, EC, LAC, and NC were set in two steps according to the topological parameters calculated by CytoNCA. And a total of 22 pivotal proteins were filtered out, including Caspase-3, BCL2L1, TP53, IL-1β, Akt1, ESR1, FN1, CCND1, VEGFA, HIF1A, EGFR, CXCL8, CCL2, CTNNB1, JUN, PPARG, FOS, NFKBIA, PTGS2, MYC, MMP9, EGF, which were strongly linked to OP (**Figures 2E, F**).

Functional Enrichment Analysis

To explore the crucial biological processes of ZGBSF in the treatment of OP, the GO functional enrichment analyses were performed. The results of GO analysis revealed that the 164 genes were enriched in 2709 GO entries, consisting of 2401 biological progress (BP), 92 cellular components (CC), and 216 molecular functions (MF) ($P < 0.05$), and the top 10 entries of BP, CC and MF were shown in **Figure 3A**. BP analysis revealed that related targets were mainly centered on cellular response to chemical stress, drug, oxidative stress, *etc.* CC analysis indicated that related targets were mainly centered on membrane microdomain, membrane raft, *etc.* Moreover, MF analysis showed that potential targets were primarily focused on

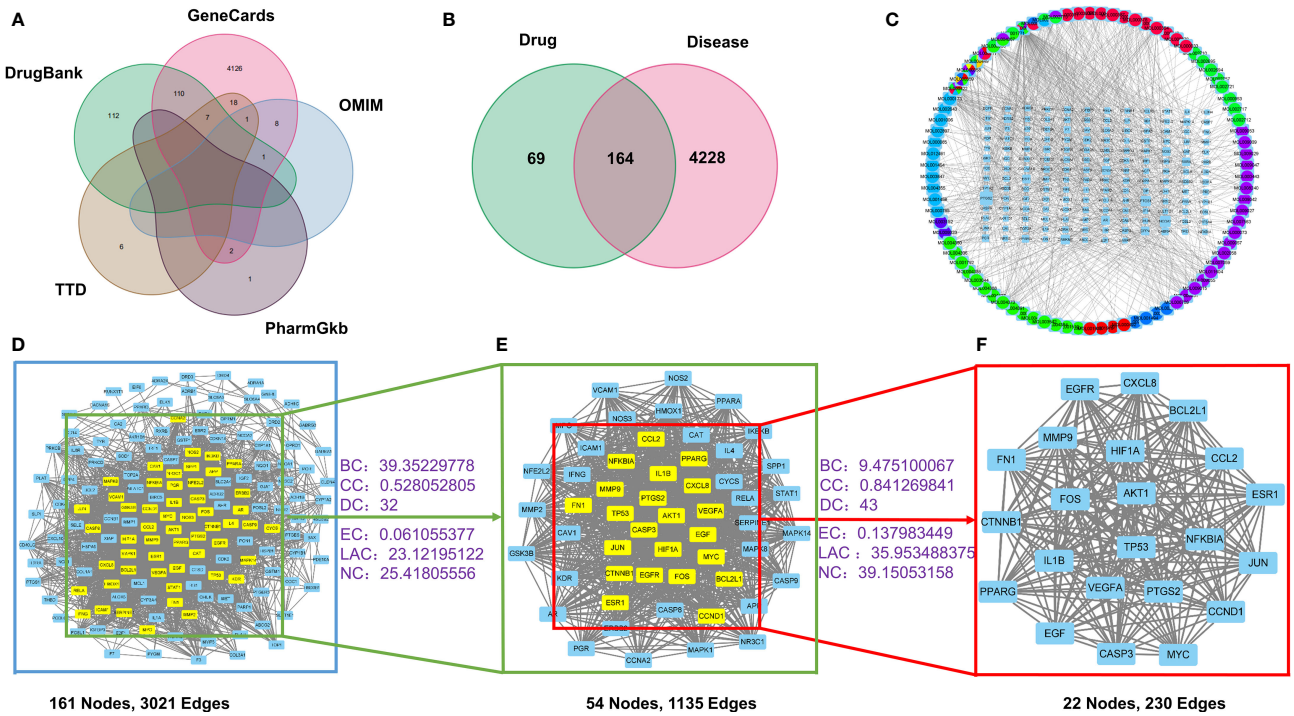

FIGURE 2 | The drug-target-disease network and PPI network construction. **(A)** The collection of predictive targets for OP. **(B)** The intersection targets of ZGBSF-related targets and OP-related targets. **(C)** The network of drug-target-disease includes 10 kinds of herbs, 86 active components, and 164 target genes. Circle represents active components and rectangle represents related targets. **(D)** PPI network of predicted targets of ZGBSF against OP. **(E)** The significant proteins of the PPI network were extracted from **(D)**. **(F)** Screening 22 key proteins of ZGBSF in the treatment of OP were extracted from **(E)**.

nuclear receptor activity, transcription factor activity, RNA polymerase II–specific DNA–binding transcription factor binding, *etc.*

To investigate the representative signaling pathways associated with the key targets, the KEGG enrichment analysis was performed. And the results showed that 160 significantly enriched signaling pathways were retrieved ($P < 0.05$). The top 30 significantly enriched signaling pathways closely correlated with OP were shown in **Figure 3B**, including apoptosis, PI3K-Akt, and TNF signaling pathways, *etc.* Furthermore, we found that apoptosis and PI3K-Akt signaling pathways were most closely related to OP in these enriched pathways, and the predicted targets corresponding to these two signaling pathways were shown in **Figures 3C, D**.

ZGBSF Ameliorates Bone Loss and the Progression of OP in OVX Mice

To verify the core pharmacological mechanism of ZGBSF in treating OP predicted by the above-mentioned network pharmacology analysis, OVX model mice were established and treated intragastrically with ZGBSF for 8 weeks. The femurs of OVX mice were harvested and radiographic alterations were assessed by μCT analysis. The results of μCT analysis showed that compared with sham mice, the bone mass of OVX mice

TABLE 2 | The top 10 key compounds of ZGBSF against OP.

Molecular ID	Ingredient	Degree	Source	OB(%)	DL
MOL000098	quercetin	108	Du Zhong, Hong Hua, Huang Qi, Niu Xi, Yin Yang Huo	46.43	0.28
MOL000006	luteolin	45	Hong Hua, Yin Yang Huo	36.16	0.25
MOL000422	kaempferol	38	Bai Shao, Du Zhong, Hong Hua, Huang Qi, Niu Xi, Yin Yang Huo	41.88	0.24
MOL000173	wogonin	35	Niu Xi	30.68	0.23
MOL002714	baicalein	25	Hong Hua, Niu Xi	33.52	0.21
MOL000378	7-O-methylisomucronulatol	24	Huang Qi	74.69	0.30
MOL000392	formononetin	23	Huang Qi	69.67	0.21
MOL000354	isorhamnetin	22	Huang Qi	49.60	0.31
MOL004373	Anhydroicaritin	21	Yin Yang Huo	45.41	0.44
MOL004391	8-(3-methylbut-2-enyl)-2-phenyl-chromone	19	Yin Yang Huo	48.54	0.25

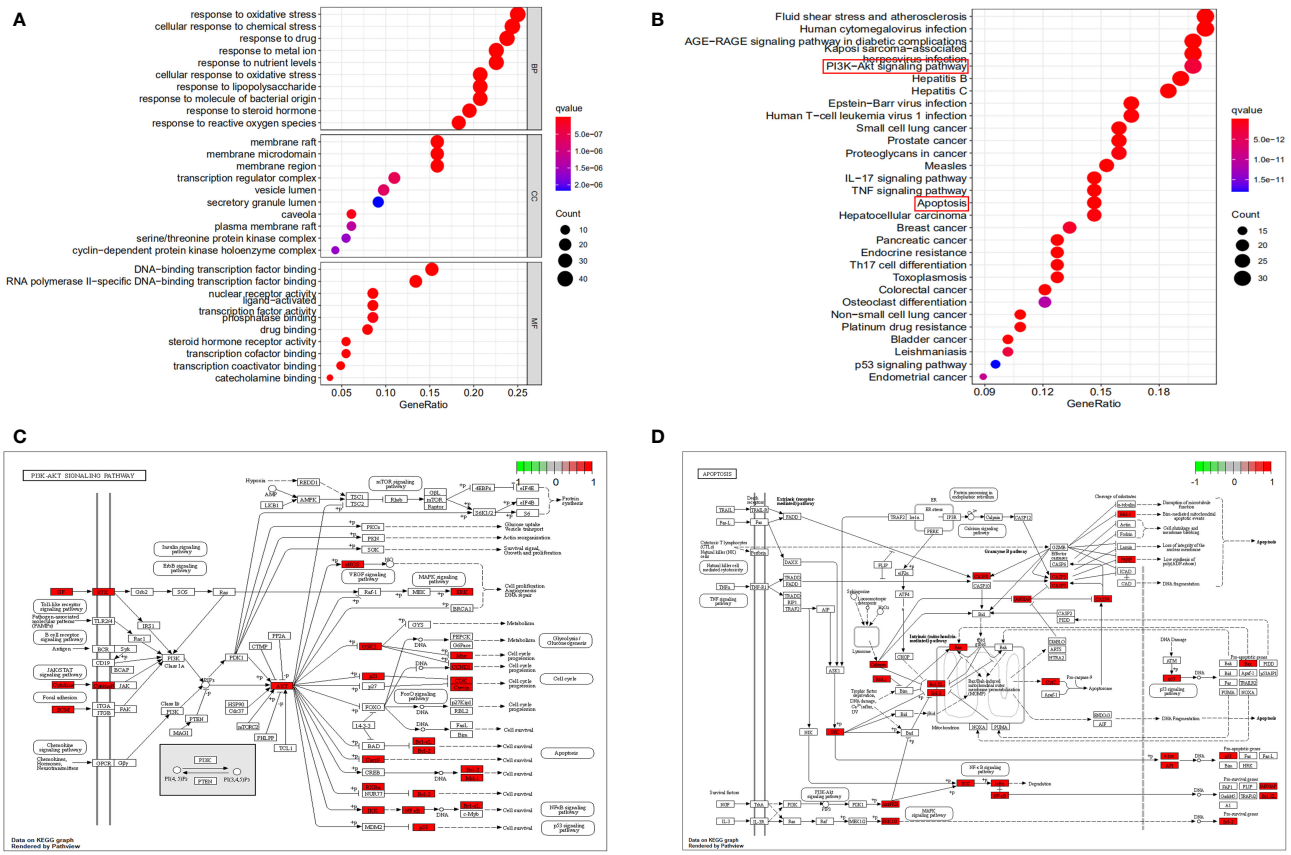

FIGURE 3 | GO and KEGG functional analysis. **(A)** The top 10 of GO enrichment analysis in Biological processes (BP), cellular components (CC) and molecular function (MF). **(B)** The top 30 signaling pathways were analyzed by KEGG. **(C, D)** The PI3K-Akt signaling pathway **(C)** and apoptosis **(D)** were described in detail. The larger the nodes, the darker the color, and the more genes were enriched.

significantly reduced, whereas ZGBSF intervention significantly restored the bone mass (**Figure 4A**). Moreover, the results of bone morphological parameter analysis showed that ZGBSF enhanced the decrease of bone mineral density (BMD), bone volume fraction (BV/TV), trabecular thickness (Tb.Th), trabecular number (Tb.N) in OVX mice. However, it had no significant recovery effect for the widened trabecular separation (Tb.Sp) (**Figures 4B–F**). In parallel, the histological changes of the femur were examined using H&E staining. The results showed that the femoral tissues of OVX mice exhibited less trabecular bone, and a large number of lipid droplets were present instead. ZGBSF administration significantly reversed these alterations (**Figures 4G–I**). All these findings showed that ZGBSF effectively attenuated bone loss and the progression of OP.

ZGBSF Promotes Osteogenesis and Fails to Inhibit the Formation of Osteoclasts

Bone homeostasis and remodelling is regulated by a balance between osteogenesis of osteoblast and osteoclastogenesis of osteoclast (37). To examine the effects of ZGBSF on osteogenesis, protein levels of Runx2, Alp, and Osx were determined by IHC analysis. The results of IHC analysis revealed that Runx2, Alp, and Osx were significantly decreased in OVX mice. The treatment of ZGBSF significantly increased the expression of Runx2, Alp, and Osx (**Figures 5A–D**). Subsequently, to explore the effect of ZGBSF on osteoclast formation, the number of osteoclasts was evaluated by TRAP staining. Compared with sham mice, the number of osteoclasts in the distal femurs of OVX mice was markedly increased. Unexpectedly, ZGBSF intervention had no significant effect on the increase of osteoclast number in OVX mice (**Figures 5E, F**).

ZGBSF Suppresses Apoptosis and Activates the PI3K-Akt Signaling Pathway of Osteoblasts

The prediction results from our network pharmacology analysis revealed that the apoptosis and PI3K-Akt signaling pathways were pivotal biological events in ZGBSF against OP. Therefore, we first determined the expression of Bcl-2, Bax, Caspase-3, and Parp, indicators of apoptosis, by IF analysis. The IF results showed that Bcl-2 was markedly decreased in the distal femur of OVX mice, while Bax, Caspase-3 and Parp were significantly

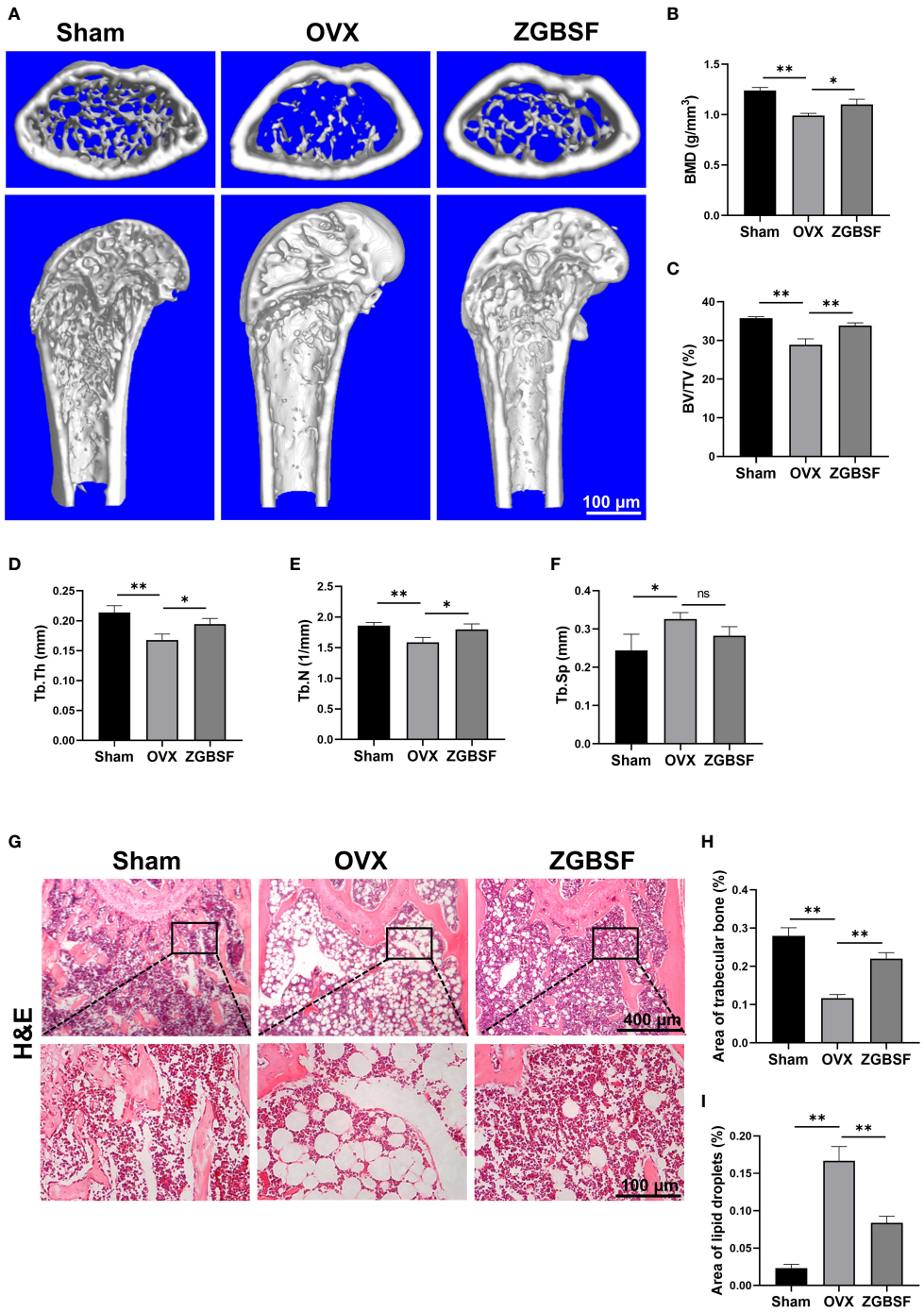

FIGURE 4 | ZGBSF ameliorates bone loss in OVX mice. **(A)** Representative μCT images of distal femoral. Quantification of bone mineral density (BMD) **(B)**, bone volume fraction (BV/TV) **(C)**, trabecular thickness (Tb.Th) **(D)**, trabecular number (Tb.N) **(E)** and trabecular separation (Tb.Sp) **(F)**. **(G)** Hematoxylin-eosin staining of the distal femur. **(H)** The area of trabecular bone (%). **(I)** The area of lipid droplets (%). Data were presented as mean ± SEM of three independent experiments. $^{*}P < 0.05$, $^{**}P < 0.01$, NS indicated no significant difference.

increased. ZGBSF significantly reversed these alterations (**Figures 6A–E**). In parallel, the anti-apoptosis effect of ZGBSF was further confirmed by TUNEL staining. The results of TUNEL staining revealed that ZGBSF significantly inhibited the increased apoptosis ratio of osteoblasts in femoral tissues of OVX mice (**Figures 6F, G**). All these findings showed that ZGBSF suppressed apoptosis of osteoblasts and contributed to osteogenesis, thus ameliorating bone loss of OVX mice.

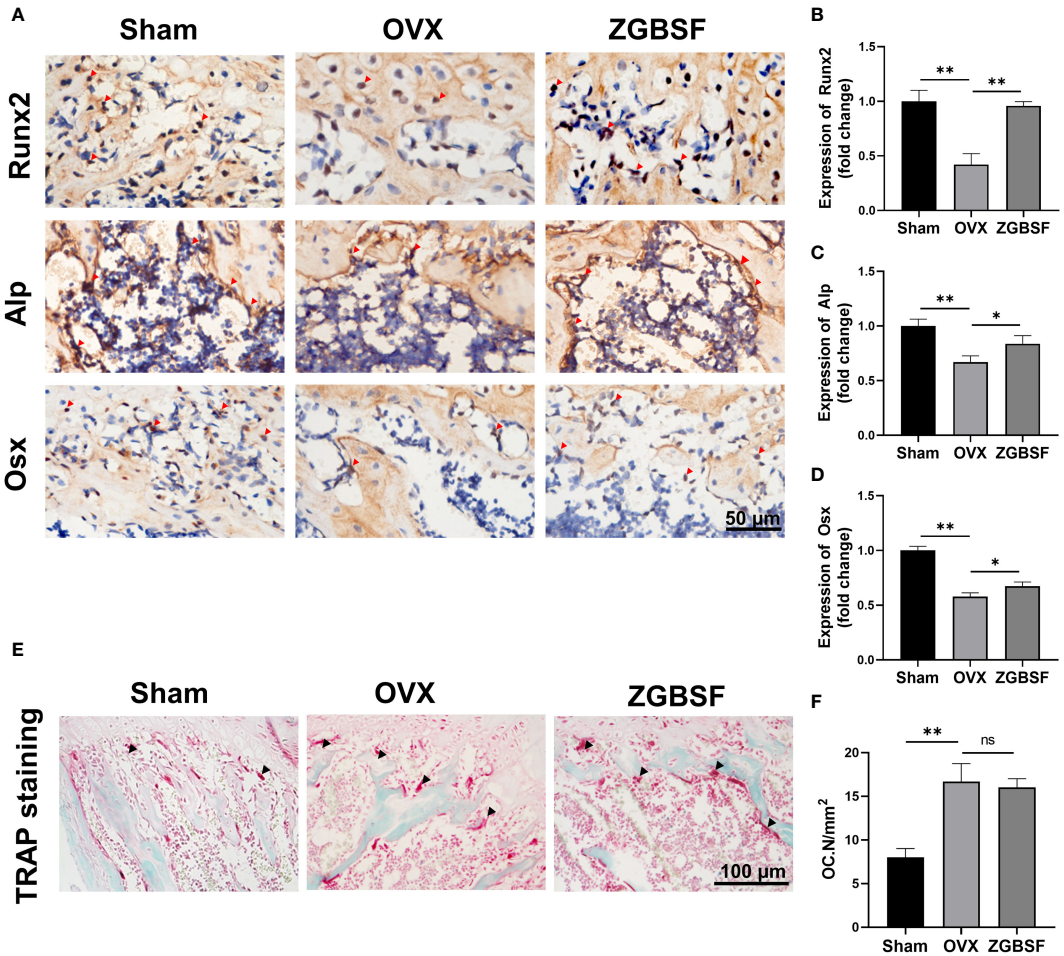

FIGURE 5 | ZGBSF promotes osteogenesis and fails to inhibit osteoclastogenesis. **(A)** Immunohistochemistry of Runx2, Alp, and Osx of the distal femur. Red arrows indicated the high expression of Runx2, Alp, and Osx. **(B–D)** The quantification of Runx2, Alp, and Osx expression. **(E)** TRAP staining of the distal femur. **(F)** The number of osteoclasts (OC.N/mm^2). The arrows represented the positive expression. Data were presented as mean ± SEM of three independent experiments. *P < 0.05, **P < 0.01, NS indicated no significant difference.

Next, to verify the effect of ZGBSF on PI3K–Akt signaling pathway predicted by KEGG enrichment analysis, the phosphorylation status of Akt1, and expression of PI3K protein were examined by IHC analysis of t-Akt1, p-Akt1, and PI3K. The IHC results showed that the levels of p-Akt1 and PI3K protein in distal femoral tissue of OVX mice were lower than those in sham mice. ZGBSF treatment significantly upregulated the expression of p-Akt1 and PI3K protein in ZGBSF mice (**Figures 7A–C**).

DISCUSSION

OP is a common chronic skeletal disease worldwide, characterized by bone loss and increased fracture risk. Fractures caused by OP are highly susceptible to disability and mortality in the elderly (38, 39). ZGBSF is a novel TCM formula, which has been proved to be an effective drug for treating OP in clinic. However, due to the diversity of components in ZGBSF, the pharmacological mechanism of its anti-OP effect is still elusive, which greatly hinders its popularization and application. Network pharmacology, a newly developed cross-discipline, has unique advantages in deciphering the molecular mechanisms of TCM on diseases with multiple components, targets, and pathways (40, 41). In this study, we deciphered the underlying molecular mechanisms of ZGBSF in the treatment of OP *via* network pharmacology analysis and *in vivo* experimental validation. We found that ZGBSF contributed to osteogenesis by inhibiting osteoblast apoptosis and activating PI3K-Akt signaling pathways, thereby attenuating bone loss and the progression of OP.

Based on network pharmacology analysis, the core compounds of TCM have made great contributions to the therapeutic effect of treating diseases (42). In the present study, we firstly discovered that the top active compounds in ZGBSF consist of quercetin, luteolin, kaempferol, baicalein, *etc.* Previous studies have shown that quercetin could inhibit oxidative stress and inflammatory

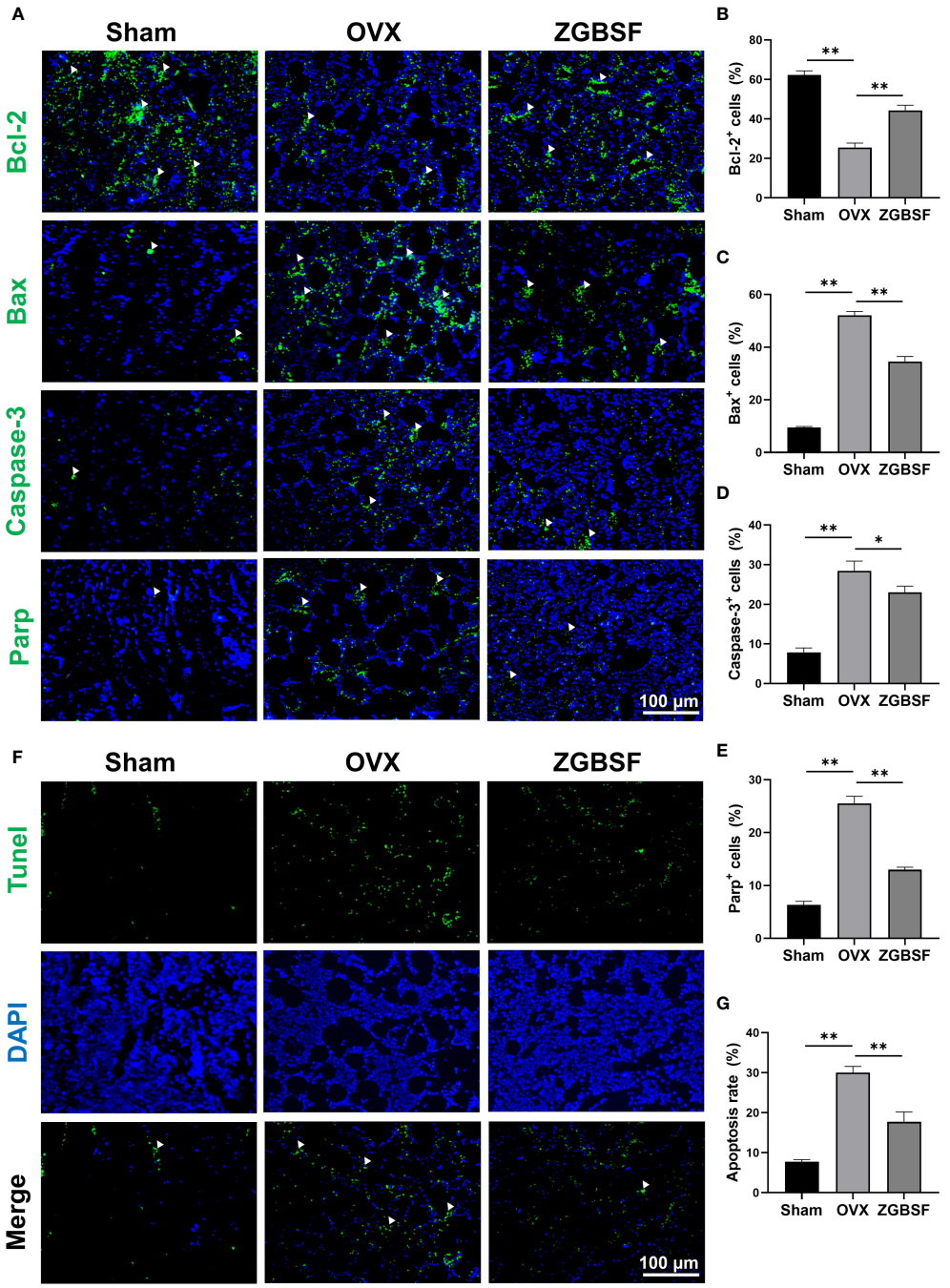

FIGURE 6 | ZGBSF suppresses apoptosis of osteoblasts to ameliorate OP in OVX mice. **(A)** Immunofluorescence of Bcl-2, Bax, Caspase-3 and Parp in distal femur. **(B–E)** The quantification of Bcl-2, Bax, Caspase-3 and Parp positive cells. **(F)** Tunel staining was performed to examine the apoptosis status of osteoblasts. **(G)** The quantification of TUNEL positive rates in the distal femur. White arrows indicated the positive expression. Data were presented as mean ± SEM of three independent experiments. $^{*}P < 0.05$, $^{**}P < 0.01$.

response as well as the apoptosis of osteoblasts, thereby promoting osteogenesis (43). *In vivo* and *in vitro* experiments also showed that luteolin and kaempferol ameliorated OP by regulating oxidative stress and osteogenesis (44, 45). In addition, baicalein contributed to the expression of OP-related proteins and extracellular matrix mineralization (46). Therefore, all these findings showed that multiple components of ZGBSF had a good therapeutic effect on OP.

To explore the underlying mechanisms of ZGBSF in the treatment of OP, the OP-related targets of core components of

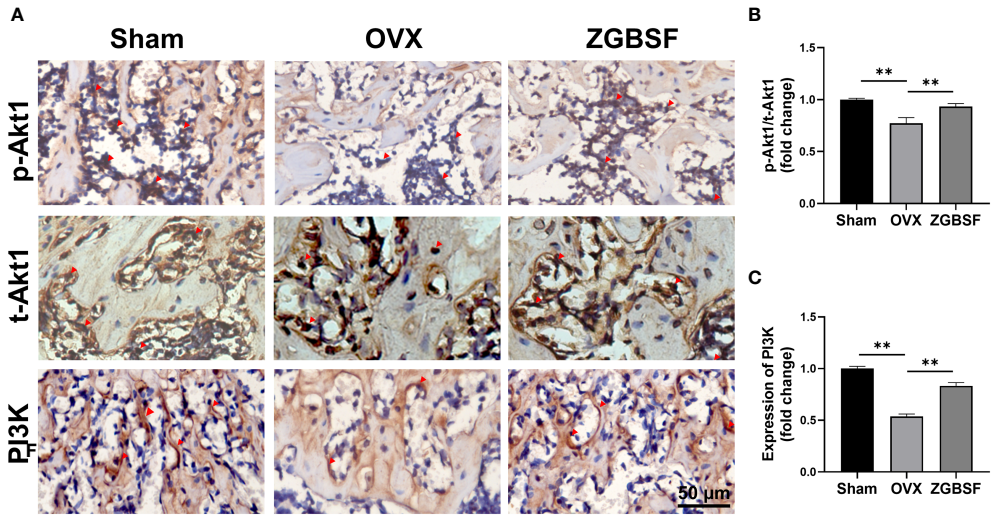

FIGURE 7 | ZGBSF activates the PI3K-Akt signaling pathway of femoral tissue. **(A)** Immunohistochemistry of t-Akt1, Akt1(S473), and PI3K of distal femur. **(B, C)** The quantification of Akt1(S473)/t-Akt1, and PI3K expression. Red arrows indicated the positive expression. Data were presented as mean ± SEM of three independent experiments. $^{**}P < 0.01$.

ZGBSF were identified by the PPI network. We found that the top targets of ZGBSF for OP included Caspase-3, BCL2L1, and TP53, which were closely related to the process of apoptosis. Caspase-3 is a critical regulator of apoptosis, which has been proven to impair bone formation (47). A recent study reported that lowering the expression of Caspase-3 by quercetin and vitamin E inhibited osteoblast apoptosis, thus alleviating OP (48). BCL2L1 is a vital apoptosis regulator gene encoding splicing variants of anti-apoptosis [Bcl-x(L)] and pro-apoptosis [Bcl-x (S)] (49). Overexpression of BCL-x(L) in osteoblasts suppressed the apoptosis of osteoblasts and increased the bone mass of trabecular bone and cortical bone (50). In addition, as a pro-apoptotic protein, TP53 is closely related to OP (51). An *in vitro* experiment revealed that downregulating the expression of p53 observably increased the expression of osteogenesis-related proteins, such as Alp and Runx2 (52). All these findings showed that Caspase-3, BCL2L1, and P53 played an important role in the progression of OP.

Previous studies have shown that the excessive apoptosis of osteoblasts may exacerbate the progression of osteoporosis (53). Inhibiting the apoptosis of osteoblasts significantly enhanced osteogenic differentiation, thereby exerting anti-OP effects (54). A recent study on OP model of rats showed that quercetin improved ovariectomy-induced osteoporosis *via* regulation of apoptosis (48). Consistent with the above studies, our KEGG enrichment analysis showed that apoptosis was involved in the intervention of ZGBSF for OP, and *in vivo* mouse OVX model evidence revealed that ZGBSF treatment significantly overturned the decreased Bcl-2 protein and increased levels of Bax, Caspase-3, Parp as well as increased DNA damage in OVX mice. The results showed that ZGBSF attenuated the apoptosis of osteoblasts.

Increasing studies revealed that the PI3K-Akt signaling pathway played an important role in the physiological and pathological processes of OP (55, 56). Activation of the PI3K-Akt signaling pathway resulted in enhanced osteogenic differentiation of human bone marrow mesenchymal stem cells (15). Similarly, another work discovered that quercetin, one of the top active compounds in ZGBSF, promoted osteogenic differentiation and mineralization *via* PI3K-Akt signaling pathway (57). Consistent with those studies, our results uncovered that the activity of the PI3K-Akt signaling pathway was decreased in OVX mice, whereas ZGBSF treatment significantly activated the activity of the PI3K-Akt signaling pathway. And ZGBSF significantly enhanced the expression of decreased osteogenic markers (Runx2, Alp, and Osx) in OVX mice. However, ZGBSF administration had no significant effect on the increase of osteoclasts number in OVX mice. All these findings revealed that the treatment of ZGBSF dramatically promoted osteogenesis by activating the PI3K-Akt signaling pathway.

In total, ZGBSF could ameliorate the progression of OP *via* multi-ingredients, multi-targets, multi-pathways mode, which was different from a single drug with few targets. Network target and signaling pathway could perfectly decipher sophisticated interactions between diseases with chemical ingredients in TCM. However, there were some limitations in this study. First, only core targets and pathways of ZGBSF were verified, which may result in a slight deviation of results. Further validation of other relevant targets and signaling pathways predicted by network pharmacology is needed in future experiments. Second, our *in vivo* animal experiment was limited to mouse OVX model, so human-derived osteoblasts were used to make the experiment more clinically relevant in a follow-up experiment.

CONCLUSION

In summary, to decipher the molecular mechanisms of ZGBSF in the treatment of OP, network pharmacology analysis coupled

with experimental validation were performed. The network pharmacology analysis revealed that ZGBSF exerted anti-OP effects *via* multi-ingredients, multi-targets, and multi-pathways, and the experimental results validated that ZGBSF promoted osteogenesis *via* inhibition of osteoblast apoptosis and activation of PI3K-Akt signaling pathway, thus ameliorating bone loss of OP. This study could provide an optimized method to elucidate the pharmacological mechanisms of ZGBSF and supply a novel candidate for the treatment of OP.

DATA AVAILABILITY STATEMENT

The original contributions presented in the study are included in the article/supplementary material. Further inquiries can be directed to the corresponding authors.

ETHICS STATEMENT

The animal study was reviewed and approved by The Ethics Committee of Zhejiang Chinese Medical University.

AUTHOR CONTRIBUTIONS

HR, PT, XL, CW contributed to the concept and design of this study. HZ, CZ, ZZ performed the computational analyses and performed the *in vivo* experiments. SaY, YB, FF, HL, YL, SxY, YG, YC, KZ, MY, WD, KT, HJ performed the experimental analysis. HZ drafted the manuscript. All the authors read, revised, and approved the final manuscript.

FUNDING

This study was financially supported by National Natural Science Foundation of China (No.: 82174140, 82174401, 82104164, 81973870, 81973881, 81904053, 81804121), China Postdoctoral Science Foundation (No.: 2018M632154), Natural Science Foundation of Zhejiang Province (No.: LY22H270003, LBY22H270008, LY19H270006, and LQ19H080001), Traditional Chinese Medical Administration of Zhejiang Province (No.: 2022ZX005, 2022ZB119, 2021ZB090), Zhejiang medical and health science and technology project (No.: 2021KY222), Research Project of Zhejiang Chinese Medical University Scientific (No.: 2021JKZDZC02, 2021JKZKTS036A, 2021JKJNTZ022B, 2019ZG25, 2018ZR06), National Undergraduate Innovation and Entrepreneurship Training Program (202110344005, 202110344025, S202110344007, 202010344004), General Research Project of Zhejiang Provincial Education Department "Special Project for the Reform of Cultivation Mode of Professional Degree Graduate Students in Higher Education Institutions" (No.: Y202145932), Postgraduate Science Research Fund of Zhejiang Chinese Medical University (No.: 2021YKJ02, 2020YKJ07).

REFERENCES

1. Cotts KG, Cifu AS. Treatment of Osteoporosis. *Jama* (2018) 319(10):1040–1. doi: 10.1001/jama.2017.21995
2. Compston JE, McClung MR, Leslie WD. Osteoporosis. *Lancet (London England)* (2019) 393(10169):364–76. doi: 10.1016/s0140-6736(18)32112-3
3. Macías I, Alcorta-Sevillano N, Rodríguez CI, Infante A. Osteoporosis and the Potential of Cell-Based Therapeutic Strategies. *Int J Mol Sci* (2020) 21(5):1653. doi: 10.3390/ijms21051653
4. Lin Z, Zheng J, Chen J, Chen M, Dong S. Antiosteoporosis Effect and Possible Mechanisms of the Ingredients of Fructus Psoraleae in Animal Models of Osteoporosis: A Preclinical Systematic Review and Meta-Analysis. *Oxid Med Cell Longev* (2021) 2021:2098820. doi: 10.1155/2021/2098820
5. Chen M, Han H, Zhou S, Wen Y, Chen L. Morusin Induces Osteogenic Differentiation of Bone Marrow Mesenchymal Stem Cells by Canonical Wnt/beta-Catenin Pathway and Prevents Bone Loss in an Ovariectomized Rat Model. *Stem Cell Res Ther* (2021) 12(1):173. doi: 10.1186/s13287-021-02239-3
6. Song N, Zhao Z, Ma X, Sun X, Ma J, Li F, et al. Naringin Promotes Fracture Healing Through Stimulation of Angiogenesis by Regulating the VEGF/VEGFR-2 Signaling Pathway in Osteoporotic Rats. *Chem-Biol Interact* (2017) 261:11–7. doi: 10.1016/j.cbi.2016.10.020
7. Cui J, Li X, Wang S, Su Y, Chen X, Cao L, et al. Triptolide Prevents Bone Loss *via* Suppressing Osteoclastogenesis Through Inhibiting PI3K-AKT-NFATc1 Pathway. *J Cell Mol Med* (2020) 24(11):6149–61. doi: 10.1111/jcmm.15229
8. Ukon Y, Makino T, Kodama J, Tsukazaki H, Tateiwa D, Yoshikawa H, et al. Molecular-Based Treatment Strategies for Osteoporosis: A Literature Review. *Int J Mol Sci* (2019) 20(10):2557. doi: 10.3390/ijms20102557
9. Chen LR, Ko NY, Chen KH. Medical Treatment for Osteoporosis: From Molecular to Clinical Opinions. *Int J Mol Sci* (2019) 20(9):2213. doi: 10.3390/ijms20092213
10. Rachner TD, Khosla S, Hofbauer LC. Osteoporosis: Now and the Future. *Lancet (London England)* (2011) 377(9773):1276–87. doi: 10.1016/s0140-6736(10)62349-5
11. Che CT, Wong MS, Lam CW. Natural Products From Chinese Medicines With Potential Benefits to Bone Health. *Molecules (Basel Switzerland)* (2016) 21(3):239. doi: 10.3390/molecules21030239
12. Zhu B, Zhang QL, Hua JW, Cheng WL, Qin LP. The Traditional Uses, Phytochemistry, and Pharmacology of Atractylodes Macrocephala Koidz.: A Review. *J Ethnopharmacol* (2018) 226:143–67. doi: 10.1016/j.jep.2018.08.023
13. Liu C, Ma R, Wang L, Zhu R, Liu H, Guo Y, et al. Rehmanniae Radix in Osteoporosis: A Review of Traditional Chinese Medicinal Uses, Phytochemistry, Pharmacokinetics and Pharmacology. *J Ethnopharmacol* (2017) 198:351–62. doi: 10.1016/j.jep.2017.01.021
14. Xu R, Zeng Q, Xia C, Chen J, Wang P, Zhao S, et al. Fractions of Shen-Sui-Tong-Zhi Formula Enhance Osteogenesis *Via* Activation of β-Catenin Signaling in Growth Plate Chondrocytes. *Front Pharmacol* (2021) 12:711004. doi: 10.3389/fphar.2021.711004
15. Ye C, Zhang W, Hang K, Chen M, Hou W, Chen J, et al. Extracellular IL-37 Promotes Osteogenic Differentiation of Human Bone Marrow Mesenchymal Stem Cells *via* Activation of the PI3K/AKT Signaling Pathway. *Cell Death Dis* (2019) 10(10):753. doi: 10.1038/s41419-019-1904-7
16. Hussain T, Tan B, Liu G, Oladele OA, Rahu N, Tossou MC, et al. Health-Promoting Properties of Eucommia Ulmoides: A Review. *Evid Based complementary Altern Med eCAM* (2016) 2016:5202908. doi: 10.1155/2016/5202908
17. Zhang W, Xue K, Gao Y, Huai Y, Wang W, Miao Z, et al. Systems Pharmacology Dissection of Action Mechanisms of Dipsaci Radix for Osteoporosis. *Life Sci* (2019) 235:116820. doi: 10.1016/j.lfs.2019.116820
18. Yang L, Fan L, Wang K, Chen Y, Liang L, Qin X, et al. Analysis of Molecular Mechanism of Erxian Decoction in Treating Osteoporosis Based on Formula

Optimization Model. *Oxid Med Cell Longev* (2021) 2021:6641838. doi: 10.1155/2021/6641838
19. An L, Lin Y, Li L, Kong M, Lou Y, Wu J, et al. Integrating Network Pharmacology and Experimental Validation to Investigate the Effects and Mechanism of Astragalus Flavonoids Against Hepatic Fibrosis. *Front Pharmacol* (2020) 11:618262. doi: 10.3389/fphar.2020.618262
20. Guo C, Kang X, Cao F, Yang J, Xu Y, Liu X, et al. Network Pharmacology and Molecular Docking on the Molecular Mechanism of Luo-Hua-Zi-Zhu (LHZZ) Granule in the Prevention and Treatment of Bowel Precancerous Lesions. *Front Pharmacol* (2021) 12:629021. doi: 10.3389/fphar.2021.629021
21. Zhang H, Yao S, Zhang Z, Zhou C, Fu F, Bian Y, et al. Network Pharmacology and Experimental Validation to Reveal the Pharmacological Mechanisms of Liuwei Dihuang Decoction Against Intervertebral Disc Degeneration. *Drug Design Dev Ther* (2021) 15:4911–24. doi: 10.2147/dddt.s338439
22. Feng W, Ao H, Yue S, Peng C. Systems Pharmacology Reveals the Unique Mechanism Features of Shenzhu Capsule for Treatment of Ulcerative Colitis in Comparison With Synthetic Drugs. *Sci Rep* (2018) 8(1):16160. doi: 10.1038/s41598-018-34509-1
23. Ru J, Li P, Wang J, Zhou W, Li B, Huang C, et al. TCMSP: A Database of Systems Pharmacology for Drug Discovery From Herbal Medicines. *J Cheminform* (2014) 6:13. doi: 10.1186/1758-2946-6-13
24. UniProt C. UniProt: A Worldwide Hub of Protein Knowledge. *Nucleic Acids Res* (2019) 47(D1):D506–D15. doi: 10.1093/nar/gky1049
25. Wishart DS, Feunang YD, Guo AC, Lo EJ, Marcu A, Grant JR, et al. DrugBank 5.0: A Major Update to the DrugBank Database for 2018. *Nucleic Acids Res* (2018) 46(D1):D1074–D82. doi: 10.1093/nar/gkx1037
26. Stelzer G, Dalah I, Stein TI, Satanower Y, Rosen N, Nativ N, et al. *In-Silico* Human Genomics With GeneCards. *Hum Genomics* (2011) 5(6):709–17. doi: 10.1186/1479-7364-5-6-709
27. Li YH, Yu CY, Li XX, Zhang P, Tang J, Yang Q, et al. Therapeutic Target Database Update 2018: Enriched Resource for Facilitating Bench-to-Clinic Research of Targeted Therapeutics. *Nucleic Acids Res* (2018) 46(D1):D1121–7. doi: 10.1093/nar/gkx1076
28. Barbarino JM, Whirl-Carrillo M, Altman RB, Klein TE. PharmGKB: A Worldwide Resource for Pharmacogenomic Information. *Wiley Interdiscip Rev Syst Biol Med* (2018) 10(4):e1417. doi: 10.1002/wsbm.1417
29. Amberger JS, Bocchini CA, Schiettecatte F, Scott AF, Hamosh A. OMIM.org: Online Mendelian Inheritance in Man (OMIM(R)), an Online Catalog of Human Genes and Genetic Disorders. *Nucleic Acids Res* (2015) 43(Database issue):D789–98. doi: 10.1093/nar/gku1205
30. He D, Huang JH, Zhang ZY, Du Q, Peng WJ, Yu R, et al. A Network Pharmacology-Based Strategy For Predicting Active Ingredients And Potential Targets Of LiuWei DiHuang Pill In Treating Type 2 Diabetes Mellitus. *Drug Des Devel Ther* (2019) 13:3989–4005. doi: 10.2147/DDDT.S216644
31. Du A, Xie Y, Ouyang H, Lu B, Jia W, Xu H, et al. Si-Miao-Yong-An Decoction for Diabetic Retinopathy: A Combined Network Pharmacological and. *In Vivo Approach Front Pharmacol* (2021) 12:763163. doi: 10.3389/fphar.2021.763163
32. Shi H, Dong C, Wang M, Liu R, Wang Y, Kan Z, et al. Exploring the Mechanism of Yizhi Tongmai Decoction in the Treatment of Vascular Dementia Through Network Pharmacology and Molecular Docking. *Ann Transl Med* (2021) 9(2):164. doi: 10.21037/atm-20-8165
33. Li Q, Hu S, Huang L, Zhang J, Cao G. Evaluating the Therapeutic Mechanisms of Selected Active Compounds in Cornus Officinalis and Paeonia Lactiflora in Rheumatoid Arthritis *via* Network Pharmacology Analysis. *Front Pharmacol* (2021) 12:648037. doi: 10.3389/fphar.2021.648037
34. Xu R, Zeng Q, Xia C, Chen J, Wang P, Zhao S, et al. Fractions of Shen-Sui-Tong-Zhi Formula Enhance Osteogenesis *Via* Activation of Beta-Catenin Signaling in Growth Plate Chondrocytes. *Front Pharmacol* (2021) 12:711004. doi: 10.3389/fphar.2021.711004
35. Fu F, Bao R, Yao S, Zhou C, Luo H, Zhang Z, et al. Aberrant Spinal Mechanical Loading Stress Triggers Intervertebral Disc Degeneration by Inducing Pyroptosis and Nerve Ingrowth. *Sci Rep* (2021) 11(1):772. doi: 10.1038/s41598-020-80756-6
36. Xia C, Zou Z, Fang L, Ge Q, Zhang P, Xu H, et al. Bushenhuoxue Formula Promotes Osteogenic Differentiation of Growth Plate Chondrocytes Through Beta-Catenin-Dependent Manner During Osteoporosis. *BioMed Pharmacother* (2020) 127:110170. doi: 10.1016/j.biopha.2020.110170
37. Zhu Y, Li Z, Zhang Y, Lan F, He J, Wu Y. The Essential Role of Osteoclast-Derived Exosomes in Magnetic Nanoparticle-Infiltrated Hydroxyapatite Scaffold Modulated Osteoblast Proliferation in an Osteoporosis Model. *Nanoscale* (2020) 12(16):8720–6. doi: 10.1039/d0nr00867b
38. Johnston CB, Dagar M. Osteoporosis in Older Adults. *Med Clinics North Am* (2020) 104(5):873–84. doi: 10.1016/j.mcna.2020.06.004
39. Vandenbroucke A, Luyten FP, Flamaing J, Gielen E. Pharmacological Treatment of Osteoporosis in the Oldest Old. *Clin Interv Aging* (2017) 12:1065–77. doi: 10.2147/cia.s131023
40. Wang X, Wang ZY, Zheng JH, Li S. TCM Network Pharmacology: A New Trend Towards Combining Computational, Experimental and Clinical Approaches. *Chin J Natural Med* (2021) 19(1):1–11. doi: 10.1016/s1875-5364(21)60001-8
41. Gao L, Cao M, Li JQ, Qin XM, Fang J. Traditional Chinese Medicine Network Pharmacology in Cardiovascular Precision Medicine. *Curr Pharm design* (2021) 27(26):2925–33. doi: 10.2174/1381612826666201112142408
42. Xia H, Liu J, Yang W, Liu M, Luo Y, Yang Z, et al. Integrated Strategy of Network Pharmacological Prediction and Experimental Validation Elucidate Possible Mechanism of Bu-Yang Herbs in Treating Postmenopausal Osteoporosis *via* ESR1. *Front Pharmacol* (2021) 12:654714. doi: 10.3389/fphar.2021.654714
43. Wong SK, Chin KY, Ima-Nirwana S. Quercetin as an Agent for Protecting the Bone: A Review of the Current Evidence. *Int J Mol Sci* (2020) 21(17):6448. doi: 10.3390/ijms21176448
44. Jing Z, Wang C, Yang Q, Wei X, Jin Y, Meng Q, et al. Luteolin Attenuates Glucocorticoid-Induced Osteoporosis by Regulating ERK/Lrp-5/GSK-3β Signaling Pathway *In Vivo* and *In Vitro*. *J Cell Physiol* (2019) 234(4):4472–90. doi: 10.1002/jcp.27252
45. Liu H, Yi X, Tu S, Cheng C, Luo J. Kaempferol Promotes BMSC Osteogenic Differentiation and Improves Osteoporosis by Downregulating miR-10a-3p and Upregulating CXCL12. *Mol Cell Endocrinol* (2021) 520:111074. doi: 10.1016/j.mce.2020.111074
46. Cai P, Lu Y, Yin Z, Wang X, Zhou X, Li Z. Baicalein Ameliorates Osteoporosis *via* AKT/FOXO1 Signaling. *Aging* (2021) 13(13):17370–9. doi: 10.18632/aging.203227
47. Liang J, Chen H, Pan W, Xu C. Puerarin Inhibits Caspase-3 Expression in Osteoblasts of Diabetic Rats. *Mol Med Rep* (2012) 5(6):1419–22. doi: 10.3892/mmr.2012.854
48. Vakili S, Zal F, Mostafavi-Pour Z, Savardashtaki A, Koohpeyma F. Quercetin and Vitamin E Alleviate Ovariectomy-Induced Osteoporosis by Modulating Autophagy and Apoptosis in Rat Bone Cells. *J Cell Physiol* (2021) 236(5):3495–509. doi: 10.1002/jcp.30087
49. Sillars-Hardebol AH, Carvalho B, Beliën JA, de Wit M, Delis-van Diemen PM, Tijssen M, et al. BCL2L1 has a Functional Role in Colorectal Cancer and its Protein Expression is Associated With Chromosome 20q Gain. *J Pathol* (2012) 226(3):442–50. doi: 10.1002/path.2983
50. Moriishi T, Fukuyama R, Miyazaki T, Furuichi T, Ito M, Komori T. Overexpression of BCLXL in Osteoblasts Inhibits Osteoblast Apoptosis and Increases Bone Volume and Strength. *J Bone Mineral Res Off J Am Soc Bone Mineral Res* (2016) 31(7):1366–80. doi: 10.1002/jbmr.2808
51. Yu T, You X, Zhou H, Kang A, He W, Li Z, et al. P53 Plays a Central Role in the Development of Osteoporosis. *Aging* (2020) 12(11):10473–87. doi: 10.18632/aging.103271
52. Yu T, Wu Q, You X, Zhou H, Xu S, He W, et al. Tomatidine Alleviates Osteoporosis by Downregulation of P53. *Med Sci Monitor Int Med J Exp Clin Res* (2020) 26:e923996. doi: 10.12659/msm.923996
53. Xiao L, Lin J, Chen R, Huang Y, Liu Y, Bai J, et al. Sustained Release of Melatonin From GelMA Liposomes Reduced Osteoblast Apoptosis and Improved Implant Osseointegration in Osteoporosis. *Oxid Med Cell Longevity* (2020) 2020:6797154. doi: 10.1155/2020/6797154
54. Wang Y, Liu J, Pang Q, Tao D. Alpinumisoflavone Protects Against Glucocorticoid-Induced Osteoporosis Through Suppressing the Apoptosis of Osteoblastic and Osteocytic Cells. *BioMed Pharmacother* (2017) 96:993–9. doi: 10.1016/j.biopha.2017.11.136
55. Kong Y, Nie ZK, Li F, Guo HM, Yang XL, Ding SF. MiR-320a was Highly Expressed in Postmenopausal Osteoporosis and Acts as a Negative Regulator in MC3T3E1 Cells by Reducing MAP9 and Inhibiting PI3K/AKT Signaling Pathway. *Exp Mol Pathol* (2019) 110:104282. doi: 10.1016/j.yexmp.2019.104282

56. Zhang Y, Cao X, Li P, Fan Y, Zhang L, Li W, et al. PSMC6 Promotes Osteoblast Apoptosis Through Inhibiting PI3K/AKT Signaling Pathway Activation in Ovariectomy-Induced Osteoporosis Mouse Model. *J Cell Physiol* (2020) 235(7-8):5511–24. doi: 10.1002/jcp.29261
57. Zhong Z, Li Y, Chen Y, Chen W, Li S, Lv X, et al. Predicting and Exploring the Mechanisms of Erzhi Pill in Prevention and Treatment of Osteoporosis Based on Network Pharmacology and Zebrafish Experiments. *Drug Design Dev Ther* (2021) 15:817–27. doi: 10.2147/dddt.s293455

Conflict of Interest: The authors declare that the research was conducted in the absence of any commercial or financial relationships that could be construed as a potential conflict of interest.

Publisher's Note: All claims expressed in this article are solely those of the authors and do not necessarily represent those of their affiliated organizations, or those of the publisher, the editors and the reviewers. Any product that may be evaluated in this article, or claim that may be made by its manufacturer, is not guaranteed or endorsed by the publisher.

frontiers in Endocrinology

ORIGINAL RESEARCH
published: 18 February 2022
doi: 10.3389/fendo.2022.839885

Comparative Efficacy of Xianling Gubao Capsules in Improving Bone Mineral Density in Postmenopausal Osteoporosis: A Network Meta-Analysis

Ming-hui Luo[1‡], Jin-long Zhao[2‡†], Nan-jun Xu[2], Xiao Xiao[1], Wen-xuan Feng[1], Zi-ping Li[1] and Ling-feng Zeng[1,2*†]*

[1] The 2nd Affiliated Hospital of Guangzhou University of Chinese Medicine, Guangzhou, China, [2] The Second Clinical Medical College of Guangzhou University of Chinese Medicine, Guangzhou, China

Objective: The clinical efficacy of Xianling Gubao capsule (XLGB) and its combination therapy in the treatment of postmenopausal osteoporosis (PMOP) was systematically evaluated by frequency-based network meta-analysis.

Methods: We searched the China National Knowledge Infrastructure (CNKI), Wanfang, SinoMed, PubMed, Embase and Cochrane Library databases to identify clinical trials of XLGB for the treatment of PMOP from the establishment of each database to November 22, 2021. The quality of the included studies was evaluated by using the risk of bias assessment tool version 2.0 (Rob 2.0) recommended by Cochrane. Stata 14.0 was applied for statistical analysis of the data, and the surface under the cumulative ranking curve (SUCRA) was used to rank the intervention measures of each outcome index.

Results: This study included 22 clinical trials (including 19 RCTs and 3 non-RCTs) involving 12 drug therapies. According to the results of the network meta-analysis and SUCRA, the best three interventions for improving lumbar bone mineral density (BMD) are XLGB+BP+calcium (83.7%), XLGB+BP (68.5.7%) and XLGB+VD (67.1%). XLGB+calcium was the best combination regimen for improving femoral neck BMD and increasing bone Gla protein (BGP) and alkaline phosphatase (ALP) contents in serum. The SUCRA values of XLGB+calcium for improving the three outcome indicators were 68.0%, 59.5% and 82.1%, respectively.

Conclusions: The results of this network meta-analysis show that combined application of XLGB can effectively improve BMD and serum BGP and ALP compared to calcium alone, VD or BP. In the future, multicenter, large-sample and double-blind clinical RCTs should be carried out to supplement and verify the results of this study.

Keywords: traditional Chinese medicine, efficacy, Xianling Gubao capsule, postmenopausal osteoporosis, network meta-analysis

OPEN ACCESS

Edited by:
Qi Wang,
Guangzhou University of Chinese Medicine, China

Reviewed by:
Alessandro de Sire,
University of Magna Graecia, Italy
Jianxiong Ma,
Tianjin Hospital, China
Tao Gui,
Jinan University, China
Claudia Cristina Biguetti,
The University of Texas at Dallas, United States

***Correspondence:**
Zi-ping Li
lzip008@163.com
Ling-feng Zeng
zenglf6778@163.com

***ORCID:**
Jin-long Zhao
orcid.org/0000-0001-7079-1336
Ling-feng Zeng
orcid.org/0000-0001-8149-242X

‡These authors have contributed equally to this work

Specialty section:
This article was submitted to Bone Research, a section of the journal Frontiers in Endocrinology

Received: *20 December 2021*
Accepted: *24 January 2022*
Published: *18 February 2022*

Citation:
Luo M-h, Zhao J-l, Xu N-j, Xiao X, Feng W-x, Li Z-p and Zeng L-f (2022) Comparative Efficacy of Xianling Gubao Capsules in Improving Bone Mineral Density in Postmenopausal Osteoporosis: A Network Meta-Analysis. Front. Endocrinol. 13:839885. doi: 10.3389/fendo.2022.839885

INTRODUCTION

Postmenopausal osteoporosis (PMOP) is a systemic metabolic bone disease characterized by decreased bone mass, increased bone fragility and easy fracture (1). PMOP generally occurs within 5 to 10 years after menopause (2). Based on epidemiological statistics, there are approximately 27.6 million patients with osteoporosis over 50 years old in EU countries, including 22 million women, with a prevalence rate of 22.1% (3). The prevalence rate of osteoporosis in women is approximately three times that in men (3). The decline in ovarian function and the decrease in estrogen secretion in postmenopausal women can lead to an imbalance in bone turnover, a decrease in bone mass and an increase in bone fragility (4). A low BMI index, low milk intake, alcohol consumption, fracture history and smoking are risk factors for PMOP, and strengthening the management of the above controllable risk factors is beneficial to reduce PMOP complications (5). At present, the main drug used for the treatment of PMOP is a bone resorption inhibitor. Bisphosphonates, estrogens and other drugs recommended in clinical practice guidelines have good clinical efficacy, but their safety remains a concern (4, 6). Therefore, it is important to seek effective drugs while improving drug safety.

In traditional Chinese medicine, osteoporosis belongs to the category of "*Guwei*", which is closely related to kidney deficiency: "The kidney stores essence and the main bone generates marrow" (7). Therefore, kidney nourishing is closely related to bone marrow regeneration. Xianling Gubao capsule (XLGB) is mainly used to clinically treat osteoporosis and osteoarthritis. XLGB includes *Epimedium*, *Dipsacus*, *Psoralea*, *Rehmannia glutinosa*, *Salvia miltiorrhiza* and *Anemarrhena asphodeloides*, which have the functions of nourishing the liver and kidney, activating blood circulation and dredging collaterals, and strengthening tendons and bones (7, 8). Kidney-tonifying herbs or compounds, such as XLGB, can regulate the proliferation and differentiation of osteoblasts and osteoclasts through a variety of signaling pathways to achieve a dynamic balance (8). XLGB is widely used in the treatment of PMOP in China, but compared with other types of drug regimens or combination therapy, an evidence-based foundation is lacking. Although XLGB is widely used in China, the comparison of efficacy and safety between XLGB and other drugs or combination therapies remains controversial (7, 8), and it is necessary to further evaluate efficacy between XLGB and other therapies. Therefore, this study used the frequency network meta-analysis method to compare the clinical efficacy of XLGB and other drug regimens for the treatment of PMOP to provide an evidence-based foundation for the rational clinical application of XLGB.

MATERIALS AND METHODS

Inclusion Criteria

The inclusion criteria were as follows. 1) Participants: female postmenopausal patients with a clear diagnosis of primary osteoporosis and clear diagnostic criteria for osteoporosis in the study. 2) Interventions and comparisons: the experimental group was treated with XLGB alone or combined with XLGB on the basis of routine intervention measures in the control group; the control group was treated with no intervention, placebo or conventional Western medicine. 3) Outcome measure: the main outcome indicators were lumbar bone mineral density (BMD) and femoral neck BMD, and secondary outcome indicators were bone Gla protein (BGP) and alkaline phosphatase (ALP); all included studies involved at least one of the above evaluation indicators. 4) Study design: randomized controlled trials (RCTs) and nonrandomized controlled trials (non-RCTs). 5) To ensure the test efficiency of this study, the number of studies included in the intervention measures was ≥ 2.

Exclusion Criteria

The exclusion criteria were as follows: 1) animal experiments and case reports; 2) studies with incorrect or incomplete data; 3) studies with unobtainable full texts; and 4) repeated published literature.

Literature Search

We searched the China National Knowledge Infrastructure (CNKI), Wanfang, SinoMed, PubMed, Embase and Cochrane Library databases to identify clinical trials of XLGB for the treatment of PMOP. The retrieval time limit was from the establishment of each database to November 22, 2021. Each database was searched using subject words combined with free words. English search terms included "Xianlingguao", "Xianling Gubao", "XLGB", "osteoporosis", "postmenopausal osteoporosis", "postmenopausal osteoporosis", "primary osteoporosis", and "PMOP". The retrieval strategy for each database is shown in **Supplementary Material 1**.

Literature Screening and Data Extraction

Two researchers followed the inclusion and exclusion criteria to independently screen the literature and extract data; any disagreements were resolved by the corresponding author. The extracted contents included basic information, bias risk factors, and outcome index data.

Bias Risk Assessment

Literature quality was evaluated using Cochrane's recommended risk of bias assessment tool version 2.0 (Rob 2.0) (9). The evaluation tool assesses the risk of bias in five areas, including bias generated in the random process, bias deviating from the established intervention, bias of missing outcome data, bias of outcome measurement and bias of selective reporting of results.

Statistical Analysis

The relative advantages and disadvantages of network meta-analysis can be evaluated by direct or indirect comparisons and the cumulative ranking probability. This study was based on the frequency framework and used Stata/MP 14.0 with the mvmeta and network packages (10–12). All indexes were analyzed using a random effect model. As the outcome indicators considered in this study were continuous variables, the mean difference (MD) was used as the effect value; the result is expressed with a 95% confidence interval (CI).

The size of the dot in the network diagram represents the sample size of the intervention, and the thickness of the line represents the amount of direct evidence between the two interventions. If there was

a closed loop in the diagram, the inconsistency test was employed to evaluate consistency between the results of direct comparison and indirect comparison. If no closed loop formed, the consistency model was directly used for analysis. The surface under the cumulative ranking curve (SUCRA) was applied to rank the interventions of each outcome index, with a greater SUCRA value indicating a better the effect of the intervention. A "comparison correction" funnel plot was used to identify a small-sample effect between studies and publication bias in the studies included.

RESULTS

Literature Search Results

We preliminarily searched 1709 relevant studies, and 784 remained after deleting duplicate studies. After reading the titles and abstracts, we screened a total of 92 articles for full-text evaluation. A total of 22 clinical studies (13–34) were included after reading the full texts with reference to our inclusion and exclusion criteria. The process and results of the literature screening are shown in **Figure 1**.

Basic Characteristics of the Included Studies

A total of 22 studies (13–34) (including 19 RCTs and 3 non-RCTs) were included: 4 three-arm (21, 23, 26, 30) tests and 18 two-arm tests (13–20, 22, 24, 25, 27–29, 31–34). The total sample size was 2016 cases, including 924 cases in the treatment group and 1092 cases in the control group. The treatment course and follow-up time included in the study ranged from 1 to 12 months. Twelve medication measures were involved: calcium, XLGB, bisphosphonate (BP), XLGB+calcium, XLGB+BP, XLGB

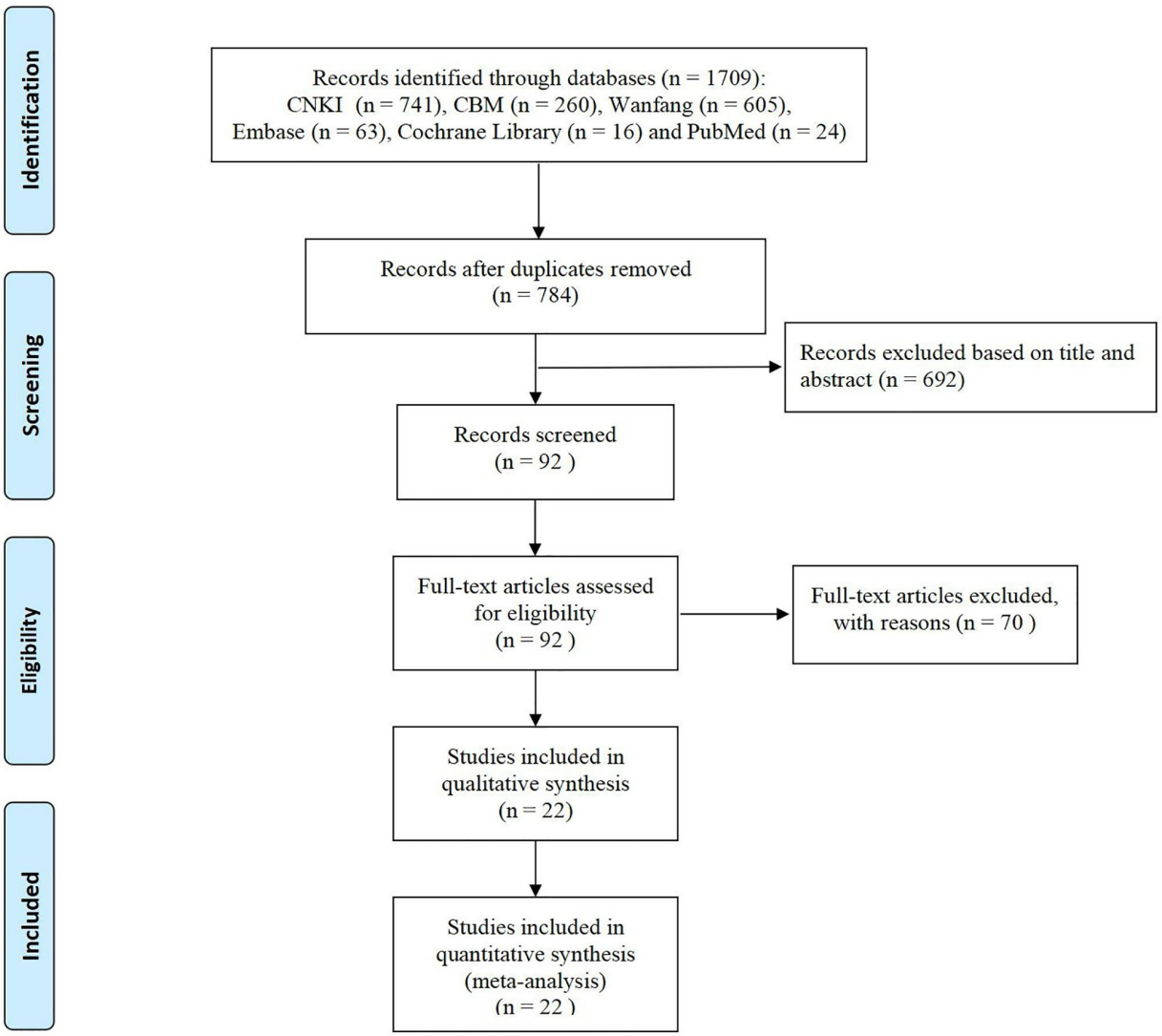

FIGURE 1 | Flow diagram of the study selection process.

+BP+calcium, XLGB+vitamin D (VD), VD, BP+calcium, calcium+VD, estrogen+calcium, and XLGB+calcium+VD. The basic information of the included studies is shown in **Table 1**.

Quality Evaluation of the Included Studies

Nineteen studies (13, 15–18, 20–32, 34) reported specific methods of random assignment or a description of "random" assignment. In 18 studies (13, 15–17, 20–32, 34), intervention was according to the research protocol, whereas the specific basic treatment was not specified in the other 4 studies (14, 17, 19, 33). The outcome index data of all studies were complete and extractable. Because 3 studies (14, 15, 33) did not implement strict blinding methods, measurement bias may have been present. No selective reports were found. Overall, the quality of the literature included was general, and a more rigorous double-blind trial design is needed. The risk assessment of the included studies is shown in **Figure 2**.

Traditional Meta-analysis

1) Lumbar BMD (**Table 2**). Compared with calcium alone, XLGB+calcium significantly improved lumbar BMD (MD = 0.13, 95% CI [0.03, 0.22]). In addition, XLGB+VD showed more advantages in improving lumbar BMD compared with VD (MD = 0.09, 95% CI [0.04, 0.14]) or XLGB (MD = -0.09, 95% CI [-0.12, -0.06]) alone. Overall, the combined application of XLGB can improve the BMD of the lumbar spine compared with

TABLE 1 | The characteristics of the included studies.

Included studies	Treatment Group 1				Treatment Group 2				Study design	Treatment course (months)
	Treatment	Sample size	Age (years)	Years since menopause (years)	Treatment	Sample size	Age (years)	Years since menopause (years)		
Zhu HM (13)	XLGB +Calcium +VD	61	65.4 ± 6.3	15.5 ± 6.4	Calcium +VD	61	64.9 ± 6.0	15.1 ± 7.2	RCT	12
Zhang H (14)	XLGB+BP +Calcium	28	68.34 ± 3.25	–	–	28	67.64 ± 3.56	–	Non - RCT	12
Wu N (15)	XLGB+BP +Calcium	33	54.2 ± 4.2	–	Calcium	23	55.6 ± 3.9	–	RCT	6
Li L (16)	XLGB+BP +Calcium	34	58.2 ± 0.3	3.5 ± 0.4	BP +Calcium	34	58.5 ± 0.3	3.2 ± 0.5	RCT	6
Ni G (17)	XLGB	35	66.3 ± 5.8	14.8 ± 4.5	XLGB+VD	45	65.1 ± 7.9	16.9 ± 7.2	RCT	2
Wang M (18)	XLGB+VD	45	65.4 ± 7.3	15.6 ± 6.4	BP	45	64.7 ± 8.2	15.2 ± 7.1	RCT	6
Lai F (19)	XLGB+BP	30	63.52	–	BP	30	63.15	–	Non - RCT	3
Dai Y (20)	XLGB +Calcium	53	55.88 ± 5.64	6.89 ± 3.59	Calcium	53	56.73 ± 5.17	7.83 ± 2.63	RCT	1
Zhang X* (21)	XLGB +Calcium	62	–	–	Estrogen +Calcium	66	–	–	RCT	12
					Calcium	50	–	–		
Wu W (22)	XLGB +Calcium	34	55.6 ± 4.3	13.6 ± 3.4	Calcium	34	56.4 ± 4.6	13.8 ± 4.1	RCT	12
Xu M* (23)	XLGB+BP	52	–	–	BP	52	–	–	RCT	6
					XLGB	52	–	–		
Cai C (24)	XLGB+BP	63	58.79 ± 8.82	5.86 ± 1.52	BP	63	59.66 ± 7.34	5.92 ± 1.55	RCT	6
Nie D (25)	XLGB+VD	35	59.8	48.6	VD	35	60.3	49.3	RCT	2
Wu Z* (26)	XLGB +Calcium	38	51.2 ± 3.2	6.3 ± 1.1	Calcium	37	56.3 ± 3.5	6.7 ± 2.0	RCT	1
					XLGB	33	55.1 ± 2.9	6.5 ± 2.3		
Wang Y (27)	XLGB+VD	50	67.81 ± 7.04	13.25 ± 5.62	VD	50	66.74 ± 6.85	13.85 ± 5.19	RCT	2
Li Y (28)	XLGB +Calcium	51	62.2 ± 2.3	9.9 ± 1.4	Calcium	51	61.8 ± 2.5	9.8 ± 1.6	RCT	–
Chen X (29)	XLGB +Calcium +VD	30	56.45 ± 5.33	5.84 ± 4.43	Calcium +VD	30	54.86 ± 5.19	5.66 ± 4.28	RCT	6
Shang Y* (30)	XLGB +Calcium	30	–	–	Estrogen +Calcium	30	–	–	RCT	6
					Calcium	30	–	–		
Liu M (31)	XLGB	34	73.50 ± 12.25	–	Calcium	34	73 ± 12.16	–	RCT	1
Song X (32)	XLGB +Calcium	31	56 ± 3.16	8.32 ± 2.67	Calcium	31	55.21 ± 2.97	7.28 ± 1.95	RCT	6
Zhou J (33)	XLGB+BP +Calcium	63	66.79 ± 8.16	12.29 ± 2.07	BP +Calcium	63	66.72 ± 8.24	13.12 ± 2.15	Non - RCT	6
Zhuang L (34)	XLGB+BP	32	59.78 ± 2.17	–	–	32	60.34 ± 2.35	–	RCT	6

*XLGB, Xianling Gubao Capsule; VD, vitamin D; BP, bisphosphonate; RCT, randomized controlled trail. *Three-arm experiment.*

BP (MD = 0.10, 95% CI [0.07, 0.13]) or BP+calcium (MD = 0.13, 95% CI [0.08, 0.18]).

2) Femoral neck BMD (**Table 3**). Compared with VD (MD = 0.03, 95% CI [0.01, 0.06]) or XLGB (MD = -0.09, 95% CI [-0.11, -0.07]) alone, XLGB+VD significantly improved femoral neck the BMD. Compared with calcium alone (MD = 0.17, 95% CI [0.06, 0.29]) or BP+calcium (MD = 0.09, 95% CI [0.03, 0.15]), combined application of XLGB displayed a synergistic role in improving the BMD of the femoral neck.

3) ALP (**Table 4**). Compared with calcium alone (MD = 4.26, 95% CI [0.53, 7.98]), XLGB+calcium significantly increased the content of ALP in serum. XLGB+BP+calcium also increased serum ALP compared with BP alone (MD = 2.82, 95% CI [0.89, 4.75]). Nevertheless, XLGB+BP (MD = -2.55, 95% CI [-4.06, -1.04]) or XLGB+BP+calcium (MD = -15.70, 95% CI [-21.51, -9.89]) combination therapy did not necessarily increase the ALP content in serum compared with BP or calcium alone.

4) BGP (**Table 5**). Compared with calcium alone, XLGB +calcium increased the content of BGP in serum (MD = 3.75, 95% CI [0.59, 6.91]), and XLGB+BP+calcium reduced serum BGP compared with BP+calcium (MD = -24.97, 95% CI [-31.66, -18.28]).

Network Meta-analysis

Network Diagram

This study included 12 interventions, 5 of which involved XLGB. The evidence network of the four outcome indicators is shown in **Figure 3**. The lines in the figure represent interventions with a direct comparison, the line thickness represents the number of studies, and the dot size represents the sample size of the intervention.

Inconsistency Test of Closed Loops

The 12 interventions of lumbar BMD formed three closed loops. See **Table 6** for the detection results of the characteristic intercirculation inconsistency factor (IF), 95% CI and intercirculation heterogeneity parameter t^2 of lumbar BMD. The IF values of the three closed loops were 0.040, 0.085, and 0.127, and the lower limit of the 95% CIs was 0, which indicates that the consistency of each closed loop was good; that is, direct comparison and indirect comparison had little impact on the results of the whole network meta-analysis. The statistical results of the reticular meta-analysis of lumbar BMD were highly reliable. The eight interventions of ALP formed two closed loops. As shown in **Table 6**, the consistency of the two closed loops of ALP was good. The seven interventions of BGP formed a closed loop, with a large lower 95% CI limit (3.40), suggesting inconsistency. Therefore, the results of the network meta-analysis of BGP need to be interpreted carefully.

Results of the Network Meta-analysis

In the comparison of lumbar BMD, 45 pairwise comparisons were formed. The results of the network meta-analysis showed obvious advantages for XLGB+calcium in improving lumbar BMD compared with calcium alone (MD = 0.13, 95% CI [0.05, 0.20]), and the difference was statistically significant. In

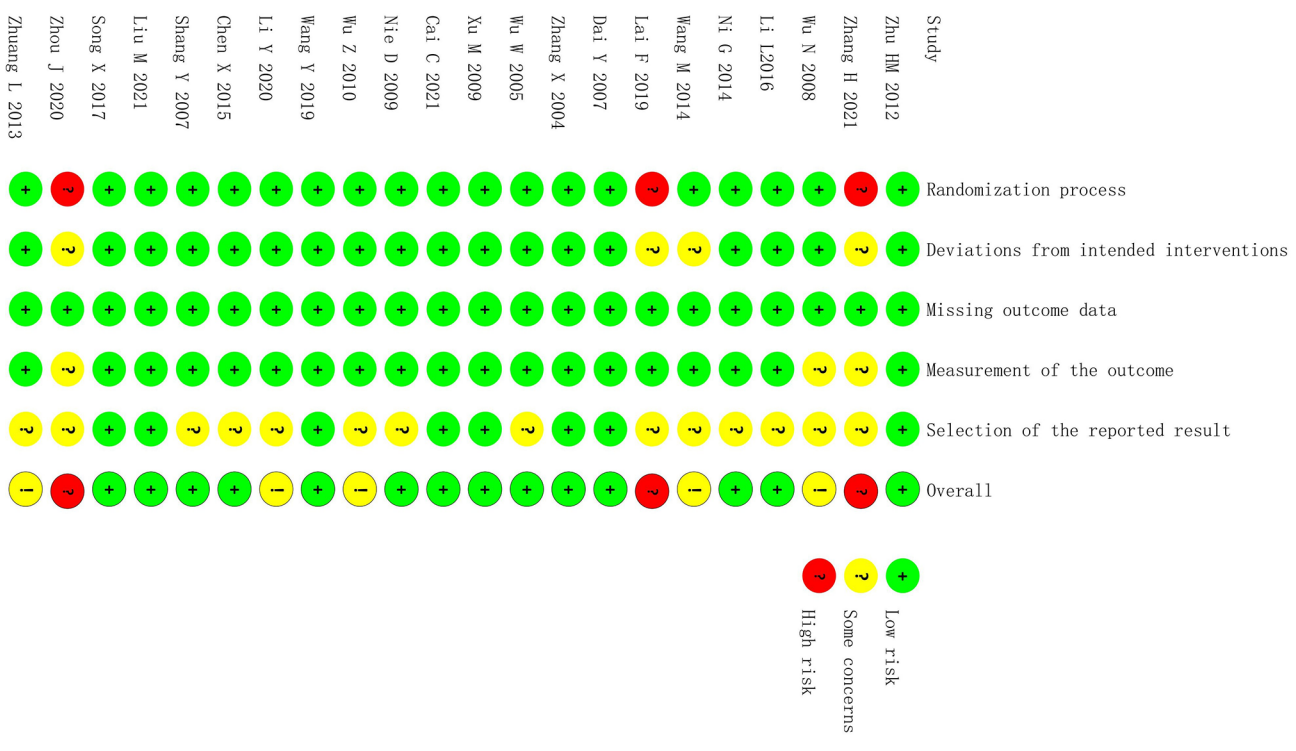

FIGURE 2 | Risk of bias.

TABLE 2 | Traditional Meta-analysis of Lumbar BMD.

Intervention	No. of studies	I^2, %	MD (95% CI)	p value
XLGB+Calcium *vs* Calcium	5	96	0.13 (0.03, 0.22)	0.01
XLGB+BP *vs* BP	3	62	0.04 (0.00, 0.08)	0.05
XLGB+Calcium+VD *vs* Calcium+VD	2	98	0.10 (-0.10, 0.30)	0.32
XLGB+BP+Calcium vs BP	1	–	0.10 (0.07, 0.13)	<0.001
XLGB vs XLGB+VD	1	–	-0.09 (-0.12, -0.06)	<0.001
XLGB+VD vs BP	1	–	0.01 (-0.02, 0.03)	0.70
XLGB+VD vs VD	1	–	0.09 (0.04, 0.14)	0.001
BP vs Calcium	1	–	0.10 (0.05, 0.15)	<0.001
XLGB+BP+Calcium vs BP+Calcium	1	–	0.13 (0.08, 0.18)	<0.001

TABLE 3 | Traditional Meta-analysis of femoral neck BMD.

Intervention	No. of studies	I^2, %	MD (95% CI)	p value
XLGB+Calcium vs Calcium	4	98	0.17 (0.06, 0.29)	0.003
XLGB+BP vs BP	2	78	0.04 (-0.03, 0.10)	0.24
XLGB+Calcium+VD vs Calcium+VD	2	97	0.08 (-0.10, 0.26)	0.38
XLGB+VD vs VD	2	23	0.03 (0.01, 0.06)	0.02
XLGB vs XLGB+VD	1	–	-0.09 (-0.11, -0.07)	<0.001
XLGB+VD vs BP	1	–	0.01 (-0.02, 0.04)	0.44
XLGB vs Calcium	1	–	0.06 (-0.00, 0.12)	0.05
XLGB+BP+Calcium vs BP+Calcium	1	–	0.09 (0.03, 0.15)	0.006

TABLE 4 | Traditional Meta-analysis of BGP.

Intervention	No. of studies	I^2, %	MD (95% CI)	p value
XLGB+Calcium *vs* Calcium	4	98	4.26 (0.53, 7.98)	0.03
XLGB+BP+Calcium vs BP+Calcium	2	99	3.23 (-30.54,-37.00)	0.85
XLGB+BP *vs* BP	1	–	-2.55 (-4.06, -1.04)	<0.001
XLGB+Calcium+VD *vs* Calcium+VD	1	–	0.45 (-2.50, 3.40)	0.76
XLGB+BP+Calcium vs BP	1	–	2.82 (0.89, 4.75)	0.004
XLGB+BP+Calcium vs Calcium	1	–	-15.70(-21.51,-9.89)	<0.001

improving femoral neck BMD, 21 pairwise comparisons were formed. The results of the network meta-analysis showed that XLGB+calcium had more advantages than calcium alone (MD = 0.17, 95% CI [0.07, 0.27]). In terms of improving the contents of serum ALP and BGP, the results of the network meta-analysis did not suggest a pairwise comparison with a significant difference. The results of the network meta-analysis of the four outcome indicators concerned in this study are shown in **Tables 7**–**10**.

SUCRA Probability Ranking

The best SUCRA probability rankings of the improvement effects of different interventions on the four outcome indicators are provided in **Table 11**. In terms of improving lumbar BMD, the best three interventions were XLGB+ BP+calcium (83.7%), XLGB+BP (68.5.7%) and XLGB+VD (67.1%). The three best interventions to improve femoral neck BMD were XLGB +calcium (68.0%), XLGB+BP (67.8%) and XLGB+VD (63.0%). The best interventions to increase the serum ALP content in were XLGB+calcium (59.5%), XLGB (52.6%) and calcium (47.8%). The best measures to improve the serum BGP content were XLGB+calcium (82.1%), estrogen+calcium (73.5%) and calcium (67.7%).

Small-Sample Effect Evaluation

A funnel plot was drawn to evaluate a small-sample effect for the four outcome indicators in this study (**Figure 4**). Different colors in the funnel chart indicate different intervention measures. We found that most dots in the funnel chart of BMD of the lumbar spine and femoral neck were roughly symmetrically distributed on both sides of the vertical line with X = 0, which suggests no publication bias for these two outcome indicators. For ALP and BGP, a high degree of publication bias and a small sample effect were suggested.

TABLE 5 | Traditional Meta-analysis of ALP.

Intervention	No. of studies	I^2, %	MD (95% CI)	p value
XLGB+Calcium *vs* Calcium	5	100	5.36(-26.04, 36.76)	0.74
XLGB+VD vs BP	1	–	-1.00(-3.03, 1.03)	0.33
XLGB vs Calcium	1	–	3.75 (0.59, 6.91)	0.02
XLGB+BP+Calcium vs BP+Calcium	1	–	-24.97 (-31.66, -18.28)	<0.001

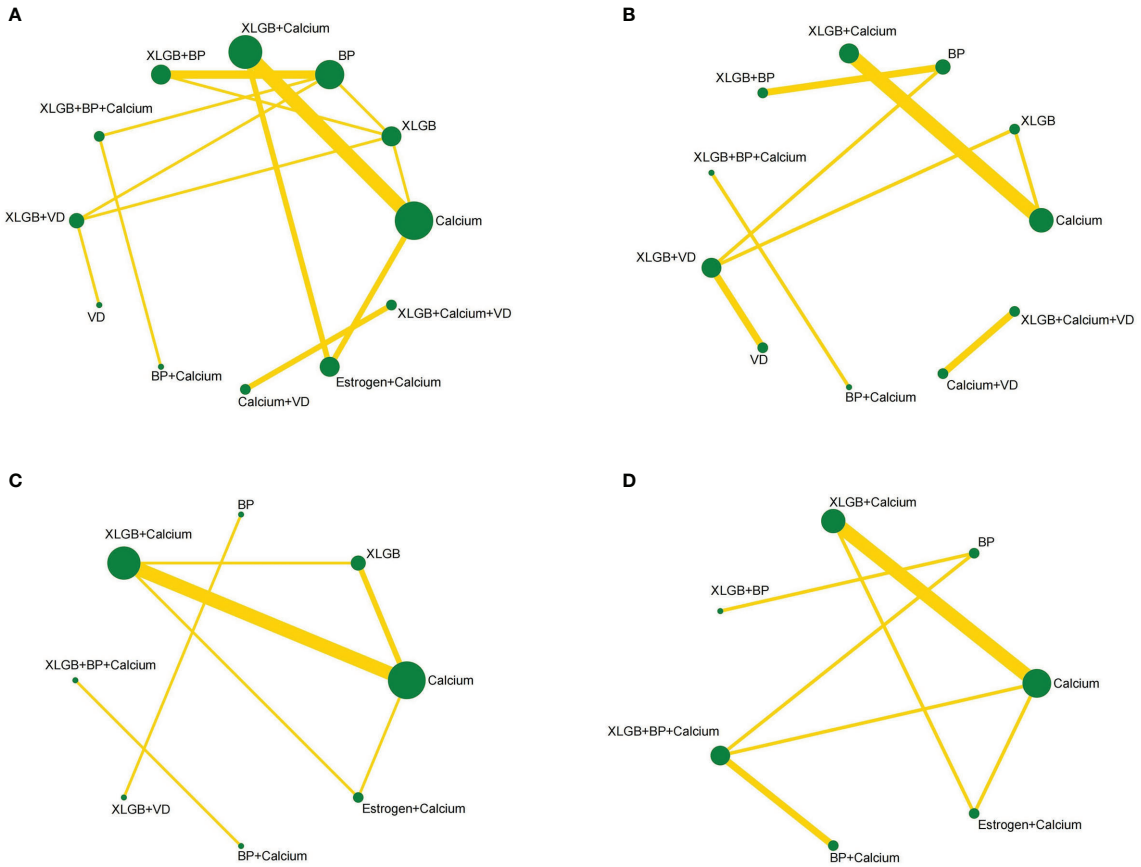

FIGURE 3 | Network diagrams depicting direct evidence used in network meta-analysis. **(A)** Network diagram of lumbar BMD. **(B)** Network diagram of BMD of femoral neck. **(C)** Network diagram of BGP. **(D)** Network diagram of ALP.

DISCUSSION

This study evaluated the efficacy of XLGB and other combined therapies for the treatment of PMOP by network meta-analysis. The results show that the combined application of XLGB can well treat PMOP. Osteoporosis is a systemic bone disease characterized by reduced bone mass and degeneration of bone microstructure, which leads to increased bone fragility and easy fracture (1). Among the types of osteoporosis, PMOP has a high incidence rate (3). XLGB is a Chinese patent medicine widely used for the treatment of osteoporosis (35–37). Due to the lack of comparisons between XLGB and other drug regimens in the treatment of PMOP, this study ranked the clinical efficacy of XLGB-related drug regimens in PMOP treatment with the help of network meta-analysis to provide an evidence-based foundation for its clinical use.

Traditional meta-analysis is a direct comparison between intervention measures, which can most intuitively compare differences in efficacy among drug regimens. In terms of improving lumbar BMD and femoral neck BMD (13, 14, 17, 18, 20–25, 27–34), combined application of XLGB can improve lumbar BMD and femoral neck BMD compared with calcium and VD alone, and XLGB+BP+calcium showed more advantages than BP

TABLE 6 | Results of the closed-loop inconsistency test.

Outcome indicators	Closed-Loop	IF	95%CI (truncated)	Loop-specific Heterogeneity(t^2)	z-value	p-value
LBMD	Calcium - XLGB+Calcium - Calcium+VD	0.127	(0.00, 0.36)	0.010	1.058	0.0290
	XLGB - BP - XLGB+VD	0.085	(0.04, 0.13)	0.000	0.023	0.000
	XLGB - BP - XLGB+BP	0.040	(0.00, 0.09)	0.000	0.027	0.142
ALP	Calcium - BP - XLGB+Calcium	71.847	(0.00, 202.01)	741.190	1.082	0.279
	Calcium - XLGB - BP	0.005	(0.00, 129.84)	1233.224	0.000	1.000
BGP	Calcium - BP - XLGB+VD	5.260	(3.40, 7.12)	0.000	5.555	0.000

TABLE 7 | Network meta-analysis of lumbar BMD.

XLGB+BP +Calcium								
0.06 (-0.13, 0.25)	XLGB+BP							
0.07 (-0.14, 0.28)	0.00 (-0.15, 0.16)	XLGB+VD						
0.10 (-0.17, 0.38)	0.04 (-0.19, 0.27)	0.04 (-0.19, 0.26)	XLGB + Calcium					
0.10 (-0.06, 0.26)	0.04 (-0.06, 0.13)	0.03 (-0.10, 0.16)	-0.00 (-0.23, 0.22)	BP				
0.13 (-0.16, 0.42)	0.07 (-0.17, 0.31)	0.06 (-0.18, 0.30)	0.03 (-0.08, 0.14)	0.03 (-0.20, 0.27)	Estrogen + Calcium			
0.13 (-0.04, 0.30)	0.07 (-0.19, 0.32)	0.06 (-0.21, 0.33)	0.03 (-0.30, 0.35)	0.03 (-0.21, 0.27)	-0.00 (-0.34, 0.33)	BP+Calcium		
0.13 (-0.07, 0.34)	0.07 (-0.07, 0.20)	0.06 (-0.07, 0.19)	0.03 (-0.16, 0.21)	0.03 (-0.09, 0.16)	0.00 (-0.20, 0.20)	0.00 (-0.27, 0.27)	XLGB	
0.16 (-0.11, 0.43)	0.09 (-0.13, 0.32)	0.09 (-0.08, 0.26)	0.05 (-0.23, 0.34)	0.06 (-0.16, 0.27)	0.03 (-0.27, 0.32)	0.03 (-0.29, 0.35)	0.03 (-0.19, 0.24)	VD
0.23 (-0.04, 0.50)	0.17 (-0.05, 0.38)	0.16 (-0.05, 0.37)	0.13 (0.05, 0.20)	0.13 (-0.08, 0.34)	0.10 (-0.01, 0.21)	0.10 (-0.21, 0.42)	0.10 (-0.07, 0.27)	0.07 (-0.20, 0.34)

TABLE 8 | Network meta-analysis of femoral neck BMD.

XLGB+Calcium						
0.00 (-0.38, 0.38)	XLGB+BP					
0.02 (-0.27, 0.32)	0.02 (-0.21, 0.26)	XLGB+VD				
0.04 (-0.31, 0.39)	0.04 (-0.10, 0.18)	0.01 (-0.18, 0.21)	BP			
0.06 (-0.27, 0.38)	0.06 (-0.22, 0.33)	0.03 (-0.10, 0.17)	0.02 (-0.22, 0.26)	VD		
0.11 (-0.11, 0.33)	0.11 (-0.19, 0.42)	0.09 (-0.10, 0.28)	0.08 (-0.20, 0.35)	0.06 (-0.18, 0.29)	XLGB	
0.17 (0.07, 0.27)	0.17 (-0.19, 0.54)	0.15 (-0.13, 0.42)	0.14 (-0.20, 0.47)	0.11 (-0.19, 0.42)	0.06 (-0.14, 0.26)	Calcium

alone. Furthermore, combined application of XLGB on the basis of BP+calcium had a good clinical effect on improving lumbar BMD. XLGB+calcium exhibited more advantages than calcium alone in increasing the content of serum BGP, and XLGB+BP+calcium had better clinical efficacy than BP alone (13–16, 20–22, 24, 28, 33). Moreover, XLGB showed better clinical efficacy than calcium in improving serum ALP content.

Network meta-analysis was used to examine differences among interventions through indirect comparisons. The results of this study show that XLGB+BP+calcium is most likely the optimal treatment for improving lumbar BMD but that XLGB+calcium is the best combination regimen for improving femoral neck BMD and increasing contents of serum BGP and ALP. Combining the results of this traditional meta-analysis and network meta-analysis, compared with the schemes of VD, BP or calcium alone, combined application of XLGB showed better clinical efficacy in improving BMD and serum BGP and ALP. In traditional Chinese medicine, orthopedic diseases such as osteoporosis are believed to be the manifestation of kidney deficiency. The kidney governs bone and generates marrow, which should be used to tonify the kidney and strengthen *Yang* (38, 39). Deficiency of the kidney and spleen is the root cause of the disease, and blood stasis is the promoting factor. Blood stasis further aggravates injury to the spleen and kidney and then accelerates the occurrence of osteoporosis (39). XLGB, which is mainly composed of *Epimedium* supplemented with *Dipsacus*, *Salvia miltiorrhiza*, *Rehmannia glutinosa* and *Anemarrhena asphodeloides*, has the effects of nourishing the liver and kidney, activating blood circulation and dredging collaterals, and strengthening tendons and bones (40). Previous studies have shown that XLGB combined with calcium or BP has a better clinical effect in the treatment of osteoporosis (7, 41), which is consistent with our conclusions. In addition, theoretical studies have shown that XLGB inhibits osteoclast activity and promotes osteoblast differentiation by regulating OPG/RANK/RANKL (42). Animal experiments have shown that XLGB increases the contents of Ca and P in rat serum, reduces the contents of ALP, OCN and DPD in serum, and increases the BMD of vertebrae as well as the

TABLE 9 | Network meta-analysis of ALP.

XLGB+Calcium			
2.76 (-61.02, 66.54)	XLGB		
5.44 (-33.30, 44.18)	2.68 (-55.84, 61.19)	Calcium	
14.99 (-63.45, 93.43)	12.23 (-83.43, 107.89)	9.55 (-68.90, 88.01)	Estrogen+Calcium

TABLE 10 | Network meta-analysis of BGP.

XLGB+Calcium						
2.17 (-20.15, 24.49)	Estrogen+Calcium					
4.82 (-7.62, 17.25)	2.65 (-19.67, 24.97)	Calcium				
19.90 (-7.98, 47.78)	17.73 (-15.75, 51.21)	15.08 (-9.88, 40.04)	XLGB+BP+Calcium			
22.46 (-14.53, 59.45)	20.29 (-21.08, 61.67)	17.65 (-17.19, 52.48)	2.56 (-22.09, 27.22)	BP		
24.93 (-19.45, 69.31)	22.76 (-25.34, 70.86)	20.12 (-22.49, 62.72)	5.03 (-29.82, 39.88)	2.47 (-22.27, 27.21)	XLGB+BP	
23.33 (-9.63, 56.28)	21.16 (-16.66, 58.97)	18.51 (-12.02, 49.04)	3.43 (-14.25, 21.10)	0.86 (-29.46, 31.19)	-1.60 (-40.67, 37.46)	BP+Calcium

TABLE 11 | Rank of efficacy of included treatments.

Outcome indicator / Treatment methods	BMD of lumbar vertebra		BMD of femoral neck		ALP		BGP	
	SUCRA value	Rank	SUCRA value	Rank	SUCRA value	Rank	SUCRA value	Rank
Calcium	11.6	10	16.9	7	47.8	3	67.7	3
XLGB	40.2	8	31.7	6	52.6	2	–	–
BP	51.9	5	54.4	4	–	–	32.8	5
XLGB + Calcium	54.8	4	68.0	1	59.5	1	82.1	1
XLGB + BP	68.5	2	67.8	2	–	–	28.5	7
XLGB + BP + Calcium	83.7	1	–	–	–	–	37.1	4
XLGB + VD	67.1	3	63.0	3	–	–	–	–
VD	34.9	9	48.3	5	–	–	–	–
BP + Calcium	42.1	7	–	–	–	–	28.4	6
Calcium + VD	–	–	–	–	–	–	–	–
Estrogen + Calcium	45.1	6	–	–	40.1	4	73.5	2
XLGB + Calcium + VD	–	–	–	–	–	–	–	–

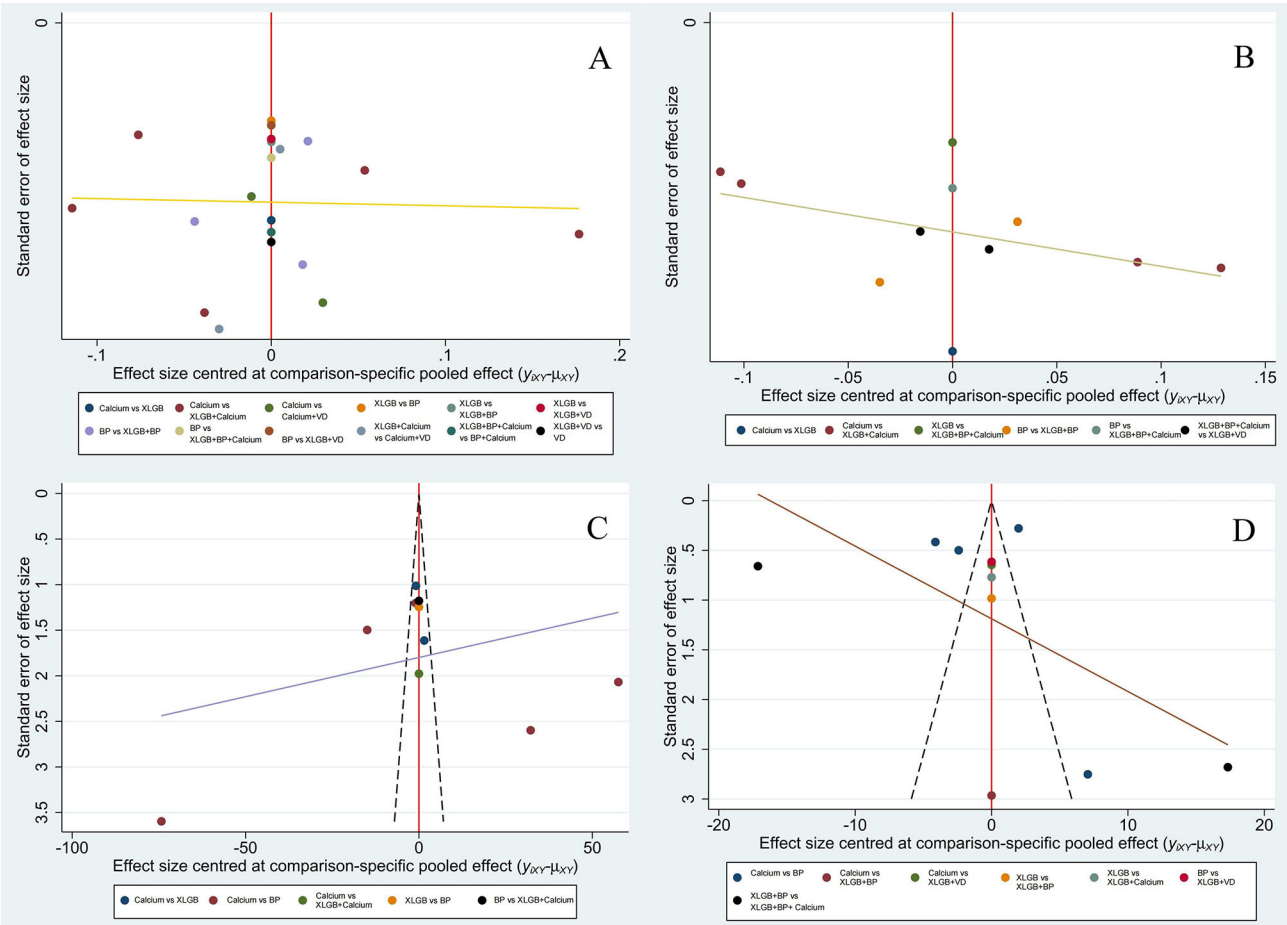

FIGURE 4 | Comparison-adjusted funnel plot of lumbar BMD **(A)**, BMD of the femoral neck **(B)**, BGP **(C)** and ALP **(D)**.

femur and tibia (43). The above results provide a theoretical basis for using XLGB to treat PMOP.

This study has the following limitations. 1) Due to the lack of direct comparison evidence for each outcome index, it was not possible to rank the probability of individual interventions. 2) Most of the included studies were small-sample studies, reducing the statistical efficiency of tour analysis. None of the studies provided strict sample-size estimation standards, which may affect authenticity. 3) We also detected statistical heterogeneity and publication bias, and a pharmacoeconomic evaluation was not included. Furthermore, the great differences in the course of treatment and follow-up time included in the literature may also affect the credibility of the results. Therefore, the conclusions of this study need to be applied in combination with clinical practice. 4) Due to the limitations of this study, further animal or cell experiments are needed to verify the results to provide a more experimental or clinical basis.

CONCLUSION

The results of this network meta-analysis show that combined application of XLGB can effectively improve BMD and serum BGP and ALP compared to calcium, VD or BP alone. In the future, multicenter, large-sample and double-blind clinical RCTs need to be carried out to supplement and validate the results of this study.

DATA AVAILABILITY STATEMENT

The original contributions presented in the study are included in the article/**Supplementary Material**. Further inquiries can be directed to the corresponding authors.

AUTHOR CONTRIBUTIONS

M-hL and J-lZ conceptualized the research question. M-hL and J-lZ participated in drafting and writing the review. N-jX, XX, W-xF, and J-lZ participated in the formulation of retrieval strategies, data acquisition, data analysis, and quality assessment. M-hL, XX, and J-lZ participated in the drawing of tables and figures. Z-pL and L-fZ participated in critical revision of the manuscript. All authors contributed to the research and approved the final manuscript.

FUNDING

This work was supported by the National Natural Science Foundation of China (No.82004383, No. 81974574), the National key research and development program (2021YFC1712804), the Project of Administration of Traditional Chinese Medicine of Guangdong Province (No.20201129), the Project of Guangdong Provincial Department of Finance (No. [2014]157, No. [2018]8), the Medical Science Research Foundation of Guangdong Province (No.A2020105, No.B2019091), the Science and Technology Planning Project of Guangzhou (No. 202102010273) and the Science and Technology Research Project of Guangdong Provincial Hospital of Chinese Medicine (No.YN2019ML08, YN2015MS15).

SUPPLEMENTARY MATERIAL

The Supplementary Material for this article can be found online at: https://www.frontiersin.org/articles/10.3389/fendo.2022.839885/full#supplementary-material

REFERENCES

1. Anastasilakis AD, Polyzos SA, Yavropoulou MP, Makras P. Combination and Sequential Treatment in Women With Postmenopausal Osteoporosis. *Expert Opin Pharmaco* (2020) 21(4):477–90. doi: 10.1080/14656566.2020.1717468
2. Ono Y, Miyakoshi N, Kasukawa Y, Akagawa M, Kimura R, Nagahata I, et al. Diagnosis of Presarcopenia Using Body Height and Arm Span for Postmenopausal Osteoporosis. *Clin Interv Aging* (2020) 15:357–61. doi: 10.2147/CIA.S231759
3. Hernlund E, Svedbom A, Ivergård M, Compston J, Cooper C, Stenmark J, et al. Osteoporosis in the European Union: Medical Management, Epidemiology and Economic Burden. *Arch Osteoporosis* (2013) 8:1–2. doi: 10.1007/s11657-013-0136-1
4. Black DM, Rosen CJ, Solomon CG. Postmenopausal Osteoporosis. *N Engl J Med* (2016) 374(3):254–62. doi: 10.1056/NEJMcp1513724
5. Migliaccio S, Francomano D, Romagnoli E, Marocco C, Fornari R, Resmini G, et al. Persistence With Denosumab Therapy in Women Affected by Osteoporosis With Fragility Fractures: A Multicenter Observational Real Practice Study in Italy. *J Endocrinol Invest* (2017) 40(12):1321–6. doi: 10.1007/s40618-017-0701-3
6. de Sire A, Baricich A, Renò F, Cisari C, Fusco N, Invernizzi M. Myostatin as a Potential Biomarker to Monitor Sarcopenia in Hip Fracture Patients Undergoing a Multidisciplinary Rehabilitation and Nutritional Treatment: A Preliminary Study. *Aging Clin Exp Res* (2020) 32(5):959–62. doi: 10.1007/s40520-019-01436-8
7. Chen J, Zheng J, Chen M, Lin S, Lin Z. The Efficacy and Safety of Chinese Herbal Medicine Xianling Gubao Capsule Combined With Alendronate in the Treatment of Primary Osteoporosis: A Systematic Review and Meta-Analysis of 20 Randomized Controlled Trials. *Front Pharmacol* (2021) 12:695832. doi: 10.3389/fphar.2021.695832
8. An J, Yang H, Zhang Q, Liu C, Zhao J, Zhang L, et al. Natural Products for Treatment of Osteoporosis: The Effects and Mechanisms on Promoting Osteoblast-Mediated Bone Formation. *Life Sci* (2016) 147:46–58. doi: 10.1016/j.lfs.2016.01.024
9. Sterne JAC, Savović J, Page MJ, Elbers RG, Blencowe NS, Boutron I, et al. RoB 2: A Revised Tool for Assessing Risk of Bias in Randomised Trials. *BMJ* (2019) 366:l4898. doi: 10.1136/bmj.l4898
10. Cipriani A, Furukawa TA, Salanti G, Chaimani A, Atkinson LZ, Ogawa Y, et al. Comparative Efficacy and Acceptability of 21 Antidepressant Drugs for the Acute Treatment of Adults With Major Depressive Disorder: A Systematic Review and Network Meta-Analysis. *Lancet* (2018) 391(10128):1357–66. doi: 10.1016/S0140-6736(17)32802-7
11. Chaimani A, Higgins JPT, Mavridis D, Spyridonos P, Salanti G, B. Haibe-Kains B. Graphical Tools for Network Meta-Analysis in STATA. *PloS One* (2013) 8(10):e76654–4. doi: 10.1371/journal.pone.0076654
12. Marotta N, Demeco A, Moggio L, Marinaro C, Pino I, Barletta M, et al. Comparative Effectiveness of Breathing Exercises in Patients With Chronic Obstructive Pulmonary Disease. *Complement Ther Clin Pract* (2020) 41:101260. doi: 10.1016/j.ctcp.2020.101260
13. Zhu HM, Qin L, Garnero P, Genant HK, Zhang G, Dai K, et al. The First Multicenter and Randomized Clinical Trial of Herbal Fufang for Treatment of Postmenopausal Osteoporosis. *Osteoporosis Int* (2012) 23(4):1317–27. doi: 10.1007/s00198-011-1577-2

14. Zhang H, Wang Y, Nie H. Efficacy of Alendronate Sodium Combined With Xianling Gubao in the Treatment of Osteoporosis in Middle-Aged and Elderly Postmenopausal Patients. *China Med Pharm* (2021) 11(17):231–4. doi: 10.3969/j.issn.2095-0616.2021.17.063
15. Wu N, Chen J, Huang J, Huang J. Clinical Study of Fushanmei Combined With Xianlinggubao in the Treatment of Osteocalcin, Calcitonin and Bone Mineral Density in Postmenopausal Osteoporosis. *Contemp Med* (2008) 147 (11):142–4.
16. Li L. Clinical Study on the Changes of Osteocalcin, Calcitonin and Bone Mineral Density of Fushanmei Combined With Xianlinggubao in the Treatment of Postmenopausal Osteoporosis. *Oriental Diet Ther Health Care* (2016) 9:230–1. doi: 10.3969/j.issn.1672-5018.2016.09.211
17. Ni G. Clinical Observation of Calcitriol Combined With Xianlinggubao in the Treatment of Postmenopausal Osteoporosis. *J New Chin Med* (2014) 46 (02):113–5. doi: 10.13457/j.cnki.jncm.2014.02.032
18. Wang M. *Clinical Study of Calcitriol Combined With Xianlinggubao in Treatment of Women With Osteoporosis*. Baoding City: Hebei University (2014).
19. Lai F, Ma L, Liang X, Liu M, Luo Z, Li J. Clinical Observation on Jintiange Capsules in the Treatment of Postmenopausal Osteoporosis. *Chin Med Modern Distance Educ China* (2019) 17(15):63–5. doi: 10.3969/j.issn.1672-2779.2019.15.026
20. Dai Y, Shen L, Yang Y, Xie J, Zhou P. Effects of Migu Tablet on Bone Mineral Density, Serum Levels of Osteoprotegerin and Its Ligand and Bone Metabolic Markers in Patients With Postmenopausal Osteoporosis. *Chin J Integrated Tradit Western Med* (2007) 27(08):696–9. doi: 10.3321/j.issn:1003-5370.2007.08.009
21. Zhang X, Han J, Qian G, He M, Li Y. Effects of Xianling Gubao Capsule on Bone Mineral Density and Cytokines in Postmenopausal Osteaporofic Patients. *Chin J Osteoporosis* (2004) 10(01):99–102.
22. Wu W, Li D, Zhi X, Han M. Preventive and Therapeutic Effects of Xianling Gubao Capsules for Postmenopausal Osteoporosis. *J Guangzhou Univ Tradit Chin Med* (2005) 22(03):191–3. doi: 10.13359/j.cnki.gzxbtcm.2005.03.008
23. Xu M, Liu B, Huang C, Tang F, Lou Y, Liang Z, et al. Clinical Observation of Xianlinggubao Plus Alendronate on Postmenopausal Osteoporosis. *J Liaoning Univ Tradit Chin Med* (2009) 11(01):94–5. doi: 10.13194/j.jlunivtcm.2009.01.96.xum.106
24. Cai C, He G. Effects of Xianling Gubao Jiaonang on Lipid Metabolism, Bone Metabolism and Bone Density in Postmenopausal Osteoporosis Patients With Obesity. *J Henan Med Coll* (2021) 33(01):27–31. doi: 10.3969/j.issn.1008-9276.2021.01.007
25. Nie D, Peng M, Lin Z, Yang L. Clinical Research on Xianling Gubao Capsule and Rocalirol Tablet in Treating 35 Cases of Postmenopausal Osteoporosis Related Pain. *Rehabil Med* (2009) 19(03):37–8. doi: 10.13261/j.cnki.jfutcm.002170
26. Wu Z. Xianling Gubao Capsule Combined With Caltech D in the Treatment of Postmenopausal Osteoporosis. *Strait Pharm J* (2010) 22(12):159–60.
27. Wang Y, Sheng C. Alfacalcidol Capsules Combined With Xianling Gubao Capsules in Treatment of Postmenopausal Osteoporosis. *Int Med Health Guidance News* (2019) 25(07):1099–102. doi: 10.3760/cma.j.issn.1007-1245.2019.07.027
28. Li Y. Effect of Xianling Gubao Capsule Combined With Calcium Acetate Capsule on Post- Menopausal Women's Osteoporosis. *World J Complex Med* (2020) 6(05):183–5. doi: 10.11966/j.issn.2095-994X.2020.06.05.61
29. Chen X, Zhu X, Lin W, Wang L, Yang S. Effect of Xianlinggubao Capsule in the Treatment of Postmenopausal Osteoporosis and its Effect on Osteoprotegerin, Receptor Activator of Nuclear Factor - κb Ligand. *Chin J Clin Pharmacol* (2015) 31(10):827–9+854. doi: 10.13699/j.cnki.1001-6821.2015.10.019
30. Shang Y, Liu Y, Li H. Clinical Observation of Xianling Gubao Capsule in the Treatment of Postmenopausal Osteoporosis. *Chin J Integrated Tradit Western Med Intensive Crit Care* (2007) 14(01):55.
31. Liu M, Yang F, Zeng L. Clinical Observation of Xianling Gubao Capsule in the Treatment of Postmenopausal Women With Osteoporosis. *Yunnan J Tradit Chin Med Materia Med* (2021) 42(06):37–40. doi: 10.16254/j.cnki.53-1120/r.2021.06.012
32. Song X. The Clinical Research Into Menopausal Osteoporosis Treated With Xianlinggubao Capsules. *Henan Tradit Chin Med* (2017) 37(04):686–8. doi: 10.16367/j.issn.1003-5028.2017.04.0244
33. Zhou J. Effects of Xianling Gubao Combined With Alendronate on Bone Metabolic Indexes, Bone Mineral Density and Symptoms of Bone Pain in Postmenopausal Osteoporosis. *Chin J Gerontol* (2020) 40(03):581–4. doi: 10.3969/j.issn.1005-9202.2020.03.041
34. Zhuang L. Xianlinggubao Combined With Fushanmei in the Treatment of Postmenopausal Osteoporosis. *Zhejiang J Integrated Tradit Chin Western Med* (2013) 23(07):558–60.
35. Wang X, He Y, Guo B, Tsang M, Tu F, Dai Y, et al. *In Vivo* Screening for Anti-Osteoporotic Fraction From Extract of Herbal Formula Xianlinggubao in Ovariectomized Mice. *PloS One* (2015) 10(2):e0118184. doi: 10.1371/journal.pone.0118184
36. Wu H, Zhong Q, Wang J, Wang M, Fang F, Xia Z, et al. Beneficial Effects and Toxicity Studies of Xian-Ling-Gu-Bao on Bone Metabolism in Ovariectomized Rats. *Front Pharmacol* (2017) 8:273. doi: 10.3389/fphar.2017.00273
37. Ai L, Yi W, Chen L, Wang H, Huang Q. Xian-Ling-Gu-Bao Protects Osteoporosis Through Promoting Osteoblast Differentiation by Targeting miR-100-5p/KDM6B/RUNX2 Axis. *In Vitro Cell Dev Biol Anim* (2021) 57 (1):3–9. doi: 10.1007/s11626-020-00530-w
38. Chen YY, Hsue YT, Chang HH, Gee MJ. The Association Between Postmenopausal Osteoporosis and Kidney-Vacuity Syndrome in Traditional Chinese Medicine. *Am J Chin Med* (1999) 27(1):25–35. doi: 10.1142/S0192415X99000057
39. Liang J, Wang F, Huang J, Xu Y, Chen G. The Efficacy and Safety of Traditional Chinese Medicine Tonifying-Shen (Kidney) Principle for Primary Osteoporosis: A Systematic Review and Meta-Analysis of Randomized Controlled Trials. *Evid Based Complement Alternat Med* (2020) 2020:1–21. doi: 10.1155/2020/5687421
40. Qin L, Zhang G, Hung W, Shi Y, Leung K, Yeung H, et al. Phytoestrogen-Rich Herb Formula "XLGB" Prevents OVX-Induced Deterioration of Musculoskeletal Tissues at the Hip in Old Rats. *J Bone Miner Metab* (2005) 23(S1):55–61. doi: 10.1007/BF03026324
41. Wang G, Liao X, Zhang Y, Xie Y. Systemic Evaluation and Meta-Analysis of Xianling Gubao Capsule in Treatment of Primary Osteoporosis in Randomized Controlled Trials. *China J Chin Materia Med* (2017) 42 (15):2829–44. doi: 10.19540/j.cnki.cjcmm.20170705.007
42. Qi X, Chen G, Shi P, Zhang Z, Fang C, Zheng S, et al. Analysis of Pharmacological Mechanism of XianlingGubao Capsule in Treating Osteoporosis Based on Network Pharmacology. *Chin J Osteoporosis* (2020) 26(5):710–8. doi: 10.3969/j.issn.1006-7108.2020.05.017
43. Liu M, Xuan Z, Zhang Y, Xu J, Sun Y, Bai Z. Effects of New Xianling Gubao Capsule on Ovariectomized Osteoporotic Rats. *Tradit Chin Drug Res Clin Pharmacol* (2018) 29(4):399–403. doi: 10.19378/j.issn.1003-9783.2018.04.004

Conflict of Interest: The authors declare that the research was conducted in the absence of any commercial or financial relationships that could be construed as a potential conflict of interest.

frontiers in Endocrinology

ORIGINAL RESEARCH
published: 08 March 2022
doi: 10.3389/fendo.2022.866641

Mechanism and Experimental Verification of *Luteolin* for the Treatment of Osteoporosis Based on Network Pharmacology

Guihong Liang[1,2†], Jinlong Zhao[2†], Yaoxing Dou[1,2], Yuan Yang[1,2], Di Zhao[2], Zhanpeng Zhou[3], Rui Zhang[3], Weiyi Yang[1] and Lingfeng Zeng[1,2*]*

[1] The 2nd Affiliated Hospital of Guangzhou University of Chinese Medicine, Guangzhou, China, [2] The Second Clinical Medical College of Guangzhou University of Chinese Medicine, Guangzhou, China, [3] School of Pharmaceutical Sciences, Guangzhou University of Chinese Medicine, Guangzhou, China

OPEN ACCESS

Edited by:
Bo Liu,
Guangdong Provincial Hospital of Chinese Medicine, China

Reviewed by:
Chen Chao,
Southern Medical University, China
Anna Piotrowska,
University School of Physical Education in Krakow, Poland
Yikai Li,
Southern Medical University, China

***Correspondence:**
Weiyi Yang
gdszyyywy@sina.com
Lingfeng Zeng
lfzeng6778@163.com

[†]These authors have contributed equally to this work

Specialty section:
This article was submitted to Bone Research, a section of the journal Frontiers in Endocrinology

Received: *31 January 2022*
Accepted: *14 February 2022*
Published: *08 March 2022*

Citation:
Liang G, Zhao J, Dou Y, Yang Y, Zhao D, Zhou Z, Zhang R, Yang W and Zeng L (2022) Mechanism and Experimental Verification of Luteolin for the Treatment of Osteoporosis Based on Network Pharmacology. Front. Endocrinol. 13:866641. doi: 10.3389/fendo.2022.866641

Purpose: To explore the molecular mechanism of *luteolin* in the treatment of osteoporosis (OP) by network pharmacological prediction and experimentation.

Methods: The target proteins of *luteolin* were obtained with the Traditional Chinese Medicine Systems Pharmacology Database and Analysis Platform (TCMSP). OP-related proteins were extracted from the Comparative Toxicogenomics Database (CTD) and GeneCards and DisGeNET databases. We imported the common protein targets of *luteolin* and OP into the STRING database to obtain the relationships between the targets. The common target proteins of *luteolin* and OP were assessed by KEGG and GO enrichment analyses with the DAVID database. Animal experiments were conducted to verify the effect of *luteolin* on bone mineral density in ovariectomised (OVX) rats. Finally, the effects of *luteolin* on key signalling pathways were verified by cell experiments *in vitro*.

Results: Forty-four targets of *luteolin* involved in the treatment of OP, including key target proteins such as TP53, AKT1, HSP90AA1, JUN, RELA, CASP3, and MAPK1, were screened. KEGG enrichment analysis found that *luteolin* inhibits OP by regulating the PI3K-Akt, TNF, oestrogen and p53 signalling pathways. The results of animal experiments showed that bone mass in the low-dose *luteolin* group (*Luteolin*-L group, 10 mg/kg), high-dose *luteolin* group (*Luteolin*-H group, 50 mg/kg) and positive drug group was significantly higher than that in the OVX group ($P<0.05$). Western blot (WB) analysis showed that the protein expression levels of Collagen I, Osteopontin and RUNX2 in bone marrow mesenchymal stem cells (BMSCs) cultured with 0.5, 1 and 5 μM *luteolin* for 48 h were significantly higher than those in the dimethyl sulfoxide (DMSO) group ($P<0.05$). *In vitro* cell experiments showed that the p-PI3K/PI3K and p-Akt/Akt expression ratios in BMSCs cultured with 0.5, 1 and 5 μM *luteolin* for 48 h were also significantly higher than those in the DMSO group ($P<0.05$).

Conclusions: *Luteolin* has multitarget and multichannel effects in the treatment of OP. *Luteolin* could reduce bone loss in OVX rats, which may be due to its ability to promote the osteogenic differentiation of BMSCs by regulating the activity of the PI3K-Akt signalling pathway.

Keywords: Traditional Chinese medicine, luteolin, osteoporosis, network pharmacology, signalling pathway, experimental verification

INTRODUCTION

Osteoporosis (OP) is a systemic bone disease involving decreased bone density and bone quality induced by human ageing, menopause and other factors, and the main characteristics of this disease are the destruction of bone microstructure and an increase in bone brittleness (1, 2). With the ageing of the global population, OP and its complications will become a major public global health problem (3, 4). It is predicted that by 2050, the medical expenses for OP-related fractures in China will reach 25.4 billion USD, nearly 30 times greater than those in 2010 (5). At present, OP is mainly treated by drug therapy, physical therapy and exercise therapy (6, 7). Although great progress has been made in the treatment of OP, therapeutic effects still do not meet clinical expectations. First, many newly developed anti-OP drugs are expensive (8), limiting their wide clinical application; in addition, adverse drug reactions (9) eventually affect patient drug compliance.

In the theoretical traditional Chinese medicine system, OP is called "*Gu Wei*", which refers to osteopenia caused by kidney deficiency. Traditional Chinese medicine has a long history of using herbal medicines to tonify the kidney and replenish *Qi* for the prevention and treatment of "*Gu Wei*". In the application of herbal traditional Chinese medicines, many kidney-tonifying herbs contain flavonoids or flavonoid monomers (10). *Luteolin* is a natural flavonoid found in various medicinal materials, vegetables and fruits, such as *honeysuckle*, *Schizonepeta tenuifolia* and *Perilla*, in its glycosylated form (11). Many studies have shown that flavonoids, such as *icariin*, *naringin* and *soybean isoflavones*, can inhibit OP through a variety of pathways and targets (10, 12–14). *Luteolin*, a flavonoid monomer, may also have great potential for the treatment of OP. Studies have focused on the mechanism of *luteolin* in the treatment of OP, but clarification of this mechanism is still needed (15, 16). This study aimed to screen the targets of *luteolin* in the treatment of OP through network pharmacology to study the network relationship among the drug, its targets and related signalling pathways. Some key targets were experimentally verified, providing a scientific basis for the mechanism of *luteolin* in the treatment of OP and drug development. A flow chart describing this study is shown in **Figure 1**.

MATERIALS AND METHODS

Network Pharmacology

Obtaining Potential Targets of *Luteolin*

The Traditional Chinese Medicine Systems Pharmacology Database and Analysis Platform (TCMSP) (https://tcmspw.com/tcmsp.php) was used to obtain the targets of *luteolin*. Human genes were identified from the target information with the UniProt database (https://www.UniProt.org/).

Acquisition of OP Target Genes

OP-related genes were obtained from the Comparative Toxicogenomics Database (CTD) (http://ctdbase.org/) and GeneCards (https://www.genecards.org/) and DisGeNET (http://www.disgenet.org/web/DisGeNET/menu/home) databases with "osteoporosis" as the keyword. The target genes of *luteolin* and OP were introduced into Venny 2.1 to screen genes related to the use of *luteolin* in the treatment of OP.

Construction of a Protein–Protein Interaction (PPI) Network and Screening of Core Targets

Common target genes of *luteolin* and OP were imported into the STRING online database (https://string-db.org) for PPI analysis. The species in the database was set to "*Homo sapiens*", and the screening confidence was ≥ 0.90. With the above parameters, a PPI network interaction diagram was obtained, and the core gene was then obtained based on the number of node connections.

Construction of a "*Luteolin*-Target" Network Diagram

The targets of *luteolin* in OP were visualized with Cytoscape 3.7.1.

Gene Function and Biological Pathway Enrichment Analyses

The target genes of *luteolin* in the treatment of OP were uploaded to the DAVID data analysis platform for KEGG pathway enrichment and GO biological process enrichment analyses. The species was limited to "*Homo sapiens*" in the database. Pathways and biological processes for which $P < 0.05$ were extracted.

Experimental Verification

Animals and Experimental Groups

A total of 20 SPF-grade female SD rats aged 1.5 months with a body weight of (200 ± 10) g were used. The above rats were purchased from the *Experimental Animal Center of Southern Medical University*. The animal certificate number is 44002100030321. The twenty rats were raised in an SPF environment at the *Experimental Animal Center of Guangdong College of Traditional Chinese Medicine*. The experimental protocol was implemented after approval by the Animal Ethics Committee of the *Guangdong Hospital of Traditional Chinese Medicine* (animal experimental ethics approval No. 2021028). Relevant experimental procedures were implemented in accordance with regulations related to *the*

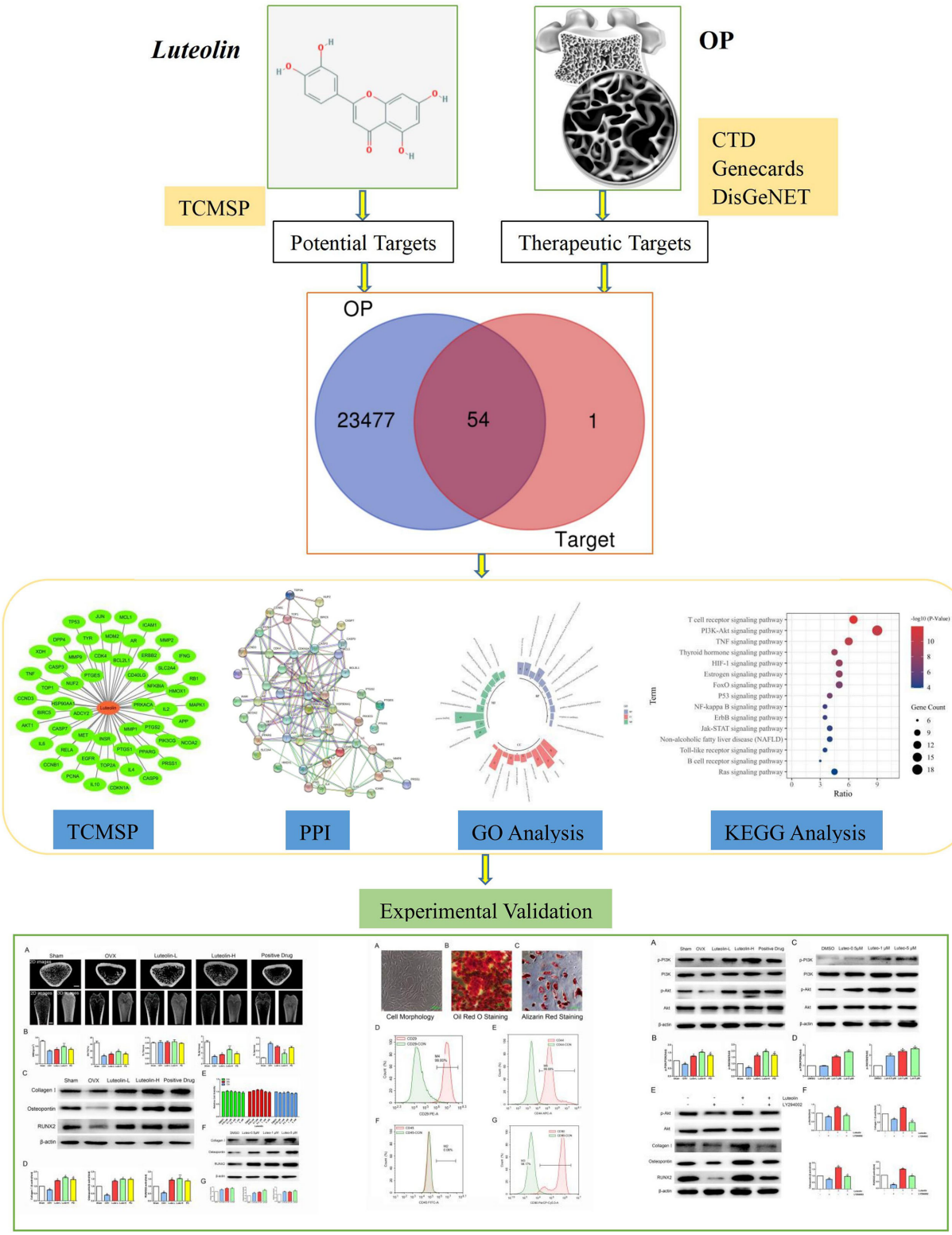

FIGURE 1 | Workflow of Luteolin in treatment of OP.

administration of experimental animals approved by the State Council of the People's Republic of China.

Construction of an OP Rat Model of Bilateral Ovariectomy and Drug Treatment

Twenty rats were divided into five groups (4 rats in each group), namely, the sham group, ovariectomised (OVX) group, low-dose *luteolin* group (*Luteolin*-L group), high-dose *luteolin* group (*Luteolin*-H) and positive drug group. After isoflurane was used to anaesthetise the rats, the rats in all groups except the sham group underwent surgery on both ovaries. For rats in the sham group, the bilateral ovaries were separated, and some adipose tissue around the ovaries was removed. Drug gavage was started 4 weeks after the operation, and *luteolin* was dissolved in carboxymethylcellulose sodium (CMC-na, C304951, Aladdin, Shanghai, China) to prepare a suspension. Alendronate sodium and vitamin D3 tablets (J201440144, Merck Sharp & Dohme Ltd., UK) were dissolved in normal saline. Experimental studies have proved that [16], *luteolin* at 25, 50, and 100 mg/kg doses can alleviate bone loss associated with glucocorticoid-induced osteoporosis induced by gavage in SD rats over 2 months. Based on the principle of reduction and optimisation in the "3R principle" of animal experiments, effective experimental data are obtained on the premise of using as few animals as possible. In this experiment, the bone mass loss of the OP model constructed by the OVX method progressed slowly. Therefore, a high dose of 50 mg/kg was selected to observe the effect of luteolin on the bone mass of OVX rats, and a lower dose of luteolin (10 mg/kg) was used to further explore whether a lower dose of luteolin can also increase the bone mass of OVX rats, representing a safer dose choice for the future treatment of OP with luteolin. Rats in the Luteolin-L group (10 mg/kg body weight) and Luteolin-H group (50 mg/kg body weight) underwent gavage once a day for 8 weeks. Rats in the positive drug group underwent gavage with alendronate sodium and vitamin D3 tablets (6.3 mg/kg) once a week for 8 weeks. Rats in the other two groups were given the same dose of drug dissolved in solvent by gavage. After 8 weeks of gavage, the rats were anaesthetised and euthanised, and the long bones of the limbs were collected for further analysis.

Micro-CT Analysis

After 4% paraformaldehyde fixation, a micro-CT scanner (ZKKS-MCT-Sharp, Guangzhou, China) was used to scan and analyse the morphology of the femur. During scanning, the femur was fixed in the fixator along the long axis. The scanning voltage was set to 70 kV, and the current was set to 100 μA. The power was 7 W, 4 frames were superimposed, the angle gain was 0.72 degrees, the scanning was carried out by rotating for one cycle, and the scanning layer was 15 μm thick. ZKKS-MicroCT 4.1 software was used to analyse the bone morphological parameters of the femoral metaphysis.

Extraction, Culture, and Identification of Rat Primary BMSCs

Bone marrow fluid was collected from the rat long shaft, and rat BMSCs were extracted by whole-bone-marrow cell culture. The cells were cultured in OriCell® rat bone marrow mesenchymal stem cell (BMSC) complete medium. Expression of the cell surface markers CD29, CD44, CD45 and CD90 was detected by flow cytometry. Osteogenic differentiation of the BMSCs was induced by rat BMSCs with an Osteogenic Differentiation Medium Kit (batch No. RASMX-90021, Saiye (Suzhou) Biotechnology Co., Ltd., Suzhou, China). Cell mineralisation was observed by Alizarin red staining. Adipogenic differentiation of the BMSCs was induced by rat BMSCs with an Adipogenic Differentiation Medium kit (batch No. RASMX-90031, Saiye (Suzhou) Biotechnology Co., Ltd., Suzhou, China). Fat droplets in the cells were observed by oil red O staining.

Cell Viability Assay

BMSCs were plated at a density of 2.5×10^3 cells/well in a 96-well plate. After culturing the cells for 24 h, 0.05 μM, 0.1 μM, or 5 μM luteolin (S2320, Selleck, USA) was added, and the cells were then incubated for a further 24, 48, or 72 h. Dimethyl sulfoxide (DMSO, D2650, Sigma, USA) was used to treat the control group. At the end of luteolin treatment, 10 μL of reagent from a Cell Counting Kit-8 (CCK-8, C0038, Beyotime, China) was added to each well, and the cells were incubated for 2 h at 37°C. The optical density (OD) at 450 nm was determined using a microplate reader (M1000 Pro, Tecan, Switzerland); four independent experiments were carried out.

Western Blot (WB) Analysis

After BMSCs were treated with the corresponding drugs, cell lysis buffer for WB and IP (P0013, Beyotime Biotechnology, China) was used to collect the total protein from the cells, and a bicinchoninic acid (BCA) quantification kit (P0012, Beyotime Biotechnology, China) was used to detect the protein concentration. A total of 20 μg of total protein was subjected to SDS–PAGE electrophoresis and then transferred to PVDF membranes. The membranes were blocked with 5% skimmed milk at room temperature for 1 h, and the following diluted antibodies were then added: anti-collagen I (1:1000, ab260043, Abcam), anti-osteopontin (1:1000, ab63856, Abcam), anti-RUNX2 (1:1000, 12556, CST), anti-β-actin (1:2000, 3700, CST), anti-PI3K (1:1000, 3358, CST), anti-Akt (1:1000, 4691, CST), anti-phospho-Akt (Ser473) (1:1000, 4058, CST), and anti-PI3K p85 (1:1000, ab182651, Abcam). The PVDF membranes were washed 3 times with 1× TBST. Finally, the samples were incubated in a refrigerator at 4°C overnight. HRP-conjugated goat anti-rabbit or anti-mouse antibodies (7074, 7076, CST, USA) were added and incubated at room temperature for 1 h. Finally, the membranes were incubated with ECL reagent (WBKLS0100, Merck, Germany) and scanned with a chemiluminescence system (Bio–Rad, USA).

Data Analysis

The data were analysed using one-way analysis of variance (ANOVA) followed by Tukey's multiple comparison test (GraphPad Prism version 5.0 for Windows).

RESULTS

Common Targets of *Luteolin* and OP

A total of 57 *luteolin* targets (including 2 invalid targets) were retrieved with the TCMSP. We obtained 36180 gene targets of

OP from the CTD, 1098 gene targets from the DisGeNET database and 2916 gene targets from the GeneCards database. After removing the duplicates, 23531 OP gene targets were obtained. After mapping the targets of *luteolin* and OP with Venny 2.1, 54 intersecting targets were obtained (**Figure 2**).

"*Luteolin*-Target" Network Diagram

Using Cytoscape 3 7.1 software, a "*luteolin*-target" network diagram was drawn (**Figure 3**). In the figure, the red node is *luteolin*, and each green node is a target.

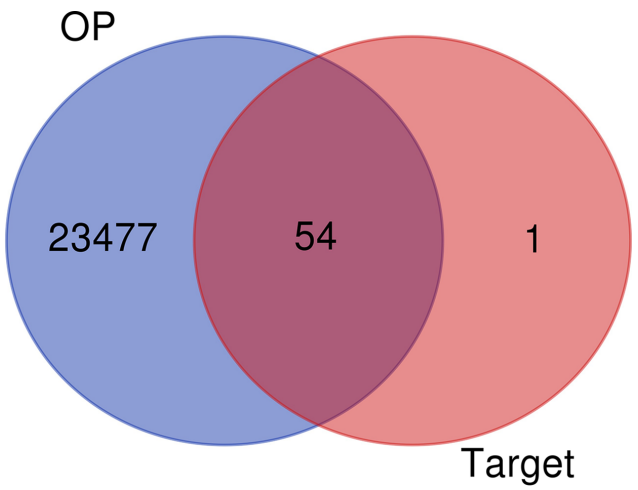

FIGURE 2 | Venn diagram of Luteolin targets and OP-related targets.

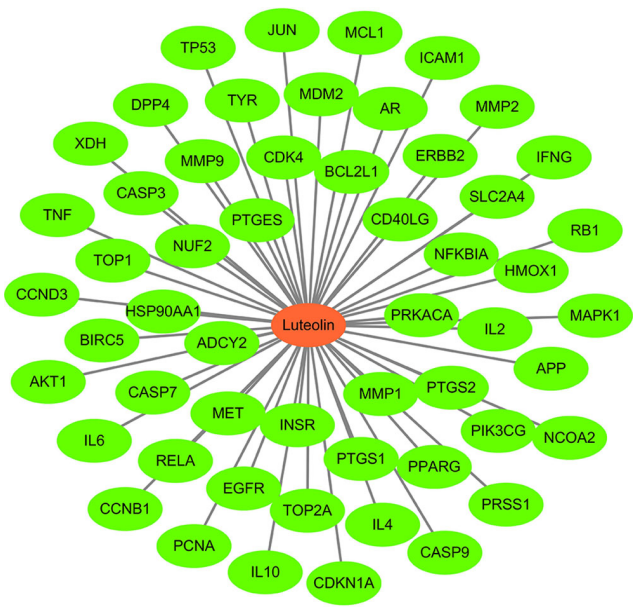

FIGURE 3 | Potential target genes related to Luteolin.

PPI Network Construction

A PPI network consisting of common targets was obtained by using the STRING 11.0 data analysis platform with the confidence set to ≥0.90. After hiding the isolated protein, a PPI network diagram was obtained. A total of 54 proteins were obtained (**Figure 4**). The degree value is often used to indicate the importance of network nodes. The larger the degree value is, the more important the node is in the network is. The top 10 most important targets in the PPI network based on degree value were TP53, AKT1, HSP90AA1, JUN, IL6, MAPK1, RELA, RB1, CASP3, and CDKN1A (**Figure 5**).

Results of GO Enrichment Analysis

The intersecting targets of *luteolin* and OP were analysed for GO functional enrichment with the DAVID data analysis platform, and the top 10 most significantly enriched biological process (BP), cell composition (CC) and molecular function (MF) terms were selected to form a GO enrichment bar graph (**Figure 6**). BP enrichment included the response to drugs, negative regulation of apoptotic processes, positive regulation of nitric oxide biosynthetic processes, and positive regulation of transcription from RNA polymerase II promoter. CC enrichment included the cytosol, nucleus, nucleoplasm, membrane raft, etc. MF enrichment included identical protein binding, enzyme binding, protein binding, protein heterodimerisation activity, and protein phosphatase binding.

Results of KEGG Enrichment Analysis

The enrichment of KEGG pathways in the intersecting targets of *luteolin* and OP were analysed with the DAVID data analysis platform. Ultimately, a total of 109 signalling pathways were obtained. After excluding obviously unrelated disease pathways, such as tumour- and liver disease-related pathways, the top 15 most significantly enriched pathways were selected and used to form a bubble diagram consisting of enriched KEGG signalling pathways (**Figure 7**). The results showed that *luteolin* may inhibit OP by regulating the T cell receiver, PI3K-Akt, TNF, HIF-1, oestrogen, FoxO and p53 signalling pathways.

Luteolin Alleviated Bone Loss in an OP Model by Promoting the Osteogenic Differentiation of BMSCs

To verify the mechanism of *luteolin* in the treatment of OP, we administered *luteolin* (low-dose group: 10 mg/kg, high-dose group: 50 mg/kg) to OVX model rats by gavage and used alendronate D3 tablets as the positive control. After 8 weeks of gavage, the femurs were collected from the rats in each group, and the distal femur was scanned by micro-CT. The imaging results showed that bone mass was significantly decreased for rats in the OVX group compared with those in the sham group. However, bone mass was significantly greater for the *Luteolin*-L group, *Luteolin*-H group and positive drug group compared with the OVX group (**Figure 8A**). An analysis of bone morphological parameters showed that the bone mineral density (BMD),

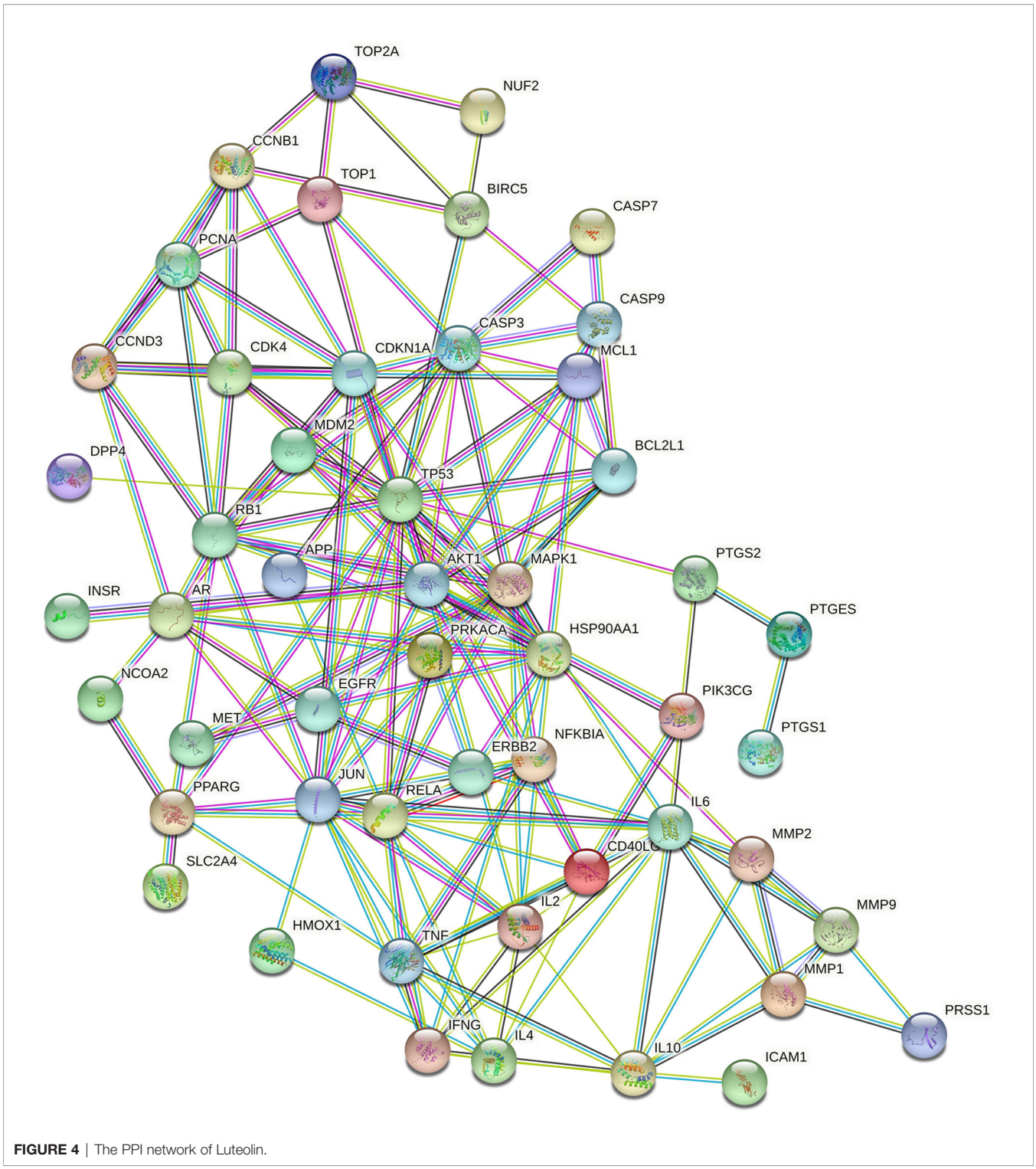

FIGURE 4 | The PPI network of Luteolin.

relative bone volume fraction (BV/TV) and trabecular number (Tb.N) were significantly lower for the OVX group than for the sham group, but the values of the *Luteolin*-L group, *Luteolin*-H group and positive drug group were significantly higher than those of the OVX group. The BMD and Tb.N values were greater for the *Luteolin*-H group than for the positive drug group. Trabecular separation (Tb.Sp) was significantly greater for the OVX group than for the sham group. Furthermore, the Tb.Sp of the *Luteolin*-H group was smaller than that of the OVX group and smaller than that of the positive drug group. There was no

FIGURE 5 | Histogram of the adjacent target number.

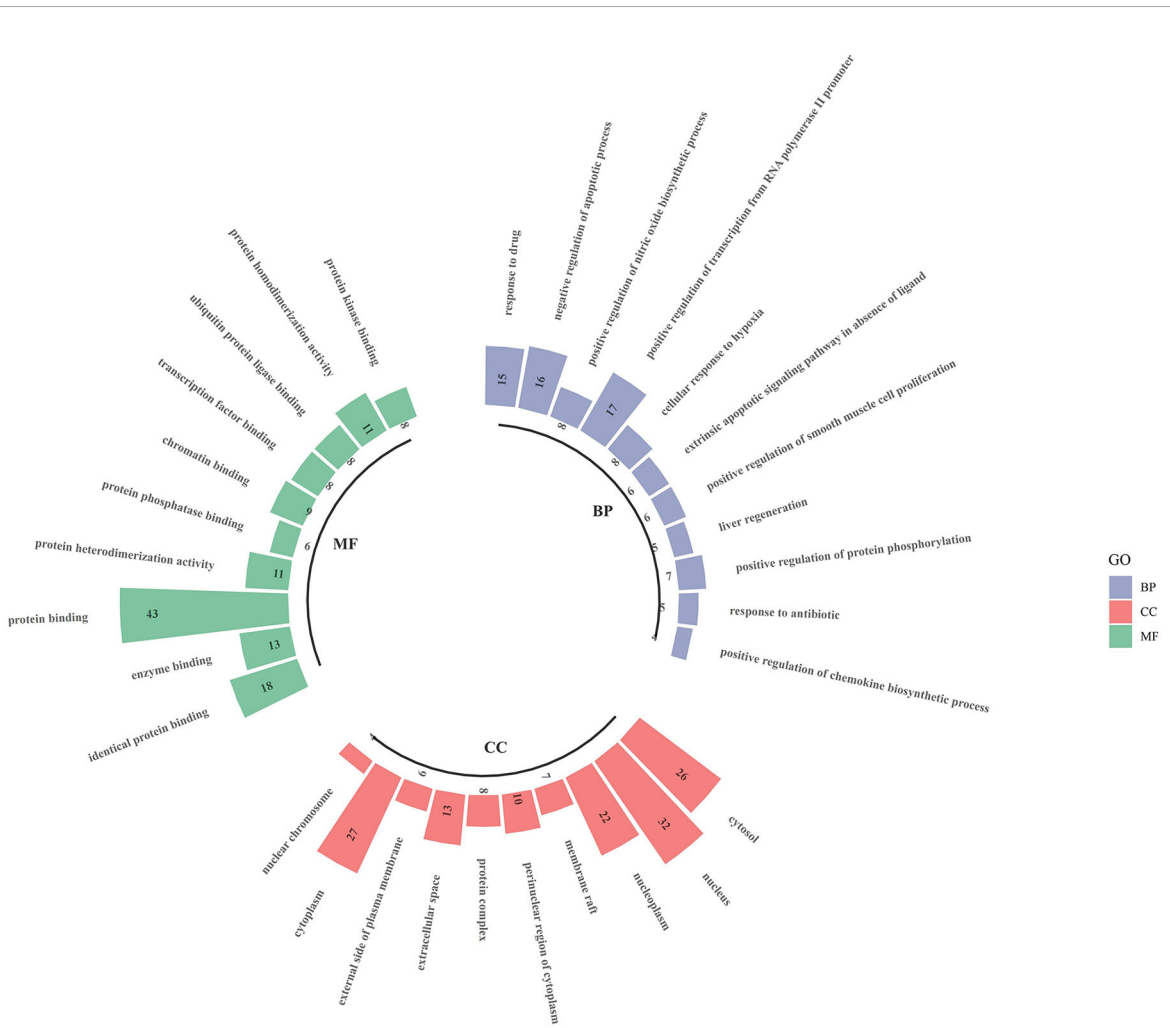

FIGURE 6 | Go enrichment analysis for targets of Luteolin against OP (TOP 10).

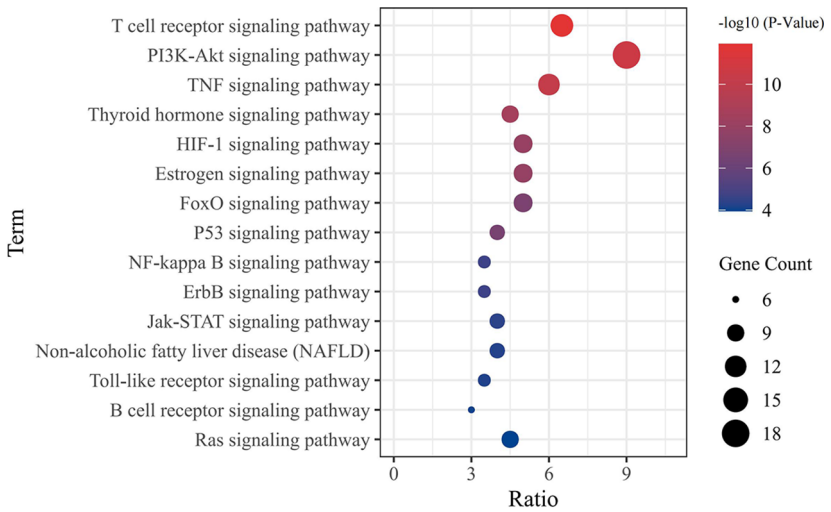

FIGURE 7 | The bubble chart of KEGG pathway analysis (TOP 15).

significant difference in trabecular thickness (Tb.Th) of the femur between the groups (**Figure 8B**). We collected long bone marrow from the rats in each group, extracted BMSCs and examined the isolated and cultured primary BMSCs. The results showed that the BMSCs grew normally after separation, and the cells were long and spindle-shaped under an inverted microscope (**Figure 9A**). After osteogenic induction, the results of alizarin red staining suggested the presence of a large number of mineralised nodules stained red (**Figure 9B**). After lipid induction, oil red O staining showed a large number of lipid droplets dyed orange (**Figure 9C**). Through fluorescent flow cytometry analysis of CD29, CD44, CD45 and CD90, the results showed that the CD29, CD44, CD45 and CD90 positivity rates were 99.00%, 99.08%, 0.08% and 98.17%, respectively (**Figures 9D–G**), in line with the biological characteristics of BMSCs. We extracted total protein from the BMSCs in each group and analysed osteogenic differentiation-related protein levels by WB. The results showed that the protein expression levels of collagen I, osteopontin and RUNX2 in BMSCs of the OVX group were significantly lower than those of the sham group, but the values of the *Luteolin*-L group, *Luteolin*-H group and positive drug group were significantly higher than those of the OVX group, and the expression of RUNX2 in the *Luteolin*-H group was also higher than that in the positive drug group (**Figures 8C, D**). To verify the effect of *luteolin* on the osteogenic differentiation of BMSCs, we further analysed the effect of *luteolin* on the viability of BMSCs and the expression of osteogenic differentiation-related proteins through *in vitro* cellular experiments. The results of CCK-8 assays showed that the viability of the BMSCs was not affected after 72 h of culture with *luteolin* at a concentration of 5 μM (**Figure 8E**). The results of WB showed that the protein expression levels of collagen I, osteopontin and RUNX2 in BMSCs cultured with *luteolin* at concentrations of 0.5, 1 and 5 μM were significantly higher than those in the DMSO group (**Figures 8F, G**). The above results show that *luteolin* could reduce bone loss in OVX rats, inhibit the progression of OP, and promote the osteogenic differentiation of BMSCs.

Luteolin Promotes the Osteogenic Differentiation of BMSCs by Activating the PI3K/Akt Signalling Pathway

Our animal experiments suggested that *luteolin* can promote the osteogenic differentiation of BMSCs, and the results of a network pharmacological analysis show that *luteolin* can regulate the PI3K/Akt signalling pathway. Therefore, we further explored the effect of *luteolin* on PI3K/Akt signalling pathway activity. The results of WB showed that the levels of phosphorylated PI3K and Akt (p-PI3K/PI3K and p-Akt/Akt) in BMSCs of the OVX group were significantly lower than those of BMSCs of the sham group. The levels BMSCs of in the *Luteolin*-L group, *Luteolin*-H group and positive drug group were higher than those in BMSCs of the OVX group (**Figures 10A, B**). After BMSCs were cultured with *luteolin* at concentrations of 0.5, 1 and 5 μM for 48 h, the relative expression of phosphorylated PI3K and Akt (p-PI3K/PI3K and p-Akt/Akt) was also significantly higher than that in the DMSO group (**Figures 10C, D**). To verify the role of the PI3K/Akt signalling pathway in the ability of *luteolin* to promote the osteogenic differentiation of BMSCs, we used the PI3K inhibitor LY294002 to inhibit the activity of the PI3K/Akt signalling pathway in BMSCs. The results of WB showed that the p-Akt/Akt expression ratio in BMSCs treated with 20 μM LY294002 was significantly lower than that in the DMSO group, indicating that LY294002 inhibited the activity of the PI3K/Akt signalling pathway in the BMSCs. LY294002 also reduced the protein expression levels of collagen I, osteopontin and

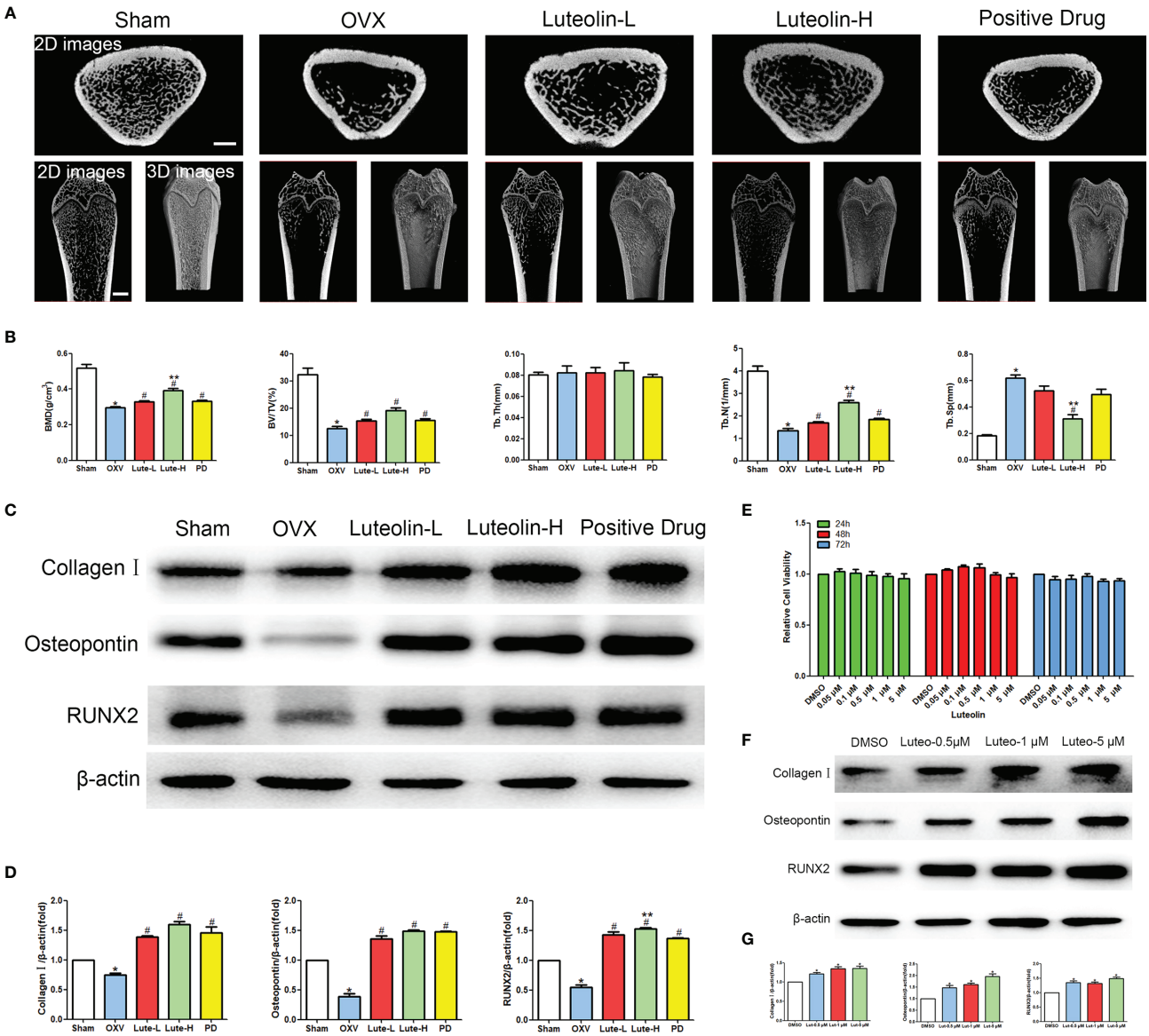

FIGURE 8 | Luteolin alleviated bone loss in OVX rats by promoting the osteogenic differentiation of BMSCs. **(A)** Micro-CT image of the femoral diaphysis (scale bars, 1 mm). **(B)** Quantitative presentation of the femoral microarchitectural parameters BMD, BV/TV, Tb.Th, Tb.N, and Tb.Sp expressed as the mean ± SD from four independent experiments. Compared with the sham group, $^{*}p < 0.05$; compared with the OVX group, $\#p < 0.05$; compared with the DG group, $^{**}p < 0.05$. **(C)** The expression levels of osteogenesis-related marker proteins (collagen I, osteopontin and RUNX2). **(D)** Comparative analysis of grey values for relevant protein bands; data are expressed as the mean ± SD from three independent experiments. Compared with the sham group, $^{*}p < 0.05$; compared with the OVX group, $\#p < 0.05$; compared with the DG group, $^{**}p < 0.05$. **(E)** BMSCs were treated with luteolin at increasing concentrations (0.05 μM, 0.1 μM, 0.5 μM, 1 μM, and 5 μM) for 24, 48 and 72 h, after which the OD value was determined by CCK-8 assay. Cell viability is expressed as the mean ± SD from four independent experiments. There was no significant difference. **(F)** BMSCs were treated with luteolin at increasing concentrations (0.5 μM, 1 μM, and 5 μM) for 48 h, after which osteogenesis-related marker protein (collagen I, osteopontin, RUNX2) expression was analysed with WB. **(G)** Comparative analysis of grey values from relevant protein bands; data are expressed as the mean ± SD from three independent experiments. Compared with the DMSO group, $^{*}p < 0.05$.

RUNX2 in the BMSCs; the protein expression levels of collagen I, osteopontin and RUNX2 in BMSCs cultured with both 20 μM LY294002 and 5 μM *luteolin* were significantly lower than those in BMSCs cultured with 5 μM *luteolin* alone (**Figures 10E, F**), suggesting that inhibiting the activity of the PI3K/Akt signalling pathway reduced the ability of *luteolin* to promote the osteogenic differentiation of BMSCs. The above results suggest that *luteolin* may promote the osteogenic differentiation of BMSCs by enhancing the activity of the PI3K/Akt signalling pathway.

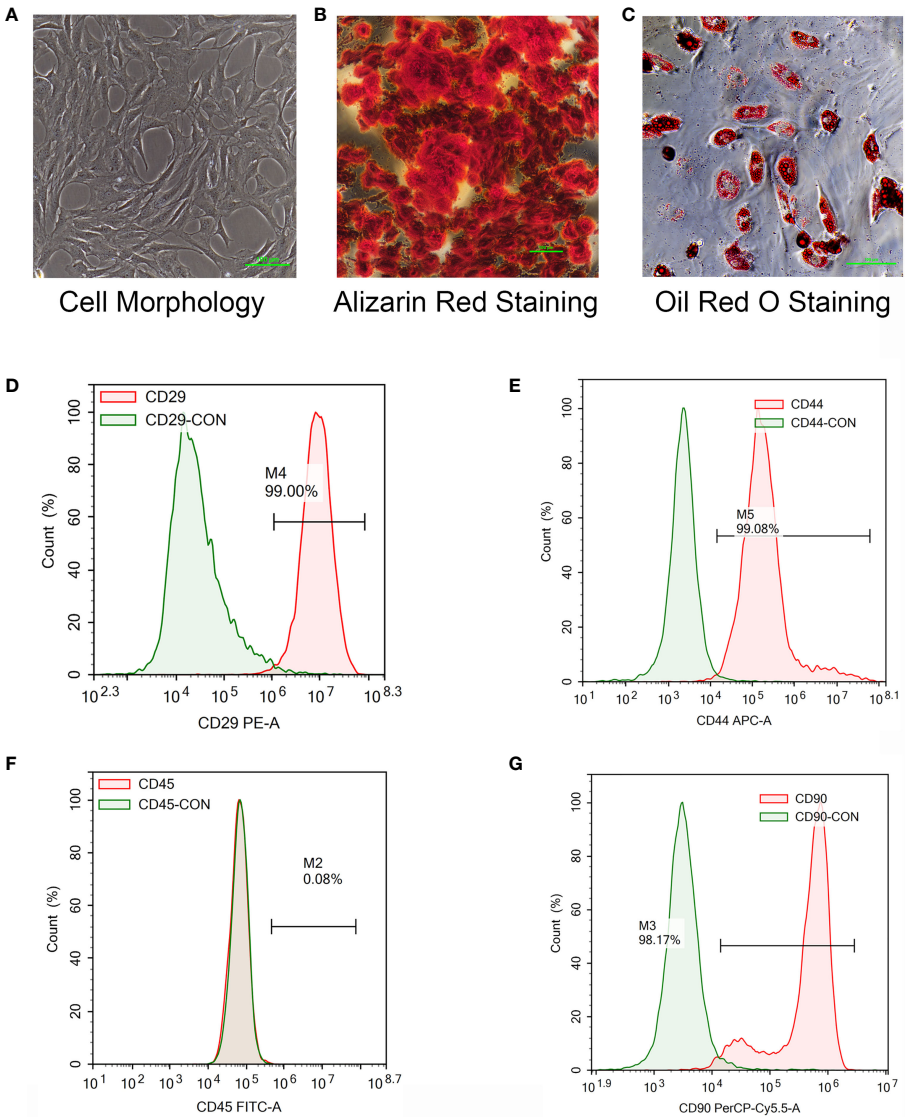

FIGURE 9 | Isolation and culture of rat primary BMSCs, the induction of osteogenic and adipogenic differentiation and the detection of cell surface markers. **(A)** The morphology of primary BMSCs from third-generation rats was observed under a microscope (×40). **(B)** After the osteogenic differentiation of third-generation BMSCs was induced with an osteogenic differentiation-inducing agent (Alizarin red staining), the formation of mineralized nodules was observed under a microscope (×100). **(C)** The adipogenic differentiation of third-generation BMSCs was induced by an adipogenic differentiation-inducing agent, and lipid droplets were enlarged and made rounder by continuous culture with maintenance medium (stained with oil red O) and observed under a microscope (×200). **(D–F)** The primary BMSCs of third-generation rats were collected and stained for CD29 **(D)**, CD44 **(E)**, CD45 **(F)** and CD90 **(G)** for 30 min. Control staining was simultaneously carried out. Fluorescence was detected with a flow cytometer, and the results were analysed.

DISCUSSION

Studies suggest that *luteolin* can reduce bone loss by reducing osteoclast activity and differentiation function (17, 18). Therefore, based on the large number of sources of *luteolin* and its great potential for the treatment of OP, in this study, we combined network pharmacology and experimental verification to explore the mechanism of *luteolin* in the treatment of OP. Through the prediction of *luteolin* and disease-related targets by network pharmacology, 54 potential targets of *luteolin* in OP were screened. PPI network analysis showed that *luteolin* may inhibit OP by regulating TP53, AKT1, JUN, RELA, CASP3, MAPK1, RB1 and CDKN1A. GO enrichment analysis found that the biological processes enriched in the targets of *luteolin* against OP include the response to drugs, negative regulation of apoptotic processes, and positive regulation of nitric oxide biosynthetic processes. The results of KEGG pathway enrichment analysis showed that *luteolin* may play a key role

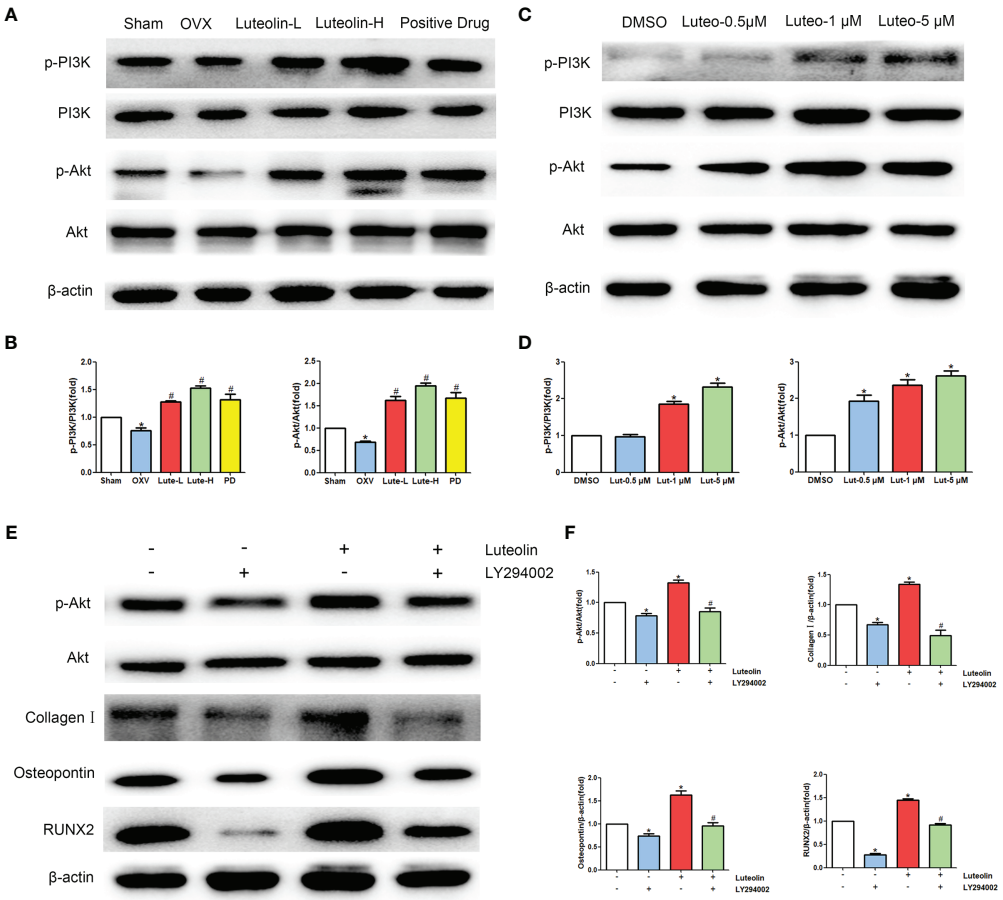

FIGURE 10 | Luteolin promotes the osteogenic differentiation of BMSCs by activating the PI3K/Akt signalling pathway. **(A)** The protein expression of p-PI3K, PI3K, p-Akt and Akt was detected by WB. **(B)** Comparative analysis of grey values from relevant protein bands; data are expressed as the mean ± SD from three independent experiments. Compared with the sham group, $*p < 0.05$; compared with the OVX group, $\#p < 0.05$. **(C)** BMSCs were treated with luteolin at increasing concentrations (0.5 μM, 1 μM, and 5 μM) for 48 h, followed by an analysis of p-PI3K, PI3K, p-Akt and Akt protein expression levels with WB. **(D)** Comparative analysis of grey values from relevant protein bands; data are expressed as the mean ± SD from three independent experiments. Compared with the DMSO group, $*p < 0.05$. **(E)** BMSCs were incubated with or without 20 μM LY294002 (S1105, Selleck, USA) and 5 μM luteolin for 48 h, followed by an analysis of collagen I, osteopontin, RUNX2, p-Akt and Akt protein expression levels by WB. **(F)** Comparative analysis of grey values from relevant protein bands; data are expressed as the mean ± SD from three independent experiments. Compared with the DMSO group, $*p < 0.05$; compared with the luteolin only group, $*p < 0.05$.

in regulating the PI3K-Akt, TNF, HIF-1, oestrogen and p53 signalling pathways. These results suggest that *luteolin* can regulate the biological processes of OP through multiple targets and pathways. The results of GO enrichment and KEGG pathway enrichment analyses showed that the degree to which the PI3K-Akt signalling pathway is enriched in targets of *luteolin* and OP is high, which may have significance and value for treating OP.

The results of animal experiments show that *luteolin* could reduce bone loss in OVX rats and upregulate the protein expression of collagen I, osteopontin and RUNX2 in BMSCs to promote osteogenic differentiation. *In vitro* cellular studies showed that *luteolin* promoted the osteogenic differentiation of BMSCs by increasing the p-PI3K/PI3K and p-Akt/Akt expression ratios, subsequently enhancing the activity of the PI3K/Akt signalling pathway. One study (19) showed that activation of the PI3K/Akt signalling pathway could stimulate the proliferation and differentiation of osteoblasts and inhibit their apoptosis. In addition, PI3K can stimulate the formation of osteoclast actin filaments and regulate cell chemotaxis, adhesion and diffusion. Inhibiting PI3K expression can reduce bone resorption of mature osteoclasts (19). Luteolin is a flavonoid monomer. Other research into the use of flavonoids for the treatment of OP has revealed that flavonoids, such as *epimedium* and *drynaria*, can regulate the activity balance of osteoblasts and osteoclasts by activating the PI3K/Akt signalling pathway (20, 21). The results of PPI analysis showed that AKT1 and TP53 are key targets of *luteolin* in the treatment of OP. Compared with that in normal mice, bone mass in AKT1- and AKT2-knockout mice are significantly decreased, suggesting that this pathway is related to enhanced bone formation (22). The PI3K/Akt signalling pathway is also negatively regulated by several

factors. For example, TP53 can negatively regulate the PI3K/Akt signalling pathway and promote the dephosphorylation of members of the PI3K/Akt signalling pathway through a series of biological effects (23, 24). Studies have shown that the PI3K-Akt signalling pathway can affect bone formation and bone cell survival, thereby controlling BMD balance (25, 26). Based on this information and our network pharmacology and experimental research results, we believe that *luteolin* may enhance the activity of the PI3K-Akt signalling pathway by interfering with target proteins such as AKT1 and TP53 to inhibit OP.

This study has the following limitations, and further theoretical and experimental research is needed in the future. First, public databases are dynamic, so the target data associated with the results of this study may change in the future. Additionally, this study did not comprehensively verify the targets and pathway results, which were theoretically derived. Other pathway and target data that were not verified in this study need to be further studied in future work.

CONCLUSIONS

Based on network pharmacology experiments and an established OP rat model, this study discusses the mechanism of *luteolin* in the treatment of OP, and the PI3K-Akt signalling pathway was selected for further experimental verification. The results show that *luteolin* can reduce bone loss in OVX rats, and upregulate the protein expression of collagen I, osteopontin and RUNX2 in BMSCs, promoting osteogenic differentiation. The possible mechanism by which *luteolin* acts against osteoporosis is the promotion of BMSC osteogenic differentiation *via* PI3K Akt signalling pathway activation regulation. This study provides new insights for the experimental and clinical treatment of OP in the future.

DATA AVAILABILITY STATEMENT

The original contributions presented in the study are included in the article/**Supplementary Material**. Further inquiries can be directed to the corresponding authors.

ETHICS STATEMENT

The animal study was reviewed and approved by the Experimental Animal Center of Guangdong College of Traditional Chinese Medicine.

AUTHOR CONTRIBUTIONS

GL, JZ, LZ, and WY contributed to the concept and design of this study. GL, JZ, YD, YY, ZZ, and RZ performed the computational analyses and performed the *in vivo* experiments. GL, JZ, YD, DZ, YY, and ZZ performed the experimental analysis. GL and JZ drafted the manuscript. All the authors read, revised, and approved the final manuscript.

FUNDING

This work was supported by the National Natural Science Foundation of China (No. No.82004383, No. 81974574), the National key research and development program (2021YFC1712804), the Project of Administration of Traditional Chinese Medicine of Guangdong Province (No.20201129, No.20225016, No.20225025), the Project of Guangdong Provincial Department of Finance (No. [2014]157), the Medical Science Research Foundation of Guangdong Province (No.A2020105, No.B2019091), the Science and Technology Planning Project of Guangzhou (No. 202102010273) and the Science and Technology Research Project of Guangdong Provincial Hospital of Chinese Medicine (No.YN2019ML08).

SUPPLEMENTARY MATERIAL

The Supplementary Material for this article can be found online at: https://www.frontiersin.org/articles/10.3389/fendo.2022.866641/full#supplementary-material

REFERENCES

1. Gkastaris K, Goulis DG, Potoupnis M, Anastasilakis AD, Kapetanos G. Obesity, Osteoporosis and Bone Metabolism. *J Musculoskelet Neuronal Interact* (2020) 20(3):372–81.
2. Fardellone P, Salawati E, Monnier LL, Goëb V. Bone Loss, Osteoporosis, and Fractures in Patients With Rheumatoid Arthritis: A Review. *J Clin Med* (2020) 9:3361. doi: 10.3390/jcm9103361
3. Johnston CB, Dagar M. Osteoporosis in Older Adults. *Med Clin N Am* (2020) 104:873–84. doi: 10.1016/j.mcna.2020.06.004
4. Rozenberg S, Bruyère O, Bergmann P, Cavalier E, Gielen E, Goemaere S, et al. How to Manage Osteoporosis Before the Age of 50. *Maturitas* (2020) 138:14–25. doi: 10.1016/j.maturitas.2020.05.004
5. Si L, Winzenberg TM, Jiang Q, Chen M, Palmer AJ. Projection of Osteoporosis-Related Fractures and Costs in China: 2010–2050. *Osteoporosis Int* (2015) 26:1929–37. doi: 10.1007/s00198-015-3093-2
6. Polzonetti V, Pucciarelli S, Vincenzetti S, Polidori P. Dietary Intake of Vitamin D From Dairy Products Reduces the Risk of Osteoporosis. *Nutrients* (2020) 12:1743. doi: 10.3390/nu12061743
7. Zhu Y, Huang Z, Wang Y, Xu W, Chen H, Xu J, et al. The Efficacy and Safety of Denosumab in Postmenopausal Women With Osteoporosis Previously Treated With Bisphosphonates: A Review. *J Orthop Transl* (2020) 22:7–13. doi: 10.1016/j.jot.2019.08.004
8. Clynes MA, Harvey NC, Curtis EM, Fuggle NR, Dennison EM, Cooper C. The Epidemiology of Osteoporosis. *Brit Med Bull* (2020) 133(1):105–17. doi: 10.1093/bmb/ldaa005
9. Iolascon G, Moretti A, Toro G, Gimigliano F, Liguori S, Paoletta M. Pharmacological Therapy of Osteoporosis: What's New? *Clin Interv Aging* (2020) 15:485–91. doi: 10.2147/CIA.S242038
10. Zhang G, Qin L, Hung WY, Shi YY, Leung PC, Yeung HY, et al. Flavonoids Derived From Herbal Epimedium Brevicornum Maxim Prevent OVX-Induced Osteoporosis in Rats Independent of Its Enhancement in Intestinal Calcium Absorption. *Bone* (2006) 38:818–25. doi: 10.1016/j.bone.2005.11.019
11. Yan H, Wei P, Song J, Jia X, Zhang Z. Enhanced Anticancer Activity *in Vitro* and *in Vivo* of Luteolin Incorporated Into Long-Circulating Micelles Based on DSPE-PEG2000 and TPGS. *J Pharm Pharmacol* (2016) 68:1290–8. doi: 10.1111/jphp.12598
12. Mu P, Hu Y, Ma X, Shi J, Zhong Z, Huang L. Total Flavonoids of Rhizoma Drynariae Combined With Calcium Attenuate Osteoporosis by Reducing

Reactive Oxygen Species Generation. *Exp Ther Med* (2021) 21:618. doi: 10.3892/etm.2021.10050
13. Shi X, Liu K, Wu L. Interventional Value of Total Flavonoids From Rhizoma Drynariae on Cathepsin K, a Potential Target of Osteoporosis. *Chin J Integr Med* (2011) 17:556–60. doi: 10.1007/s11655-010-0792-1
14. Wang J, Jiang J, Xie Y, Wei X, Li J, Duan J, et al. Population Pharmacokinetics of Naringin in Total Flavonoids of Drynaria Fortunei (Kunze) J. Sm. In Chinese Women With Primary Osteoporosis. *Chin J Integr Med* (2012) 18:925–33. doi: 10.1007/s11655-012-1296-0
15. Zheng L. Luteolin Stimulates Proliferation and Inhibits Late Differentiation of Primary Rat Calvarial Osteoblast Induced by High-Dose Dexamethasone *via* Sema3A/NRP1/Pleixin A1. *Curr Pharm Biotechnol* (2021) 22:1538–45. doi: 10.2174/1389201021666201216150442
16. Jing Z, Wang C, Yang Q, Wei X, Jin Y, Meng Q, et al. Luteolin Attenuates Glucocorticoid-Induced Osteoporosis by Regulating ERK/Lrp-5/GSK-3β Signaling Pathway *In Vivo* and *In Vitro*. *J Cell Physiol* (2019) 234:4472–90. doi: 10.1002/jcp.27252
17. Li N, Cornelissen D, Silverman S, Pinto D, Si L, Kremer I, et al. An Updated Systematic Review of Cost-Effectiveness Analyses of Drugs for Osteoporosis. *Pharmacoeconomics* (2021) 39:181–209. doi: 10.1007/s40273-020-00965-9
18. Kim T, Jung JW, Ha BG, Hong JM, Park EK, Kim H, et al. The Effects of Luteolin on Osteoclast Differentiation, Function *In Vitro* and Ovariectomy-Induced Bone Loss. *J Nutr Biochem* (2011) 22:8–15. doi: 10.1016/j.jnutbio.2009.11.002
19. Shi D, Dong M, Lu Y, Niu W. PI3K/Akt Signaling Pathway and Bone Destruction: Problems and Mechanisms. *Chin J Tissue Eng Res* (2020) 24:3716–22. doi: 10.3969/j.issn.2095-4344.2728
20. Qu H, Zheng J. Research Progress on the Anti-Osteoporosis Effect of Plant Flavones. *Chin J Osteoporos* (2021) 27:1529–33. doi: 10.3969/j.issn.1006-7108.2021.10.024
21. Zhang J, Ren Y, Zhang S. Recent Advances in Anti-Osteoporosis Effects and Drug Delivery System of Icaritin. *Chin Pharm J* (2021) 56:781–4. doi: 10.11669/cpj.2021.10.001
22. Peng XD, Xu PZ, Chen ML, Hahn-Windgassen A, Skeen J, Jacobs J, et al. Dwarfism, Impaired Skin Development, Skeletal Muscle Atrophy, Delayed Bone Development, and Impeded Adipogenesis in Mice Lacking Akt1 and Akt2. *Genes Dev* (2003) 17:1352–65. doi: 10.1101/gad.1089403
23. Diehl N, Schaal H. Make Yourself at Home: Viral Hijacking of the PI3K/Akt Signaling Pathway. *Viruses* (2013) 5:3192–212. doi: 10.3390/v5123192
24. Nielsen-Preiss SM, Silva SR, Gillette JM. Role of PTEN and Akt in the Regulation of Growth and Apoptosis in Human Osteoblastic Cells. *J Cell Biochem* (2003) 90:964–75. doi: 10.1002/jcb.10709
25. Roncevic J, Djoric I, Selemetjev S, Jankovic J, Dencic TI, Bozic V, et al. MMP-9-1562 C/T Single Nucleotide Polymorphism Associates With Increased MMP-9 Level and Activity During Papillary Thyroid Carcinoma Progression. *Pathology* (2019) 51:55–61. doi: 10.1016/j.pathol.2018.10.008
26. Adapala NS, Barbe MF, Tsygankov AY, Lorenzo JA, Sanjay A. Loss of Cbl-PI3K Interaction Enhances Osteoclast Survival Due to P21-Ras Mediated PI3K Activation Independent of Cbl-B. *J Cell Biochem* (2014) 115:1277–89. doi: 10.1002/jcb.24779

Conflict of Interest: The authors declare that the research was conducted in the absence of any commercial or financial relationships that could be construed as a potential conflict of interest.

Publisher's Note: All claims expressed in this article are solely those of the authors and do not necessarily represent those of their affiliated organizations, or those of the publisher, the editors and the reviewers. Any product that may be evaluated in this article, or claim that may be made by its manufacturer, is not guaranteed or endorsed by the publisher.

frontiers in Endocrinology

ORIGINAL RESEARCH
published: 24 March 2022
doi: 10.3389/fendo.2022.874849

Effects of Icariin on Modulating Gut Microbiota and Regulating Metabolite Alterations to Prevent Bone Loss in Ovariectomized Rat Model

Shanshan Wang[1†], Shengjie Wang[1,2†], Xiaoning Wang[1,3†], Yunteng Xu[1,2], Xin Zhang[1,2], Yidan Han[1,2], Hui Yan[1,4], Linglong Liu[1,4], Lili Wang[2], Hongzhi Ye[2] and Xihai Li[1,3]*

[1] College of Integrative Medicine, Fujian University of Traditional Chinese Medicine, Fuzhou, China, [2] Academy of Integrative Medicine, Fujian University of Traditional Chinese Medicine, Fuzhou, China, [3] Key Laboratory of Fujian University of Traditional Chinese Medicine, Fuzhou, China, [4] Basic Discipline Laboratory of Integrative Medicine, Fujian University of Traditional Chinese Medicine, Fuzhou, China

OPEN ACCESS

Edited by:
Jun Liu,
Guangdong Provincial Academy of Chinese Medical Sciences, China

Reviewed by:
Wumei Xu,
Yunnan Normal University, China
Jie Wang,
Wuhan Institute of Physics and Mathematics (CAS), China
Hongting Jin,
Zhejiang Chinese Medical University, China

***Correspondence:**
Xihai Li
lixihaifz@163.com

[†]These authors have contributed equally to this work

Specialty section:
This article was submitted to Bone Research, a section of the journal Frontiers in Endocrinology

Received: 13 February 2022
Accepted: 28 February 2022
Published: 24 March 2022

Citation:
Wang S, Wang S, Wang X, Xu Y, Zhang X, Han Y, Yan H, Liu L, Wang L, Ye H and Li X (2022) Effects of Icariin on Modulating Gut Microbiota and Regulating Metabolite Alterations to Prevent Bone Loss in Ovariectomized Rat Model. Front. Endocrinol. 13:874849. doi: 10.3389/fendo.2022.874849

Postmenopausal osteoporosis (PMOP) is an estrogen deficiency-induced bone loss, which has been shown an association with an altered gut microbiota (GM). Gut microbiota-bone axis has been recognized as a crucial mediator for bone homeostasis. Icariin (ICA) is an effective agent to delay bone loss by regulating the bone homeostasis. Thus, we hypothesize that ICA can prevent bone loss by modulating GM and regulating metabolite alterations. The effects of ICA on bone metabolism improvement in ovariectomized (OVX) rats and their relationships with the GM and fecal metabolites were investigated. Micro-computed tomography (micro-CT) and hematoxylin-eosin (HE) staining showed a typical bone boss in OVX group, while ICA or estradiol (E2) administration exhibited positive effects on bone micro-architecture improvement. The GM such as Actinobacteria, Gammaproteobacteria, Erysipelotrichi, Erysipelotrichales, Enterobacteriales, Actinomycetales, *Ruminococcus* and *Oscillospira* significantly correlated to serum bone Gla-protein (BGP), receptor activator of nuclear factor-κB (RANK), receptor activator of nuclear factor-κB ligand (RANKL), osteoprotegerin (OPG) and tartrate resistant acid phosphatase (TRACP). Further *t*-test revealed a substantial variation of the GM and fecal metabolites in different treatments. Among them, *Lachnoclostridium*, *Butyricimonas*, *Rikenella*, *Paraprevolla*, *Adlercreutzia*, *Enterorhabdus*, *Anaerovorax*, *Allobaculum*, *Elusimicrobium*, *Lactococcus*, *Globicatella* and *Lactobacillus* were probably the key microbial communities driving the change of bile acid, amino acid and fatty acid, thereby leading to an improvement of PMOP. The significant up-regulation of L-Saccharopine, 1-Aminocyclohexadieneacid and linoleic acid after ICA administration suggested important contributions of amino acid and fatty acid metabolisms in the prevention and treatment of PMOP. Taken together, our study has provided new perspectives to better understand the effects of ICA on PMOP improvement

by regulating GM and the associated fecal metabolites. Our findings contribute to develop ICA as a potential therapy for PMOP.

Keywords: icariin, postmenopausal osteoporosis, gut microbiota, metabolic pathway, bile acid, amino acid, fatty acid

INTRODUCTION

Postmenopausal osteoporosis (PMOP) is a worldwide disease often observed in the ageing woman. A high prevalence and a lack of effective therapy have made it the leading cause of disease burden (1). The pathophysiological mechanisms underlying PMOP are complicated and not fully understood. Estrogen as well as other medicines including bisphosphonates, denosumab and parathyroid hormone (PTH) analogs are popular choices for the prevention and treatment of PMOP (2–5). However, several undesirable side effects of the above drugs on women's health limit their wide and long-term administration (2, 6). It is still urgent to find more alternative choices to prevent and treat PMOP.

Icariin (ICA), 2-(4′-methoxyphenyl)-3-rhamnoside-5-hydroxyl-7-glucoside-8-(3′-methyl-2-butylene)-4-chromanone, as the main active flavonoid ingredient of Herba Epimedii, has been widely used in treating bone and joint diseases (7). Although there is insufficient clinical evidence, ICA has shown great efficacy for the treatment of PMOP in many studies (8, 9). ICA administration increased bone mineral density (BMD) and serum osteoprotegerin (OPG), but decreased serum bone Gla-protein (BGP) concentration in ovariectomized (OVX) rats (10). Receptor activator of nuclear factor-κB (RANK) and receptor activator of nuclear factor-κB ligand (RANKL) play vital roles in the collapse of cartilage and subchondral bone, while the result can be inhibited by ICA (11). Also, ICA has shown ability in decreasing the serum levels of tartrate-resistant acid phosphatase (TRACP) and consequent reducing the bone resorption (12). These findings suggest that ICA has potential drug target for treating PMOP.

So far, several possible mechanisms underlying bone loss improvement under ICA administration have been reported. The mostly-studied regulation mechanism towards PMOP is to accelerate bone formation through Wnt/β-catenin signaling pathway (10, 13, 14). This signaling pathway often co-functions with bone morphogenetic proteins (BMPs) or ERα to promote osteogenic differentiation under ICA treatment (14, 15). Recently, others potential regulating mechanisms such as the enhancement of IGF-I coupled non-genomic ERα signaling (16), the promotion of signal transducer and activator of transcription (STAT) (17) and the stimulation of mitogen-activated protein kinase (MAPK) (11) have also been reported. Noticeably, both MAPK and Wnt/β-catenin signaling pathways are involved in the IL-1β-induced expression of OPG, RANKL and RANK (11). This indicates that anti-inflammation is an important process in ICA-induced PMOP improvement, which can also be regulated by IGF-I signaling pathway (16, 18).

Another power driving the PMOP improvement is gut microbiota (GM) alteration. The roles of GM-bone axis in PMOP regulation have been increasingly noticed (19). It was reported that a suppression of bone loss with the administration of *Agastache rugosa* extract was regarded to be associated with the induction of osteoblast differentiation due to the alteration of GM (20). The significant correlations between GM and serum RANK, OPG and TRACP or inflammatory factors suggested a potential role of GM-bone axis in improving PMOP (21). More and more studies have also shown an influence of the altered GM on gut homeostasis *via* regulating bile acid, amino acid and fatty acid metabolisms, thereby leading to an improvement of PMOP (22–24). Correspondingly, those GM capable of bile acid, amino acid and fatty acid metabolisms were already used to prevent PMOP in OVX model (18, 24). It is apparent that ICA can modulate GM to improve the intestinal barrier function through regulating p38 MAPK and NF-κB signaling pathway or inhibiting intestinal inflammation (25–27). As such, we hypothesize that the therapeutic effects of ICA on PMOP may be closely associated with GM-bone axis regulation.

In present study, we employed OVX rat as a model to evaluate the effects of ICA on PMOP improvement at GM-bone axis. The following validations were implemented: 1) the effects of ICA administration on bone micro-architecture and serum physiological indexes, 2) the composition and abundance of GM and their correlations with serum biomarkers and 3) the relationships between GM and fecal metabolites and their potential roles in improving PMOP. We believe that the results have provided compelling evidence of ICA in regulating GM-bone axis that may contribute to the development of ICA as a novel therapy for PMOP.

MATERIALS AND METHODS

Ethical Approval

All the animal experiments were performed in accordance with the Guide for the Care and Use of Laboratory Animals published by the US National Institutes of Health (NIH Publication, 8th edition, 2011). Before experiment, the principles and guidelines were also approved by the Laboratory Animal Welfare and Ethics Committee of Fujian University of Traditional Chinese Medicine ((Min) SYXK 2019-0007).

Experimental Animals and Dietary Treatments

Sixty 2-months old female specific-pathogen-free (SPF) Sprague-Dawley (SD) rats weighting from 180 to 220 g were purchased from Shanghai Laboratory Animal Co. Ltd. (Shanghai, China; animal license NO. SCXK (Hu) 2017-0005). The rats were allowed to acclimate to animal room for 1 week before experiment. The acclimated animals were randomly divided

into 4 groups, including control group (Sham, n = 15), ovariectomy group (OVX, n = 15), ovariectomy plus ICA administration group (OVX+ICA, n = 15) and ovariectomy plus estradiol (E2) administration group (OVX+E2, n = 15). The OVX rats were obtained according to Jiang et al. (6) with a slight modification. Briefly, the rats were anesthetized with pentobarbital sodium (100 mg/kg i.p.) and the ovaries were removed to establish PMOP model. After surgery, the established rats were intramuscularly injected penicillin (200,000 units per rat) for 3 days to prevent infection and housed in individual cage. As to Sham group, a given amount of adipose tissue around ovary was removed to mimic the ovariectomy.

A commercial rodent diet and water were provided during the whole period of 12 weeks. Icariin or E2 at a concentration of 20 mg/kg/d or 0.1 mg/kg/d dissolved in 0.9% saline was administered intragastrically to animals in experimental groups every day. In contrast, the animals in Sham and OVX groups were administered 0.9% saline with the same dose of 0.5 mL as OVX+ICA and OVX+E2 groups. Animals in all groups were housed in SPF room at a temperature of 22-26°C and a relative humidity of 40%-70% with 12 h/12 h light/night cycle in the Laboratory Animal Center of Fujian University of Traditional Chinese Medicine.

Microtomographic Observation and Histomorphometric Analysis of Lumbar

After the last administration, the rats were fasted for 12 h. Live rats were scanned on micro-computed tomography (micro-CT; Guangzhou Zhongke Kesheng Medical Technology Co., LTD) to examine the structure and morphology of the lumbar. The micro-CT scan indexes were set at a voxel resolution of 20 μm, a beam angle increment of 0.72°, an X-ray voltage of 70 kV, an X-ray power of 7 W, a current intensity of 100 μA and an exposure time of 100 ms for a total of scanning time of 10 min. For each run, 3 groups of bones and a calibration phantom were analyzed in pairs to standardize the grayscale values and maintain the consistency of all samples. The calibrated three-dimensional (3D) images were reconstructed by MedProject (28). The typical histomorphometric indexes, i.e., trabecular bone mineral content (BMD) and bone volume fraction (BV/TV), were analyzed by ZZKS-Micro-CT4.1. More details about the assessed regions of interest (ROI) and the growth plate reference slice for ROI selection can be obtained from Fu et al. (29).

After micro-CT scanning, the rats were euthanized and the lumbar tissues were separated carefully. The obtained lumbar was fixed with 4% paraformaldehyde for 24 h, followed by thrice wash in Milli-Q water for 1 min per run and decalcified in 10% ethylenediaminetetraacetic acid (EDTA) for 8 weeks. A fresh EDTA was added to the system to renew the solution every two days. Before slicing, the decalcified lumbar was dehydrated by ethyl alcohol at the concentrations of 70%, 80%, 90%, 95% (4 h per run) and 100% (thrice, 20 min, 30 min and 70 min per run), transparentized twice by xylene (15 min and 30 min per run), waxed thrice (20 min by soft paraffin (two runs) and 40 min by hard paraffin), and finally embedded by paraffin as required (30). The embedded lumbar was sectioned to a 4-μm thick slice on a RM2135 Slicer (Leica, Germany). After dewaxing, the hydrated slices were stained with hematoxylin eosin (HE) for histomorphometric analysis (29).

Serum Biochemical Analysis

All venous blood was collected from the abdominal aorta of the rats under anesthesia and stored in a sterile vacuum tube. A total of 5 mL of blood were stayed statically for 4-5 h at room temperature and then centrifuged at 4°C, 3500 r/min for 15 min (Eppendorf 5430R, Germany). The serum in supernatant was transferred to a new tube and stored at -80°C before use. The biochemical indexes including bone Gla-protein (BGP), OPG, RANK, RANKL and TRACP were tested by enzyme-linked immunosorbent assay (ELISA) according to the manufacturer's instructions (31).

Gut Microbiota Analysis Based on High-Throughput Sequencing

One hundred mg of the fresh feces were collected and stored in sterile containers under -80°C until further analysis. Bacterial genomic DNA was extracted by using a FastDNA® SPIN Kit for Soil (MP Biomedicals, USA), while DNA concentrations and quality were determined by a Nanodrop® ND-1000 UV-vis spectrophotometer (NanoDrop technologies, Wilmington, DE, USA) and 1.0% agarose gel electrophoresis. For each treatment, 10 samples were used for high-throughput sequencing. All obtained samples were diluted to 1 ng/μL with sterile Milli-Q water.

The V3-V4 variable region of 16S rRNA were amplified using the barcoded primers 5'-ACTCCTACGGGAGCAGCA-3' (27F) and 5'-GGACTACHVGGGTWTCTAAT-3' (1492R). The amplification system of polymerase chain reaction (PCR) contained 30 ng of sample DNA, 1 μL of each of the 5 μM primer, 12.5 μL of 2 × Taq Plus Master Mix, 3 μL of 2 ng μL^{-1} Bovine Serum Albumin (BSA) and 7.5 μL of sterile Milli-Q water. The PCR programs consisted of a total of 30 cycles including 2 min at 95°C, 20 s at 95°C, 30 s at 55°C and 30 s at 72°C, and a final extension for 5 min at 72°C (32). The amplicons were purified and recovered by a AxyPrepDNA Gel Extraction Kit (AXYGEN), followed by a library construction by using NEB Next®Ultra™DNA Library Prep Kit for Illumina (NEB, USA) following manufacturer's instructions. The library quality was assessed on a Qubit2.0 Fluorometer (Thermo Scientific) and Agilent Bioanalyzer 2100 system. Finally, the established amplicons were pooled in equimolar proportion and paired-end sequenced on Illumina HiSeq2500 platform.

The paired-end reads of original DNA fragments were merged using Flash (v1.20) and Pear (v0.96) according to the overlap of the reverse complementary sequences. After removing the chimera and short or low-quality reads, the established sequences were analyzed by Uparse software package using the Uparse-OTU and Uparse-OTUref algorithms. In short, the sequences with ≥ 97% similarity were assigned to a same OTU. Following, the clear data were submitted to NCBI-SRA database with the accession number PRJNA807063. In our study, the

representative sequences for each OTU were picked to annotate their taxonomic information by using RDP Classifier algorithm. To evaluate the change of GM among treatments, the community distribution and relative abundance of GM were taxonomically analyzed from the levels of phylum to species. However, only those microbial communities ranking top 10 of the relative abundance were used for further analysis. Moreover, the potential GM involved in PMOP improvement were screened by correlating them to serum biomarkers BGP, OPG, RANK, RANKL and TRACP based on Spearman analysis (SPSS, version 21). Furthermore, the significant up-regulation and down-regulation of the GM at different taxonomic levels between Sham and OVX, OVX+ICA and OVX, OVX+E2 and OVX were also fully evaluated. Statistical analysis was performed by *t*-test at $p = 0.05$ using GraphPad Prism for Windows (Version 6.01, USA). Finally, the key phylotypes of GM in each treatment were identified by Linear Discriminant Analysis (LDA) Effect Size (LefSe) analysis with both LDA value calculation and cladogram construction (33).

Fecal Metabolite Analysis

The fresh feces (~100 mg) were mixed thoroughly with 100 μL sterile Milli-Q water (vortical vibration for 1 min) and 100 μL methanol-acetonitrile solution (v/v = 1:1) (vortical vibration for 1 min), respectively, and ultrasonically treated for 1 h at 4°C. The mixture was stayed statically for 1 h to precipitate the proteins at -20°C and centrifuged for 20 min at 4°C and 14000 r/min. The obtained supernatants were subsequently freeze-dried (FreeZone 6 plus, Labconco, USA) for 48 h and stored at -80°C until further use. Before analysis, each sample was re-dissolved by 100 μL methanol-acetonitrile-water solution (v/v/v = 2:2:1) with 5 min of vortical vibration and centrifuged again for 20 min at 4°C and 14000 r/min.

Liquid chromatography coupled with mass spectrometry/mass spectrometry (LC-MS/MS) analysis was performed on an Agilent 1290 Infinity LC (Agilent, USA) with an AB Triple TOF 5600/6600 MS system (AB SCIEX, USA). An ACQUITY UPLC BEH Amide C18 column (1.7 μm, 2.1 mm × 100 mm; Waters, UK) and an ACQUITY UPLC HSS T3 column (1.8 μm, 2.1 mm × 100 mm; Waters, UK) were used for the reversed phase separation. The column oven was maintained at 25°C. The flow rate of LC was 0.3 mL/min and the mobile phase consisted of solvent A (water + 25 mM ammonium acetate + 25 mM ammonium hydroxide) and solvent B (acetonitrile). Gradient elution conditions were set as follows: 0-0.5 min, 95% B; 0.5-7 min, linear decrease of B from 95% to 65%; 7-8 min, linear decrease of B from 65% to 40%; 8-9 min, 40% B; 9-9.5 min, linear increase of B from 40% to 95%; 9.1-12 min, 95% B. The injection volume for each sample was 3 μL. The samples in autosampler were stayed at 4°C in the whole analysis process.

Both positive (POS) and negative (NEG) modes of electrospray ionization (ESI) were used for the detection of fecal metabolites. The ESI conditions for Agilent 5600 system were gas temperature of 250°C, drying gas of 16 L/min, nebulizer of 20 psig, sheath gas temperature of 400°C, sheath gas flow of 12 L/min, Vcap of 3000 V, nozzle voltage of 0 V. Other conditions include fragment of 175 V, mass range of 50-1200, acquisition rate of 4 Hz and cycle time of 250 ms. The obtained ions were further identified by AB Triple TOF 6600 system with ion source gas1 of 40 and gas2 of 80, curtain gas of 30, source temperature of 650°C, IonSapary voltage floating of ±5000 V (POS and NEG modes). As to secondary ion MS (SIMS or MS2) analysis, the data were obtained by using information dependent acquisition (IDA; exclude isotopes within 4 Da, candidate ions to monitor per cycle: 10) in high sensitivity mode with de-clustering potential of ±60 V (POS and NEG modes), and collision energy of 35 ± 15 eV. Data collection was performed according to mass range of 50-300, 290-600, 590-900 and 890-1200 (four times for each internal) to increase the spectrum collection efficiency. The structure of the collected ions was identified by MetDDA and LipDDA developed by Shanghai Applied Protein Technology Co. Ltd (Shanghai, China).

Univariate analysis and multivariate analysis were used to identify the potential key metabolites. While the fold change (FC) analysis can identify the differential metabolites between treatments, *t*-test helps to verify whether a significant difference is present. The variable importance for the projection (VIP) obtained from orthogonal partial least squares discriminant analysis (OPLS-DA) model, along with FC and *p*-value, is also an important index for evaluating the differences among treatments. In our study, the metabolites screened by VIP > 1, FC > 1.2 (up-regulation) or < 0.8333 (down-regulation) and *p*-value < 0.05 were regarded as the significant differential candidates. To have a full evaluation of the annotated metabolites and their differences in expression patterns in different samples, we used the qualitative expression levels of the significant differential metabolites for hierarchical clustering analysis of each group.

Correlation Analysis Between GM and Fecal Metabolites

To evaluate whether can gut microbes influence bone metabolisms through changing the compositions of fecal metabolites, the relationships between the relative abundance of significant differential GM in genus level (*t*-test; *p*-value < 0.05) and the significant differential metabolites (VIP > 1 and *p*-value < 0.05) were correlatively analyzed. The analyses included correlation coefficient calculation (Spearman), Spearman correlation analysis-based network mapping (Cytoscape 3.5.1) and Spearman correlation analysis-based hierarchical clustering heat mapping (R 3.4.2 Heatmap package). It was considered that there was a significant relationship between GM and fecal metabolites when *p*-value was < 0.05. Finally, each paired GM and fecal metabolite with significant correlation was fully compared with previous studies to evaluate their potential roles in PMOP prevention and (or) treatment under ICA administration.

Statistical Analysis

All the experiments were repeated independently at least three times. The results are presented as the mean ± standard deviation (SD). R package and SPSS 21.0 (IBM, USA) were used to perform Spearman and *t*-test analyses as required. Significant differences were calculated according to one-way analysis of variance (ANOVA) by Tukey's multiple comparisons test at $p = 0.05$

using GraphPad Prism for Windows (Version 6.01, USA) unless otherwise noted.

RESULTS

Verification of Therapeutic Effects of ICA on PMOP

Micro-CT images show that the bone trabecular of SD rats in Sham group is of close arrangement, regular shape, uniform thickness and consistent direction (**Figures 1A1–A3**). The ovariectomy can lead to an obvious loss of the bone trabecula, which becomes thinner with a fractured structure, an irregular arrangement and a wider spacing, thereby forming cavities in the located area (**Figure 1B1–B3**). Either ICA or E2 administration exhibited positive effects on improving the trabecular micro-architecture (**Figures 1C1–C3, D1–D3**). Both BMD and BV/TV in local area of the lumbar vertebra also verified a significant bone loss in OVX rats ($p < 0.01$), while ICA and E2 administration significant increased BMD by 38% ($p < 0.05$) and 44% ($p < 0.05$) and BV/TV by 47% ($p < 0.05$) and 53% ($p < 0.01$), respectively (**Figures 1E, F**). These results showed that ICA prevented estrogen deficiency-induced PMOP in OVX rats.

Besides *in situ* micro-CT observation, a HE staining was also performed in this study to evaluate the bone trabecular structure in different treatments. **Figure 2** shows a histology structure of the fifth lumbar vertebra stained by HE. As expected, a regular mesh network of the bone trabecula was observed in Sham group (**Figure 2A**). However, a typical trabecular structure was missing, instead a considerable structure change and emerging adipocytes in marrow cavity were found in OVX group (**Figure 2B**). The HE staining also showed us a clear improvement of the bone trabecula in PMOP rats administrated with ICA or E2 (**Figure 2C**). These results verified a potential role of ICA, served as an estrogen-like substitution, in improving the estrogen-deficient symptoms.

Regulation of ICA on Serum Biomarkers Associated With Bone Metabolisms

Compared to Sham group, the serum BGP in OVX rats significantly increased from 2.1 to 3.3 ng/L ($p < 0.01$) (**Figure 3A**). When administrated with ICA, serum BGP concentration decreased to 2.4 ng/L ($p < 0.05$), close to those observed in Sham and OVX+E2 groups (**Figure 3A**). The serum RANK concentrations in Sham, OVX, OVX+ICA and OVX+E2 followed a similar trend to BGP, being up to 1339 pg/mL in OVX group and 935-1117 pg/mL in other treatments (**Figure 3B**). However, both ovariectomy and ICA or E2 administration did not significant change the concentration of serum RANKL (**Figure 3C**), a biomarker that can be bound to RANK to enhance osteoclastogenesis (34). Unlike RANKL, OPG, as another ligand of RANK, in the serum of OVX rats was significantly down-regulated to 1572 pg/mL by 31% lower than Sham group ($p < 0.05$) (**Figure 3D**). Either ICA or E2 administration improved the dysfunction of ovary, resulting in a significant up-regulation of serum OPG concentration ($p < 0.01$) (**Figure 3D**). Besides, we also determined the serum TRACP concentration and found an increase of TRACP by 38% in OVX group ($p < 0.05$) and a similar concentration in OVX+ICA and OVX+E2 as compared to Sham group (**Figure 3E**). These results showed that ICA administration was of great ability to influence bone metabolisms *via* regulating serum BGP, RANK, RANKL, OPG and TRACP to a desirable concentration.

Verification of GM-Bone Axis Targets Involved in ICA-Mediated Improvement of PMOP

In phylum level, Firmicutes and Bacteroidetes predominated in all treatments, being the lowest abundance of Firmicutes by 55% and the highest abundance of Bacteroidetes by 35% both observed in OVX+ICA group (**Figure 4A**). These phylum communities in Sham, OVX and OVX+E2 groups were 69%-70% and 20%-25%, respectively (**Figure 4A**). In other taxonomic levels, it was apparent that the dominant GM belonging to Firmicutes included the genera *Ruminococcus*, *Clostridium*, *Lactobacillus*, *Oscillospira* and SMB53 group, the families Ruminococcaceae, Clostridiaceae, Lachnospiraceae, Lactobacillaceae and S24-7 group, the orders Clostridiales and Lactobacillales, and the classes Clostridia and Bacilli (**Figure 4B**; **Supplementary Figure S1**). As to those GM belonging to Bacteroidetes, the genera *Prevotella* and *Paraprevotella* in Prevotellaceae, a family belonging to the order of Bacteroidales in the class of Bacteroidia, were likely to be dominant in rat gut (**Figure 4B**; **Supplementary Figure S1**). Statistical analysis suggested that the dominant GM mainly be positively correlated with RANK and TRACP and negatively correlated with RANKL and OPG (**Table 1**). The most eye-catching genera were *Ruminococcus* and *Oscillospira*, which probably contributed to the significant up-regulation of RANK and TRACP and down-regulation of OPG (**Table 1**). It was also worth noting that some nondominant GM belonging to Actinobacteria, Gammaproteobacteria, Erysipelotrichi, Enterobacteriales and Acetinomycetales were important in regulating serum RANK and RANKL concentrations (**Table 1**).

Among treatments, a total of 4 plyla, 4 classes, 5 orders, 10 families, 17 genera and 7 species varied significantly based on *t*-test at $p = 0.05$ (**Figure 5**). Specifically, the families Streptococcaceae and Marinifilaceae, the genera *Butyricimonas* and *Lactococcus* and the species *Ruminococcus bromii* and *Butyricimonas synergistica* was significantly up-regulated in OVX as compared to Sham group (**Figure 5**). By comparing OVX+ICA to OVX, the phylum Elusimicrobia, an unidentified class in Elusimicrobia, the order Elusimicrobiales, the families Prevotellaceae and Elusimicrobiaceae and the genus *Elusimicrobium* and an unidentified genus in Corynebacteriaceae were significantly up-regulated (**Figure 5**). Moreover, the ovariectomy also resulted in a significant down-regulation of the phylum Actinobacteria, an unidentified class in Actinobacteria, the genera *Lachnoclostridium*, *Negativibacillus*, *Rikenella* and *Harryflintia*, and the species Lachnospiraceae bacterium A2 (**Figure 5**). Furthermore, more significant differential GM was found in OVX+ICA vs OVX and OVX+E2

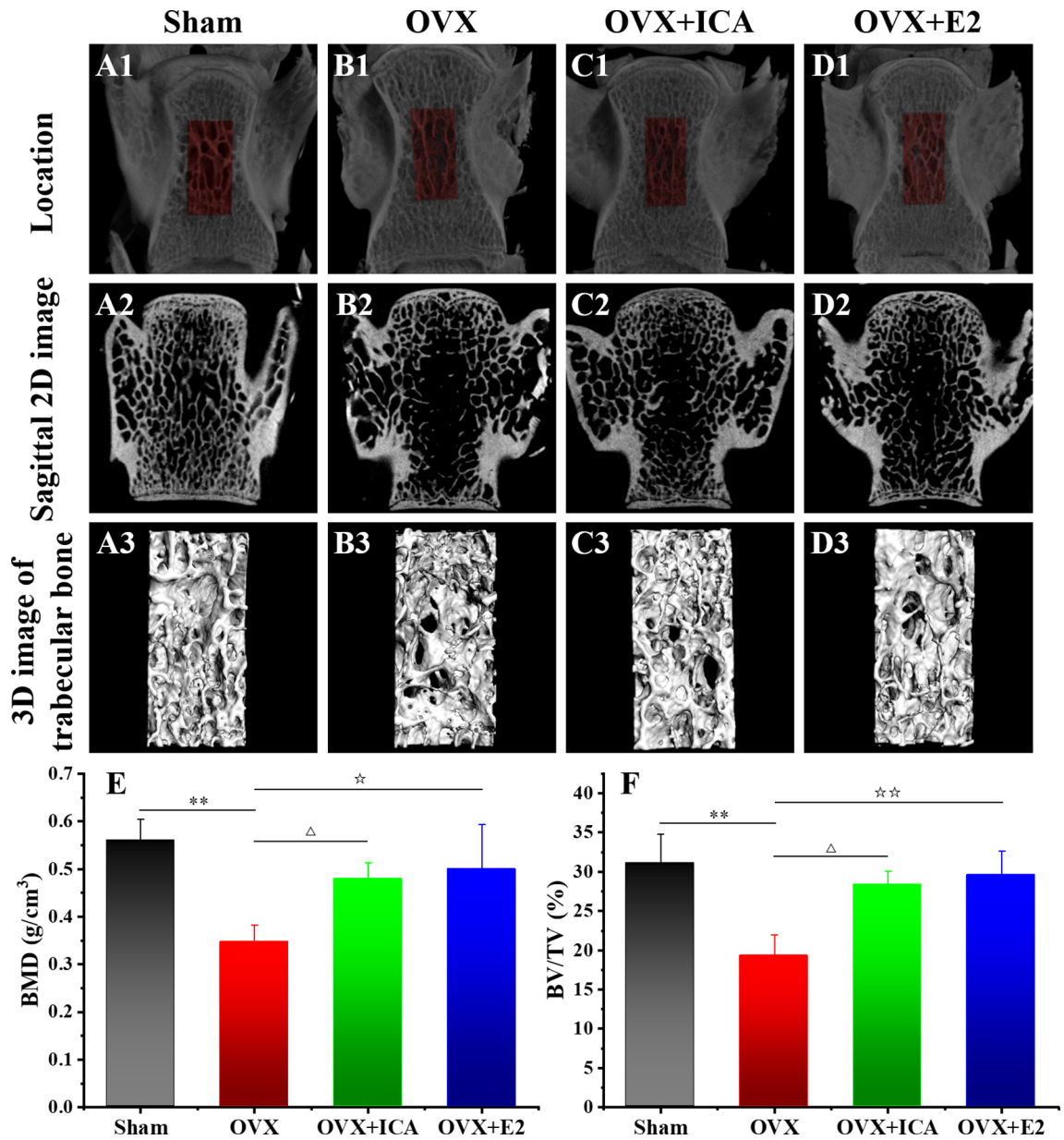

FIGURE 1 | Therapeutic effects of different treatments on the bone histomorphometry of PMOP model. Micro-CT images of the bone structure for Sham **(A1–A3)**, OVX **(B1–B3)**, OVX+ICA **(C1–C3)** and OVX+E2 **(D1–D3)** (n = 6). Morphometric analysis of BMD **(E)** and BV/TV **(F)** in local area (three samples per group at each time point). $^{\triangle,\star}p < 0.05$, $^{\star\star,\star\star}p < 0.01$.

vs OVX as compared to another two comparisons (**Figure 5**). One information needed to be noted was that some GM such as Streptococcaceae, *Butyricimonas* and *Lactococcus* having a significant up-regulation trend in OVX significantly decreased in OVX+ICA (**Figure 5**). *Globicatella* was another genus belonging to Lactobacillales in Firmicutes like *Lactococcus* that down-regulated in OVX+ICA (**Figure 5**). While Streptococcaceae, Christensenellaceae, *Adlercreutzia* and *Helicobacter rodentium* showed the same down-regulation trend in both OVX+ICA and OVX+E2, only the first one was up-regulated in OVX group (**Figure 5**).

Although the predominant GM in all treatments belonged to Firmicutes and Bacteroidetes, the key phylotypes making the sample in each treatment distinguishable from others were varied. As shown in **Figure 6** and **Supplementary Figure S2**, the key phylotypes of GM in Sham group showed higher diverse than those observed in other treatments. In OVX group, the genus *Oscillospira* and the family Erysipelotrichaceae in Firmicutes and the genus *Butyricimonas* belonging to Odoribacteraceae in Bacteroidetes were abundant GM (**Figure 6**; **Supplementary Figure S2**). However, the rats administrated with ICA or E2

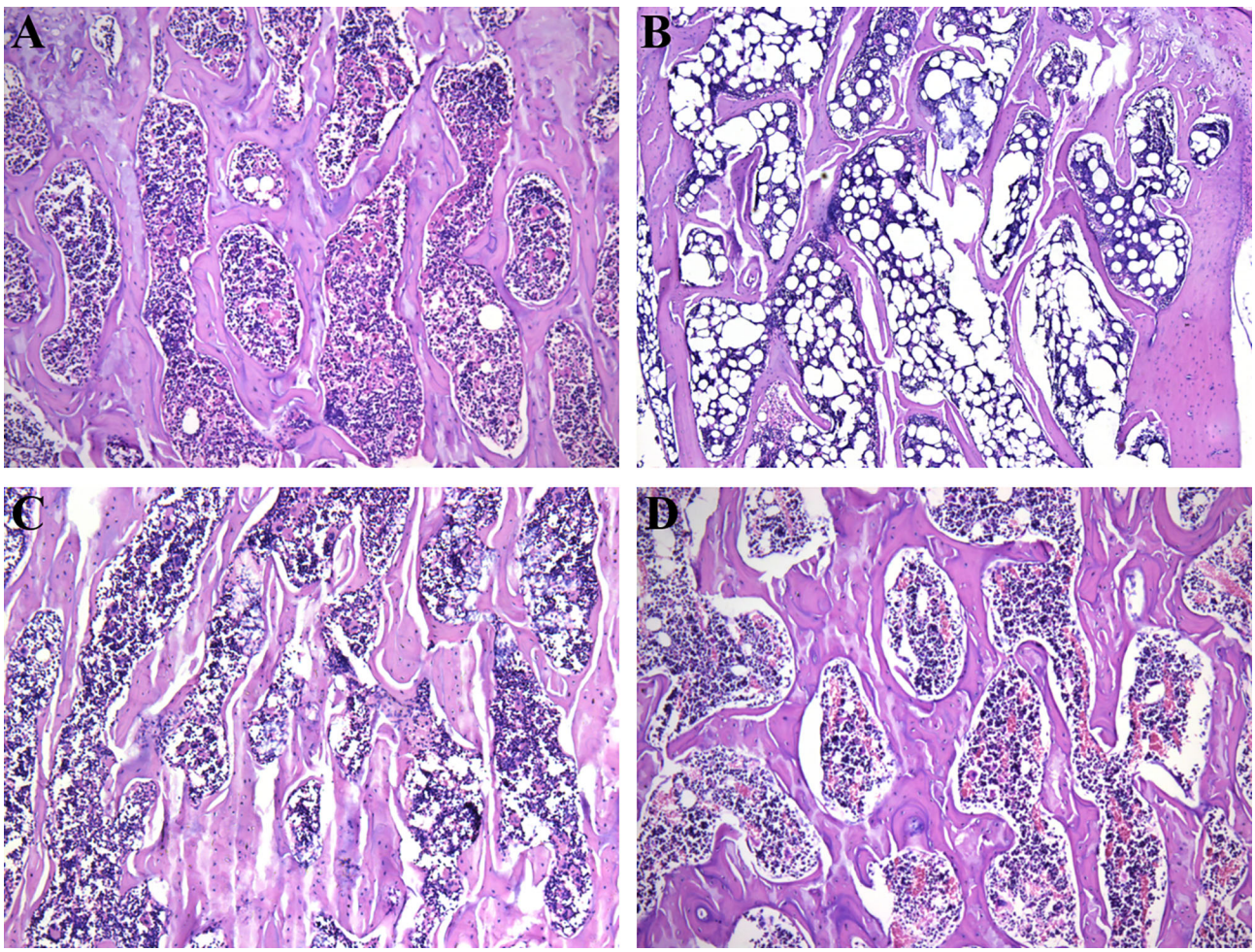

FIGURE 2 | Therapeutic effects of different treatments on the bone trabecular structure (100 ×) of PMOP model. **(A-D)** represent the HE images of Sham, OVX, OVX+ICA and OVX+E2 groups, respectively.

harbored major GM such as *Paraprevotella* and *Prevotella* in Bacteroidetes or *Lactobacillus* in Firmicutes, respectively (**Figure 6**; **Supplementary Figure S2**). The presence of Erysipelotrichi, Erysipelotrichales, Lactobacillales, Lactobacillaceae, Paraprevotellaceae, Prevotellaceae, *Paraprevotella*, *Prevotella*, *Oscillospira* and *Butyricimonas* was in accordance with the results as shown in **Figure 5**. These data showed that different treatments modulated specific GM, and the diverse GM might co-work to regulate the estrogen homeostasis and bone metabolism.

Identification of Key Fecal Metabolites Correlated to ICA Administration

Based on metabonomic analysis in POS mode, a total of 15 metabolites were significantly up- or down-regulated between Sham and OVX groups (**Supplementary Table S1**). Among which, 3-Amino-3-(4-Hydroxyphenyl)propanoate, nicotinate, 1-Palmitoylglycerol, Ile-Leu, xanthosine, N-Tigloylglycine, 1-Aminocyclohexanecarboxylic acid, D-Alanyl-D-alanine (D-Ala-D-Ala), L-saccharopine, stearidonic acid, Pro-Asn, triethanolamine and 2'-O-methylcytidine were significantly up-regulated, while N-(omega)-Hydroxyarginine and D-Pipecolinic acid were significantly down-regulated (**Supplementary Table S1**). Compared to OVX, ICA administration resulted in a significant up-regulation of 6 out of 9 differential metabolites, being the highest FC of 6.74 (NG, NG-dimethyl-L-arginine (ADMA); VIP = 2.80; $p < 0.001$) (**Supplementary Table S1**). 1-Aminocyclohexanecarboxylic acid and L-Saccharopine followed similar trend in both Sham vs OVX and OVX+ICA vs OVX (**Supplementary Table S1**). However, most significant differential metabolites between OVX+E2 and OVX were similar to Sham vs OVX and OVX+ICA vs OVX except for Leu-Gly, phenylenthylamine, Thr-Val and Leu-Thr, while only 1-Aminocyclohexanecarboxylic acid was found in all comparisons (**Supplementary Table S1**). The comparison between OVX+E2 and OVX+ICA showed that only D-Ala-D-Ala and ADMA those also observed in OVX+E2 vs OVX or OVX+ICA vs OVX were down- and up-regulated, respectively (**Supplementary Table S1**). A hierarchical clustering heat map

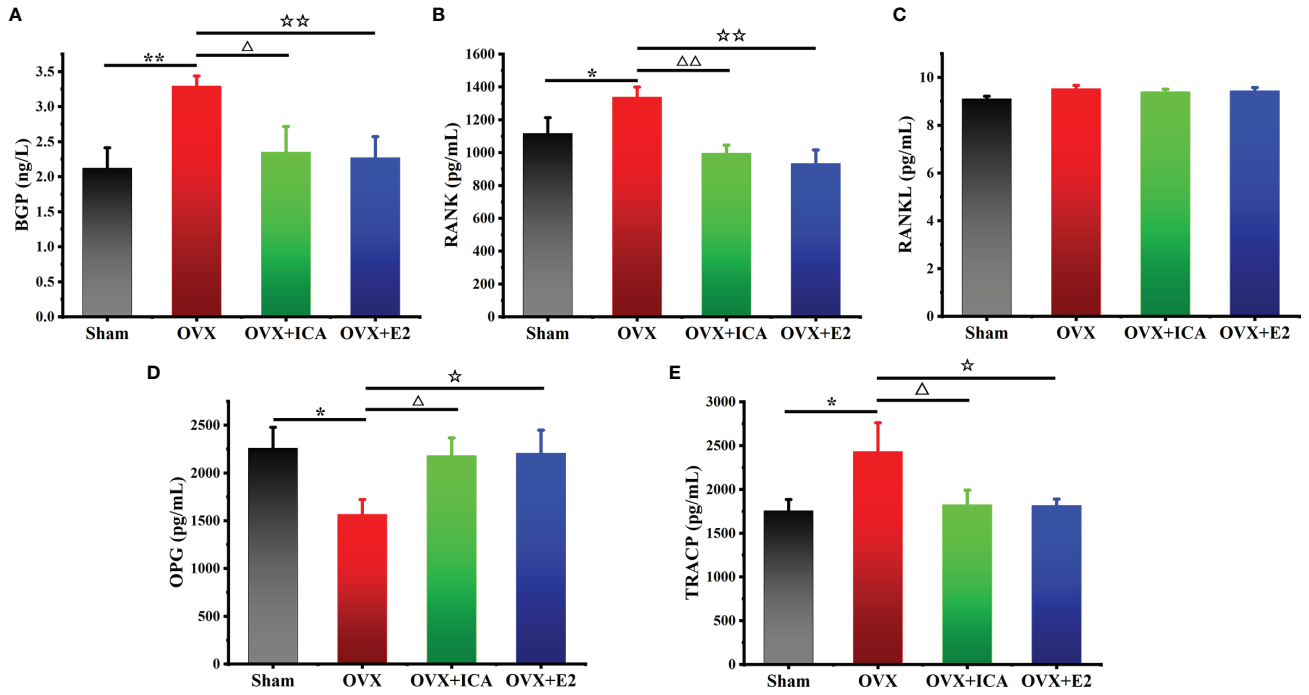

FIGURE 3 | Therapeutic effects of different treatments on serum concentrations of BGP **(A)**, OPG **(B)**, RANK **(C)**, RANKL **(D)** and TRACP **(E)** in PMOP model (n = 6). $^{*,\triangle,\star}p < 0.05$, $^{**,\triangle\triangle,\star\star}p < 0.01$.

showed that the significant differential metabolites in different samples within the same group were similar and varied in different groups (**Supplementary Figure S3A**).

A NEG mode-based analysis also identified several significant differential metabolites in different treatments. Briefly, except for deoxycholic acid and 3-Methyladipic acid, other metabolites including tetrahydrocorticosterone, N-Acetyl-L-phenylalanine, 1-Oleoyl-L-.alpha.-lysophosphatidic acid, lithocholic acid, D-Glucosamine 6-phosphate, succinate, propionic acid, adynerin, 15(S)-15-methyl PGF2alpha, cholic acid, glutaric acid and suberic acid were up-regulated significantly in Sham vs OVX (**Supplementary Table S1**). In OVX+ICA vs OVX, only two metabolites linoleic acid and guanosine were significantly up- and down-regulated, respectively (**Supplementary Table S1**). Unlike the results observed in POS mode, NEG mode only identified 4 metabolites being found in all the three comparisons (**Supplementary Table S1**; **Supplementary Figure S3B**). Interestingly, there were 4 metabolites, i.e., 15(S)-15-methyl PGF2alpha, lithocholic acid, lumichrome and linoleic acid, observed in one or two of the above comparisons showed significant difference between OVX+ICA vs OVX+E2 (**Supplementary Table S1**).

Collectively, ovariectomy, ICA or E2 administration resulted in a considerable change of 66 metabolites (**Supplementary Table S1**), those of which observed in two or three of the treatments might be important in the development or improvement of PMOP. They were tetrahydrocorticosterone, adynerin, 3-Amino-3-(4-Hydroxyphenyl) propanoate, stearidonic acid, triethanolamine, D-Ala-D-Ala, lithocholic acid, 1-Aminocyclohexanecarboxylic acid, L-Saccharopine, suberic acid, ADMA, Arg-Met, lumichronme, linoleic acid and deoxyinosine (**Supplementary Table S1**).

Unveiling Mechanisms Underlying ICA-Mediated Bone Metabolism Regulation Based on GM-Fecal Metabolite Relationships

The results of the correlation coefficient calculation between significant differential GM and fecal metabolites were given in **Supplementary Table S2**. Six GM in genera *Lactococcus*, *Butyricimonas*, *Negativibacillus*, *Rikenella*, *Lachnoclostridium* and *Harryflintia* were significantly correlated to 23 fecal metabolites in Sham vs OVX (**Figure 7**). Among which, *Lachnoclostridium* correlated significantly to most of the given metabolites, followed by *Lactococcus* and *Rikenella*, but *Butyricimonas*, *Negativibacillus* and *Harryflintia* only significantly correlated to one or two metabolites (**Figure 7**; **Supplementary Table S2A**). The network analysis showed that *Lachnoclostridium*, *Lactococcus*, *Harryflintia*, *Butyricimonas* and *Rikenella* had a higher correlation with 1-Aminocyclohexanecarboxylic acid, 1-Oleoyl-L-.alpha.-lysophosphatidic acid, 15(S)-15-methyl PGF2alpha, 2'-O-methylcytidine, 3-Amino-3-(4-hydroxyphenyl)propanoate, adynerin, D-Ala-D-Ala, D-Glucosamine 6-phosphate, deoxycholic acid, L-Saccharopine, N-(omega)-Hydroxyarginine, N-Acetyl-L-phenylalanine, nicotinate, propionic acid, stearidonic acid, succinate, tetrahydrocorticosterone and xanthosine (**Supplementary Figure S4**; **Supplementary Table S2A**).

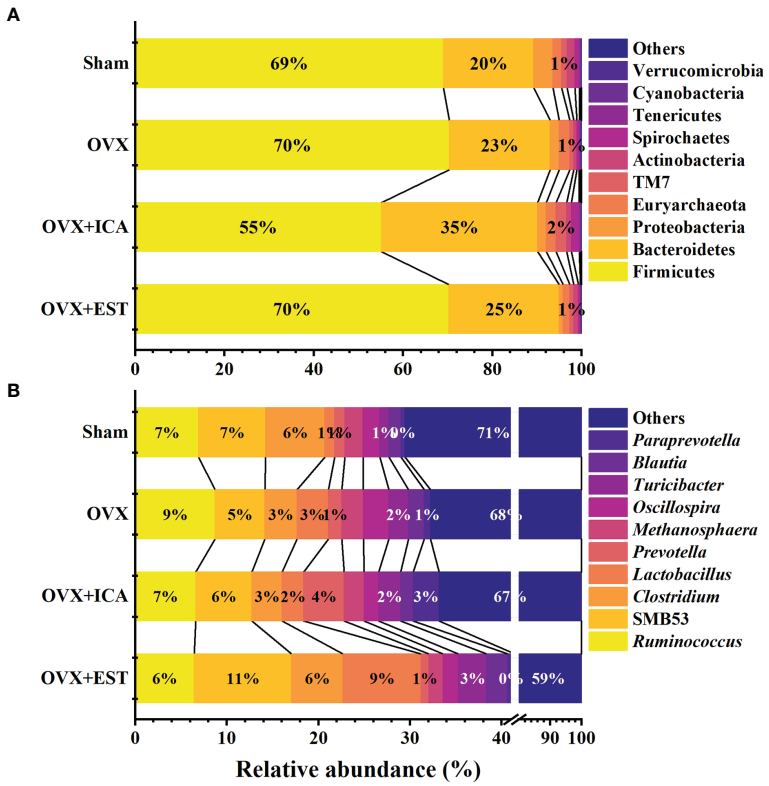

FIGURE 4 | Therapeutic effects of different treatments on the relative abundance of GM at the taxonomic levels of phylum **(A)** and genus **(B)** (n = 10). Only the Latin manes of the top 10 GM were given, while the low abundant ones were put together and shown as ''Others''.

TABLE 1 | Pearson analysis of the correlations between GM and serum biomarkers probably associated with bone metabolisms.

GM[a]		BGP	RANK	RANKL	OPG	TRACP
p_Actinobacteria	Pearson's r	-0.750	-0.267	-0.989*[b]	0.700	-0.700
	p-value	0.250	0.733	0.011	0.300	0.300
c_Gammaproteobacteria	Pearson's r	0.744	0.951*	0.089	-0.770	0.761
	p-value	0.256	0.049	0.911	0.230	0.239
c_Erysipelotrichi	Pearson's r	0.629	0.952*	-0.116	-0.676	0.671
	p-value	0.371	0.048	0.884	0.324	0.329
o_Enterobacteriales	Pearson's r	0.867	0.995**[c]	0.254	-0.900	0.899
	p-value	0.133	0.005	0.746	0.100	0.101
o_Erysipelotrichales	Pearson's r	0.629	0.952*	-0.116	-0.676	0.671
	p-value	0.371	0.048	0.884	0.324	0.329
o_Actinomycetales	Pearson's r	-0.878	-0.472	-0.952*	0.841	-0.841
	p-value	0.122	0.528	0.0480	0.159	0.159
g_*Ruminococcus*	Pearson's r	0.941	0.970*	0.418	-0.962*	0.961*
	p-value	0.059	0.030	0.582	0.038	0.039
g_*Oscillospira*	Pearson's r	0.924	0.954*	0.409	-0.951*	0.953*
	p-value	0.076	0.0460	0.591	0.0490	0.0470

[a]*p, phylu; c, class; o, order; g, genus.*
[b]** Significant correlation at p-value of 0.05 based on Two-tailed test.*
[c]*** Significant correlation at p-value of 0.01 based on Two-tailed test.*

As to OVX+ICA and OVX, the significant correlation was found between the GM such as unidentified_Corynebacteriaceae, *Elusimicrobium*, unidentified_Ruminococcaceae, *Parvibacter*, *Globicatella*, *Lactococcus* and *Adlercreutzia* and the metabolites such as Leu-ALA, guanosine, deoxyinosine, ADMA, Arg-Met, L-Saccharopine, 1-Aminocyclohexanecarboxylic acid, linoleic acid and 21-Hydroxypregnenolone (**Figure 8**). The key GM were *Elusimicrobium*, *Lactococcus* and *Globicatella*, which showed high correlation with ADMA, guanosine, 1-Aminocyclohexanecarboxylic acid, Arg-Met, 21-Hydroxypregnenolone, deoxyinosine and

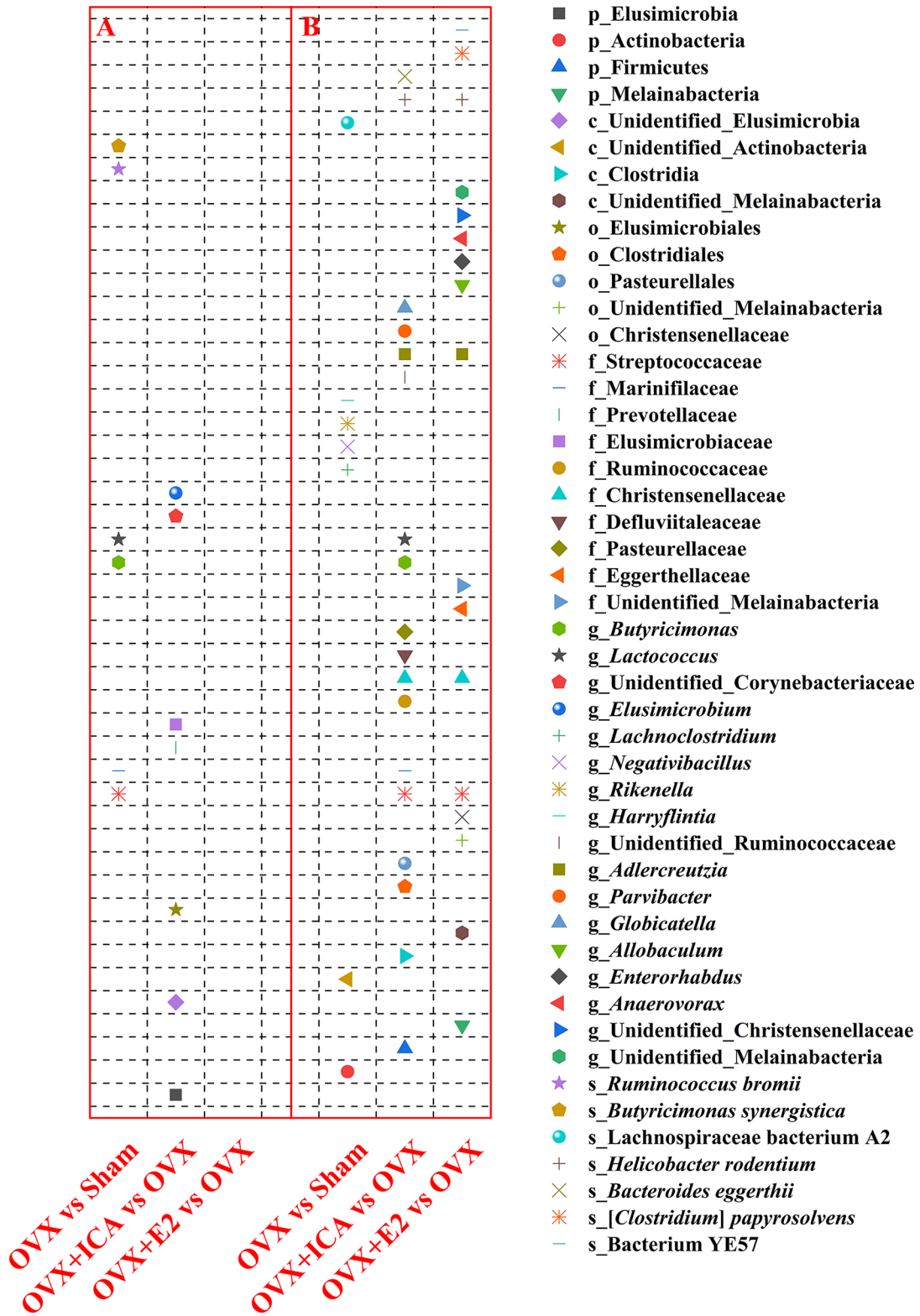

FIGURE 5 | Therapeutic effects of different treatments on the GM at different taxonomic levels by significant up-regulation **(A)** and down-regulation **(B)** between paired treatments (n = 10). The statistical analysis was performed by *t*-test at $p = 0.05$ using GraphPad Prism for Windows (Version 6.01, USA).

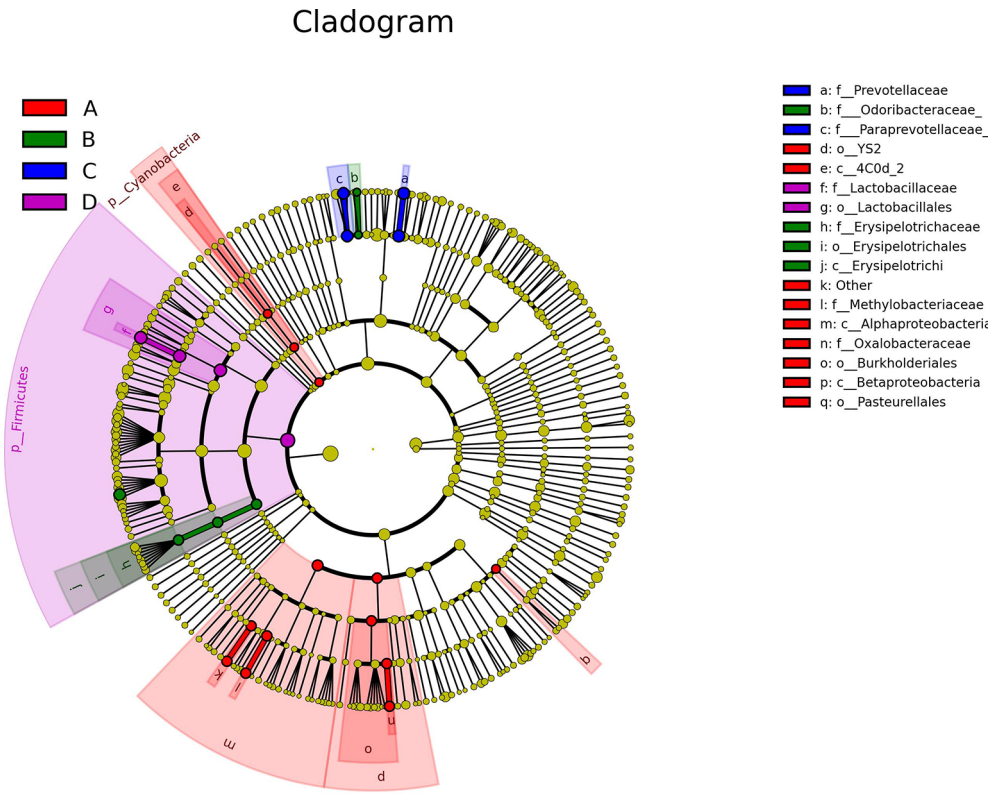

FIGURE 6 | Therapeutic effects of different treatments on the structure and key phylotypes of the GM displayed by cladogram based on LefSe analysis (n = 10). The levels represent, from the inner to outer rings, phylum, class, order, family, genus and species, which can identify the specific community or species that make a significant difference in sample classification. **(A-D)** represent Sham, OVX, OVX+ICA and OVX+E2 groups, respectively.

L-Saccharopine (**Supplementary Figure S5**; **Supplementary Table S2B**).

Unlike Sham vs OVX and OVX+ICA vs OVX, no positive correlation with statistical significance between GM and fecal metabolites in OVX+E2 vs OVX was found (**Figure 9**). Most of the key metabolites were correlated to at least one of the significant differential GM such as *Anaerovorax*, unidentified_Christensenellaceae, unidentified_Melainabacteria, *Allobaculum*, *Enterorhabdus* and *Adlercrutzia* (**Figure 9**; **Supplementary Table S2C**). The most eye-catching GM was *Adlercreutzia*, also observed in OVX+ICA, that correlated to most of the key metabolites (**Supplementary Figure S6**). Finally, we analyzed the correlation of GM and fecal metabolites between OVX+ICA and OVX+E2. The results showed that *Paraprevotella*, *Lactobacillus* and *Butyrivibrio* were significantly correlated to most of the significant differential metabolites except for L-Phenylalanine (**Figure 10**; **Supplementary Table S2D**).

DISCUSSION

In this study, ICA with an estrogen-like function improved the bone micro-architecture and the serum biomarkers associated with bone metabolism in OVX rats. Different treatments modulated specific GM and regulated fecal metabolite alterations. Several key GM were correlated to bile acid, amino acid and fatty acid, suggesting their potential roles in regulating the bone homeostasis. Such metabolites significantly correlated to the significant differential GM could be probably the targets to further understand the underlying metabolisms in regulating PMOP. These findings have provided new evidence for using ICA as a potential therapy for PMOP at the level of GM-bone axis.

Verification of *In Vivo* Therapeutic Effects of ICA on Inhibiting Bone Loss

The estrogen deficiency-induced PMOP has a typical symptom of bone metabolic disorder, which can stimulate RANKL production to prolong the life span of osteoclasts and reduce the life span of osteoblasts (35). Hormone replacement therapy is often used to prevent or ameliorate bone loss by promoting osteocalcin gene expression (4). The use of E2 in prevention and treatment of PMOP has been widely used for a long time (36, 37). Recent study further verified that E2 administration was able to increase BMD and BV/TV probably by changing miRNAs expression (5). As an alternative candidate for estrogen replacement due to its structural similarity with E2, ICA has shown outstanding effects on the improvement of PMOP (9).

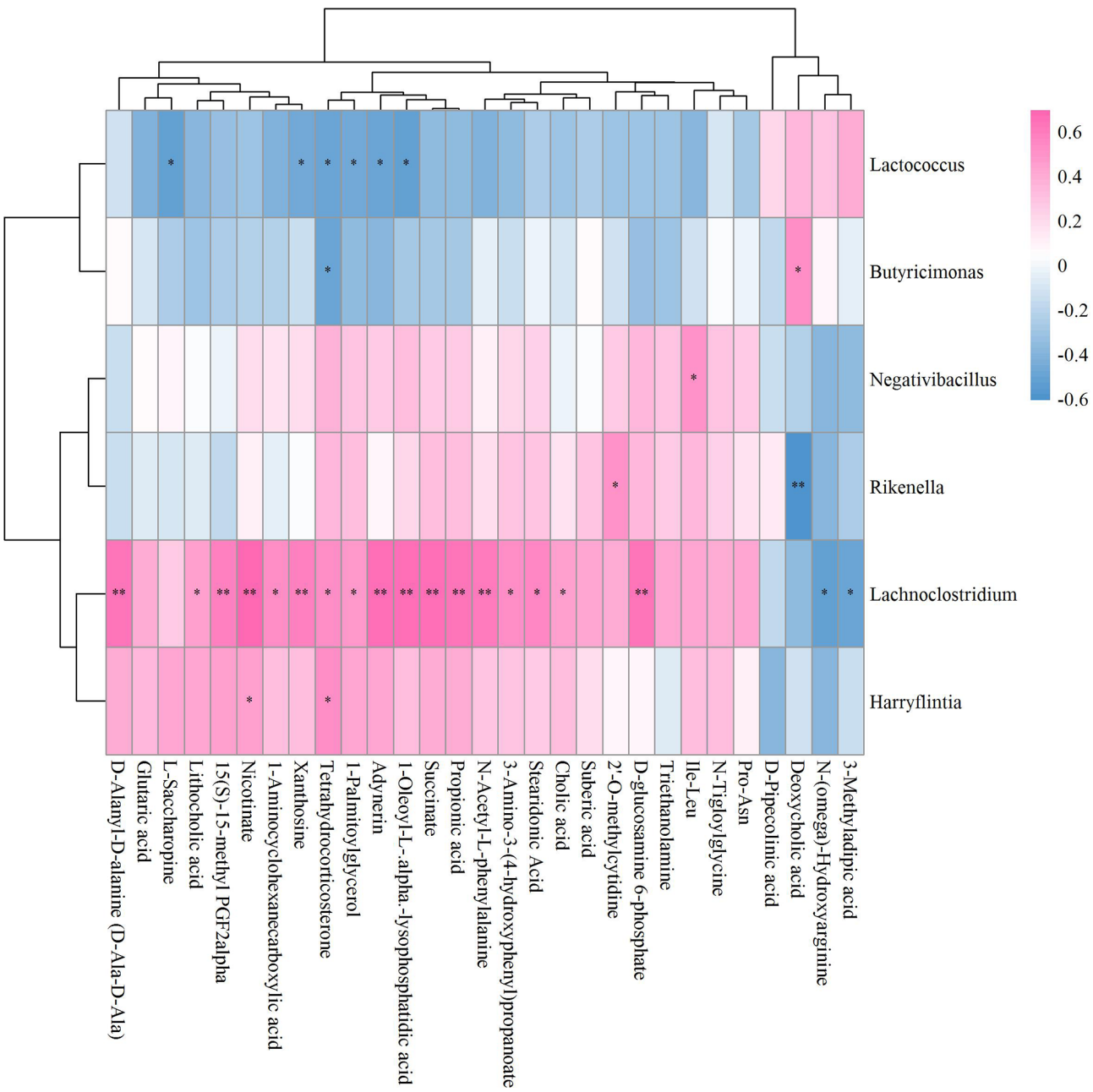

FIGURE 7 | Hierarchical clustering heat map of the significant differential GM and fecal metabolites in Sham and OVX groups based on Spearman correlation analysis (n = 10). * and ** mean a significant correlation between GM and fecal metabolites was found based on $p < 0.05$ and $p < 0.01$, respectively.

Here, we found a great ability of ICA administration to improve the micro-architecture of bone trabecula and increase BMD and BV/TV in OVX rats (**Figure 1**), in accordance with the recent studies from Wei et al. (14) and Zhou et al. (16). A significant decrease of BGP and RANK and increase of OPG in OVX rat serum suggested a direct evidence of ICA-induced osteogenic differentiation (38), which was probably mediated *via* Wnt/β-catenin pathway like other TCMs such as *radix Salviae miltiorrhizae* (RSM) and Liuwei Dihuang (10, 13, 39, 40). Other signaling pathways including IGF-I coupled non-genomic ERα and STAT associated with ICA-induced OP improvement have also been documented (16, 17), but whether the pathways RANKL/RANK/TRAF6 and OPG/RANKL/cathepsin K identified in other TCMs (39, 41) can be activated by ICA still warrants further investigations. As to another biomarker of bone sorption, TRACP can also be up-regulated following ovariectomy and decreased to a normal level of control (38). It is noting that the decrease of adipocytes also indicates a

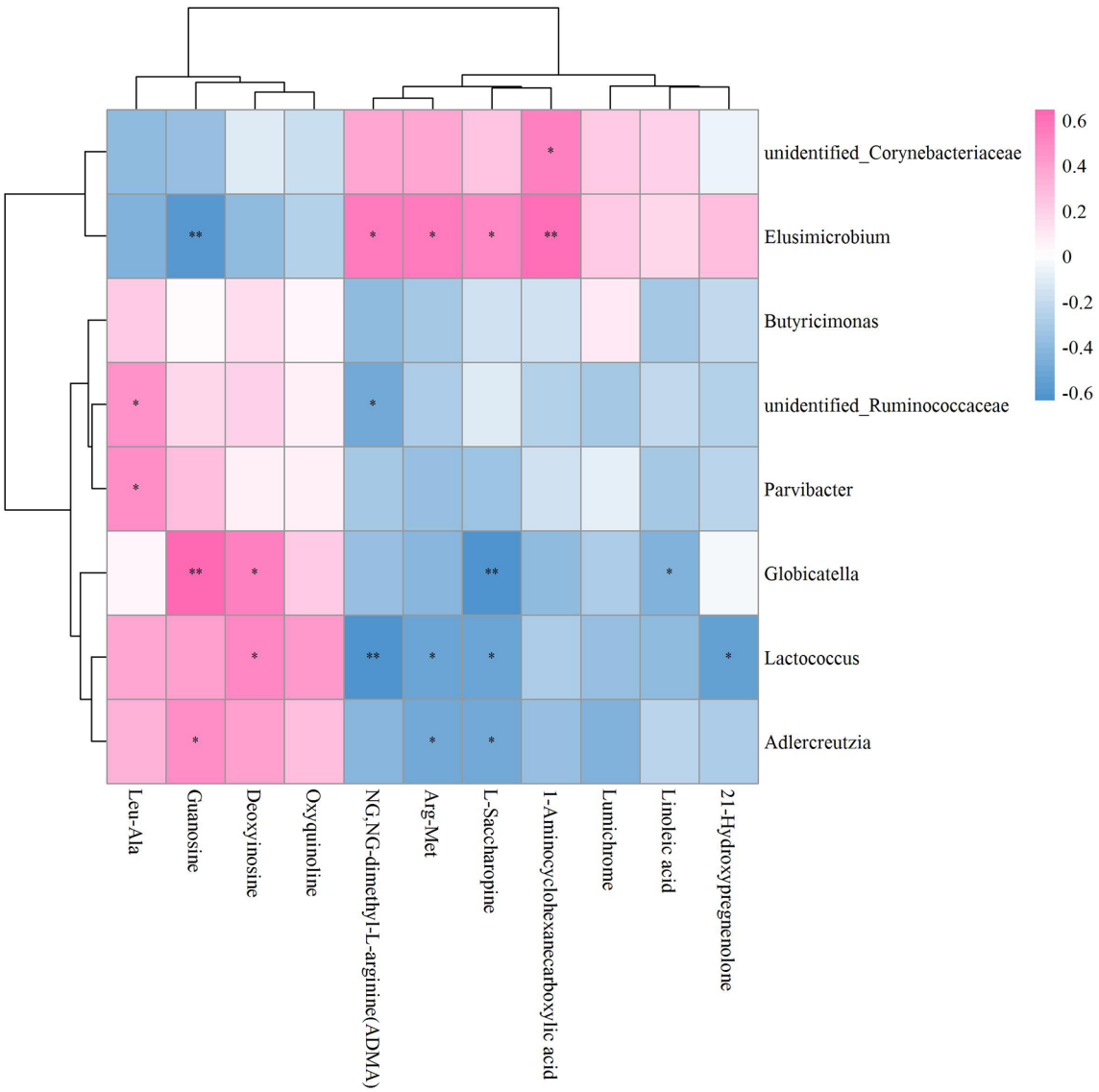

FIGURE 8 | Hierarchical clustering heat map of the significant differential GM and fecal metabolites in OVX+ICA and OVX groups based on Spearman correlation analysis (n = 10). * and ** mean a significant correlation between GM and fecal metabolites was found based on $p < 0.05$ and $p < 0.01$, respectively.

positive effect of ICA on osteogenic differentiation, which is probably due to the inhibition of AMPK/mTOR signaling pathway (42, 43) or the activation of RhoA-TAZ signaling pathway (44). Apparently, similar to E2 or other reported TCMs, ICA has played an equal role in improving bone metabolisms through regulating serum BGP, RANK, RANKL, OPG and TRACP concentrations.

Verification of GM-Related Targets Towards PMOP Regulation by High-Throughput Sequencing and Metabolomic Analyses

Gut microbes are involved in the regulation of bone homeostasis mainly *via* intestinal barrier and nutrient absorption (involving SCFAs), immunoregulation (Th-17 and T-reg cells balance) and regulation of intestinal-brain axis (involving 5-HT) (19). Several studies have found a higher abundance of Firmicutes and lower abundance of Bacteroidetes in OVX rats than Sham group (20, 25). In our study, ICA administration reversed the abundances of Firmicutes and Bacteroidetes (**Figure 4A**), in accordance with the findings from Xiong et al. (25) and Hong et al. (20) although the microbial compositions in genus level were different (**Figure 4B**). In fact, several key genera such as *Prevotella*, *Barnesiella*, *Lactococcus*, *Streptococcus* and *Ruminococcus* correlating to serum indexes of bone homeostasis and inflammation (TNF-α and IL-17) have been reported (21). Here, we detected a significant correlation of *Ruminococcus* with RANK, OPG and TRACP (**Table 1**) as reported by Ma et

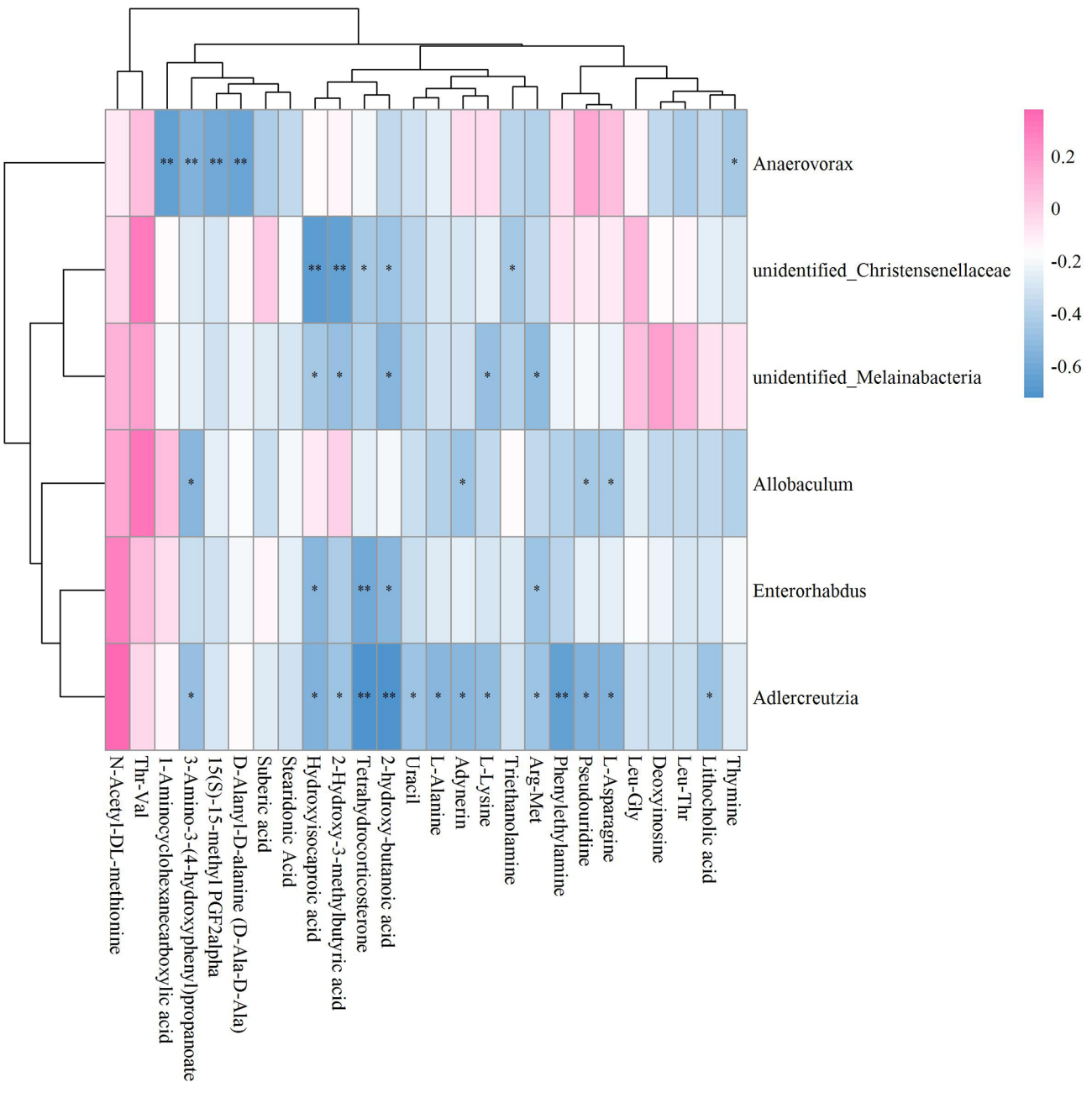

FIGURE 9 | Hierarchical clustering heat map of the significant differential GM and fecal metabolites in OVX+E2 and OVX groups based on Spearman correlation analysis (n = 10). * and ** mean a significant correlation between GM and fecal metabolites was found based on $p < 0.05$ and $p < 0.01$, respectively

al. (45), implying that ICA can modulate GM to influence serum indexes to regulate bone metabolisms. Moreover, ICA administration-induced improvement of intestinal barrier function has been proven to be associated with GM by inhibiting NF-κB or p38 MAPK signaling pathway (25, 26). Combining our results with those from other studies suggest that both the inhibition of NF-κB pathway to reduce bone resorption and the activation of Wnt/β-catenin pathway to enhance bone formation after E2 analogues administration may be associated with GM (21, 46). Therefore, further investigations on the effects of ICA on the prevention and treatment of PMOP can be performed by determining the inflammatory factors and correlating the data to GM and serum indexes.

Different treatments modulate specific microbial communities, *t*-test is able to identify the significant differential GM (47). By emphasizing on the cases for OVX and OVX+ICA, 3 GM with significant difference were identified (**Figure 5**). Except for *Butyricimonas*, both Streptococcaceae and *Lactococcus*

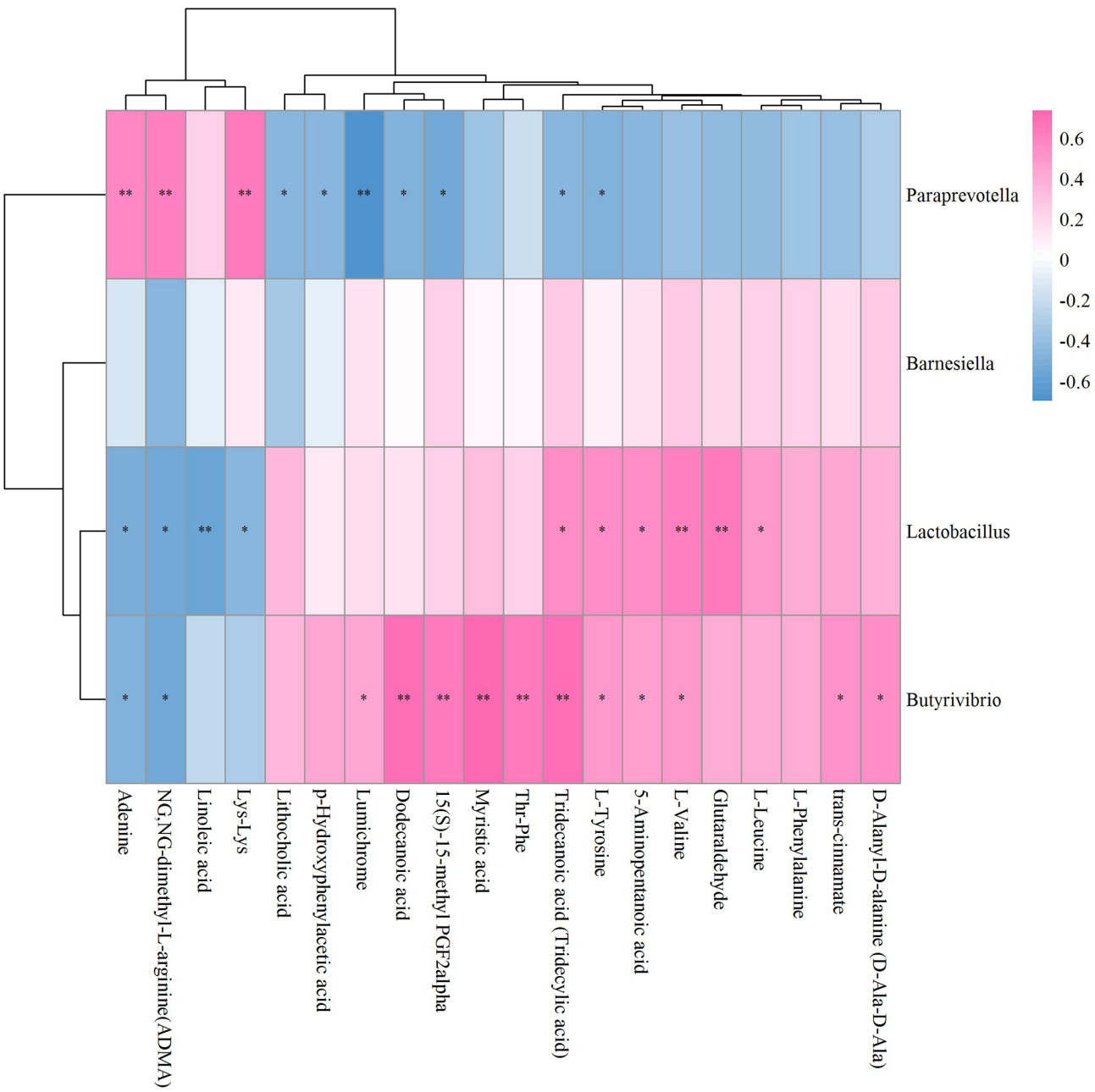

FIGURE 10 | Hierarchical clustering heat map of the significant differential GM and fecal metabolites in OVX+ICA and OVX+E2 groups based on Spearman correlation analysis (n = 10). * and ** mean a significant correlation between GM and fecal metabolites was found based on $p < 0.05$ and $p < 0.01$, respectively.

are belonging to Firmicutes. Although Streptococcaceae, *Lactococcus* and *Butyricimonas* were not significantly correlated to serum indexes (**Table 1**), the first two were reported to have close relationships with IL-17, TNF-α and Wnt1 according to Li J. et al. (21). In contrast, other GM correlated well to serum indexes have not shown significant difference between treatments (**Figure 5**; **Table 1**). In other words, the high abundant and significant different GM among treatments likely involved in different processes to regulate bone metabolism due to the complex mechanisms as previously described (19). Interestingly, Streptococcaceae, Christensenellaceae, *Adlercreutzia* and *Helicobacter rodentium* followed similar trend in OVX+ICA vs OVX and OVX+E2 vs OVX, again verifying the potential roles of ICA, as an analogue of E2, in the prevention and treatment of PMOP (9). Since LefSe analysis and LDA obtain unique GM in one group apart from others, they provide more information about the key phylotypes in each treatment (20, 33). In summary, the significant differential GM between treatments and the key

phylotypes in each treatment suggest a full picture of the interactions between ICA and GM.

Besides the modulation towards GM, different treatments also resulted in a considerable change of the fecal metabolites (**Supplementary Table S1**). Bile acid is an important compound which has been reported to have vital roles in bone metabolism (48, 49). The primary bile acid (e.g., cholic acid) is synthesized in liver and modified to secondary products such as lithocholic acid, deoxycholic acid and their conjugated species in gut by microbes, finally enters portal veins (50). The hepatoenteral circulation maintains the stability of bile acid metabolism, thus both the serum and fecal bile acids have been used to evaluate their roles in bone metabolisms (51, 52). In our study, the ovariectomy enhanced cholic acid and lithocholic acid assimilation but promoted deoxycholic acid loss, which was likely attributed to the PMOP development as reported previously (52, 53). However, the regulation of bile acid metabolism might be one of the possible mechanisms to improve PMOP by E2 but not ICA administration (**Supplementary Table S1**). It has shown that the overconsumption of *n*-6 polyunsaturated fatty acids (PUFA) may result in a high *n*-6 to *n*-3 ration and thus lead to an increased pathogenesis of PMOP by promoting low-grade chronic inflammation (LGCI) (54). The anti-inflammatory role of stearidonic acid (a *n*-3 PUFA derived from linoleic acid) in improving PMOP have been widely studied (54), which was also supported by our data that E2 administration promoted a significant increase of stearidonic acid (FC = 1.49, $p < 0.001$). It was interesting to note that ICA administration also significantly up-regulated the precursor of stearidonic acid, i.e., linoleic acid, by FC of 1.36 ($p < 0.05$), which was 1.32 times of E2 group ($p < 0.05$). The relationships between linoleic acid and bone biology have been widely studied and recently verified to promote bone formation in OVX rats by co-working with ultraviolet B treatment (55, 56). L-Saccharopine is an important metabolite in amino acid metabolism and often decrease during the progression of OP and PMOP (57, 58). While ovariectomy resulted in a significant decrease of L-Saccharopine (FC = 0.69, $p < 0.05$), the ICA administration significantly up-regulated it by FC of 1.47 ($p< 0.05$), similar to the effects of velvet collagen hydrolysate (57) and sialoglycoprotein (58). Since its vital roles in amino acid metabolism and PMOP improvement, we conclude that L-Saccharopine can be an important biomarker to further evaluate the mechanisms of ICA towards PMOP prevention and treatment. In our study, we also noted a significant alteration of 1-Aminocyclohexanecarboxylic acid in OVX as well as the ICA and E2 administrated rats (**Supplementary Table S1**). 1-Aminocyclohexanecarboxylic acid is an antistaphylococcal amino acid and has been used to prepare 4-Aminophenoxyacetic acid, a novel class of reversible cathepsin K inhibitors (59–61). However, whether ICA and E2, similar to RSM, possesses the ability to improve PMOP *via* OPG/RANKL/cathepsin K signaling pathway with the aid of 1-Aminocyclohexanecarboxylic acid warrants further study (39).

Other metabolites involved in the regulation of PMOP when administrated with E2 were also found in this study (**Supplementary Table S1**). Unlike typical glucocorticoids, which have systematic side effects such as OP, abdominal obesity and glaucoma, tetrahydrocorticosterone has shown outstanding potentials in defensing inflammation with fewer side effects (62). Here, we found a down-regulation of tetrahydrocorticosterone by 40 times in OVX rats as compared to Sham group ($p < 0.001$), while E2 significantly increased its production (FC = 1.82, $p < 0.001$). Several studies have also shown the relationship between 2-Hydroxy-butanoic acid and TRACP (63), the effects of L-Lysine on stimulating the osteoblast proliferation and synthetic activity (64), the transformation between L-Alanine and tryptophane and its roles in regulating PMOP (65), and the prevention of bone loss by enhancing L-Asparagine production and OPG increase (66, 67). It seemed that, however, ICA-induced improvement of PMOP cannot be associated with the above-mentioned metabolites although no significant difference between ICA and E2 treatments were observed (**Supplementary Table S1**). These results showed that ICA had different mechanisms for the treatment of PMOP as compared to E2 administration.

Exploration of Potential GM-Bone Axis Mechanisms Underlying Therapeutic Effects of ICA on PMOP

It has well-documented that the gut microbial alterations can impair bone strength and tissue material properties (68). *Lachnoclostridium* is an abundant GM having key correlations with bone mass (69, 70), which was supported by our results that this genus significantly correlated to most of the significant differential metabolites (**Figure 7**). While *Butyricimonas* can regulate bile acid by influencing vitamin D absorption (24), no study has so far shown the role of *Rikenella* in bile acid metabolism. As to *Adlercreuztia*, it can function in bone metabolism by regulating cholic acid, exactly lithocholic acid in this study, like *Gordonibacter* and *Parvibacter*, which belong to the same family of *Adlercreutzia*, Eggerthellaceae (52). Our data showed that the down- and up-regulation of L-Saccharopine, a lysine degradation intermediate (71), in OVX and ICA groups were associated with *Lactococcus*, as well as the genera *Elusimicrobium*, *Globicatella* and *Adlercreutzia* (**Figure 7**). Other amino acids such as 1-Aminocyclohexanecarboxylic acid, L-Asparagine, L-Lysine, L-Alanine and 2-Hydroxy-butanoic acid significantly correlated to *Lachnoclostridium*, *Elusimicrobium*, *Anaerovorax*, *Adlercreutzia*, *Allobaculum* and *Enterorhabdus*, which were in line with the finding that the association of GM with PMOP was mediated by amino acid metabolism (72). More and more studies have verified that several lactic acid bacteria are capable of the biohydrogenation of linoleic acid (73). Recent study also revealed the prevention of PMOP in OVX rats by *Saururus chinensis* extract due to the involvement of linoleic acid (22). In our study, the GM significantly correlated to metabolites were belonging to two independent families Aerococcaceae (*Globicatella*) and Lactobacillaceae (*Lactobacillus*) in the same order Lactobacillales of Firmicutes (**Figures 8**, **10**). Of which, *Lactobacillus* has been widely used to prevent PMOP in OVX model (18, 74, 75). As indicated, the IGF-I signaling pathway was involved in this process (18).

Taken together, the ovariectomy mainly disrupted bile acid metabolism to induce PMOP (**Figure 11A**), while ICA

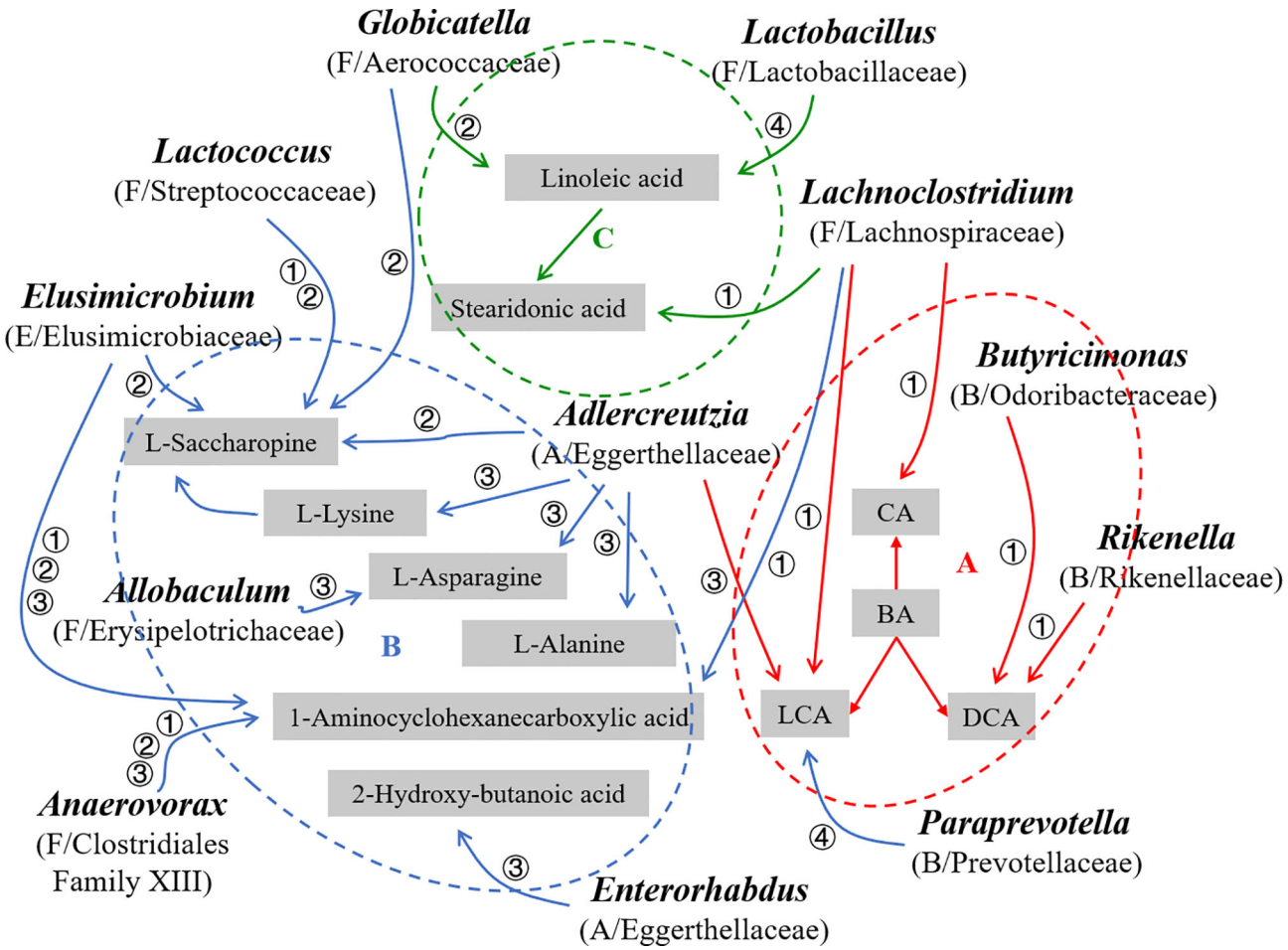

FIGURE 11 | Schematic diagram of the GM and key metabolites probably associated with PMOP development and (or) improvement in OVX rats (n = 10). The red (→, A, o), blue (→, B, o) and green (→, C, o) information represent bile acid, amino acid and fatty acid metabolisms, respectively. A, Actinobacteria; B, Bacteroidetes; F, Firmicutes; E. Elusimicrobia; BA, Bile acid, CA, Cholic acid, LCA, Lithocholic acid, DCA, Deoxycholic acid; ①, ②, ③ and ④ mean Sham vs OVX, OVX+ICA vs OVX, OVX+E2 vs OVX and OVX+ICA vs OVX+E2, respectively.

administration restored the bone metabolism homeostasis through amino acid and fatty acid metabolism (**Figure 11B**), and E2 intervention treatment activated both bile acid and amino acid metabolisms to improve PMOP (**Figure 11C**). We concluded that the improvement of PMOP after ICA or E2 administration was probably in part achieved by GM-mediated bile acid, amino acid and fatty acid metabolisms.

CONCLUSIONS

In this study, ICA exhibited great ability in protecting bone by regulating GM-bone axis in OVX rats. Both GM modulation and fecal metabolite alteration were induced by ICA administration to improve PMOP. The underlying mechanisms included GM-regulated changes of the serum biomarkers RANK, RANKL, OPG and TRACP, and alterations of the fecal metabolites such as bile acid, amino acid and fatty acid. Our data provided evidence for ICA as a novel potential therapy for PMOP, and shed lights onto the PMOP pathogenesis from a new perspective.

DATA AVAILABILITY STATEMENT

The original contributions presented in the study are publicly available. This data can be found here: NCBI, PRJNA807063.

ETHICS STATEMENT

The animal study was reviewed and approved by The Laboratory Animal Welfare and Ethics Committee of Fujian University of Traditional Chinese Medicine.

AUTHOR CONTRIBUTIONS

Conceptualization, XL. Data Curation, SSW, SJW, XW, YX, and XL. Funding acquisition, SSW and XL. Sources, XL. Investigation, SJW and YX. Methodology, SJW, XW, YX, XZ, YH, LW, HZY, and XL. Supervision, HZY and XL. Writing—original draft, SSW and XL. Writing—review and editing, SSW, SJW, XW, YX, XZ, YH, HY, LL, LW, HZY, and XL. All authors contributed to the article and approved the submitted version.

FUNDING

This work was funded by the National Natural Science Foundation of China (No. 82074461), the Natural Science Foundation of Fujian Province (No. 2021J01364), the Chen Keji Development Fund of Integrative Medicine (No. 2020004) and the Research Start-up Fund of Fujian University of Traditional Chinese Medicine (No. X2020011-Talent).

ACKNOWLEDGMENTS

We would like to thank Dr. Yong-He Han at College of Environmental Science and Engineering of Fujian Normal University and three reviewers for their helpful suggestions which have help us to improve the manuscript.

SUPPLEMENTARY MATERIAL

The Supplementary Material for this article can be found online at: https://www.frontiersin.org/articles/10.3389/fendo.2022.874849/full#supplementary-material

REFERENCES

1. Lorentzon M, Johansson H, Harvey NC, Liu E, Vandenput L, McCloskey EV, et al. Osteoporosis and Fractures in Women: The Burden of Disease. *Climacteric* (2022) 25(1):4–10. doi: 10.1080/13697137.2021.1951206
2. Gennari L, Rotatori S, Bianciardi S, Nuti R, Merlotti D. Treatment Needs and Current Options for Postmenopausal Osteoporosis. *Expert Opin Pharmacother* (2016) 17(8):1141–52. doi: 10.1080/14656566.2016.1176147
3. Ma YL, Marin F, Stepan J, SophiaIsh-Shalom, Möricke R, Hawkins F, et al. Comparative Effects of Teriparatide and Strontium Ranelate in the Periosteum of Iliac Crest Biopsies in Postmenopausal Women With Osteoporosis. *Bone* (2011) 48(5):972–8. doi: 10.1016/j.bone.2011.01.012
4. Rahnama M, Jastrzębska-Jamrogiewicz I, Jamrogiewicz R, Trybek G. Analysis of the Influence of Hormone Replacement Therapy on Osteocalcin Gene Expression in Postmenopausal Women. *BioMed Res Int* (2015) 2015:416929. doi: 10.1155/2015/416929
5. Xu X, Zhang P, Li X, Liang Y, Ouyang K, Xiong J, et al. MicroRNA Expression Profiling in an Ovariectomized Rat Model of Postmenopausal Osteoporosis Before and After Estrogen Treatment. *Am J Trans Res* (2020) 12(8):4251–63.
6. Jiang Z, Li Z, Zhang W, Yang Y, Han B, Liu W, et al. Dietary Natural N-Acetyl-D-Glucosamine Prevents Bone Loss in Ovariectomized Rat Model of Postmenopausal Osteoporosis. *Molecules* (2018) 23(9):2302. doi: 10.3390/molecules23092302
7. Wu H, Kim M, Han J. Icariin Metabolism by Human Intestinal Microflora. *Molecules* (2016) 21:1158. doi: 10.3390/molecules21091158
8. Tang D, Ju C, Liu Y, Xu F, Wang Z, Wang D. Therapeutic Effect of Icariin Combined With Stem Cells on Postmenopausal Osteoporosis in Rats. *J Bone Miner Metab* (2018) 36:180–8. doi.org/10.1007/s00774-017-0831-x
9. Xu J-h, Yao M, Ye J, Wang G-d, Wang J, Xue-jun C, et al. Bone Mass Improved Effect of Icariin for Postmenopausal Osteoporosis in Ovariectomy-Induced Rats: A Meta-Analysis and Systematic Review. *Menopause: J North Am Menopause Soc* (2016) 23(10):1152–7. doi: 10.1097/GME.0000000000000673
10. Chen G, Wang C, Wang J, Yin S, Gao H, Xiang L, et al. Antiosteoporotic Effect of Icariin in Ovariectomized Rats Is Mediated *via* the Wnt/β-Catenin Pathway. *Exp Ther Med* (2016) 12:279–87. doi: 10.3892/etm.2016.3333
11. Wang Z, Ding L, Zhang S, Jiang T, Yang Y, Li R. Effects of Icariin on the Regulation of the OPG–RANKL–RANK System are Mediated Through the MAPK Pathways in IL–1β–Stimulated Human SW1353 Chondrosarcoma Cells. *Int J Mol Med* (2014) 34(6):1720–6. doi: 10.3892/ijmm.2014.1952
12. Zhang Z-B, Yang Q-T. The Testosterone Mimetic Properties of Icariin. *Asian J Androlo* (2006) 8(5):601–5. doi: 10.1111/j.1745-7262.2006.00197.x
13. Gao J, Xiang S, Wei X, Yadav RI, Han M, Zheng W, et al. Icariin Promotes the Osteogenesis of Bone Marrow Mesenchymal Stem Cells Through Regulating Sclerostin and Activating the Wnt/β-Catenin Signaling Pathway. *BioMed Res Int* (2021) 2021:6666836. doi: 10.1155/2021/6666836
14. Wei Q, Zhang J, Hong G, Chen Z, Deng W, He W, et al. Icariin Promotes Osteogenic Differentiation of Rat Bone Marrow Stromal Cells by Activating the Erα-Wnt/β-Catenin Signaling Pathway. *Biomed Pharmacother* (2016) 84:931–9. doi: 10.1016/j.biopha.2016.09.107
15. Li X-F, Xu H, Zhao Y-J, Tang D-Z, Xu G-H, Holz J, et al. Icariin Augments Bone Formation and Reverses the Phenotypes of Osteoprotegerin-Deficient Mice Through the Activation of Wnt/β-Catenin-BMP Signaling. *Evidence-Based Complement Altern Med* (2013) 2013:652317. doi: 10.1155/2013/652317
16. Zhou L, Poon CC-W, Wong K-Y, Cao S, Dong X, Zhang Y, et al. Icariin Ameliorates Estrogen-Deficiency Induced Bone Loss by Enhancing IGF-I Signaling *via* Its Crosstalk With non-Genomic Erα Signaling. *Phytomedicine* (2021) 82:153413. doi: 10.1016/j.phymed.2020.153413
17. Xu H, Zhou S, Qu R, Yang Y, Gong X, Hong Y, et al. Icariin Prevents Oestrogen Deficiency–Induced Alveolar Bone Loss Through Promoting Osteogenesis *via* STAT3. *Cell Prolif* (2020) 53(2):e12743. doi: 10.1111/cpr.12743
18. Yan J, Herzog JW, Tsang K, Brennan CA, Bower MA, Garrett WS, et al. Gut Microbiota Induce IGF-1 and Promote Bone Formation and Growth. *Proc Natl Acad Sci USA* (2016) 113(47):E7554–63. doi: 10.1073/pnas.1607235113
19. Ding K, Hua F, Ding W. Gut Microbiome and Osteoporosis. *Aging Dis* (2020) 11(2):438–47. doi: 10.14336/AD.2019.0523
20. Hong S, Cha KH, Kwon DY, Son YJ, Kim SM, Choi J-H, et al. *Agastache Rugosa* Ethanol Extract Suppresses Bone Loss *via* Induction of Osteoblast Differentiation With Alteration of Gut Microbiota. *Phytomedicine* (2021) 84:153517. doi: 10.1016/j.phymed.2021.153517
21. Li J, Yang M, Lu C, Han J, Tang S, Zhou J, et al. Tuna Bone Powder Alleviates Glucocorticoid-Induced Osteoporosis *via* Coregulation of the NF-κb and Wnt/β-Catenin Signaling Pathways and Modulation of Gut Microbiota Composition and Metabolism. *Mol Nutr Food Res* (2020) 65(5):1900861. doi: 10.1002/mnfr.201900861
22. Lee S, Jang GJ, Yoo M, Hur HJ, Sung MJ. *Saururus Chinensis* Prevents Estrogen Deficiency-Induced Osteoporosis in Rats: A Metabolomic Study Using UPLC/Q-TOF MS. *Appl Sci* (2021) 11:1392. doi: 10.3390/app11041392
23. Ling C-w, Miao Z, Xiao M-l, Zhou H, Jiang Z, Fu Y, et al. The Association of Gut Microbiota With Osteoporosis Is Mediated by Amino Acid Metabolism: Multiomics in a Large Cohort. *J Clin Endocrinol Metab* (2021) 106(10):e3852–64. doi: 10.1210/clinem/dgab492
24. Robles-Vera I, Callejo M, Ramos R, Duarte J, Perez-Vizcaino F. Impact of Vitamin D Deficit on the Rat Gut Microbiome. *Nutrients* (2019) 11(11):2564. doi: 10.3390/nu11112564
25. Xiong W, Ma H, Zhang Z, Jin M, Wang J, Xu Y, et al. Icariin Enhances Intestinal Barrier Function by Inhibiting NF-κb Signaling Pathways and Modulating Gut Microbiota in a Piglet Model. *RSC Adv* (2019) 9:37947–56. doi: 10.1039/C9RA07176H

26. Xiong W, Huang J, Li X, Zhang Z, Jin M, Wang J, et al. Icariin and Its Phosphorylated Derivatives Alleviate Intestinal Epithelial Barrier Disruption Caused by Enterotoxigenic *Escherichia Coli* Through Modulate P38 MAPK *In Vivo* and *In Vitro*. *FASEB J* (2020) 34:1783–801. doi: 10.1096/fj.201902265R
27. Zhang H, Zhuo S, Song D, Wang L, Gu J, Ma J, et al. Icariin Inhibits Intestinal Inflammation of DSS-Induced Colitis Mice Through Modulating Intestinal Flora Abundance and Modulating P-P65/P65 Molecule. *Turkish J Gastroenterol* (2021) 32(4):382–92. doi: 10.5152/tjg.2021.20282
28. Yang S, Wang L, Feng S, Yang Q, Yu B, Tu M. Enhanced Bone Formation by Strontium Modified Calcium Sulfate Hemihydrate in Ovariectomized Rat Critical-Size Calvarial Defects. *Biomed Mater* (2017) 12(3):035004. doi: 10.1088/1748-605X/aa68bc
29. Fu C, Xu D, Wang C-Y, Jin Y, Liu Q, Meng Q, et al. Alpha-Lipoic Acid Promotes Osteoblastic Formation in H_2O_2-Treated MC3T3-E1 Cells and Prevents Bone Loss in Ovariectomized Rats. *J Cell Physiol* (2015) 230 (9):2184–201. doi: 10.1002/jcp.24947
30. Zhang Y, Xiang C, Wang Y, Duan Y, Liu C, Jin Y, et al. lncRNA LINC00152 Knockdown had Effects to Suppress Biological Activity of Lung Cancer *via* EGFR/PI3K/AKT Pathway. *Biomed Pharmacother* (2017) 94:644–51. doi: 10.1016/j.biopha.2017.07.120
31. Ye M, Zhang C, Jia W, Shen Q, Qin X, Zhang H, et al. Metabolomics Strategy Reveals the Osteogenic Mechanism of Yak (*Bos Grunniens*) Bone Collagen Peptides on Ovariectomy-Induced Osteoporosis in Rats. *Food Funct* (2020) 11:1498–512. doi: 10.1039/C9FO01944H
32. Han Y-H, Yin D-X, Jia M-R, Wang S-S, Chen Y, Rathinasabapathi B, et al. Arsenic-Resistance Mechanisms in Bacterium *Leclercia Adecarboxylata* Strain As3-1: Biochemical and Genomic Analyses. *Sci Total Environ* (2019) 690:1178–89. doi: 10.1016/j.scitotenv.2019.07.098
33. Segata N, Izard J, Waldron L, Gevers D, Miropolsky L, Garrett WS, et al. Metagenomic Biomarker Discovery and Explanation. *Genome Biol* (2011) 12: R60. doi: 10.1186/gb-2011-12-6-r60
34. Zhang B, Yang L-L, Ding S-Q, Liu J-J, Dong Y-H, Li Y-T, et al. Anti-Steoporotic Activity of an Edible Traditional Chinese Medicine *Cistanche Deserticola* on Bone Metabolism of Ovariectomized Rats Through RANKL/RANK/TRAF6-Mediated Signaling Pathways. *Front Pharmacol* (2019) 10:1412. doi: 10.3389/fphar.2019.01412
35. Gutierrez-Buey G, Restituto P, Botella S, Monreal I, Colina I, Rodríguez-Fraile M, et al. Trabecular Bone Score and Bone Remodelling Markers Identify Perimenopausal Women at High Risk of Bone Loss. *Clin Endocrinol* (2019) 91 (3):391–9. doi: 10.1111/cen.14042
36. Ettinger B. Prevention of Osteoporosis: Treatment of Estradiol Deficiency. *Obstet Gynecol* (1988) 72(5):S12–7.
37. Warming L, Ravn P, Nielsen T, Christiansen C. Safety and Efficacy of Drospirenone Used in a Continuous Combination With 17β-Estradiol for Prevention of Postmenopausal Osteoporosis. *Climacteric* (2004) 7(1):103–11. doi: 10.1080/13697130310001651535
38. He J-p, Feng X, Wang J-f, Shi W-g, Li H, Danilchenko S, et al. Icariin Prevents Bone Loss by Inhibiting Bone Resorption and Stabilizing Bone Biological Apatite in a Hindlimb Suspension Rodent Model. *Acta Pharmacol Sin* (2018) 39:1760–7. doi: 10.1038/s41401-018-0040-8
39. Liu H, Zhu R, Wang L, Liu C, Ma R, Qi B, et al. *Radix Salviae Miltiorrhizae* Improves Bone Microstructure and Strength Through Wnt/β-Catenin and Osteoprotegerin/Receptor Activator for Nuclear Factor-κb Ligand/Cathepsin K Signaling in Ovariectomized Rats. *Phytother Res* (2018) 32(12):2487–500. doi: 10.1002/ptr.6188
40. Xia B, Xu B, Sun Y, Xiao L, Pan J, Jin H, et al. The Effects of Liuwei Dihuang on Canonical Wnt/β-Catenin Signaling Pathway in Osteoporosis. *J Ethnopharmacol* (2014) 153(1):133–41. doi: 10.1016/j.jep.2014.01.040
41. Ma X, Liu J, Yang L, Zhang B, Dong Y, Zhao Q. *Cynomorium Songaricum* Prevents Bone Resorption in Ovariectomized Rats Through RANKL/RANK/TRAF6 Mediated Suppression of PI3K/AKT and NF-κb Pathways. *Life Sci* (2018) 209:140–8. doi: 10.1016/j.lfs.2018.08.008
42. Han Y-Y, Song M-Y, Hwang M-S, Hwang J-H, Park Y-K, Jung H-W. *Epimedium Koreanum* Nakai and Its Main Constituent Icariin Suppress Lipid Accumulation During Adipocyte Differentiation of 3T3-L1 Preadipocytes. *Chin J Natural Medicines* (2016) 14(4):671–6. doi: 10.1016/S1875-5364(16)30079-6
43. Li H, Yuan Y, Zhang Y, Zhang X, Xu LG. Icariin Inhibits AMPK-Dependent Autophagy and Adipogenesis in Adipocytes *In Vitro* and in a Model of Graves' Orbitopathy *In Vivo*. *Front Physiol* (2017) 8:45. doi: 10.3389/fphys.2017.00045
44. Ye Y, Jing X, Li N, Wu Y, Li B, Xu T. Icariin Promotes Proliferation and Osteogenic Differentiation of Rat Adipose-Derived Stem Cells by Activating the RhoA-TAZ Signaling Pathway. *Biomed Pharmacother* (2017) 88:384–94. doi: 10.1016/j.biopha.2017.01.075
45. Ma S, Qin J, Hao Y, Shi Y, Fu L. Structural and Functional Changes of Gut Microbiota in Ovariectomized Rats and Their Correlations With Altered Bone Mass. *Aging* (2020) 12(11):10736–53. doi: 10.18632/aging.103290
46. Srivastava RK, Dar HY, Mishra PK. Immunoporosis: Immunology of Osteoporosis—Role of T Cells. *Front Immunol* (2018) 9:657. doi: 10.3389/fimmu.2018.00657
47. Huazano-García A, Shin H, López MG. Modulation of Gut Microbiota of Overweight Mice by Agavins and Their Association With Body Weight Loss. *Nutrients* (2017) 9(9):821. doi: 10.3390/nu9090821
48. Dubreuil M, Ruiz-Gaspà S, Guañabens N, Peris P, Álvarez L, Monegal A, et al. Ursodeoxycholic Acid Increases Differentiation and Mineralization and Neutralizes the Damaging Effects of Bilirubin on Osteoblastic Cells. *Liver Int* (2013) 33(7):1029–38. doi: 10.1111/liv.12153
49. Zhao Y-X, Song Y-W, Zhang L, Zheng F-J, Wang X-M, Zhuang X-H, et al. Association Between Bile Acid Metabolism and Bone Mineral Density in Postmenopausal Women. *Clinics* (2020) 75:e1486. doi: 10.6061/clinics/2020/e1486
50. Chen W, Wei Y, Xiong A, Li Y, Guan H, Wang Q, et al. Comprehensive Analysis of Serum and Fecal Bile Acid Profiles and Interaction With Gut Microbiota in Primary Biliary Cholangitis. *Clin Rev Allergy Immunol* (2020) 58:25–38. doi: 10.1007/s12016-019-08731-2
51. Hanly R, Ryan N, Snelling H, Walker-Bone K, Dizdarevic S, Peters AM. Association Between Bile Acid Turnover and Osteoporosis in Postmenopausal Women. *Nucl Med Commun* (2013) 34(6):597–600. doi: 10.1097/MNM.0b013e3283608993
52. Wen K, Tao L, Tao Z, Meng Y, Zhou S, Chen J, et al. Fecal and Serum Metabolomic Signatures and Microbial Community Profiling of Postmenopausal Osteoporosis Mice Model. *Front Cell Infect Microbiol* (2020) 10:535310. doi: 10.3389/fcimb.2020.535310
53. Ruiz-Gaspà S, Guañabens N, Jurado S, Dubreuil M, Combalia A, Peris P, et al. Bile Acids and Bilirubin Effects on Osteoblastic Gene Profile. Implications in the Pathogenesis of Osteoporosis in Liver Diseases. *Gene* (2020) 725:144167. doi: 10.1016/j.gene.2019.144167
54. Kelly OJ, Gilman JC, Kim Y, Ilich JZ. Long-Chain Polyunsaturated Fatty Acids may Mutually Benefit Both Obesity and Osteoporosis. *Nutr Res* (2013) 33:521–33. doi: 10.1016/j.nutres.2013.04.012
55. Shan Z, Zhao Y, Qiu Z, Angxiu u, Gu Y, Luo J, et al. Conjugated Linoleic Acid Prompts Bone Formation in Ovariectomized Osteoporotic Rats and Weakens Osteoclast Formation After Treatment With Ultraviolet B. *Ann Trans Med* (2021) 9(6):503. doi: 10.21037/atm-21-934
56. Watkins BA, Seifert MF. Conjugated Linoleic Acid and Bone Biology. *J Am Coll Nutr* (2000) 19(4):478S–86S. doi: 10.1080/07315724.2000.10718951
57. Li N, Zhao L, Lin Z, Li J, Li H, Sun J, et al. Metabonomics Study of the Anti-Osteoporosis Effect of Velvet Collagen Hydrolysate Using Rapid Resolution Liquid Chromatography Combined With Quadrupole Time-of-Flight Tandem Mass Spectrometry. *J Liquid Chromatogr Relat Technol* (2015) 83:117–22. doi: 10.1080/10826076.2014.883540
58. Zhan Q, Dai Y, Wang F, Mai X, Fu M, Wang P, et al. Metabonomic Analysis in Investigating the Anti-Osteoporotic Effect of Sialoglycoprotein Isolated From Eggs of *Carassius Auratus* on Ovariectomized Mice. *J Funct Foods* (2019) 61:103514. doi: 10.1016/j.jff.2019.103514
59. Costa AG, Cusano NE, Silva BC, Cremers S, Bilezikian JP. Cathepsin K: Its Skeletal Actions and Role as a Therapeutic Target in Osteoporosis. *Nat Rev Rheumatol* (2011) 7:447–56. doi: 10.1038/nrrheum.2011.77
60. Fujii A, Bush JH, Shores KE, Johnson RG, Garascia RJ, Cook ES. Probiotics: Antistaphylococcal Activity of 4-Aminocyclohexanecarboxylic Acid, Aminobenzoic Acid, and Their Derivatives and Structure–Activity Relationships. *J Pharm Sci* (1977) 66(6):844–8. doi: 10.1002/jps.2600660628
61. Shinozuka T, Shimada K, Matsui S, Yamane T, Ama M, Fukuda T, et al. 4-Aminophenoxyacetic Acids as a Novel Class of Reversible Cathepsin K

Inhibitors. *Bioorg Med Chem Lett* (2006) 16:1502–5. doi: 10.1016/j.bmcl.2005.12.053
62. Gastaldello A, Livingstone DEW, Abernethie AJ, Tsang N, Walker BR, Hadoke PWF, et al. Safer Topical Treatment for Inflammation Using 5α-Tetrahydrocorticosterone in Mouse Models. *Biochem Pharmacol* (2017) 129:73–84. doi: 10.1016/j.bcp.2017.01.008
63. Yu Z, Huang J, Zhou Z. Icariin Protects Against Cage Layer Osteoporosis by Intervening in Steroid Biosynthesis and Glycerophospholipid Metabolism. *Anim Dis* (2021) 1:1. doi: 10.1186/s44149-021-00001-z
64. Torricelli P, Fini M, Giavaresi G, Giardino R, Gnudi S, Nicolini A, et al. L-Arginine and L-Lysine Stimulation on Cultured Human Osteoblasts. *Biomed Pharmacother* (2002) 56:492–7. doi: 10.1016/S0753-3322(02)00287-1
65. Liu X, Zhang S, Lu X, Zheng S, Li F, Xiong Z. Metabonomic Study on the Anti-Osteoporosis Effect of *Rhizoma Drynariae* and Its Action Mechanism Using Ultra-Performance Liquid Chromatography–Tandem Mass Spectrometry. *J Ethnopharmacol* (2012) 139(1):311–7. doi: 10.1016/j.jep.2011.11.017
66. Manoury B, Mazzeo D, Li DN, Billson J, Loak K, Benaroch P, et al. Asparagine Endopeptidase can Initiate the Removal of the MHC Class II Invariant Chain Chaperone. *Immunity* (2003) 18(4):489–98. doi: 10.1016/S1074-7613(03)00085-2
67. Sharma D, Yu Y, Shen L, Zhang G-F, Karner CM. SLC1A5 Provides Glutamine and Asparagine Necessary for Bone Development in Mice. *eLife* (2021) 10:e71595. doi: 10.7554/eLife.71595
68. Guss JD, Horsfield MW, Fontenele FF, Sandoval TN, Luna M, Apoorva F, et al. Alterations to the Gut Microbiome Impair Bone Strength and Tissue Material Properties. *J Bone Miner Res* (2017) 32(6):1343–53. doi: 10.1002/jbmr.3114
69. Chen F, Wei Q, Xu D, Wei Y, Wang J, Amakye WK, et al. The Associations of Gut Microbiota and Fecal Short-Chain Fatty Acids With Bone Mass Were Largely Mediated by Weight Status: A Cross-Sectional Study. *Eur J Nutr* (2021) 60:4505–17. doi: 10.1007/s00394-021-02597-x
70. Martinis MD, Ginaldi L, Allegra A, Sirufo MM, Pioggia G, Tonacci A, et al. The Osteoporosis/Microbiota Linkage: The Role of miRNA. *Int J Mol Sci* (2020) 21(23):8887. doi: 10.3390/ijms21238887
71. Leandro J, Houten SM. Saccharopine, a Lysine Degradation Intermediate, Is a Mitochondrial Toxin. *J Cell Biol* (2019) 218(2):391–2. doi: 10.1083/jcb.201901033
72. Li B, Liu M, Wang Y, Gong S, Yao W, Li W, et al. Puerarin Improves the Bone Micro-Environment to Inhibit OVX-Induced Osteoporosis *via* Modulating SCFAs Released by the Gut Microbiota and Repairing Intestinal Mucosal Integrity. *Biomed Pharmacother* (2020) 132:110923. doi: 10.1016/j.biopha.2020.110923
73. Kuhl GC, Lindner JDD. Biohydrogenation of Linoleic Acid by Lactic Acid Bacteria for the Production of Functional Cultured Dairy Products: A Review. *Foods* (2016) 5(1):13. doi: 10.3390/foods5010013
74. Kim JG, Lee E, Kim SH, Whang KY, Oh S, Imm J-Y. Effects of a *Lactobacillus Casei* 393 Fermented Milk Product on Bone Metabolism in Ovariectomised Rats. *Int Dairy J* (2009) 19:690–5. doi: 10.1016/j.idairyj.2009.06.009
75. Liu X, Fan J-B, Hu J, Li F, Yi R, Tan F, et al. *Lactobacillus Fermentum* ZS40 Prevents Secondary Osteoporosis in Wistar Rat. *Food Sci Nutr* (2020) 8(9):5182–91. doi: 10.1002/fsn3.1824

Conflict of Interest: The authors declare that the research was coducted in the absence of any commercial or financial relationships that could be construed as a potential conflict of interest.

Publisher's Note: All claims expressed in this article are solely those of the authors and do not necessarily represent those of their affiliated organizations, or those of the publisher, the editors and the reviewers. Any product that may be evaluated in this article, or claim that may be made by its manufacturer, is not guaranteed or endorsed by the publisher.

frontiers in Endocrinology

ORIGINAL RESEARCH
published: 31 March 2022
doi: 10.3389/fendo.2022.860649

Network Pharmacological Study on Mechanism of the Therapeutic Effect of Modified Duhuo Jisheng Decoction in Osteoporosis

Xudong Huang[1†], Zhou Zhou[1†], Yingyi Zheng[2], Guoshuai Fan[1], Baihe Ni[1], Meichen Liu[1], Minghua Zhao[1], Lingfeng Zeng[3] and Weiguo Wang[1,4*]*

[1] First Clinical Medical College, Shandong University of Traditional Chinese Medicine, Jinan, China, [2] School of Basic Medical Science, Zhejiang University of Traditional Chinese Medicine, Hangzhou, China, [3] The Second Affiliated Hospital of Guangzhou University of Chinese Medicine, Guangzhou, China, [4] Affiliated Hospital of Shandong University of Traditional Chinese Medicine, Jinan, China

Background: Modified Duhuo Jisheng Decoction (MDHJSD) is a traditional Chinese medicine prescription for the treatment of osteoporosis (OP), but its mechanism of action has not yet been clarified. This study aims to explore the mechanism of MDHJSD in OP through a combination of network pharmacology analysis and experimental verification.

Methods: The active ingredients and corresponding targets of MDHJSD were acquired from the Traditional Chinese Medicine System Pharmacology (TCMSP) database. OP-related targets were acquired from databases, including Genecards, OMIM, Drugbank, CTD, and PGKB. The key compounds, core targets, major biological processes, and signaling pathways of MDHJSD that improve OP were identified by constructing and analysing the relevant networks. The binding affinities between key compounds and core targets were verified using AutoDock Vina software. A rat model of ovariectomized OP was used for the experimental verification.

Results: A total of 100 chemical constituents, 277 targets, and 4734 OP-related targets of MDHJSD were obtained. Subsequently, five core components and eight core targets were identified in the analysis. Pathway enrichment analysis revealed that overlapping targets were significantly enriched in the tumour necrosis factor-alpha (TNF-α) signaling pathway, an inflammation signaling pathway, which contained six of the eight core targets, including TNF-α, interleukin 6 (IL-6), transcription factor AP-1, mitogen-activated protein kinase 3, RAC-alpha serine/threonine-protein kinase, and caspase-3 (CASP3). Molecular docking analysis revealed close binding of the six core targets of the TNF signaling pathway to the core components. The results of experimental study show that MDHJSD

OPEN ACCESS

Edited by:
Bo Liu,
Guangdong Provincial Hospital of Chinese Medicine, China

Reviewed by:
Hailing Xin,
Second Military Medical University, China
Heshu Sulaiman Rahman,
University of Sulaimani, Iraq
Pengfei Yu,
Suzhou TCM Hospital Affiliated to Nanjing University of Chinese Medicine, China
Changliang Peng,
The Second Hospital of Shandong University, China

***Correspondence:**
Weiguo Wang
wjbwwg@hotmail.com
Lingfeng Zeng
zenglf6768@163.com

[†]These authors have contributed equally to this work

Specialty section:
This article was submitted to Bone Research, a section of the journal Frontiers in Endocrinology

Received: *23 January 2022*
Accepted: *07 March 2022*
Published: *31 March 2022*

Citation:
Huang X, Zhou Z, Zheng Y, Fan G, Ni B, Liu M, Zhao M, Zeng L and Wang W (2022) Network Pharmacological Study on Mechanism of the Therapeutic Effect of Modified Duhuo Jisheng Decoction in Osteoporosis. Front. Endocrinol. 13:860649. doi: 10.3389/fendo.2022.860649

can protect bone loss, inhibit the inflammatory response, and downregulate the expression levels of TNF-α, IL-6, and CASP3 in ovariectomized rats.

Conclusion: The mechanism of MDHJSD in the treatment of OP may be related to the regulation of the inflammatory response in the bone tissue.

Keywords: osteoporosis, network pharmacology, TNF signaling pathway, molecular docking, Modified Duhuo Jisheng Decoction

INTRODUCTION

Osteoporosis (OP) is a systemic disease characterised by a decreased bone strength and damaged bone microstructure (1). OP increases bone brittleness, which is an important factor in causing fracture, and seriously affects human health and the quality of life of patients (2, 3). There are approximately 200 million patients with OP worldwide, and with the ageing population worldwide, its incidence rate has increased each year (4). Therefore, OP has become a global health concern. Presently, the treatment methods for OP mainly improve the clinical symptoms of patients by slowing bone loss, promoting bone formation, and inhibiting bone resorption, but these treatments have certain limitations (5, 6). Modified Duhuo Jisheng Decoction (MDHJSD) is derived from Duhuo Jisheng Decoction(DHJSD), a classic prescription for Bei Ji Qian Jin Yao Fang written by Sun Simiao in the Tang Dynasty. Contemporary studies have found that DHJSD has a good curative effect in the treatment of OP (7, 8). Wang Weiguo, deputy chief physician of The Affiliated Hospital of Shandong University of Traditional Chinese Medicine, combined with the clinical symptoms of OP patients, added and subtraction DHJSD, and finally obtain the self-drafted formula MDHJSD was composed of 10 herbs: including Cornus officinalis, Divaricate saposhniovia root, Gentiana macrophylla, Angelica pubescens, Spatholobus suberctu, Rhizoma Chuanxiong, Astragalus membranaceus, Eucommia ulmoides, TyTPae pollen and Rhizoma drynariae. Its reasonable curative effect has been clinically verified. However, the material basis and molecular mechanisms of MDHJSD in the treatment of OP are not yet elucidated.

Based on the theories of system biology and bioinformatics, network pharmacology explores the interaction between biomolecules and targets *in vivo* from the perspective of a systematic level and biological network, which can effectively predict the drug efficacy and its mechanisms (9, 10) to close the gap between modern medicine and traditional Chinese medicine. Therefore, it is widely used in research studies on traditional Chinese medicines. In this study, the network pharmacology method was used to integrate the information of drug active components, drug and disease targets, construct the network of the therapeutic effect of MDHJSD on OP, and reveal the material basis and mechanism of MDHJSD in the treatment of OP. The binding ability between the ligand and receptor was evaluated by molecular docking analysis, and some key genes were verified using animal experiments. The research process is shown in **Figure 1**.

Abbreviations: OP, Osteoporosis; MDHJSD, Modified Duhuo Jisheng Decoction; DHJSD, Duhuo Jisheng Decoction; TNF-α, Tumor necrosis factor-alpha; IL-6, Interleukin 6; CASP3, Caspase-3; OB, Oral bioavailability; DL, Drug-likeness; PPI, Protein-protein interaction; KEGG, Kyoto Encyclopaedia of Genomes; BP, Biological pathways; CC, Cell localization; MF, Molecular function; CO, Cornus officinalis; DSR, Divaricate saposhniovia root; GM, Gentiana macrophylla; AP, Angelica pubescens; SS, Spatholobus suberctu; RCX, Rhizoma Chuanxiong; AM, Astragalus membranaceus; EU, Eucommia ulmoides; TP, TyTPae pollen; RD, Rhizoma drynariae; BMD, Bone mineral density; CRP, C-reactive protein.

MATERIALS AND METHODS

Screening Effective Chemical Components and Action Targets of MDHJSD

We used the Traditional Chinese Medicine System Pharmacology (TCMSP) database (http://www.tcmspw.com/tcmsp.php) (11) of traditional Chinese medicine ingredients to search for MDHJSD constituent medicines (dogwood, fangfeng, qinjie, duhuo, jixueteng, chuanxiong, astragalus, eucommia, puhuang, and drynariae) to obtain all chemical and pharmacological data. According to the key parameters of oral bioavailability (OB) and drug-likeness (DL), the chemical components satisfying an OB ≥ 30% and a DL ≥ 0.18 were identified as being the active ingredients in MDHJSD. Additionally, the TCMSP database was used to screen the targets of the active ingredients of MDHJSD, and the drug targets were corrected and deduplicated in the Uniprot database (https://www.uniprot.org/) (12).

Search for OP-Related Targets

A search using the Genecards, OMIM, Drugbank, CTD, and PGKB databases and using 'osteoporosis' as the keyword was conducted from which the OP-related targets were retrieved, and the final ones were obtained by taking the correlation score as the reference union set. We then drew a Wayne diagram to determine the intersections of the MDHJSD and OP targets.

Construction of the Drug-Active Ingredient-Target Network

Microsoft Excel was used to sort the obtained drug active ingredients and intersection targets. The data were then imported into Cytoscape software, and a 'drug-active ingredient-target' network model was built, in which the nodes represent traditional Chinese medicines, ingredients, and targets,

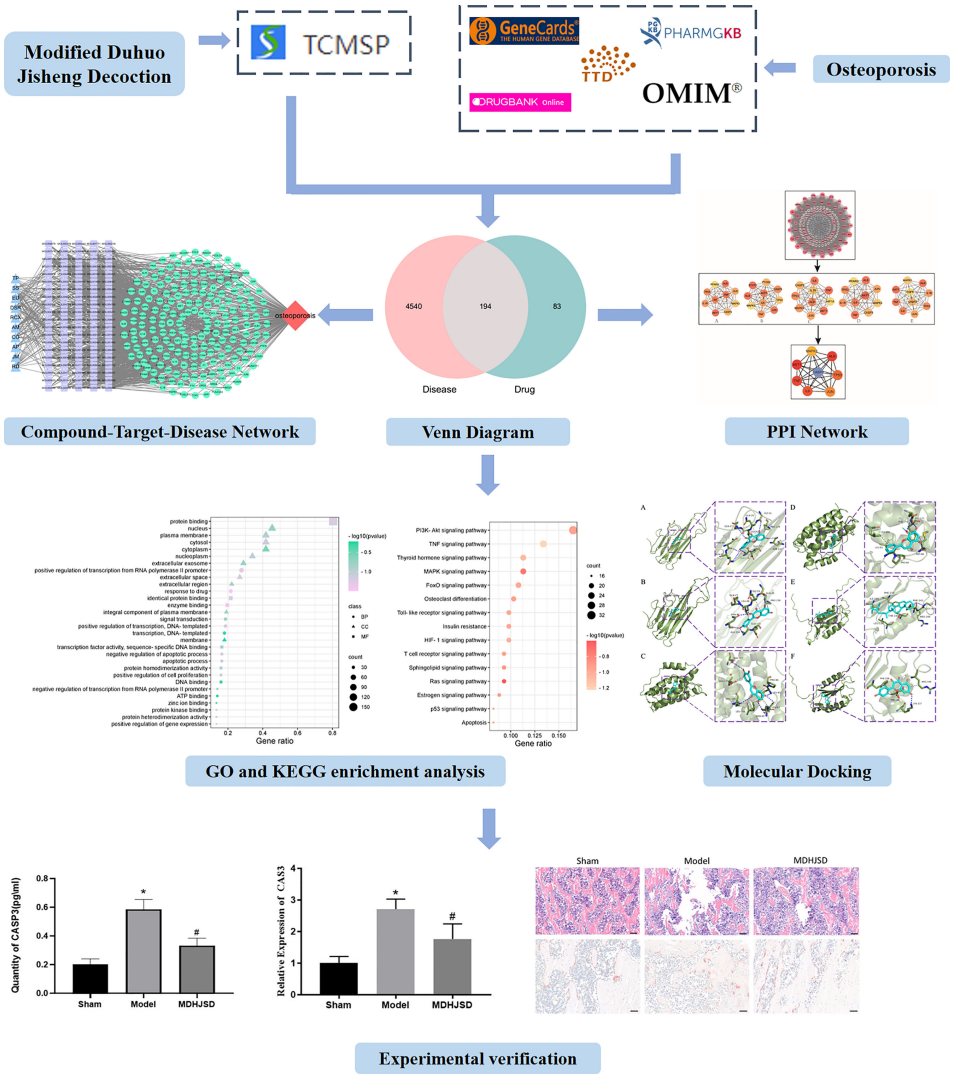

FIGURE 1 | The research process. Compared with control operation group, $^{*}P < 0.05$; Compared with the model group, $^{\#}P < 0.05$.

and in which the edges represent the relationship role between the three, using the number of associations of each node to calculate the 'degree' value.

Construction of the Protein-Protein Interaction (PPI) Network and Screening of Key Targets

The intersection target between the MDHJSD active ingredient target and OP disease target was imported into the STRING database (https://www.string-db.org/cgi/input.pl), and '*Homo sapiens*' was selected to obtain the PPI relationship (13). When importing the results into Cytoscape 3 7.2, the software constructed the interaction network diagram of 'MDHJSD active ingredient OP target', screened the common targets by using the closeness, degree, EPC, MCC, and MNC algorithms, and finally obtained the core target.

Gene Ontology Biological Process (GO) and Kyoto Encyclopaedia of Genomes (KEGG) Pathway Enrichment Analyses

The David 6.8 (https://david.ncifcrf.gov/home.jsp) database was used to perform a GO enrichment analysis and KEGG pathway annotation analysis on the intersection targets of diseases and drugs (14), and bubble diagrams were drawn for the analysis of the biological processes of the first 15 KEGG pathways, which are significantly enriched, and the top 10 BP (biological pathways), CC (cell localization) and MF (molecular function) identified in the GO analysis.

Docking of Effective Components With Key Target Genes and Molecules

In the drug-active ingredient-target network, the top five core compounds of MDHJSD in the treatment of OP were screened

according to the 'degree' value, the 2D structure of the core compound was obtained in the PubChem database, and the 3D structure of the core target was obtained from the PDB database (15). After the compound was processed by Chem3D software, the analysis of molecular docking between the core compound and core target was carried out using AutoDock Vina software. The binding energy was used to evaluate the binding degree between the molecular compounds and targets. PyMOL software was used to visually display the docking results for those molecules exhibiting a high degree of combination.

Establishment of the Experimental Animal Model of OP

Thirty-six female Sprague-Dawley rats aged 8–9 weeks and weighing 230–280 g were provided by Jinan Pengyue Experimental Animal Breeding Co., Ltd. Standard feed was made available at room temperature, and the rats were provided free access to drinking water and adaptive feeding for 5 days. The 36 rats were divided into 3 groups, with 12 rats in each group: the control, model, and treatment groups. Ovariectomies were performed in the model and treatment groups, and a similar incision without an ovariectomy was made in the control operation group, followed by suturing. Oophorectomy was followed by normal diet for 4 weeks, and MDHJSD administration was started after model establishment. The treatment group was administered 256.5 mg/kg/d MDHJSD by gavage, and the model and control operation groups were administered normal saline at the same dosage. After 3 weeks of administering continuous treatment, the abdominal aortic blood of the rats was collected under chloral hydrate anaesthesia, and the bilateral femurs were removed. All procedures were reviewed and approved by the experimental animal ethics committee of the Affiliated Hospital of Shandong University of Traditional Chinese Medicine (2020-48).

Bone Morphometric Assessments

The rat femur was exfoliated and the muscle on the bone was removed. The femur was decalcified with 5% EDTA and embedded in paraffin blocks, and 5 mm sections were cut through a continuous incision in the sagittal plane. The sections were stained with hematoxylin and eosin (H&E) to observe the changes of bone trabecular and bone marrow cavity, and the activity of osteoclasts was detected by TRAP staining.

Validation of Key Targets Through Real-Time Quantitative Reverse Transcription Polymerase Chain Reaction

When referring to relevant research findings (16), TNF-α, IL-6, and CASP3 were found to play an important role in the pathogenesis of OP, so we chose these three targets for inclusion in the experimental verification. Three key targets were verified by real-time quantitative reverse transcription polymerase chain reaction (qRT-PCR). The primers were designed and synthesized by the solid-phase phosphorous amide tri-ester method, and the sequences of the primers are shown in **Table 1**.

The rat femoral bone tissue (50 mg) was weighed, RNA was extracted with a Spark Easy Bone Tissue RNA Kit (Sparkjade, China), and a Spark Script II RT Plus Kit (Sparkjade, China) was used for the reverse transcription reaction. The two-step reaction procedure (Roche LightCycler480 II, Switzerland) was applied with pre-denaturation at 95°C for 10 min, and then 44 cycles of reaction at 95°C for 15 s and 60°C for 60 s were performed. Gene expression data were analysed using the $2^{-\Delta\Delta Ct}$ method.

Enzyme Linked Immunosorbent Assay (ELISA) Analysis

Blood samples were taken and centrifuged for 30 min, from which the serum was obtained. According to the instructions of the ELISA kit, the optical density (OD) was measured using a microplate reader at a wavelength of 450 nm, and the protein expression levels of TNF-α (JYM0635Ra, ELISA LAB), IL-6 (JYM0646Ra, ELISA LAB) and CASP3 (ab281235, abcam) were quantified.

Statistical Analysis

SPSS 21.0 software was used for the statistical analysis of the experimental data, and all data are expressed as the mean ± standard deviation. One-way analysis of variance was used for comparisons between multiple groups, the results of which were considered statistically significant at $P < 0.05$.

RESULTS

Screening of MDHJSD Active Ingredients and Therapeutic Targets for OP

A total of 100 active ingredients from 10 formulations derived from MDHJSD (**Supplementary Appendix 1**) were retrieved from the TCMSP database according to the screening criteria of OB ≥ 30% and DL ≥ 0.18, and these corresponded to 277 targets. A total of 4734 targets related to OP treatment were obtained from five databases: the Genecards, OMIM, PharmGkb, DrugBank, and CTD. Using an online Venn diagram editing website (http://bioinformatics.psb.ugent.be/webtools/Venn/), we input the potential targets screened by OP and the targets that

TABLE 1 | The primer sequences used in the qRT-PCR analysis performed in this study.

Gene Name	BP	Forward primer (5′-3′)	Reverse primer (5′-3′)
GAPDH	70	TGAACGGGAAGCTCACTGGC	CATGTGAGATCCACGACGGACA
TNF-α	111	ATGGGCTCCCTCTCATCAGTTCC	CCTCCGCTTGGTGGTTTGCTAC
IL-6	110	ACTTCCAGCCAGTTGCCTTCTTG	TGGTCTGTTGTGGGTGGTATCCTCTAC
CASP3	136	GCGGTATTGAGACAGACAGTGGAAC	AACCATGACCCGTCCCTTGAATTTC

MDHJSD active ingredients act on and found 194 common genes (**Figure 2**), which are the potential target genes of MDHJSD in the treatment of OP (**Supplementary Appendix 2**).

Construction of the Traditional Chinese Medicine-Active Ingredient-Target Network Diagram

The 10 traditional Chinese medicines, 100 active ingredients, and 194 intersecting target annotation relationships and classification obtained were imported into Cytoscape software, and the traditional Chinese medicine-active ingredients-target network diagram of MDHJSD in the treatment of OP was drawn (**Figure 3**). The square node in **Figure 2** represents the active ingredients, the triangle nodes represent the 10 traditional Chinese medicines of MDHJSD, and the circle nodes represent the targets related to the active ingredients and OP treatment. As shown in **Figure 2**, this network has 305 nodes and 92720 edges. Quercetin has the closest relationship with the therapeutic targets, with a total of 113 targets, followed by luteolin with 50 targets and kaempferol with 43 targets. It is considered that these active components may be the core components of MDHJSD in the treatment of OP.

PPI Network Construction and Key Target Screening

The 194 intersection targets were imported into the STRING database to obtain the PPI relationship, and imported into

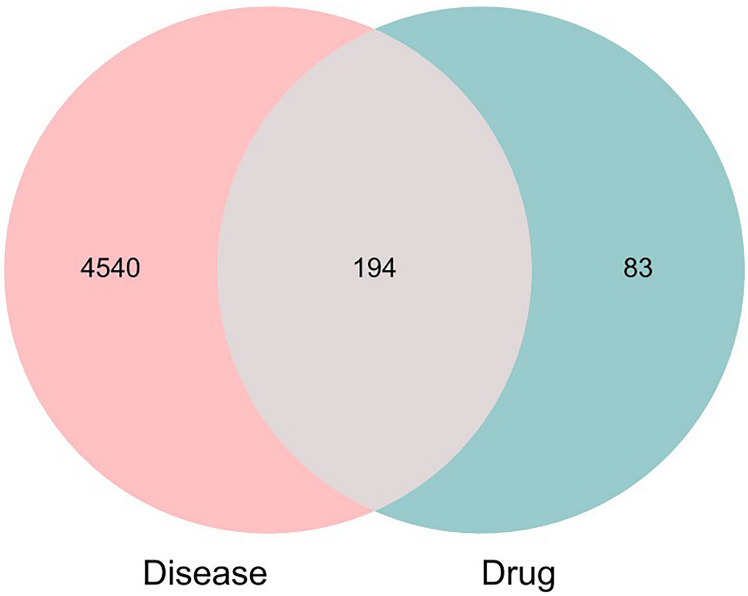

FIGURE 2 | Venn diagram exhibiting the intersection of the MDHJSD targets and OP targets.

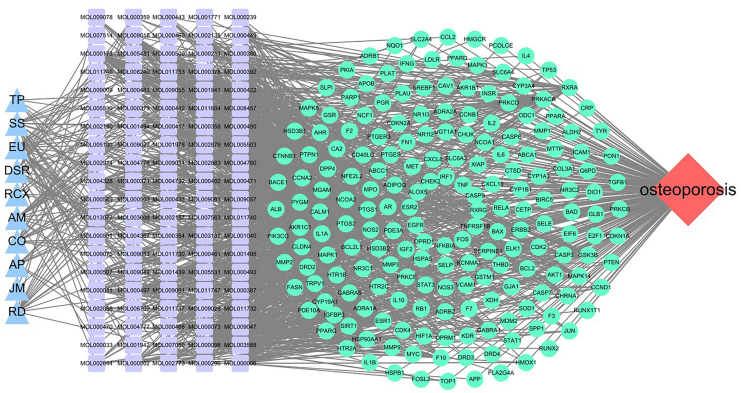

FIGURE 3 | A medicine-ingredients-targets-disease network of four parts. Red: disease; Blue: medicine; Cyan: 194 potential common targets; Purple: active ingredients of MDHJSD.

Cytoscape 3.7.2 software to construct a PPI interaction map (17) (**Supplementary Appendix 3**). Finally, eight core targets using the closeness, degree, EPC, MCC, and MNC algorithms in the Cytohubba plug-in (**Figure 4**) were determined: IL-6, RAC-alpha serine/threonine-protein kinase (AKT1), mitogen-activated protein kinase 3 (MAPK3), CASP3, TNF, transcription factor AP-1 (JUN), cellular tumour antigen p53 (TP53), and albumin (ALB).

GO Enrichment Analysis and KEGG Pathway Analysis of OP Targets in MDHJSD Therapy

We used the DAVID database and its expansion package to perform gene ontology (GO) enrichment analysis ($P < 0.05$) for the common targets between the drugs and disease. A total of 593 biological pathways, 70 cell localisations, and 121 molecular functions were obtained. GO enrichment analysis of disease-related genes was carried out with R software and its extension package, and the top 10 items of BP, CC and MF enrichment were visualized (**Figure 5**). The abscissa in the figure represents the gene enrichment rate (%), and the size of the icon represents the number of genes enriched in the process. The larger the icon, the more genes that were enriched. The icon colour represents the significance of enrichment, and the more purple, the more significant the enrichment. The results showed that BP was mainly related to the positive regulation of transcription from RNA polymerase II promoter, response to drug, transcription of DNA templates, etc. CC mainly included the nucleus, cytosol, plasma membrane, cytoplasm, etc. MF mainly included the protein binding, identity protein binding, enzyme binding, etc.

To further understand the potential pathway of MDHJSD in the treatment of OP, we performed KEGG channel enrichment analysis and obtained 125 signal channels ($P < 0.05$). Fifteen pathways related to OP were screened, including the PI3K-Akt, TNF, thyroid hormone, and MAPK signaling pathways. The channels are then visualised according to the number of key genes in these channels (**Figure 6**). The results showed that the top three enriched signaling pathways were the PI3K-Akt, TNF, and thyroid hormone signaling pathways. The TNF signaling pathway is constituted by six of the eight core targets: *TNF-α, IL-6, JUN, MAPK3, AKT1*, and *CASP3*, so this pathway may mediate the anti-OP effect of MDHJSD.

Verification of Molecular Docking

The eight core targets screened in the PPI network analysis were associated with the top five active components of 'degree' in the drug-active ingredient-target network (**Table 2**). Considering the binding energy as an evaluation of docking degree, it was

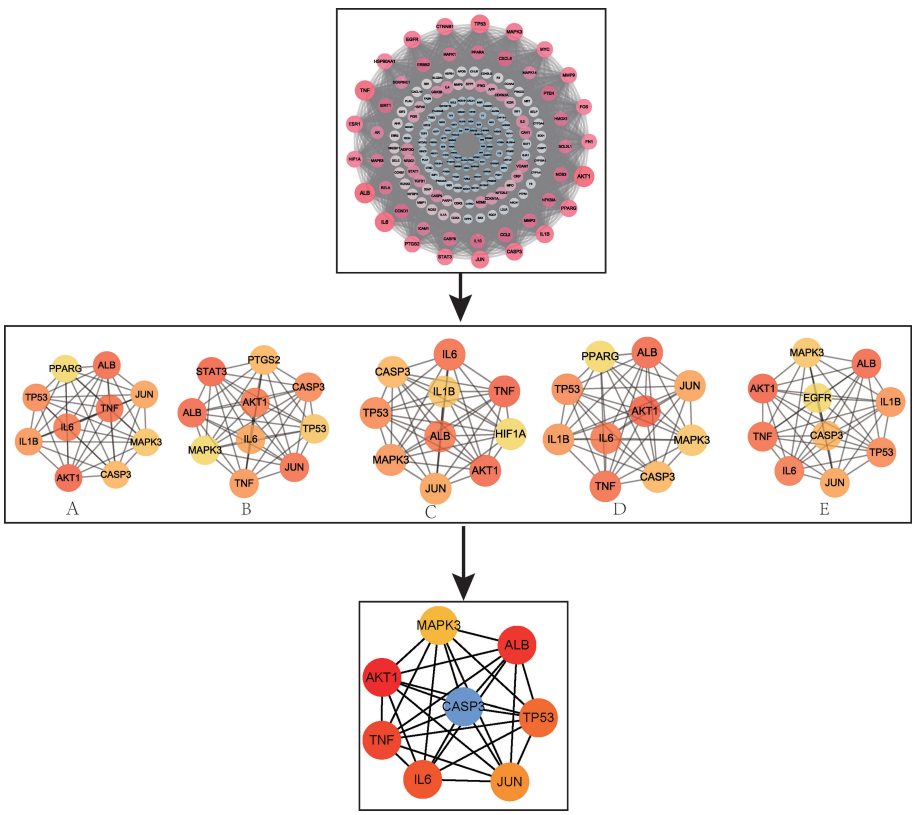

FIGURE 4 | PPI network and screening of core targets. **(A)** MNC; **(B)** MCC; **(C)** EPC; **(D)** Degree; **(E)** Closeness.

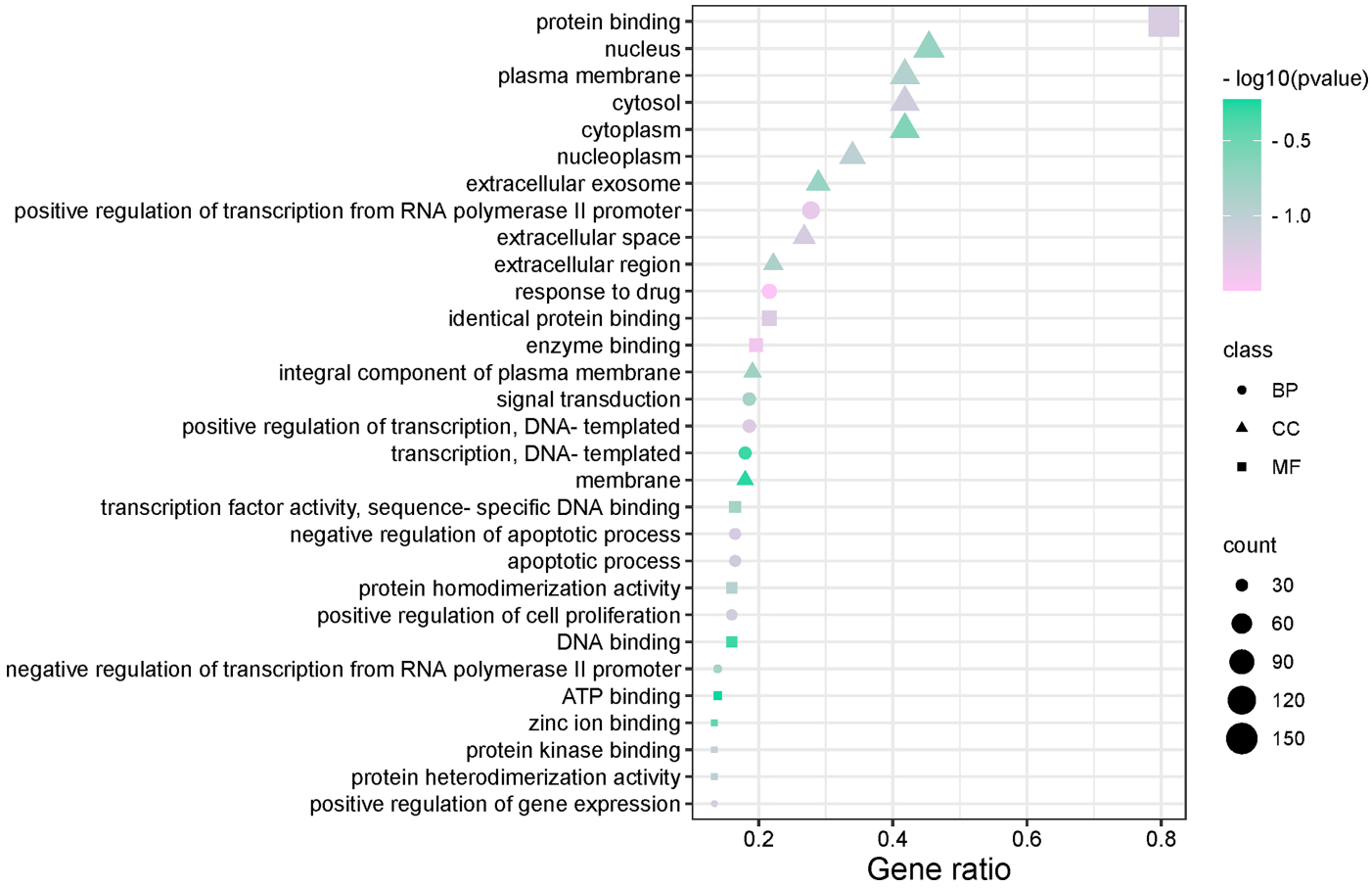

FIGURE 5 | The top 10 remarkably enriched genes from the GO analysis (BP, CC, and MF).

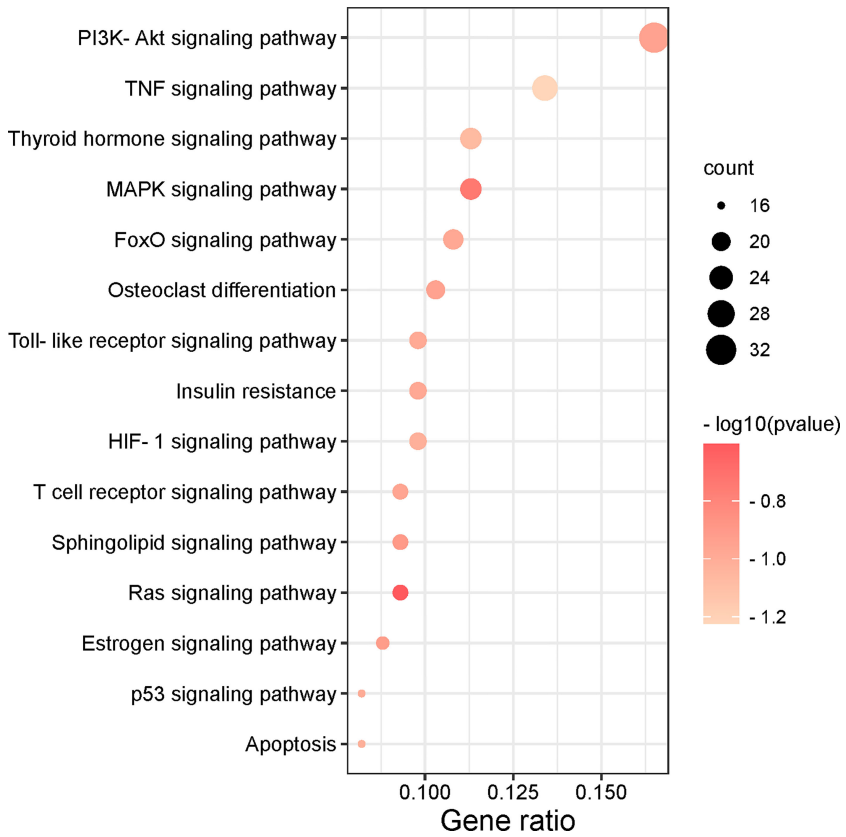

FIGURE 6 | The top 15 remarkably enriched signaling pathways from the KEGG analysis for the signaling pathway of potential target genes of MDHJSD in OP.

considered that the binding energy ≤-5 kcal/mol indicates that they can be combined, and ≤-7 kcal/mol indicates that they have a good binding ability (18). We drew the hot spot diagram of the docking results (**Figure 7**). The colour of the square in the diagram is biased to red, indicating that the binding energy between the corresponding component and the target protein is low and the binding degree is high. The colour is blue, indicating that the binding energy between the corresponding component and the target protein is high and the binding degree is poor. It can be observed from **Figure 6** that the core components and core targets have a good binding ability. Six pairs of binding relationships were selected: TNF and quercetin, TNF and kaempferol, IL-6 and luteolin, IL-6 and wogonin, CASP3 and beta-sitosterol, and CASP3 and kaempferol, which were visualized by PyMOL software (**Figure 8**).

TABLE 2 | Top 5 active ingredients in the 'degree' analysis.

NO	Molecule ID	Molecule name	Degree
1	MOL000098	quercetin	116
2	MOL000006	luteolin	51
3	MOL000422	kaempferol	47
4	MOL000173	wogonin	39
5	MOL000358	beta-sitosterol	32

Effect of MDHJSD on Morphology of Femur Bone in Rats

H&E staining (**Figure 9A**) showed that trabecular bone in the Sham group were evenly distributed and in normal morphology, while trabecular bone in the Model group were sparse and disorderly with wider spacing. Compared with Model group, the distribution of trabecular bone in MDHJSD group was more uniform, and the density of trabecular bone was roughly restored. TRAP staining (**Figure 9B**) showed that the number of osteoclasts was reduced in MDHJSD group compared with Model group, indicating that MDHJSD could inhibit osteoclasts proliferation in oophorectomy rats.

MDHJSD Effect on mRNA Expression Levels of Key Targets

The qRT-PCR results showed (**Figure 10**) that, compared with the control-operated group, the mRNA expression levels of TNF-α, IL-6, and CASP3 in the bone tissue of the model group and the treatment group were significantly increased ($P < 0.05$). Compared with the model group, the mRNA expression levels of TNF-α, IL-6, and CASP3 in the bone tissue of the treatment group were significantly decreased ($P < 0.05$). The results showed that MDHJSD could reduce the mRNA expression levels of TNF-α, IL-6, and CASP3 in the bone tissue of the rats induced with OP.

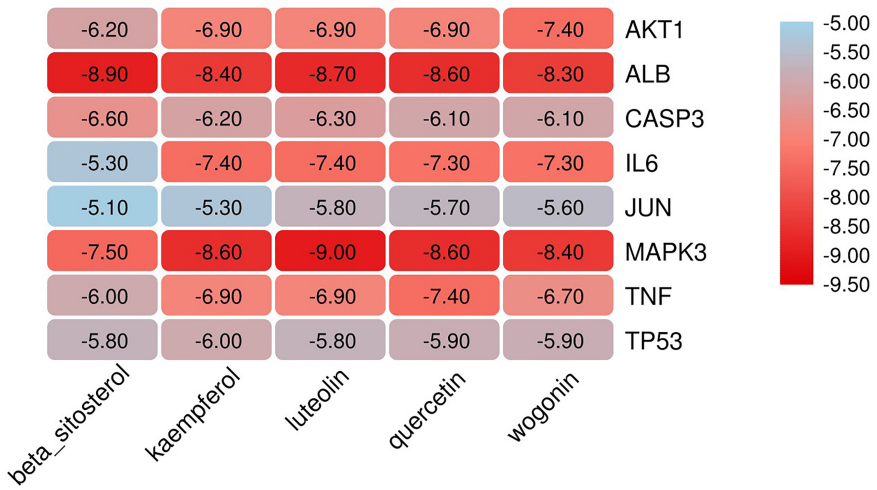

FIGURE 7 | Docking heat-map of the core components and core targets. Affinity: kcal/mol.

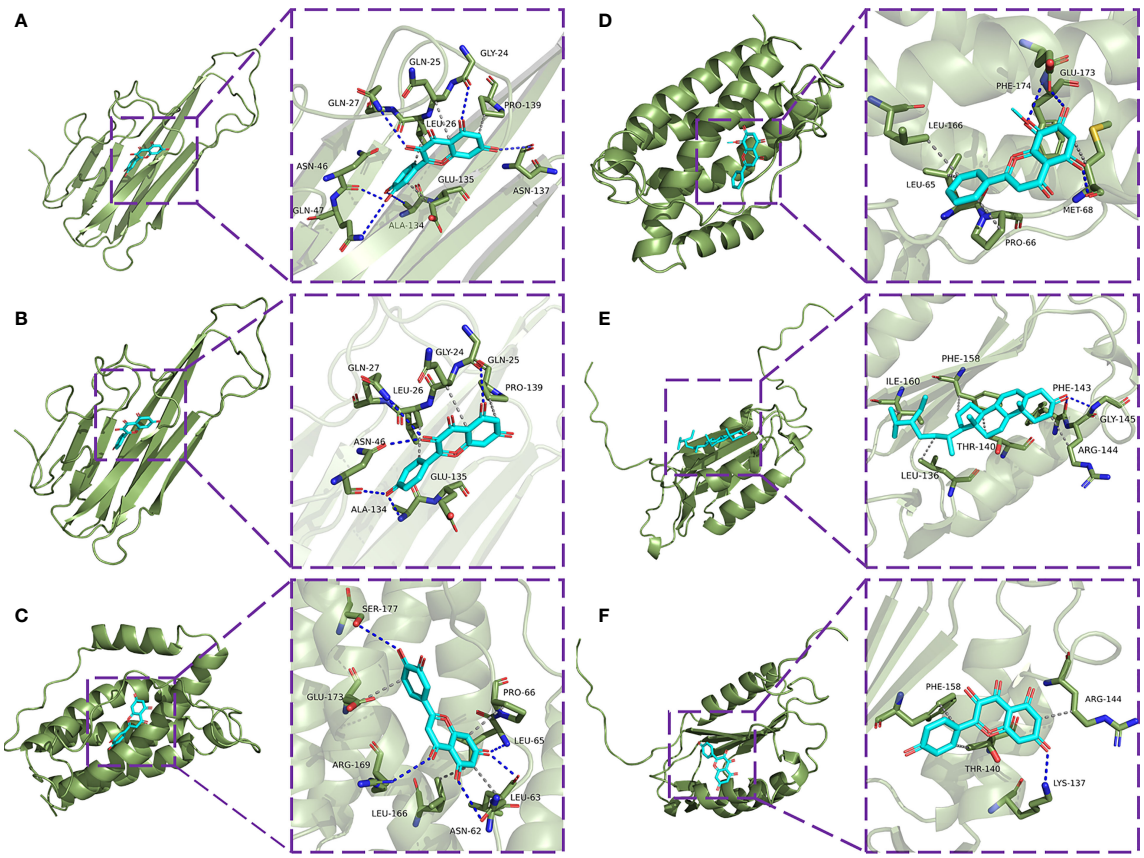

FIGURE 8 | Molecular docking model diagram. **(A)** Molecular docking of TNF-α with quercetin. **(B)** Molecular docking of TNF with kaempferol. **(C)** Molecular docking of IL-6 with luteolin. **(D)** Molecular docking of IL-6 with wogonin. **(E)** Molecular docking of CASP3 with beta-sitosterol. **(F)** Molecular docking of CASP3 with kaempferol.

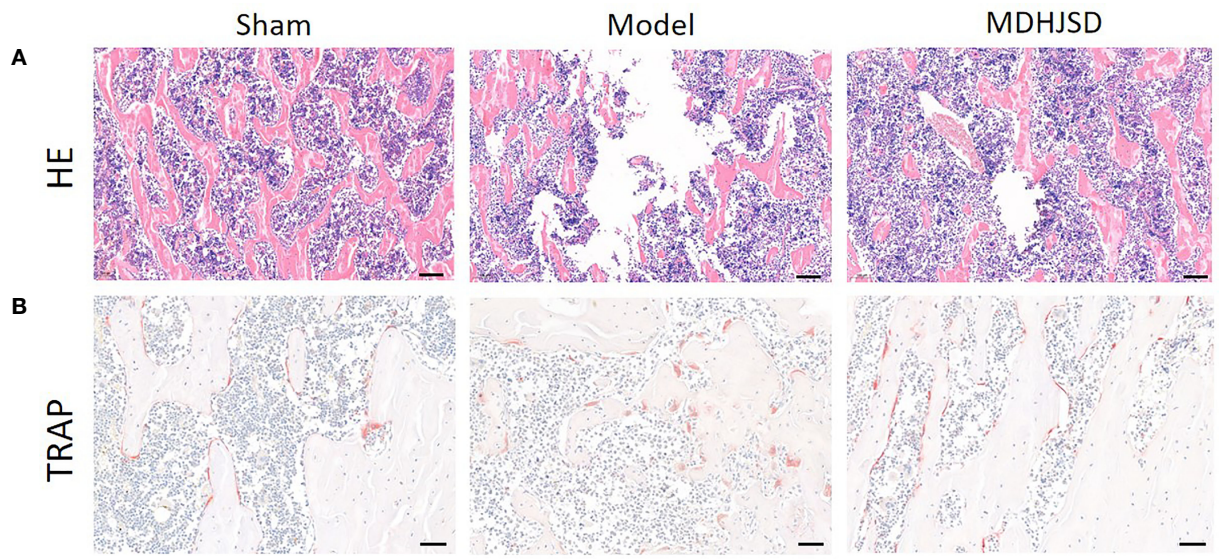

FIGURE 9 | The pathological sections of femur of rats in each group at the end of the 3th week; **(A)** H&E staining: Scale bar = 100μm, 100×; **(B)** TRAP staining: Scale bar = 50μm, 200×.

Related Protein Expression

The ELISA results showed (**Figure 11**) that compared with the rats in the control-operated group, the expression levels of TNF-α, IL6, and CASP3 in the serum of the model group and the treatment group were significantly increased ($P < 0.05$). Compared with the model group, the expression levels of the TNF-α, IL-6, and CASP3 proteins in the treatment group were significantly decreased ($P < 0.05$), and the differences for which were statistically significant. The ELISA results were consistent with the qRT-PCR results.

DISCUSSION

The process of bone remodelling occurs throughout the human body and is a coordinated process of repairing small fractures and maintaining bone mass. Under normal circumstances, bone formation and bone resorption always maintain homeostasis. When bone resorption is faster than bone formation, the balance of bone remodelling is disrupted (19), resulting in a decrease in bone content per unit volume and a decrease in bone density, which eventually leads to the development of OP (20). As the pathogenesis of OP is the result of a combination of factors and multiple targets and pathways are involved in the pathological process (21), the current therapeutic efficacies of single-target drugs are lower than expected. Traditional Chinese medicine has the advantages of having multiple components and multiple targets in the treatment of diseases (22), so it has a high clinical value in the treatment of OP. In previous clinical trials, we found that MDHJSD can clearly improve the clinical symptoms of patients with OP and reduce the incidence of fractures (especially elderly patients), but its mechanism of action has not yet been elucidated. It has good prospects for use in the treatment of OP and provides more therapeutic strategies for the treatment of OP. This study aimed to analyse the mechanism of action of MDHJSD in the treatment of OP through network pharmacology and to verify the identified mechanism using animal experiments.

One hundred active components and 277 corresponding targets of MDHJSD were retrieved, and 4734 OP-related targets were obtained, including 194 overlapping targets.

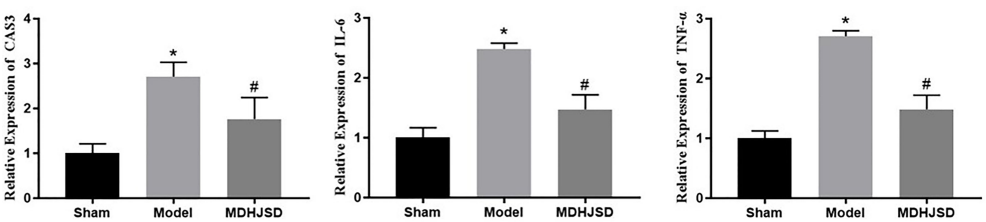

FIGURE 10 | Effect on key target mRNA expression levels. Compared with control operation group, $^{*}P < 0.05$; Compared with the model group, $^{\#}P < 0.05$.

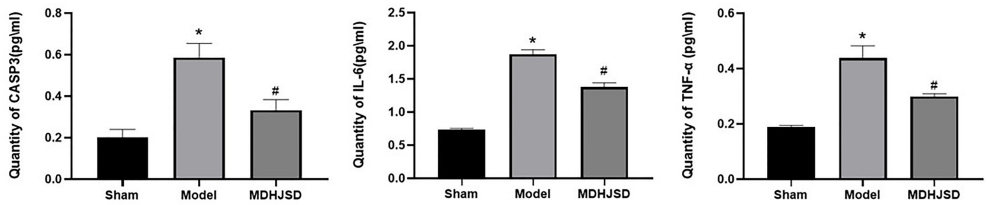

FIGURE 11 | Expression levels of the related proteins. Compared with control operation group, $^{*}P < 0.05$; Compared with the model group, $^{\#}P < 0.05$.

Finally, five active components, including quercetin, luteolin, kaempferol, wogonin, and beta-sitosterol, were screened according to the degree value. The PPI network was analysed by the Cytohubba plug-in, and the final eight core genes were obtained: IL-6, AKT1, MAPK3, CASP3, TNF, JUN, TP53, and ALB. According to the results of the pathway enrichment analysis, it was found that overlapping targets were significantly enriched in the PI3K-Akt, TNF, and thyroid hormone signaling pathways. In the molecular docking verification, the results showed that TNF-α, IL-6, and CASP3 had good docking activity with the five core active components, indicating that they may be the potential active components and targets of MDHJSD in the treatment of OP.

As far as we know, the inflammatory response plays an important role in the occurrence and development of OP. Many inflammatory factors play a key role in OP, which can not only lead to obstacles in bone formation but also strengthen bone resorption activities and cause the imbalance of bone reconstruction (23, 24). Clinical observation shows that systemic osteoporosis occurs simultaneously with periodic systemic inflammation, and local osteoporosis occurs simultaneously with local inflammatory areas (25). Pasco's study on osteoporosis found that the risk of fracture increased 24-32% for each SD increase in CRP levels in older women (26). Ding and collaborators studied 168 men and women with an average age of 63 years and found that increased bone loss was associated with higher levels of systemic inflammation during a 3-year follow-up (27). Therefore, some scholars believe that postmenopausal inflammatory factors, such as TNF -α and IL-6, are the factors leading to accelerated bone mineral density (BMD) decline (28, 29).

TNF-α is an important mononuclear inflammatory factor that can degrade organic bone by inhibiting extracellular matrix deposition. Relevant studies found that TNF-α can not only inhibit the transformation of mesenchymal stromal cells (MSCs) to osteoblasts by regulating the expression of Runx2 but also inhibit the expression of osterix (OSX; Sp7) and affect the development and maturation of osteoblasts (30, 31). In addition, TNF-α can also regulate the expression of insulin like growth factor I (IGF-I), inhibit the differentiation of osteoblasts, affect bone formation, directly or indirectly promote the production of macrophage colony stimulating factor, and accelerate the bone resorption process in osteoclasts (32, 33). In addition, abundant evidence that TNF-α can induce osteoblast apoptosis, disrupt the balance of bone remodeling, and lead to loss of bone content (34, 35). IL-6 is a multifunctional inflammatory factor that plays an important role in a variety of biological bone activities (36, 37). Experimental studies have found that IL-6 can induce osteocyte differentiation, promote osteoclast formation, enhance osteoclast activity, accelerate bone resorption, and aggravate the degree of OP (38–40). Thus, IL-6 plays an important role in the occurrence of OP.

The aim of the experimental verification in this study was to construct an OP animal model by oophorectomy. The results showed that MDHJSD could significantly reduce femoral TNF-α in ovariectomized rats. The relative mRNA expression levels of IL-6 and CASP3 and the expression levels of the related proteins in serum osteoblasts protected from TNF-α induced apoptosis. MDHJSD may protect bone loss in ovariectomized rats by regulating TNF signaling channels.

STUDY LIMITATIONS

Due to the limited time and funds of this study, the relationship between MDHJSD dose and efficacy in the treatment of OP was not studied. In addition, this study was a preliminary exploratory experiment to explore the mechanism of MDHJSD improving OP, and the mechanism of MDHJSD treating OP was not fully clarified. Therefore, in the following work, the research group will further discuss the above problems, and provide a certain scientific basis for the wide application of MDHJSD in clinical practice. Anyway, we still found that MDHJSD can significantly improve the progress of OP, and its mechanism may be related to the inhibition of inflammatory response, which will provide some scientific reference for further mechanism research.

CONCLUSIONS

In conclusion, this study screened the key targets and pathways involved in the anti-OP effect by MDHJSD through network pharmacology, further using molecular docking analysis to clarify the mechanism of its therapeutic effect, and finally verified that MDHJSD can significantly reduce TNF-α in bone tissue through animal experimental research in the mRNA expression levels of IL-6 and CASP3. Therefore, we speculated that MDHJSD can effectively treat OP by inhibiting the inflammatory response, reducing bone resorption, and promoting bone shape.

DATA AVAILABILITY STATEMENT

The original contributions presented in the study are included in the article/**Supplementary Material**. Further inquiries can be directed to the corresponding authors.

ETHICS STATEMENT

The animal study was reviewed and approved by the experimental animal ethics committee of the Affiliated Hospital of Shandong University of traditional Chinese medicine (2020-48).

AUTHOR CONTRIBUTIONS

WW and LZ conceived this project. XH and ZZ designed the study,acquisition of data, analysis and interpretation of data. GF, YZ, and BN searched the literature data. XH and ZZ drafted the manuscript. ML and MZ revision of the manuscript. All authors contributed to the article and approved the submitted version.

FUNDING

Shandong Provincial Scientific and Technological Innovation Program for Medical Workers (No.202014), Science and Technology Project of Shandong Health Science and Technology Association (No.2017004).

SUPPLEMENTARY MATERIAL

The Supplementary Material for this article can be found online at: https://www.frontiersin.org/articles/10.3389/fendo.2022.860649/full#supplementary-material

REFERENCES

1. Marwick C. Consensus Panel Considers Osteoporosis. *JAMA* (2000) 283:2093–5. doi: 10.1001/jama.283.16.2093-JMN0426-3-1
2. Migliorini F, Maffulli N, Colarossi G, Eschweiler J, Tingart M, Betsch M. Effect of Drugs on Bone Mineral Density in Postmenopausal Osteoporosis: A Bayesian Network Meta-Analysis. *J Orthop Surg Res* (2021) 16:533. doi: 10.1186/s13018-021-02678-x
3. Dai W, Sun Y, Zhong G. A Network Pharmacology Approach to Estimate the Active Ingredients and Potential Targets of Cuscutae Semen in the Treatment of Osteoporosis. *Med Sci Monit* (2020) 26:e920485. doi: 10.12659/MSM.920485
4. Zeng Q, Li N, Wang Q, Feng J, Sun D, Zhang Q, et al. The Prevalence of Osteoporosis in China, a Nationwide, Multicenter DXA Survey. *J Bone Miner Res* (2019) 34:1789–97. doi: 10.1002/jbmr.3757
5. Khosla S, Hofbauer LC. Osteoporosis Treatment: Recent Developments and Ongoing Challenges. *Lancet Diabetes Endocrinol* (2017) 5:898–907. doi: 10.1016/S2213-8587(17)30188-2
6. Canalis E. New Treatment Modalities in Osteoporosis. *Endocr Pract* (2010) 16:855–63. doi: 10.4158/EP10048.RA
7. Xiong Z, Zheng C, Chang Y, Liu K, Shu L, Zhang C. Exploring the Pharmacological Mechanism of Duhuo Jisheng Decoction in Treating Osteoporosis Based on Network Pharmacology. *Evid Based Complement Alternat Med* (2021) 2021:5510290. doi: 10.1155/2021/5510290
8. Li J, Wang W, Feng G, Du J, Kang S, Li Z, et al. Efficacy and Safety of Duhuo Jisheng Decoction for Postmenopausal Osteoporosis: A Systematic Review and Meta-Analysis. *Evid Based Complement Alternat Med* (2020) 2020:6957825. doi: 10.1155/2020/6957825
9. Luo TT, Lu Y, Yan SK, Xiao X, Rong XL, Guo J. Network Pharmacology in Research of Chinese Medicine Formula: Methodology, Application and Prospective. *Chin J Integr Med* (2020) 26:72–80. doi: 10.1007/s11655-019-3064-0
10. Hopkins AL. Network Pharmacology. *Nat Biotechnol* (2007) 25:1110–1. doi: 10.1038/nbt1007-1110
11. Ru J, Li P, Wang J, Zhou W, Li B, Huang C, et al. TCMSP: A Database of Systems Pharmacology for Drug Discovery From Herbal Medicines. *J Cheminform* (2014) 6:13. doi: 10.1186/1758-2946-6-13
12. Szklarczyk D, Santos A, von Mering C, Jensen LJ, Bork P, Kuhn M. STITCH 5: Augmenting Protein-Chemical Interaction Networks With Tissue and Affinity Data. *Nucleic Acids Res* (2016) 44:D380–4. doi: 10.1093/nar/gkv1277
13. Szklarczyk D, Gable AL, Lyon D, Junge A, Wyder S, Huerta-Cepas J, et al. STRING V11: Protein-Protein Association Networks With Increased Coverage, Supporting Functional Discovery in Genome-Wide Experimental Datasets. *Nucleic Acids Res* (2019) 47:D607–13. doi: 10.1093/nar/gky1131
14. Jiao X, Sherman BT, Huang da W, Stephens R, Baseler MW, Lane HC, et al. DAVID-WS: A Stateful Web Service to Facilitate Gene/Protein List Analysis. *Bioinformatics* (2012) 28:1805–6. doi: 10.1093/bioinformatics/bts251
15. Burley SK, Berman HM, Kleywegt GJ, Markley JL, Nakamura H, Velankar S. Protein Data Bank (PDB): The Single Global Macromolecular Structure Archive. *Methods Mol Biol* (2017) 1607:627–41. doi: 10.1007/978-1-4939-7000-1_26
16. Zhang Q, Song X, Chen X, Jiang R, Peng K, Tang X, et al. Antiosteoporotic Effect of Hesperidin Against Ovariectomy-Induced Osteoporosis in Rats *via* Reduction of Oxidative Stress and Inflammation. *J Biochem Mol Toxicol* (2021) 35:e22832. doi: 10.1002/jbt.22832
17. Doncheva NT, Morris JH, Gorodkin J, Jensen LJ. Cytoscape StringApp: Network Analysis and Visualization of Proteomics Data. *J Proteome Res* (2019) 18:623–32. doi: 10.1021/acs.jproteome.8b00702
18. Li B, Rui J, Ding X, Yang X. Exploring the Multicomponent Synergy Mechanism of Banxia Xiexin Decoction on Irritable Bowel Syndrome by a Systems Pharmacology Strategy. *J Ethnopharmacol* (2019) 233:158–68. doi: 10.1016/j.jep.2018.12.033
19. Rodan GA, Martin TJ. Therapeutic Approaches to Bone Diseases. *Science* (2000) 289:1508–14. doi: 10.1126/science.289.5484.1508
20. Cummings SR, Melton LJ. Epidemiology and Outcomes of Osteoporotic Fractures. *Lancet* (2002) 359:1761–7. doi: 10.1016/S0140-6736(02)08657-9
21. Yang TL, Shen H, Liu A, Dong SS, Zhang L, Deng FY, et al. A Road Map for Understanding Molecular and Genetic Determinants of Osteoporosis. *Nat Rev Endocrinol* (2020) 16:91–103. doi: 10.1038/s41574-019-0282-7
22. Zhang ND, Han T, Huang BK, Rahman K, Jiang YP, Xu HT, et al. Traditional Chinese Medicine Formulas for the Treatment of Osteoporosis: Implication for Antiosteoporotic Drug Discovery. *J Ethnopharmacol* (2016) 189:61–80. doi: 10.1016/j.jep.2016.05.025
23. Gillet C, Spruyt D, Rigutto S, Dalla Valle A, Berlier J, Louis C, et al. Oleate Abrogates Palmitate-Induced Lipotoxicity and Proinflammatory Response in Human Bone Marrow-Derived Mesenchymal Stem Cells and Osteoblastic Cells. *Endocrinology* (2015) 156:4081–93. doi: 10.1210/en.2015-1303
24. Miyamoto T. Mechanism Underlying Post-Menopausal Osteoporosis: HIF1alpha Is Required for Osteoclast Activation by Estrogen Deficiency. *Keio J Med* (2015) 64:44–7. doi: 10.2302/kjm.2015-0003-RE
25. Yun AJ, Lee PY. Maldaptation of the Link Between Inflammation and Bone Turnover may be a Key Determinant of Osteoporosis. *Med Hypotheses* (2004) 63:532–7. doi: 10.1016/S0306-9877(03)00326-8
26. Pasco JA, Kotowicz MA, Henry MJ, Nicholson GC, Spilsbury HJ, Box JD, et al. High-Sensitivity C-Reactive Protein and Fracture Risk in Elderly Women. *JAMA* (2006) 296:1353–5. doi: 10.1001/jama.296.11.1353
27. Ding C, Parameswaran V, Udayan R, Burgess J, Jones G. Circulating Levels of Inflammatory Markers Predict Change in Bone Mineral Density and

Resorption in Older Adults: A Longitudinal Study. *J Clin Endocrinol Metab* (2008) 93:1952–8. doi: 10.1210/jc.2007-2325
28. Weitzmann MN, Pacifici R. Estrogen Deficiency and Bone Loss: An Inflammatory Tale. *J Clin Invest* (2006) 116:1186–94. doi: 10.1172/JCI28550
29. Lencel P, Magne D. Inflammaging: The Driving Force in Osteoporosis? *Med Hypotheses* (2011) 76:317–21. doi: 10.1016/j.mehy.2010.09.023
30. Gilbert L, He X, Farmer P, Rubin J, Drissi H, van Wijnen AJ, et al. Expression of the Osteoblast Differentiation Factor RUNX2 (Cbfa1/AML3/Pebp2alpha A) Is Inhibited by Tumor Necrosis Factor-Alpha. *J Biol Chem* (2002) 277:2695–701. doi: 10.1074/jbc.M106339200
31. Lu X, Gilbert L, He X, Rubin J, Nanes MS. Transcriptional Regulation of the Osterix (Osx, Sp7) Promoter by Tumor Necrosis Factor Identifies Disparate Effects of Mitogen-Activated Protein Kinase and NF Kappa B Pathways. *J Biol Chem* (2006) 281:6297–306. doi: 10.1074/jbc.M507804200
32. Kanazawa K, Kudo A. Self-Assembled RANK Induces Osteoclastogenesis Ligand-Independently. *J Bone Miner Res* (2005) 20:2053–60. doi: 10.1359/JBMR.050706
33. Gilbert L, He X, Farmer P, Boden S, Kozlowski M, Rubin J, et al. Inhibition of Osteoblast Differentiation by Tumor Necrosis Factor-Alpha. *Endocrinology* (2000) 141:3956–64. doi: 10.1210/endo.141.11.7739
34. Glass GE, Chan JK, Freidin A, Feldmann M, Horwood NJ, Nanchahal J. TNF-Alpha Promotes Fracture Repair by Augmenting the Recruitment and Differentiation of Muscle-Derived Stromal Cells. *Proc Natl Acad Sci USA* (2011) 108:1585–90. doi: 10.1073/pnas.1018501108
35. Osta B, Benedetti G, Miossec P. Classical and Paradoxical Effects of TNF-Alpha on Bone Homeostasis. *Front Immunol* (2014) 5:48. doi: 10.3389/fimmu.2014.00048
36. Blanchard F, Duplomb L, Baud'huin M, Brounais B. The Dual Role of IL-6-Type Cytokines on Bone Remodeling and Bone Tumors. *Cytokine Growth Factor Rev* (2009) 20:19–28. doi: 10.1016/j.cytogfr.2008.11.004
37. Wong PK, Campbell IK, Egan PJ, Ernst M, Wicks IP. The Role of the Interleukin-6 Family of Cytokines in Inflammatory Arthritis and Bone Turnover. *Arthritis Rheum* (2003) 48:1177–89. doi: 10.1002/art.10943
38. Yu H, Herbert BA, Valerio M, Yarborough L, Hsu LC, Argraves KM. FTY720 Inhibited Proinflammatory Cytokine Release and Osteoclastogenesis Induced by Aggregatibacter Actinomycetemcomitans. *Lipids Health Dis* (2015) 14:66. doi: 10.1186/s12944-015-0057-7
39. Clowes JA, Riggs BL, Khosla S. The Role of the Immune System in the Pathophysiology of Osteoporosis. *Immunol Rev* (2005) 208:207–27. doi: 10.1111/j.0105-2896.2005.00334.x
40. Caetano-Lopes J, Canhao H, Fonseca JE. Osteoimmunology–the Hidden Immune Regulation of Bone. *Autoimmun Rev* (2009) 8:250–5. doi: 10.1016/j.autrev.2008.07.038

Conflict of Interest: The authors declare that the research was conducted in the absence of any commercial or financial relationships that could be construed as a potential conflict of interest.

Publisher's Note: All claims expressed in this article are solely those of the authors and do not necessarily represent those of their affiliated organizations, or those of the publisher, the editors and the reviewers. Any product that may be evaluated in this article, or claim that may be made by its manufacturer, is not guaranteed or endorsed by the publisher.

frontiers | Frontiers in Endocrinology

SYSTEMATIC REVIEW
published: 07 April 2022
doi: 10.3389/fendo.2022.870277

Chinese Proprietary Medicine Xianling Gubao Capsule for Osteoporosis: A Systematic Review and Meta-Analysis of Randomized Clinical Trials

Bai-Ru Cheng[1], Rou-Yan Wu[1], Qin-Yang Gao[1†], Kai-Xin Jiang[2†], Shuang-Sang Li[2‡], Shi-Hao Qi[2‡], Ming-Yi Yuan[2‡] and Jian-Ping Liu[3]*

[1] The First School of Clinical Medicine (Dongzhimen Hospital), Beijing University of Chinese Medicine, Beijing, China, [2] The Second School of Clinical Medicine (Dongfang Hospital), Beijing University of Chinese Medicine, Beijing, China, [3] Centre for Evidence-Based Chinese Medicine, Beijing University of Chinese Medicine, Beijing, China

Objective: To assess the benefit and harm of Chinese medicine Xianling Gubao (XLGB) capsule compared to conventional medication or placebo to inform clinical practice.

Methods: We included randomized controlled trials (RCTs) with Jadad score ≥3 of XLGB capsule compared to pharmaceutical medication, placebo, or no treatment for primary osteoporosis. We conducted searches in EMBASE, Cochrane CENTRAL, MEDLINE, China National Knowledge Infrastructure, VIP, Wanfang, and Chinese Biomedical Literature Database (Sino-Med) from their inception till November 13th, 2021. Study selection and data extraction were done by two authors independently. The methodological quality of the RCTs was assessed using Cochrane's risk of bias tool. The effect size was presented as risk ratio (RR) or mean difference (MD) with their 95% confidence interval (CI).

Results: Our searches identified 2292 records and after exclusions, eight trials involving 846 participants were included. There was no statistically significant difference between conventional medications with or without XLGB on new fracture (RR: 0.50, 95% CI: [0.13, 1.87]). Quality of life by SF-36 questionnaire of XLGB plus calcium carbonate, vitamin D_3, and calcitriol was improved than that of without XLGB (MD: 6.72 scores, 95% CI: [2.82, 10.62]). XLGB increased bone mineral density similarly as calcium carbonate plus vitamin D_3 (MD: 0.21, 95% CI: [-0.16, 0.58]) or as alendronate sodium, calcium carbonate plus vitamin D_3 (MD: 0.00, 95% CI: [-0.10, 0.10]), but it had no additional effect as an add-on treatment to conventional medications (MD: 0.13, 95% CI: [-0.12, 0.37]). XLGB relieved pain *via* visual analog scale more effectively when

OPEN ACCESS

Edited by:
Jun Liu,
Guangdong Provincial Academy of Chinese Medical Sciences, China

Reviewed by:
Guoyan (Emily) Yang,
Western Sydney University, Australia
Heng Yin,
Nanjing University of Chinese Medicine, China
Guo-qing Zheng,
Zhejiang Chinese Medical University, China

***Correspondence:**
Jian-Ping Liu
Liujp@bucm.edu.cn

†These authors have contributed equally to this work

‡These authors have contributed equally to this work

Specialty section:
This article was submitted to Bone Research, a section of the journal Frontiers in Endocrinology

Received: *06 February 2022*
Accepted: *11 March 2022*
Published: *07 April 2022*

Citation:
Cheng B-R, Wu R-Y, Gao Q-Y, Jiang K-X, Li S-S, Qi S-H, Yuan M-Y and Liu J-P (2022) Chinese Proprietary Medicine Xianling Gubao Capsule for Osteoporosis: A Systematic Review and Meta-Analysis of Randomized Clinical Trials. Front. Endocrinol. 13:870277. doi: 10.3389/fendo.2022.870277

combined with medications (MD: -1.55 score, 95% CI: [-2.47, -0.63]). XLGB as monotherapy did not increase adverse events (RR: 0.63, 95% CI: [0.28, 1.41]), or as an add-on treatment (RR: 0.25, 95% CI: [0.03, 2.16]).

Conclusion: This systematic review shows that XLGB capsule appears to be safe and has a beneficial effect on the quality of life and pain relief when used alone or in combination with conventional medications in osteoporosis patients. Further large, rigorous trials are warranted to test its long-term benefit.

Keywords: Xianling Gubao capsule, Chinese proprietary medicine, osteoporosis, quality of life, bone mineral density, systematic review, meta-analysis

1 INTRODUCTION

Osteoporosis is characterized by the deformation of bone's microarchitecture and fragility of bones, resulting in the increment of fractures, especially in postmenopausal women. Its diagnosis criteria vary (1), resulting in a wide range of reported incidence, fractures are a great threat for osteoporosis patients since they not only cause pain or humpback but also impair dignity and quality of life. Therefore, reducing fractures has become the primary goal in osteoporosis control (2).

Current therapies include physical activity, nutrient supplements, antiresorptive drugs, and anabolic drugs, while pharmacologic treatments are the most recommended (3, 4). Exercise and balance programs such as Tai-Chi have been proved to improve coordination, reducing falling-downs, consequently lowering fracture rates (5). Lifestyle changes such as quitting cigarette smoking or reducing alcohol intake help increase bone mineral density (BMD) and reduce the risk of falls (6). Nutrient supplements calcium and vitamin D have a controversial effect preventing fractures (7), and it was found to increase cardiovascular events, especially myocardial infarction (8). Pharmacologic agents such as alendronate, zoledronic acid, and calcitonin aim at preventing bone resorption or stimulating bone formation and have been shown to improve BMD and reduce the risk of fractures. The recommended therapy for women with low BMD and a fracture risk or history includes all the means mentioned above, but in China, some patients would also seek help from traditional Chinese medicine (TCM).

Xianling Gubao (XLGB) capsule is the most recommended Chinese proprietary medicine for osteoporosis treatment. It was approved by the China Food and Drug Administration in 2002 (9). It contains *Longspur epimedium* (Yin Yang Huo), *Radix dipsaci* (Xuduan), *Salvia miltiorrhiza* (Danshen), *Rhizoma anemarrhenae* (Zhimu), *Rehmannia glutinosa* (Dihuang), and *Psoralea corylifolia* (Bu Gu Zhi). Based on network pharmacology and molecular docking, the identified components such as icariin, quercetin, and luteolin, may aim at WnT, TNF, MAPK, PI3K-Akt pathways, relating to targets including STAT3, MAPK14, JUN, IL-2, and EGFR, which are important in bone homeostasis (10). XLGB capsule was found to downregulate RANKL mRNA and upregulate osteoprotegerin mRNA, which combines with RANKL to reduce osteoclasts, finally inhibiting bone destruction (11). It was also reported that the combination of six typical absorbed constituents of XLGB capsule could promote MC3T3-E1 cells' differentiation and mineralization (12). In TCM theory, most bone diseases pertain to the deficiency of the kidney and the blood stasis in meridians which causes pain, thus, this formula could nourish the liver and the kidney, promote blood circulation, and remove meridian obstruction, to strengthen the muscles and bones. There is an increasing number of clinical trials on XLGB capsule in China (13–16). Although most trials present positive findings, some of them are of low quality, lacking blinding or proper randomization methods. Therefore, we thought it necessary to do a systematic review of randomized trials with adequate quality to provide reliable evidence for the clinical use of XLGB capsule.

2 METHODS

2.1 Search Strategy

We retrieved publications using computerized searches by EMBASE, Cochrane CENTRAL, MEDLINE, China National Knowledge Infrastructure, Wanfang, VIP, and Chinese Biomedical Literature Database (Sino-Med), with no limit on inception date or language. The last search date was November 13th, 2021. The search strategy for MEDLINE (*via* PubMed) is listed in **Appendix 1**.

2.2 Inclusion Criteria

Study design: parallel-group, randomized clinical trials regardless of blinding in all languages. There was no limit on the number of participants. Studies with a Jadad score ≥3 were included [using the Jadad scale (17)].

Patients with primary osteoporosis, diagnosed according to any clearly defined criteria were included, regardless of age, gender, or ethnic origin. Those whose chief complaint was a recent fracture and those with secondary osteoporosis such as diabetes-induced, rheumatoid arthritis-induced, or corticosteroid-induced osteoporosis were excluded.

Intervention: Chinese proprietary medicine Xianling Gubao capsule with a minimum treatment duration of three months.

Control intervention could be no treatment, placebo, or conventional pharmaceutical medicine (such as alendronate, zoledronic acid, hormone replacement therapy, bisphosphonate, calcitonin, calcium, and vitamin D).

Co-intervention was allowed as long as the Xianling Gubao group received the same conventional pharmaceutical medicine as at least one comparison group and the only difference between them was the add-on Xianling Gubao capsule.

2.3 Outcome Measures

2.3.1 Primary Outcomes

1. Number of individuals with new fractures; 2. Quality of life (QoL) is measured by a validated tool or scale.

2.3.2 Secondary Outcomes

1. Bone mineral density (BMD); detected by one of the following methods of examination: single-photon absorptiometry (SPA), dual photon absorptiometry (DPA), quantitative computed tomography (QCT), dual-energy X-ray absorptiometry (DXA), or peripheral dual-energy X-ray absorptiometry (pDXA); 2. Biochemical indicators: serum calcium (Ca), phosphorus (P), bone alkaline phosphatase (BALP), OC (osteocalcin), TRACP (tartrate-resistant acid phosphatase); 3. Pain, muscle fatigue, and limited mobility; 4. Number and types of adverse events.

2.4 Study Selection

Two authors (BR Cheng and RY Wu) independently screened the titles and abstracts of all records. We retrieved the full texts of potentially eligible studies for further identification. Any uncertainty or discrepancy was resolved by discussion with a third author (JP Liu).

2.5 Data Extraction

Two authors (MY Yuan and SS Li) independently extracted data using a predesigned data form using Excel (version Microsoft Excel 2016). Extracted data were checked together, and any disagreements were resolved by discussion with SH Qi.

2.6 Risk of Bias Assessment

Since only RCTs were included, the risk of bias was assessed through Cochrane's risk of bias Tool for Randomized Trials (RoB) (18). Two authors (QY Gao and KX Jiang) independently assessed the risk of bias. Disagreements were resolved by discussion with a third author (BR Cheng). The risk of bias was assessed through the following five domains: 1) bias arising from the randomization process; 2) bias due to deviations from intended interventions; 3) bias due to missing outcome data; 4) bias in the measurement of the outcome; 5) bias in the selection of the reported result.

2.7 Data Analysis and Synthesis

We provided a narrative synthesis of the findings from the included studies and worked with the data within a meta-analysis, through Review Manager 5.3. Heterogeneity related to the results of the studies was assessed using both the chi-square test and the I^2 statistic. If data had been sufficiently homogenous (I^2 <50%), we would pool the results using a fixed-effect model, with a mean difference (MD) for continuous outcomes (in our review referring to QoL, BMD, Ca, P, BALP, OC, TRACP, and VAS score) and risk ratio (RR) for dichotomous outcomes (referring to the number of individuals with new fractures and adverse events), and calculated 95% confidence interval (CI) and two-sided *p* values for each outcome. We provided summaries of effect estimates for each study by calculating RR or MD. We considered an I^2 value greater than 50% as high heterogeneity. If there had been high heterogeneity across included studies, we would use a random-effect model or only provide a narrative synthesis of the findings.

3 RESULTS

3.1 Study Selection

Database searches initially identified 2292 records published in English or Chinese. The last search date was November 13th, 2021. After removing duplications, 1512 articles were screened by their titles and abstracts. 130 reports were sought for retrieval of full text but we failed to find two of them, as they had no available resources online, and 128 out of 130 reports were assessed for eligibility. A flowchart (**Figure 1**) with the number of included studies at each step was established, including reasons for excluding studies. Eight trials were finally included in the qualitative and quantitative synthesis.

3.2 Study Characteristics

Table 1 presents the characteristics of the included studies, and five out of the eight studies were master's or doctor's thesis, and three were published studies in journals. The included eight studies involved 846 participants (ranging from 60 to 180). The conventional treatments in the control groups included calcium carbonate and vitamin D_3, calcitriol, alendronate sodium, and carbocalcitonin, as well as the combination of some of them. The treatment duration ranged from three to twelve months.

3.3 Risk of Bias of Individual Studies

Figures 2, **3** are summaries of each included studies' risk of bias. Overall, all included studies were of unclear or high risks, which was mostly contributed by lack of randomization sequence concealment and absence of blinding process. All studies had a proper randomization process, but none reported blinding of participants, personnel, or outcome assessment except 1 triple-blinded study, using a placebo (26). Only one study reported randomization concealment using sealed envelopes (22). Subjective outcomes such as the VAS score and the QoL score could have been biased due to the lack of participant blinding, but objective outcomes like bioindicator levels are less likely to be biased.

3.4 Primary Outcomes

3.4.1 Number of Individuals With New Fractures

Only one trial reported this outcome (23). In the twelve-month follow-up after the six-month treatment, there was no significant difference between XLGB plus medications (carbocalcitonin, calcium carbonate, vitamin D_3, and calcitriol) and medications on reported new fracture onset (3/42 versus 6/42; RR: 0.50, 95% CI: [0.13, 1.87]).

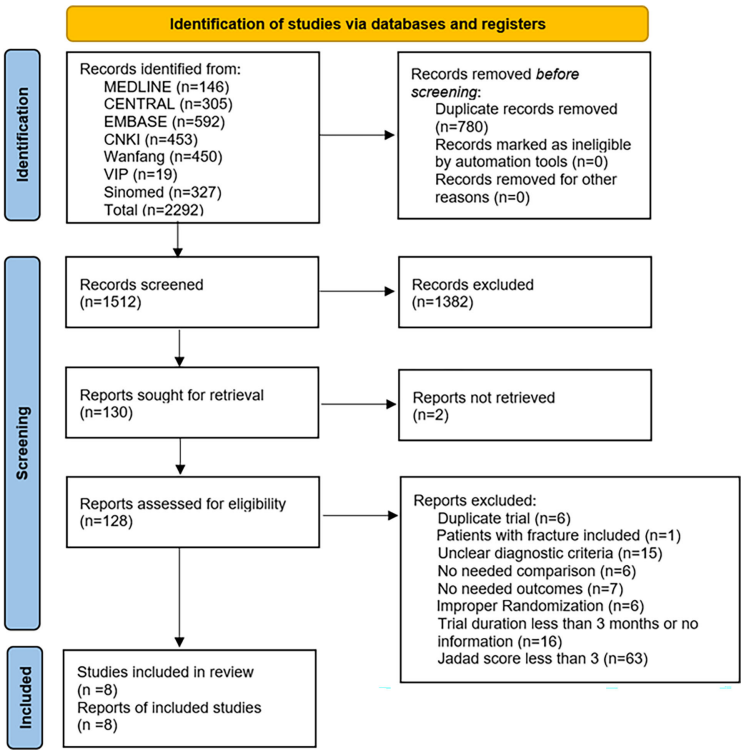

FIGURE 1 | Flowchart of the study selection process.

3.4.2 Quality of Life (QoL)

Only one trial used the SF-36 health survey questionnaire (eight domains with total scores of 100) to assess patients' quality of life (17). It showed a significant difference between calcium carbonate, vitamin D_3, and calcitriol with or without XLGB (MD: 6.72 scores, 95% CI: [2.82, 10.62]) (19).

3.5 Secondary Outcomes

3.5.1 Bone Mineral Density (BMD)

Five trials reported BMD of the lumbar spine. Two reported BMD in T scores and one did not mention the place where the BMD was detected (21), making its result unable to be pooled. In two comparisons where the units were g/cm^2 and T score, XLGB increased bone mineral density to a similar extent as calcium carbonate plus vitamin D_3 (MD: 0.21, 95% CI: [-0.16, 0.58]), or as alendronate sodium, calcium carbonate plus vitamin D_3 (MD: 0.00, 95% CI: [-0.10, 0.10]), but it had no additional effect as an add-on to conventional medications (MD: 0.13, 95% CI: [-0.12, 0.37]), though differences were seen another comparison (T score) of carbocalcitonin, calcium carbonate, vitamin D_3, and calcitriol with or without XLGB (MD: 0.11, 95% CI: [0.09, 0.13]).

3.5.2 Biochemical Indicators

3.5.2.1 Serum Calcium and Phosphorus Levels

No comparison showed a difference between XLGB plus conventional treatment and the conventional treatment, but in one study (25), serum calcium and phosphorus levels in XLGB group were significantly lower than calcium carbonate plus vitamin D_3 group (**Table 2**).

3.5.2.2 BALP, Osteocalcin, and TRACP5b Levels

XLGB plus calcium carbonate and vitamin D_3 resulted in a higher level of BALP than that of calcium carbonate and vitamin D_3 (MD: 6.67 U/L, 95% CI: [1.88, 11.46]), but XLGB alone was no better than calcium carbonate plus vitamin D_3 (MD: 6.79 U/L, 95% CI: [-23.99, 37.57]).

A higher osteocalcin level was observed in XLGB group compared to the calcium carbonate and vitamin D_3 group. The combination of the two treatments showed no differences in osteocalcin than calcium carbonate and vitamin D_3 alone (**Table 2**).

The results of the TRACP5b level were also conflicting. It was decreased in XLGB plus conventional treatment group compared to calcium carbonate, vitamin D_3, plus calcitriol group but was higher in XLGB group compared to alendronate sodium plus calcium carbonate and vitamin D_3 (**Table 2**).

3.5.3 Pain, Muscle Fatigue, and Limited Mobility

No trials reported fatigue or limited mobility. VAS score (0-10 scale) was used by all studies to measure pain. XLGB plus conventional medications significantly relieved pain than conventional medications (MD: -1.55, 95% CI: [-2.47, -0.63]). Compared to alendronate sodium plus calcium carbonate and vitamin D_3, XLGB alone did not show significant difference (MD: -0.12, 95% CI: [-0.82, 0.58]).

TABLE 1 | Characteristics of randomized controlled trials on Xianling Gubao capsule for osteoporosis.

Study	Condition	Sample Size (Experiment/control)	Experiment	Comparators	Duration (months)	Jadad Score (points out of 5)
Feng et al. (19)	Senile osteoporosis	30/30	Calcium carbonate and vitamin D_3 600mg Qd Calcitriol 0.25μg Qd Xianling Gubao capsule 1.5g Tid	Calcium carbonate and vitamin D_3 600mg Qd Calcitriol 0.25μg Qd	12	3
Li (20)	Senile osteoporosis	30/30	Calcium carbonate and vitamin D_3 600mg Bid Xianling Gubao capsule 1.5g Tid	Calcium carbonate and vitamin D_3 600mg Bid	3	3
Liu and Bai (21)	Senile osteoporosis	76/74	Alendronate sodium 70mg Qw Calcium carbonate 500mg Qd Xianling Gubao capsule 1.0g Bid	Alendronate sodium 70mg Qw Calcium carbonate 500mg Qd	6	3
Ouyang (22)	Postmenopausal osteoporosis	30/30	Calcium carbonate and vitamin D_3 600mg Qd Xianling Gubao capsule 1.5g Bid	Calcium carbonate and vitamin D_3 600mg Qd	3	3
Xu (23)	Senile osteoporosis	42/42	Carbocalcitonin 10IU Biw* Calcium carbonate and vitamin D_3 600mg Bid Calcitriol 0.25μg Bid Xianling Gubao capsule 1.5g Bid	Carbocalcitonin 10IU Biw* Calcium carbonate and vitamin D_3 600mg Bid Calcitriol 0.25μg Bid	6	3
You (24)	Postmenopausal osteoporosis	20/20	Xianling Gubao capsule 1.5g Bid	Alendronate sodium 70mg Qw Calcium carbonate and vitamin D_3 600mg Qd	6	3
Zhang (25)	Senile osteoporosis	30/30	Xianling Gubao capsule 1.5g Bid	Calcium carbonate and vitamin D_3 600mg Bid	3	3
Zhu et al. (26)#	Postmenopausal osteoporosis	61/61	Calcium carbonate 500mg Qd Vitamin D_3 200IU Qd Xianling Gubao capsule 3g/day	Calcium carbonate 500mg Qd Vitamin D_3 200IU Qd	12	4
Zhu et al. (26)#	Postmenopausal osteoporosis	58/61	Calcium carbonate 500mg Qd Vitamin D_3 200IU Qd Xianling Gubao capsule 6g/day	Calcium carbonate 500mg Qd Vitamin D_3 200IU Qd	12	4

Qd, once daily; Bid, twice daily; Tid, three times daily; g, gram; mg, milligram; μg, microgram; Qw, once per week; Biw, twice per week.
**intramuscular-injection; #Zhu 2012 contains 2 intervention groups and 1 control group.*

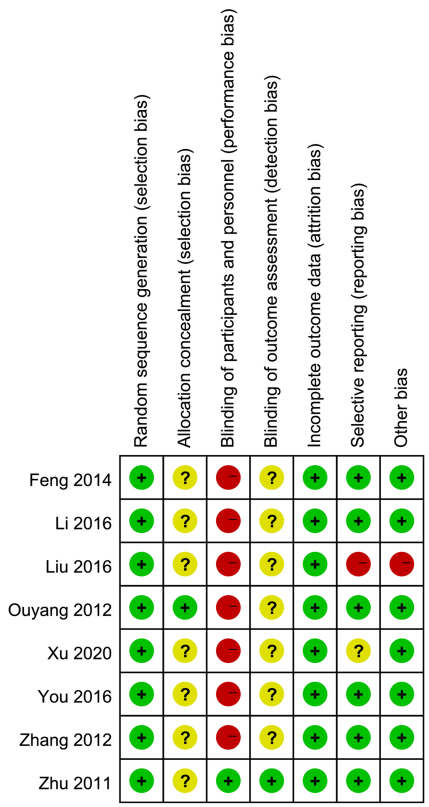

FIGURE 2 | Risk of bias summary: a review of authors' judgments about each risk of bias item for each included study.

3.5.4 Number and Types of Adverse Events

There was no significant difference in the overall rate of any adverse events between XLGB (both used alone and as add-on treatment) and conventional medication. No severe adverse events were reported. The reported adverse events in XLGB group included one case with headache, one losing appetite, one red flush, five gastrointestinal reactions, and one constipation. (**Table 3**).

3.6 Summary of the Evidence

Due to the small number of included trials, for primary outcomes–number of new fractures and quality of life–the results were not pooled, and XLGB did not significantly reduce fractures but improved quality of life. **Table 2** presents the full results of all secondary outcomes. For bone mineral density, the direct comparison of XLGB to conventional treatments had insufficient data, but the effect of XLGB as an add-on treatment was not significant. For calcium, phosphorus, and osteocalcin levels, pooled results showed no differences in the conventional treatment with or without XLGB. It was shown that XLGB significantly reduced TRACP5b levels and VAS score, indicating that it could inhibit bone deformation and relieve pain. **Table 3** shows safety outcomes, where XLGB did not result in more adverse events when added to conventional medications or compared to them.

4 DISCUSSION

This systematic review and meta-analysis investigated the efficacy and safety of XLGB capsule in patients with primary osteoporosis. Overall, XLGB capsule is a safe treatment that improved quality of life and reduces pain as an add-on treatment compared to conventional medications, including calcium carbonate, vitamin D_3, calcitriol, alendronate sodium, and carbocalcitonin, or the combination of some of them, and XLGB plus conventional treatments had a better effect than conventional medications alone. Its effects on new fractures, bone mineral density, serum calcium, and serum phosphorous levels were not significant. The results of BALP, osteocalcin, and TRACP5b levels were controversial, which could be a result of insufficient data.

XLGB capsule is a Chinese proprietary medicine made of six herbs, making its components difficult to be fully analyzed. Based on network pharmacology and molecular docking, the identified components were cryptotanshinone, chryseriol, kaempferol, anhydroicaritin, quercetin, and luteolin, which might aim at WnT, TNF, MAPK, PI3K-Akt pathways, relating to targets including STAT3, MAPK14, JUN, IL-2, and EGFR (10). Among the mentioned molecules, flavonoids such as quercetin, luteolin,

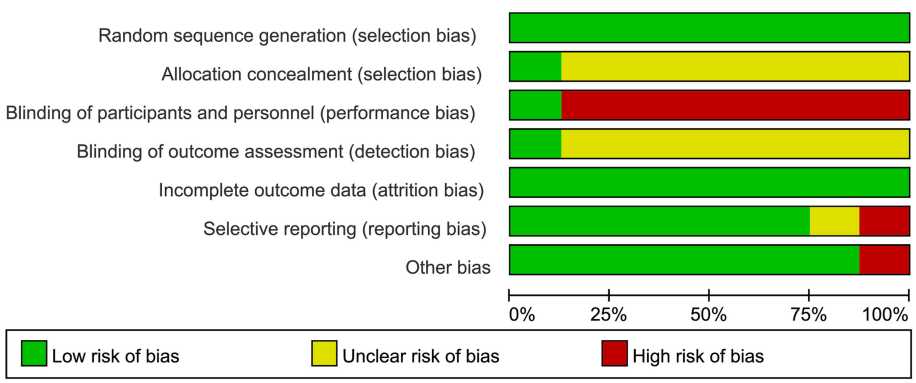

FIGURE 3 | Risk of bias graph: A review of authors' judgments about each risk of bias item presented as percentages across all included studies.

TABLE 2 | Mean differences of continuous outcomes.

	Study ID	MD [95% CI]	*P* value
Bone mineral density (lumbar spine, g/cm^2)			
XLGB plus conventional versus conventional treatment	Feng et al. (19)	0.06 [-0.00, 0.12]	0.06
	Li (20)	0.04 [0.02, 0.06]	0.0001
	Ouyang (22)	0.54 [0.51, 0.56]	<0.00001
	Zhu et al. (26)	0.00 [-0.04, 0.04]	1.00
	Zhu et al. (26)	0.00 [-0.03, 0.03]	1.00
	Pooled result	0.13 [-0.12, 0.37]	0.31
XLGB versus calcium carbonate and vitamin D_3	Zhang (25)	0.03 [-0.02, 0.08]	0.17
Bone mineral density (T score)			
XLGB plus carbocalcitonin, calcium carbonate, vitamin D_3, and calcitriol versus carbocalcitonin, calcium carbonate, vitamin D_3, and calcitriol	Xu (23)	0.11 [0.09, 0.13]	<0.00001
XLGB versus alendronate sodium, calcium carbonate and vitamin D_3	You (24)	-0.05 [-0.25, 0.15]	0.63
	You (24)	0.02 [-0.09, 0.13]	0.73
	Pooled result	0.00 [-0.10, 0.10]	0.56
Serum calcium (Ca, mmol/L)			
XLGB plus conventional versus conventional treatment	Feng et al. (19)	0.02 [-0.10, 0.14]	0.73
	Ouyang (22)	-0.20 [-0.33, -0.07]	0.002
	Pooled result	-0.09 [-0.30, 0.13]	0.01
XLGB versus calcium carbonate and vitamin D_3	Zhang (25)	-0.24 [-0.29, -0.19]	<0.00001
Phosphorus (P, mmol/L)			
XLGB plus conventional versus conventional treatment	Feng et al. (19)	-0.01 [-0.12, 0.10]	0.86
	Ouyang (22)	-0.09 [-0.28, 0.10]	0.35
	Pooled result	-0.03 [-0.13, 0.07]	0.48
XLGB versus calcium carbonate and vitamin D_3	Zhang (25)	-0.24 [-0.34, -0.14]	<0.00001
Bone alkaline phosphatase (BALP, U/L)			
XLGB plus calcium carbonate and vitamin D_3 versus calcium carbonate and vitamin D_3	Ouyang (22)	6.67 [1.88, 11.46]	0.006
XLGB versus alendronate sodium, calcium carbonate and vitamin D_3	You (24)	6.79 [-23.99, 37.57]	0.67
Osteocalcin (OC, μg/L)			
XLGB plus conventional versus conventional treatment	Li (20)	0.47 [0.41, 0.53]	<0.00001
	Xu (23)	0.12 [0.09, 0.15]	<0.00001
	Zhu et al. (26)	0.45 [-2.50, 3.40]	0.76
	Zhu et al. (26)	0.76 [-2.32, 3.84]	0.63
	Pooled result	0.30 [-0.03, 0.64]	0.08
XLGB versus calcium carbonate and vitamin D_3	Zhang (25)	0.37 [0.33, 0.42]	<0.00001
Tartrate-resistant acid phosphatase 5b (TRACP5b, nmol/L)			
XLGB plus conventional versus conventional treatment	Feng et al. (19)	-0.95 [-1.48, -0.42]	0.0004
	Ouyang (22)	-0.49 [-0.83, -0.15]	0.005
	Pooled result	-0.67 [-1.11, -0.23]	0.003
XLGB versus alendronate sodium, calcium carbonate and vitamin D_3	You (24)	0.36 [0.10, 0.62]	0.007
Pain (VAS score)			
XLGB plus conventional versus conventional treatment	Feng et al. (19)	-0.99 [-1.38, -0.60]	<0.00001
	Li (20)	-1.16 [-1.78, -0.54]	0.0002
	Liu and Bai (21)	-2.88 [-3.19, -2.57]	<0.00001
	Ouyang (22)	-1.94 [-2.48, -1.40]	<0.00001
	Xu (23)	-0.79 [-1.02, -0.56]	<0.00001
	Pooled result	-1.55 [-2.47, -0.63]	0.0009
XLGB versus alendronate sodium, calcium carbonate and vitamin D_3	You (24)	-0.12 [-0.82, 0.58]	0.74

XLGB, Xianling Gubao capsule; MD, Mean difference; CI, Confidence interval; VAS, Visual analogue scale.
**lumbar spine; #femoral neck.*

icariin are widely believed to be the main components. Quercetin, kaempferol, and icariin inhibit RANKL activation and OPG/RANK/RANKL is important in osteoclastic differentiation (27, 28). Luteolin stimulates osteoblast proliferation *via* Semaphorin 3A/Neuropilin-1/Plexin A1 pathway (29), and cryptotanshinone improves osteoblastic differentiation and reduces E_2 to inhibit bone absorption (30, 31). Also, PI3K-Akt, TNF, and MAPK pathways have to do with osteoblastic differentiation, which promotes bone formation (32, 33). Furthermore, by analyzing the absorbed components in rats' serum after intragastric administration by HPLC-MS/MS analysis, Yao et al. confirmed 15 components including sweroside, epimedin B, isopsoralen, asperosaponin VI, and neobavaisoflavone, which came from four herbs - *Longspur epimedium*, *Radix dipsaci*, *Rhizoma anemarrhenae*, and *Psoralea corylifolia* - in the formula (34). Sweroside interacts with membrane estrogen receptor-α and p38 pathway to promote osteoblastic differentiation and mineralization (35). Epimedin B downregulates PI3K-Akt, MAPK, and PPAR signaling pathways, which are mentioned above to result in bone destruction in mice (36) and have estrogen-like effects (37). Some other compounds like

TABLE 3 | Risk ratio of any adverse events.

	Study ID	RR [95% CI]	*P* value
Any adverse events			
XLGB plus conventional versus conventional treatment	Feng et al. (19)	1.00 [0.22, 4.56]	1.00
	Liu and Bai (21)	0.61 [0.21, 1.78]	0.82
	Xu (23)	0.33 [0.04, 3.08]	0.76
	Zhu (26)	1.19 [0.61, 2.33]	0.61
	Pooled result	0.90 [0.54, 1.50]	0.69
XLGB versus conventional treatment	You (24)	0.33 [0.01, 7.72]	0.82
	Zhang (25)	0.20 [0.01, 4.00]	0.58
	Pooled result	0.25 [0.03, 2.16]	0.59

XLGB, Xianling Gubao capsule; RR, Risk ratio; CI, Confidence interval.

isopsoralen, asperosaponin VI, and neobavaisoflavone have also been proved to either enhance osteogenesis or inhibit osteoclast activation (38–42). Moreover, Wu found that the combination of six typical absorbed constituents of XLGB capsule could promote MC3T3-E1 cells' differentiation and mineralization, which were not seen in any single-constituent groups, suggesting that there may be some unknown interactive mechanism of the combination (12). Moreover, Ren et al., found that XLGB capsule downregulated RANKL mRNA and upregulated the mRNA of osteoprotegerin, which combines with RANKL to reduce osteoclasts, finally inhibiting bone destruction (11). By analyzing and testing the components of XLGB capsule, we expect new phytomedicines which are more effective and with fewer adverse events.

One previous meta-analysis in Chinese reviewed the efficacy and safety of XLGB capsule in osteoporosis (43). Significant improvement in BMD, VAS, ALP, Ca, and BGP from XLGB was found, but it did not report quality of life or pain, and the difference in BMD was only slightly statistically significant that it may have limited clinical significance. Although the review specified primary osteoporosis, it included different osteoporosis. In addition, the review included randomized trials without any limitation to trial quality or treatment duration. Trials without proper randomization procedures may exaggerate the treatment effect. Compared to this review, our review has some strengths: 1) the first meta-analysis on this topic written in English and only included RCTs with adequate randomization, making the results more reliable; 2) our primary outcomes focusing on new fractures and quality of life, which are important to patients.

However, we do have some limitations: 1) the small number of included trials since we limited our inclusion criteria to those trials with moderate quality (Jadad score ≥3); 2) lack of placebo-controlled, double-blind trial, and add-on trials make blinding to participants or investigators not possible; 3) although we included trials with an adequate generation of allocation sequence, no trial reported allocation concealment, which may cause performance bias in outcome measurement such as VAS and quality of life; 4) small sample sizes (60-180 patients) of included trials may be underpowered for the effect estimates; and 5) the conventional medications used in control groups were diverse, including different combinations, so it was difficult to do subgroup analysis to investigate their efficacy respectively.

Clinicians should be aware that current evidence for XLGB capsule is limited due to small trials or a high risk of bias. Therefore, we suggest more solid evidence before the recommendation of its clinical use. We encourage placebo-controlled, double-blind trials with long follow up to test its efficacy and safety for primary osteoporosis. Only when we are confident of its efficacy would we suggest add-on trials of XLGB to current medications, especially paying attention to clinical outcomes such as the number of new fractures and quality of life.

5 CONCLUSION

This systematic review shows that XLGB capsule appears to be safe and may be used alone or with conventional treatments to improve osteoporosis patients' quality of life and relieve pain. However, current evidence for its efficacy is limited especially for long-term outcomes such as new fractures.

DATA AVAILABILITY STATEMENT

The original contributions presented in the study are included in the article/supplementary material. Further inquiries can be directed to the corresponding author.

AUTHOR CONTRIBUTIONS

B-RC and J-PL conceived this review topic. B-RC, R-YW, and J-PL drafted the study protocol. B-RC and R-YW did database searches, removed duplications, screened titles, abstracts, and full texts of included papers. K-XJ and Q-YG assessed the risk of bias and extracted data. Outcome data were extracted by M-YY and S-SL, checked, and discussed with S-HQ. Data analyses were done by B-RC and discussed with all other members. Finally, the manuscript was revised by J-PL. All authors contributed to the article and approved the submitted version.

FUNDING

This review was supported by the National Natural Science Foundation project (No. 81830115), and J-PL was partially supported by the NCCIH grant (AT001293 with sub-award No. 020468C). The funders have no role in the review design, conduct, interpretation, and writing of the report.

REFERENCES

1. Amin S, Achenbach SJ, Atkinson EJ, Khosla S, Melton LJ3rd. Trends in Fracture Incidence: A Population-Based Study Over 20 Years. *J Bone Miner Res* (2014) 29(3):581–9. doi: 10.1002/jbmr.2072
2. Black DM, Rosen CJ. Clinical PracticePostmenopausal Osteoporosis. *N Engl J Med* (2016) 374(3):254–62. doi: 10.1056/NEJMcp1513724
3. Qaseem A, Forciea MA, McLean RM, Denberg TD, Barry MJ, Cooke M, et al. Treatment of Low Bone Density or Osteoporosis to Prevent Fractures in Men and Women: A Clinical Practice Guideline Update From the American College of Physicians. *Ann Intern Med* (2017) 166(11):818–39. doi: 10.7326/M15-1361
4. Camacho PM, Petak SM, Binkley N, Diab DL, Eldeiry LS, Farooki A, et al. American Association of Clinical Endocrinologists/American College of Endocrinology Clinical Practice Guidelines for the Diagnosis and Treatment of Postmenopausal Osteoporosis-2020 Update. *Endocr Pract* (2020) 26(Suppl 1):6–8. doi: 10.4158/GL-2020-0524SUPPL
5. Sinaki M. Exercise for Patients With Osteoporosis: Management of Vertebral Compression Fractures and Trunk Strengthening for Fall Prevention. *PM R* (2012) 4(11):882–8. doi: 10.1016/j.pmrj.2012.10.008
6. Zhu K, Prince RL. Lifestyle and Osteoporosis. *Curr Osteoporos Rep* (2015) 13 (1):52–9. doi: 10.1007/s11914-014-0248-6
7. Bauer DC. Calcium Supplements and Fracture Prevention. *New Engl J Med* (2014) 370(4):387–8. doi: 10.1056/NEJMc1314100
8. Bolland MJ, Grey A, Avenell A, Gamble GD, Reid IR. Calcium Supplements With or Without Vitamin D and Risk of Cardiovascular Events: Reanalysis of the Women's Health Initiative Limited Access Dataset and Meta-Analysis. *BMJ* (2011) 342:d2040. doi: 10.1136/bmj.d2040
9. Ma Y-Z, Wang Y-P, Liu Q, Li C-L. 2018 China Guideline for the Diagnosis and Treatment of Senile Osteoporosis. *Chin J Gerontol* (2019) 39(11):2557–75. doi: 10.3969/j.issn.1005-9202.2019.11.001
10. Guan J-L, Wang Q-Y, Liu P, Xi W-Q, Zhang Q-D, Guo W-S. Molecular Mechanism of Xianling Gubao Decoction in the Treatment of Osteoporosis Based on Network Pharmacology and Molecular Docking. *J Liaoning Univ Tradit Chin Med* (2021) 23(02):57–65. doi: 10.13194/j.issn.1673-842x.2021.02.014
11. Ren S-Y, Zhang Q-H, Yan X-Z. Effect of Xianling Gubao Capsules on Microstructure of Fractured Bone in Ovariectomized Rats and Regulation Mechanism of OPG/RANKL Signaling. *Chin Tradit Patent Med* (2021) 43 (01):67–72. doi: 10.3969/j.issn.1001-1528.2021.01.013
12. Wu Q-C. *Discovery of Bioactive Constituents From Absorbed Constituents of XLGB With Promoting Differentiation and Mineralization Activity on MC3T3-E1 Cells and Preliminary Study on Action Mechanism of Sweroside [Master's Thesis]*. Guangzhou, Guangdong, China: Jinan University (2019).
13. Lai Y-H, Shen J-L. Clinical Effect of Xianling Gubao Capsule Combined With Calcitriol in the Adjuvant Treatment of Osteoporosis. *Chin J Clin Ration Drug Use* (2021) 14(19):106–8. doi: 10.15887/j.cnki.13-1389/r.2021.19.041
14. Liu M-F, Yang F, Zeng L-J. Clinical Observation of Xianling Gubao Capsule in the Treatment of Postmenopausal Women With Osteoporosis. *Yunnan J Tradit Chin Med Materia Med* (2021) 42(06):37–40. doi: 10.16254/j.cnki.53-1120/r.2021.06.012
15. Ma J-T, Qv C, Fu W-B. Effects of Zoledronic Acid Combined With Xianling Gubao Capsule on Bone Metabolism and Carotid Intimal Thickness in Elderly Postmenopausal Osteoporosis Patients. *J Med Theory Pract* (2021) 34 (24):4292–3. doi: 10.19381/j.issn.1001-7585.2021.24.029
16. Fu Y-F, Shi D-L. Effects of Xianling Gubao Capsule Combined With Zoledronic Acid Intravenous Drip and Calcium Carbonate D3 Tablet on Bone Mineral Density and Bone Turnover in Elderly Patients With Osteoporosis. *Chin J Gerontol* (2021) 41(22):5015–7. doi: 10.3969/j.issn.1005-9202.2021.22.043
17. Jadad AR, Moore RA, Carroll D, Jenkinson C, Reynolds DJ, Gavaghan DJ, et al. Assessing the Quality of Reports of Randomized Clinical Trials: Is Blinding Necessary? *Control Clin Trials* (1996) 17(1):5–8. doi: 10.1016/0197-2456(95)00134-4
18. Higgins JPT, Altman DG, Gøtzsche PC, Jüni P, Moher D, Oxman AD, et al. The Cochrane Collaboration's Tool for Assessing Risk of Bias in Randomised Trials. *BMJ* (2011) 343:d5928. doi: 10.1136/bmj.d5928
19. Feng M-M, Shi C-L, Gu P, Lv H, Zhang G-L, Liang Y-G, et al. Clinical Research of the Treatment of Primary Osteoporosis in Elder Patient With Combined Use of Xianlinggubao and Calcium. *Tianjin Pharm* (2014) 26 (2):44–7.
20. Li W-J. *The Clinical Study of the Effect of Jingu Capsule in OC and PINP Level of Senile Osteoporosis Patient [Master's Thesis]*. Guangzhou, Guangdong, China: Guangzhou University of Chinese Medicine (2016).
21. Liu B-Y, Bai R. Clinical Study of Xianling Gubao Capsule on Middle-Aged and Elderly Patients With Osteoporosis. *Shaanxi J Tradit Chin Med* (2016) 37 (10):1364–5. doi: 10.3969/j.issn.1000-7369.2016.10.045
22. Ouyang J-J. *Study of the Clinical Observation and Related Experiments on Treating Postmenopausal Osteoporosis of Kidney Yang Deficiency With Mild Moxibustion [Doctor's Thesis]*. Guangzhou, Guangdong, China: Guangzhou University of Chinese Medicine (2012).
23. Xu H-J. *Clinical Observation on the Therapeutic Effect of Wenshenqianggu Pill on Senile Osteoporosis of Spleen Kidney Yang Deficiency Type [Master's Thesis]*. Lanzhou, Gansu, China: Gansu University of Chinese Medicine (2020).
24. You Z-Q. *Clinical Observation of Bushen Juanbi Decoction in the Treatment of Postmenopausal Osteoporosis (Kidney Deficiency and Blood Stasis Syndrome) [Master's Thesis]*. Changsha, Hunan, China: Hunan University of Chinese Medicine (2016).
25. Zhang J. *Clinical Study of Gushibao Capsule on Primary Osteoporosis [Master's Thesis]*. Shijiazhuang, Hebei, China: Hebei Medical University (2012).
26. Zhu HM, Qin L, Garnero P, Genant HK, Zhang G, Dai K, et al. The First Multicenter and Randomized Clinical Trial of Herbal Fufang for Treatment of Postmenopausal Osteoporosis. *Osteoporos Int* (2012) 23(4):1317–27. doi: 10.1007/s00198-011-1577-2
27. Huang J, Yuan L, Wang X, Zhang T-L, Wang K. Icaritin and its Glycosides Enhance Osteoblastic, But Suppress Osteoclastic, Differentiation and Activity *In Vitro*. *Life Sci* (2007) 81(10):832–40. doi: 10.1016/j.lfs.2007.07.015
28. Qi X-J, Chen G-M, Shi P-Y, Zhang Z-P, Fang C-S, Zheng S-J, et al. Analysis of Pharmacological Mechanism of XianlingGubao Capsule in Treating Osteoporosis Based on Network Pharmacology. *Chin J Osteoporos* (2020) 26 (05):710–8+30. doi: 10.3969/j.issn.1006-7108.2020.05.017
29. Zheng L. Luteolin Stimulates Proliferation and Inhibits Late Differentiation of Primary Rat Calvarial Osteoblast Induced by High-Dose Dexamethasone *via* Sema3A/NRP1/Pleixin A1. *Curr Pharm Biotechnol* (2021) 22(11):1538–45. doi: 10.2174/1389201021666201216150442
30. Khosla S. New Insights Into Androgen and Estrogen Receptor Regulation of the Male Skeleton. *J Bone Miner Res* (2015) 30(7):1134–7. doi: 10.1002/jbmr.2529
31. Lee S-Y, Choi D-Y, Woo E-R. Inhibition of Osteoclast Differentiation by Tanshinones From the Root of Salvia Miltiorrhiza Bunge. *Arch Pharm Res* (2005) 28(8):909–13. doi: 10.1007/BF02973876
32. Huang RL, Yuan Y, Tu J, Zou GM, Li Q. Opposing TNF-α/IL-1β- and BMP-2-Activated MAPK Signaling Pathways Converge on Runx2 to Regulate BMP-2-Induced Osteoblastic Differentiation. *Cell Death Dis* (2014) 5:e1187. doi: 10.1038/cddis.2014.101
33. Zuo C, Zhao X, Shi Y, Wu W, Zhang N, Xu J, et al. TNF-α Inhibits SATB2 Expression and Osteoblast Differentiation Through NF-κb and MAPK Pathways. *Oncotarget* (2018) 9(4):4833–50. doi: 10.18632/oncotarget.23373
34. Yao Z-H, Dai Y, Geng J-L, Lin S-Y, Wu X-M, Yao X-S. HPLC-MS/MS Analysis of the Absorbed Blood Components in Serum After Intragastric Administration of Xianlinggubao to Rats. *J Instrumental Anal* (2013) 32 (04):420–6. doi: 10.3969/j.issn.1004-4957.2013.04.005
35. Wu Q-C, Tang X-Y, Dai Z-Q, Dai Y, Xiao H-H, Yao X-S. Sweroside Promotes Osteoblastic Differentiation and Mineralization *via* Interaction of Membrane Estrogen Receptor-α and GPR30 Mediated P38 Signalling Pathway on MC3T3-E1 Cells. *Phytomedicine* (2020) 68:153146. doi: 10.1016/j.phymed.2019.153146
36. Diao X, Wang L, Zhou Y, Bi Y, Zhou K, Song L. The Mechanism of Epimedin B in Treating Osteoporosis as Revealed by RNA Sequencing-Based Analysis. *Basic Clin Pharmacol Toxicol* (2021) 129(6):450–61. doi: 10.1111/bcpt.13657
37. Xu F, Ding Y, Guo Y, Liu B, Kou Z, Xiao W, et al. Anti-Osteoporosis Effect of Epimedium *via* an Estrogen-Like Mechanism Based on a System-Level Approach. *J Ethnopharmacol* (2016) 177:148–60. doi: 10.1016/j.jep.2015.11.007

38. Ren Y, Song X, Tan L, Guo C, Wang M, Liu H, et al. A Review of the Pharmacological Properties of Psoralen. *Front Pharmacol* (2020) 11:571535. doi: 10.3389/fphar.2020.571535
39. Ge L, Cui Y, Cheng K, Han J. Isopsoralen Enhanced Osteogenesis by Targeting AhR/Erα. *Molecules* (2018) 23(10):2–7. doi: 10.3390/molecules 23102600
40. Liu K, Liu Y, Xu Y, Nandakumar KS, Tan H, He C, et al. Asperosaponin VI Protects Against Bone Destructions in Collagen Induced Arthritis by Inhibiting Osteoclastogenesis. *Phytomedicine* (2019) 63:153006. doi: 10.1016/j.phymed.2019.153006
41. Weng Z-B, Gao Q-Q, Wang F, Zhao G-H, Yin F-Z, Cai B-C, et al. Positive Skeletal Effect of Two Ingredients of Psoralea Corylifolia L. @ on Estrogen Deficiency-Induced Osteoporosis and the Possible Mechanisms of Action. *Mol Cell Endocrinol* (2015) 417:103–13. doi: 10.1016/j.mce.2015.09.025
42. Chen H, Fang C, Zhi X, Song S, Gu Y, Chen X, et al. Neobavaisoflavone Inhibits Osteoclastogenesis Through Blocking RANKL Signalling-Mediated TRAF6 and C-Src Recruitment and NF-κb, MAPK and Akt Pathways. *J Cell Mol Med* (2020) 24(16):9067–84. doi: 10.1111/jcmm.15543
43. Wang G-Q, Liao X, Zhang Y-L, Xie Y-M. Systemic Evaluation and Meta-Analysis of Xianling Gubao Capsule in Treatment of Primary Osteoporosis in Randomized Controlled Trials. *China J Chin Materia Med* (2017) 42 (15):2829–44. doi: 10.19540/j.cnki.cjcmm.20170705.007

Conflict of Interest: The authors declare that the research was conducted in the absence of any commercial or financial relationships that could be construed as a potential conflict of interest.

Publisher's Note: All claims expressed in this article are solely those of the authors and do not necessarily represent those of their affiliated organizations, or those of the publisher, the editors and the reviewers. Any product that may be evaluated in this article, or claim that may be made by its manufacturer, is not guaranteed or endorsed by the publisher.

APPENDIX 1

Search strategy for MEDLINE (*via* PubMed):

1. bone diseases, metabolic[mh]
2. osteoporosis[mh]
3. bone density[all fields]
4. bone loss[all fields]
5. osteomalacia[tw]
6. osteodystrophy[tw]
7. osteopenia[tw]
8. bone mass[tw]
9. densitometry[mh]
10. fractures, bone[mh]
11. #1 OR #2 OR #3 OR #4 OR #5 OR #6 OR #7 OR #8 OR #9 OR #10
12. xianlinggubao[tw]
13. xianling gubao[tw]
14. XLGB[tw]
15. xian-ling-gu-bao[tw]
16. drugs, chinese herbal[mh]
17. herbal medicine[mh]
18. plants, medicinal[mh]
19. medicine, traditional[mh]
20. #12 OR #13 OR #14 OR #15 OR #16 OR #17 OR #18 OR #19
21. randomized controlled trial[pt]
22. controlled clinical trial [pt]
23. randomized [tiab]
24. placebo [tiab]
25. clinical trials as topic [mesh:noexp]
26. randomly [tiab]
27. trial [ti]
28. #21 OR #22 OR #23 OR #24 OR #25 OR #26 OR #27
29. animals [mh] NOT humans [mh]
30. #28 NOT #29
31. #11 AND #20 AND #30

frontiers | Frontiers in Endocrinology

ORIGINAL RESEARCH
published: 25 April 2022
doi: 10.3389/fendo.2022.849544

Quercetin Attenuates Osteoporosis in Orchiectomy Mice by Regulating Glucose and Lipid Metabolism *via* the GPRC6A/AMPK/mTOR Signaling Pathway

Jie Sun[1], Yalan Pan[2†], Xiaofeng Li[3†], Lining Wang[1,4], Mengmin Liu[1,4], Pengcheng Tu[1], Chengjie Wu[1], Jirimutu Xiao[5], Qiuge Han[1,4], Weiwei Da[3,4], Yong Ma[1,4*] and Yang Guo[1*]*

[1] Laboratory of New Techniques of Restoration & Reconstruction of Orthopedics and Traumatology, Nanjing University of Chinese Medicine, Nanjing, China, [2] School of Nursing, Nanjing University of Chinese Medicine, Nanjing, China, [3] Department of Orthopedics and Traumatology, Shanghai Municipal Hospital of Traditional Chinese Medicine, Shanghai University of Traditional Chinese Medicine, Shanghai, China, [4] School of Chinese Medicine, School of Integrated Chinese and Western Medicine, Nanjing University of Chinese Medicine, Nanjing, China, [5] Mongolian Medicine College, Inner Mongolia Medical University, Hohhot, China

Quercetin, a flavonoid found in natural medicines, has shown a role in disease prevention and health promotion. Moreover, because of its recently identified contribution in regulating bone homeostasis, quercetin may be considered a promising agent for improving bone health. This study aimed to elucidate the role of quercetin in androgen deprivation therapy-induced osteoporosis in mice. C57BL/6 mice were subjected to orchiectomy, followed by quercetin treatment (75 and 150 mg/kg/d) for 8 weeks. Bone microstructure was then assessed by micro-computed tomography, and a three-point bending test was used to evaluate the biomechanical parameters. Hematoxylin and eosin (H&E) staining was used to examine the shape of the distal femur, gastrocnemius muscle, and liver. The balance motion ability in mice was evaluated by gait analysis, and changes in the gastrocnemius muscle were observed *via* Oil red O and Masson's staining. ELISA and biochemical analyses were used to assess markers of the bone, glucose, and lipid metabolism. Western blotting analyses of glucose and lipid metabolism-related protein expression was performed, and expression of the GPCR6A/AMPK/mTOR signaling pathway-related proteins was also assessed. After 8 weeks of quercetin intervention, quercetin-treated mice showed increased bone mass, bone strength, and improved bone microstructure. Additionally, gait analysis, including stride length and frequency, were significantly increased, whereas a reduction of the stride length and gait symmetry was observed. H&E staining of the gastrocnemius muscle showed that the cross-sectional area of the myofibers had increased significantly, suggesting that quercetin improves balance, motion ability, and muscle mass. Bone metabolism improvement was defined by a reduction of serum levels of insulin, triglycerides, total cholesterol, and low-density

OPEN ACCESS

Edited by:
Jun Liu,
Guangdong Provincial Academy of Chinese Medical Sciences, China

Reviewed by:
Emre Karakus,
University of Giessen, Germany
Li Su,
Shanghai University, China
Bo Shuai,
Huazhong University of Science and Technology, China
Gaoyan Kuang,
The First Hospital of Hunan University of Chinese Medicine, China

***Correspondence:**
Weiwei Da
dww2348285@163.com
Yong Ma
mayong@njucm.edu.cn
Yang Guo
drguoyang@njucm.edu.cn

[†]These authors have contributed equally to this work

Specialty section:
This article was submitted to Bone Research, a section of the journal Frontiers in Endocrinology

Received: *06 January 2022*
Accepted: *16 March 2022*
Published: *25 April 2022*

Citation:
Sun J, Pan Y, Li X, Wang L, Liu M, Tu P, Wu C, Xiao J, Han Q, Da W, Ma Y and Guo Y (2022) Quercetin Attenuates Osteoporosis in Orchiectomy Mice by Regulating Glucose and Lipid Metabolism via the GPRC6A/AMPK/mTOR Signaling Pathway. Front. Endocrinol. 13:849544. doi: 10.3389/fendo.2022.849544

lipoprotein, whereas levels of insulin-like growth factor-1 and high-density lipoprotein were increased after quercetin treatment. Expression of proteins involved in glucose uptake was increased, whereas that of proteins involved in lipid production was decreased. Moreover, the GPRC6A and the phospho-AMPK/AMPK expression ratio was elevated in the liver and tibia tissues. In contrast, the phospho-mTOR/mTOR ratio was reduced in the quercetin group. Our findings indicate that quercetin can reduce the osteoporosis induced by testosterone deficiency, and its beneficial effects might be associated with the regulation of glucose metabolism and inhibition of lipid metabolism *via* the GPCR6A/AMPK/mTOR signaling pathway.

Keywords: quercetin, glucose metabolism, lipid metabolism, androgen deprivation therapy-induced osteoporosis, Gprc6a/AMPK/mTOR signaling pathway

INTRODUCTION

Androgens, including testosterone and its precursors, are vital for the musculoskeletal and endocrine-reproductive systems (1). In men 30–90 years of age, the testosterone levels slowly decrease by 1% annually (2, 3). Similarly, chronic illnesses, such as diabetes and obesity, and endocrine treatments, such as androgen deprivation therapy (ADT) after prostate cancer, can alter testosterone levels (1, 4). Low testosterone levels, referred to as "testosterone deficiency", can result in several symptoms, including erectile dysfunction, lack of energy or tiredness, depression and anxiety, bone mineral density (BMD) decline, and hair loss (1, 5, 6). These symptoms impair the lives of older men; thus, testosterone deficiency is considered a serious public health concern in the current aging society.

Similar to estrogen deficiency, the apparent relationship between bioavailable serum testosterone levels and the etiology of osteoporosis in elderly men has been clarified. A recent study examining 5540 subjects 20–59 years of age found that the lumbar BMD was positively associated with serum testosterone levels (7). Moreover, after excluding the main risk factors for fractures, serum testosterone levels were also correlated closely with fracture risk (8). The negative impact of testosterone reduction on the bone health is more unequivocal in the setting of ADT. A recent study in Korea showed that patients receiving ADT were more inclined to have newly developed osteoporosis and osteoporotic fractures (4). Thus, testosterone performs a central role in maintaining BMD and musculoskeletal health in older men.

Although the therapeutic regimens of testosterone deficiency-induced osteoporosis has not yet been fully established, the effectiveness of testosterone combined with bisphosphonate is well established (9). However, despite its beneficial effects on bone health, testosterone therapy may cause other problems, including decreased sperm production and fertility, cardiovascular disease, and prostate cancer or hyperplasia (1, 9).

Owing to the increased risk of disease from testosterone replacement therapy, investigators have shifted their focus to natural compounds that promote testosterone secretion and bone quality. Quercetin, a natural flavonol found in herbal medicines, as well as in fruits and vegetables (10). Quercetin possesses various pharmacological benefits, including antioxidative, anti-inflammatory, and antiapoptotic effects (10, 11). Recent studies have also shown that quercetin can promote testosterone secretion and ameliorate ovariectomy-induced osteoporosis *in vitro* and *in vivo* (12–15). Furthermore, it can decrease blood pressure, hyperlipidemia, and hyperglycemia, thus addressing the key problematics of testosterone therapy. However, the literature on quercetin and testosterone deficiency-induced osteoporosis is very limited.

The G-protein-coupled receptor class C group 6 member A (GPRC6A), expressed in the liver and muscles, is closely involved in the regulation of glucose and lipid metabolism (16–18). Previous research has found that GPRC6A(-/-) male mice exhibit osteoporosis and metabolic syndrome, such as increased weight and higher fat content, hyperglycemia, hyperphosphatemia, hypercalciuria, and feminization (17). In addition, computer simulations support that quercetin binds to GPCR6A and may trigger related genomic-mediated effects (19). Thus, GPRC6A may provide a novel insight into the molecular basis of quercetin treatment for testosterone deficiency-induced osteoporosis.

Here, orchiectomy was used to generate a testosterone deficiency mouse model and verify the potential therapeutic role of quercetin on testosterone deficiency-induced osteoporosis. To elucidate the possible mechanisms underlying osteoporosis induced by testosterone deficiency and the bone-protective effects of quercetin, relevant markers of glucose and lipid metabolism and components of the GPCR6A/AMPK/mTOR signaling pathway were investigated.

MATERIALS AND METHODS

Animals

In the standard barrier facility of the Experimental Animal Center of Nanjing University of Chinese Medicine, 48 male C57BL/6 mice (12 weeks old) were fed and raised. The animal room had a controlled temperature: 24 ± 2°C, and humidity: 60 ± 2%, with a 12:12 h dark-light cycle. Animal studies described in this manuscript have been approved by the Nanjing University of Chinese Medicine Institutional Animal Care and Use Committee (NO. ACU170804).

Orchiectomy Procedure and Experimental Grouping

Orchiectomy is a typical model of osteoporosis secondary to testosterone deficiency. As in a previous study (20), the surgical procedure was performed under sterile conditions, and all mice were anesthetized by an intraperitoneal injection of 1% sodium pentobarbital (60 mg/kg body weight). A ventral midline incision of approximately 1.5 cm was made in the scrotum to expose the tunica after skin preparation. The connective tissue was gently teased away, the blood vessels supplying the testes were isolated and ligated, and the testis and epididymis were removed through the incision. Finally, tetracycline ointment was applied to prevent infection after the incision was closed. In the sham-operated group, surgical procedure similar to that used for the removal of the testis and epididymis was utilized.

All treatment dosing regimens began 8 weeks after surgery. The sham-operated group (sham, n=12) received saline at a dose of 0.001 mL/kg/d. In addition to the sham-operated group, mice that underwent orchiectomy (n=36) were randomly divided into four groups. For this study, we set two different concentrations and the mice were grouped as follows: (a) the model group (model) and the sham-operated group (sham) received equivalent volumes of saline, (b) the low-quercetin group (QL) received 75 mg/kg/d of quercetin, and (c) the high-quercetin group (QH) received 150 mg/kg/d of quercetin. Saline or drugs were administered by gavage once daily for 8 weeks. The mice were anesthetized for blood collection from the retro-orbital vein and then euthanized. The liver, gastrocnemius, femur, and tibia were removed and collected carefully. The right gastrocnemius, femurs, tibias were stored in 4% paraformaldehyde, while the left gastrocnemius, femurs, tibias were stored in -80°C for further measurement.

Gait Analysis

Gait analysis was conducted using a ventral plane videography instrumentation (MSI, USA). All mice first ran at least seven adaptive runs as training before being formally recorded. After the adaptive runs, the mice were exercised and recorded by the camera at a running speed of 12 cm/s in the same direction. Stride length, stride length coefficient of variation (CV), stride frequency, and gait symmetry were analyzed to assess the ability of dynamic balance.

Micro-Computed Tomography (Micro-CT)

For bone microarchitecture analysis of the trabecular bone, micro-CT (Skyscan 1176, Germany) was used. The parameters were set as follows: voxel size 9 μm, voltage 55 kV, and current 70 mA. After completion of the scan, the region of interest (ROI) was selected from a distance of 0.3 to 0.6 mm from the highest point on the distal femur growth plate. The 3D images were analyzed and the bone features, including BMD, volume/tissue volume (BV/TV), trabecular thickness (Tb.Th), trabecular number (Tb.N), and trabecular separation (Tb.Sp), were measured.

Biomechanical Parameter Analysis

The right femurs was collected for the biomechanical three-point bending test and performed on a servohydraulic test system (MTS acumen3, USA) at 0.01 mm/s with peak load and recorded. The biomechanical parameter of stiffness, maximum load, maximum deflection, and fracture energy were then calculated from displacement and force.

Hematoxylin and Eosin (H&E) Staining

The femur was decalcified in a decalcifying liquid for 4–6 weeks after fixation in 4% paraformaldehyde, whereas the liver and gastrocnemius muscle were only fixed in 4% paraformaldehyde prior to the next step. Next, the femur, liver, and muscle were dehydrated by gradient ethanol, and then cleared with xylene solution. Specimens were then embedded in paraffin, and serial sections were generated at 5 μm thickness. The sections were stained with hematoxylin and eosin. Then sections observe alterations in the bone microstructure through an inverted microscope (Leica, DM1000).

TRAP Staining

TRAP staining kit (Sigma, 387A)was used and the specific experimental steps were performed as the manufacturer's instructions and as previously described (21). The osteoclast area to bone surface (OCs/BS) ratios were quantified.

Masson's and Oil Red O Staining

The sections were prepared as before and then stained according to the protocol of Masson's staining kit protocol (Yeasen, 60532ES58). The red stain represented the muscle fibers and blue stains represented the collagen fibers, and the muscle fiber area and collagen fiber area were calculated.

The gastrocnemius muscle and liver were fixed and embedded in the OCT compound. Next, the slices were placed in Oil Red O solution for 8 min for staining. The slices were washed twice with 60% isopropyl alcohol and re-stained by hematoxylin. Finally, the slices were photographed, and the area of the lipid droplet formation was analyzed.

ELISA

All kits were provided by Nanjing Jin Yibai Biological Technology Company (China). The expression serum of testosterone (Jin Yibai, JEB-12629), β-isomer of C-terminal telopeptide of type I collagen (β-CTX, Jin Yibai, JEB-12299), TRAP (Jin Yibai, JEB-12833), IL-6 (Jin Yibai, LA128802H), bone alkaline phosphatase (B-ALP, Jin Yibai, JEB-12359), Osteocalcin (OCN, Jin Yibai, JEB-17685), insulin-like growth factor-1 (IGF-1, Jin Yibai, JEB-12259), and insulin (Mercodia, 10-1247-01) were measured based on the standard sandwich ELISA protocol.

Biochemical Analysis

Triglyceride, total cholesterol, high-density lipoprotein (HDL), low-density lipoprotein (LDL) and free fatty acid (FFA) levels were detected using the automatic biochemical analyzer (AU680, Beckman).

Western Blotting

The left tibia, gastrocnemius muscle and liver was lysed in RIPA lysis buffer containing a protease inhibitor cocktail. The samples were sonicated and incubated on ice for 30 min and then the insoluble material was removed by centrifuging at 12000 rpm for

5min. The protein in the supernatant was collected and then quantified by BCA kit (Yeasen, 20201ES76). A 10% SDS-PAGE was used, and electrophoresis was performed with a voltage of 140 V. Subsequently, the gel was transferred onto PVDF membranes with a constant electric current of 400 mA. After the PVDF membranes were blocked using blocking solution for 15 min, the membranes were incubated with anti-Gprc6a (1:4000; SAB, 47990), anti-AMPK (1:4000; CST, 2757), anti-p-AMPK (1:2000; CST, 50081), anti-RUXN2 (1:4000; Proteintech, 20700-1-AP), anti-Osterix (1:4000; Abcam, ab94744), and anti-GAPDH (1:5000; Proteintech, 10494-1-AP) overnight at 4°C and then incubated with the secondary antibody (1:10000; Proteintech, 20536-1-AP) for 2 h on a horizontal shaker at normothermia. Finally, the membrane was moistened using ECL reagent and the image was exposed to obtain the bands.

Quantitative Real-Time PCR (qRT-PCR)

Total RNA was extracted using the Bone RNA Kit and Cell/Tissue Total RNA Kit (Yesaen, 19211ES60), and then 1st Strand cDNA Synthesis Kit (Yesaen, 11119ES60) was used to RNA reverse transcription. The Hieff qPCR SYBR Green PCR Master Mix (Yesaen, 11201ES03) was used for q-PCR analysis. Each value was adjusted using β-actin as the reference. The $2^{-\Delta\Delta Ct}$ method was used to analyze PCR array results. The qPCR primers sequences are as follows:OCN: Forward 5' CTGAAAAGCCCACAGATA CCAG3' and Reverse 5' TGGAGAGGGTTGTTAGTGTGTC3'. RUNX2: Forward 5' ATGCTTATTCGCCTCACAAA3' and Reverse 5' GCACTCACTGACTCGGTTGG3'. Osterix: Forward 5' ATGGCGTCCTCTCTGCTTG3' and Reverse 5' TGAA AGGTCAGCGTATGGCTT3' β-actin: Forward 5' GGCTG TATTCCCCTCCATCG 3' and Reverse 5' CCAGTTGGTAA CAATGCCATGT 3'.

Statistical Analysis

The raw data and generated statistics were analyzed using the SPSS software (v 23.0). The data were transformed and presented as the mean ± standard deviation (SD) and were analyzed using the Kruskal–Wallis one-way analysis of variance (ANOVA) when the data were not normally distributed. Differences were considered significant when $P < 0.05$. The GraphPad Prism software 9.0.0 was used to generate the figures.

RESULTS

Changes in the Serum Levels of Testosterone

Upon orchiectomy, due to the absence of the testes and epididymides, the serum testosterone levels decreased rapidly. As expected, the testosterone levels increased after 8 weeks of quercetin treatment both for the low-quercetin group (QL, 75 mg/kg/d) and the high-quercetin group (QH, 150 mg/kg/d) as compared with the model group receiving saline solution ($p<0.01$, **Figure 1A**). Simultaneously, the serum levels of undercarboxylated osteocalcin (uOCN), which promotes testosterone secretion, increased accordingly ($p<0.01$, **Figure 1B**).

Quercetin Improves Bone Microstructure Upon Orchiectomy

To measure the bone volume and bone microstructure in mice that underwent orchiectomy, micro-CT scans were employed and the characteristics of the distal femoral trabecular bone were evaluated. As shown in **Figure 2A**, the bone trabeculae was significantly lower in the model group than the sham-operated group. Further data analysis showed that volume/tissue volume (BV/TV) and trabecular thickness (Tb.Th) were higher and trabecular separation (Tb.Sp) was markedly lower in both the low- and the high-quercetin groups than in the model group ($p<0.01$); additionally, the high-quercetin group had significantly increased bone mineral density (BMD, $p<0.01$) and trabecular number (Tb.N, $p<0.01$) levels (**Figures 2B–F**). Next, we investigated the microstructure of the distal femoral trabecular bone using H&E staining (**Figure 3E**). The distal femoral had lesser bone trabecula and thinner cortical bones in the model group than the sham-operated group. In addition, increased bone trabecula, fewer lipid droplets, and better intertrabecular connectivity were observed in the low- and high-quercetin groups. These data suggest that after 8 weeks of treatment, bone

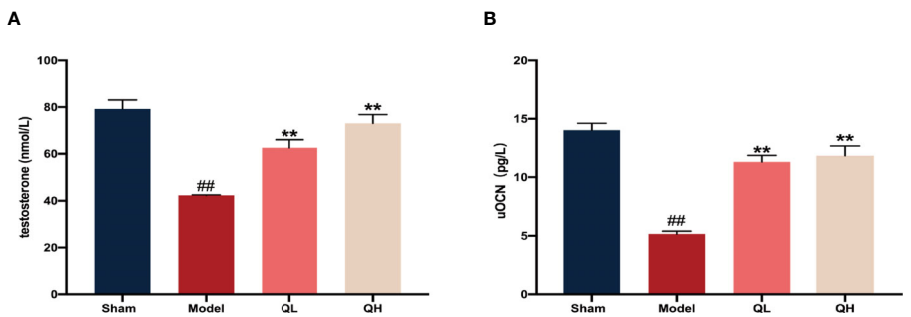

FIGURE 1 | Changes in serum levels of testosterone and undercarboxylated osteocalcin (uOCN) in mice that have undergone orchiectomy. **(A)** Serum testosterone levels in the sham-operated (sham), model (model), low- (QL), and high-quercetin groups (QH). **(B)** Serum uOCN levels in all treatment and control groups. ##$p<0.01$ vs. sham group; **$p<0.01$ vs. model group.

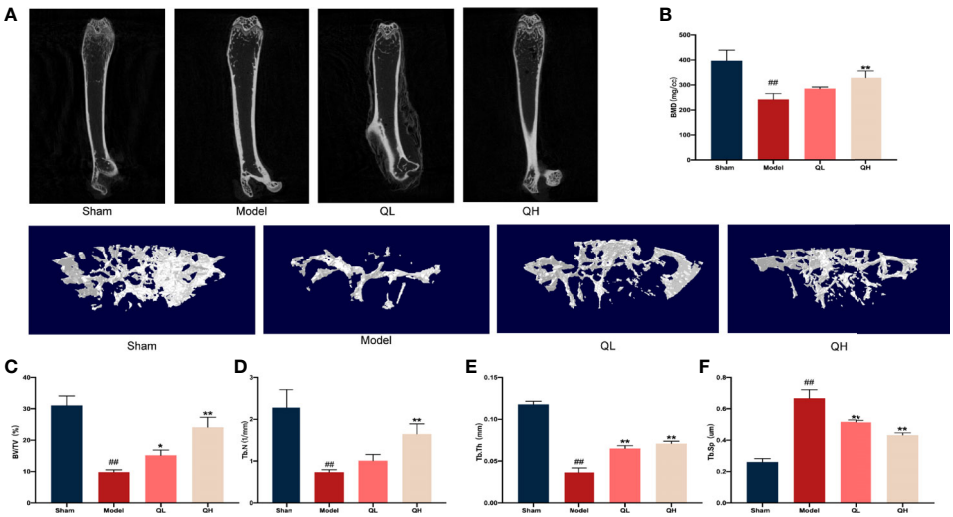

FIGURE 2 | Quercetin induced improvement of bone microstructure in mice that underwent orchiectomy. **(A)** 2D images and 3D reconstruction of the distal femur by micro-computed tomography. **(B)** Bone mineral density **(**BMD) of the distal femur. **(C–F)** Changes in bone characteristics, including bone volume/tissue volume (BV/TV), trabecular number (Tb. N), trabecular thickness (Tb. Th), and trabecular separation (Tb.Sp). ##p<0.01 vs. sham group; *p<0.05, **p<0.01 vs. model group.

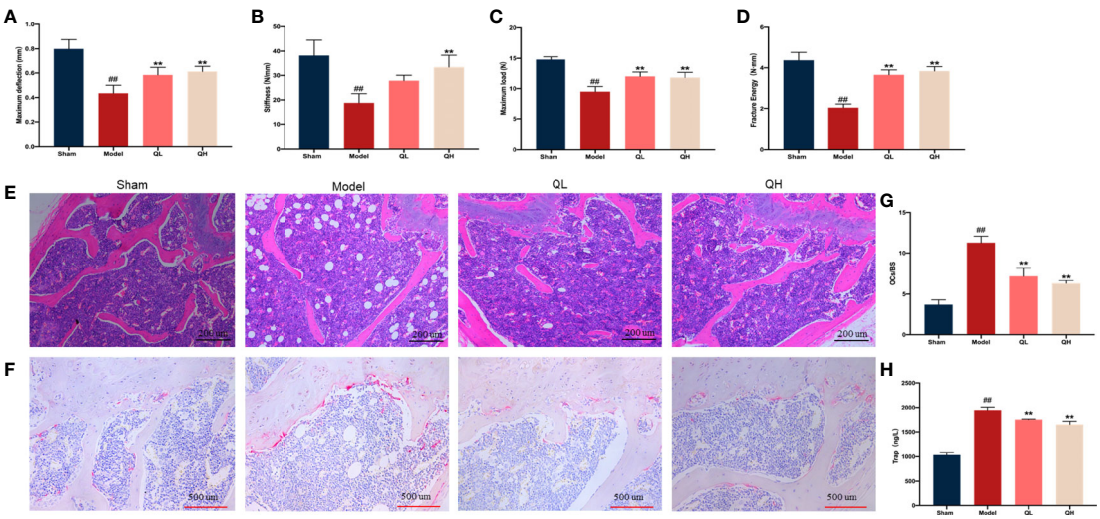

FIGURE 3 | Effects of quercetin on the biomechanical characteristics and capacity for bone resorption in mice that underwent orchiectomy. **(A–D)** Changes in the biomechanical characteristics in femur: including the maximum load and deflection, fracture energy, and stiffness. **(E)** The effects of quercetin on bone microstructure in the distal femoral bone, visualized by H&E staining. **(F)** Effects of quercetin on the bone resorption in mice that underwent orchiectomy, visualized by TRAP staining. **(G)** Osteoclast surface/bone surface (OC.s/BS). **(H)** Changes in serum levels of TRAP in mice that have undergone orchiectomy. ##p<0.01 vs. sham group; **p<0.01 vs. model group.

density improved and the high-dose quercetin effectively increased BMD and improved bone microarchitecture in mice that had undergone orchiectomy. In addition, bone resorption of the distal femoral trabecular bone was observed directly by TRAP staining (**Figures 3F**). We found that quercetin administration alleviated bone loss after orchiectomy in mice and decreased the OCs/BS ratio (**Figures 3G**). Subsequently, the levels of serum TRAP were measured and the changes after quercetin administration is consistent with TRAP staining (**Figures 3H**).

Quercetin Improves Biomechanical Parameters Upon Orchiectomy

Fresh femurs were evaluated using a three-point bending test to determine the biomechanical status of the cortical bone. The

maximum load and deflection, fracture energy, and stiffness were significantly lower in the model group than in the sham-operated group (**Figures 3A–D**) and increased in both the low- and high-quercetin groups when compared with the model ($p<0.01$). In addition, stiffness was significantly higher in the high-quercetin group than in the model group ($p<0.01$).

Quercetin Improves the Balance Motion Ability Upon Orchiectomy

The musculoskeletal system is a dynamic system that requires a strong balance. A decreased compliance of the body was observed in the muscle system when the skeletal system was changed. After treatment with high dose of quercetin, we found that the stride length and frequency significantly increased ($p<0.01$), whereas stride length CVs and gait symmetry decreased correspondingly ($p<0.01$, **Figures 4A–E**). The same trend was observed for low doses of quercetin; however, the increase in stride frequency was not significantly (**Figure 4B**). These findings suggest that quercetin improves balance motion ability, subsequently preventing falls and reducing the fracture risk often experienced with osteoporosis.

Quercetin Improves Morphological Changes in the Gastrocnemius Muscle Upon Orchiectomy

To examine the effect of quercetin on morphological changes, H&E staining of the gastrocnemius muscle was performed (**Figures 5A, B**). The average cross-sectional area of myofibers decreased notably in the model group, along with an obvious broadening of the interstitial spaces among the muscle fibers. Furthermore, the cross-sectional area of the myofibers was significantly higher in the low- and high-quercetin groups than in the model group ($p<0.05$ and $p<0.01$, respectively), indicating that fiber atrophy was attenuated. We further used Masson's staining to visualize the changes in the collagen fiber area. We found that the percentage of the collagen fiber area of gastrocnemius muscle in the model group was significantly higher than that in the sham-operated group ($p<0.01$), whereas there was an evident decrease in the collagen fiber area percentage of the low- and the high-quercetin groups ($p<0.05$ and $p<0.01$, respectively, **Figures 5C, D**). Finally, lipid accumulation in the gastrocnemius muscle was assessed by Oil Red O staining, and the results showed that the area of lipid droplets in the low- and high-quercetin groups was smaller than that in the model group ($p<0.01$, **Figures 5E, F**). These results indicate that quercetin may promote morphological changes in the gastrocnemius muscle by improving muscle mass and decreasing collagen fiber area and lipid droplets.

Quercetin Alleviates Bone Loss and Increases Bone Formation After Orchiectomy in Mice

To determine the impact of quercetin on bone homeostasis in mice that had undergone orchiectomy, markers of bone resorption (β-CTX, and IL-6) and bone formation (OCN and B-ALP) were evaluated using ELISA. Following orchiectomy, the serum levels of β-CTX, and IL-6 were markedly elevated in the model group when compared with the sham group ($p<0.01$). However, after 8 weeks of quercetin treatment, levels of these markers were decreased in the mice ($p<0.01$, **Figures 6A, B**). The serum levels of OCN significantly decreased whereas B-ALP increased after orchiectomy (**Figures 6C, D**). Quercetin treatment induced a significant increase in OCN and decrease in B-ALP ($p<0.01$). Moreover, the mRNA and protein expression of OCN, RUNX2, and Osterix were also analyzed (**Figures 6E–G**). The protein levels of OCN, RUNX2, and Osterix were significantly upregulated after 8 weeks of quercetin treatment ($p<0.01$, **Figures 6E, F**) as were the mRNA levels ($p<0.01$, **Figure 6G**).

Quercetin Improves Lipid Metabolism Upon Orchiectomy

Histological abnormalities in liver upon orchiectomy and quercetin treatment were evaluated. As shown in **Figure 7A**, the structure of the liver was normal in the sham-operated group, whereas the fat vacuole, which is a typical sign of fat degeneration, was clearly

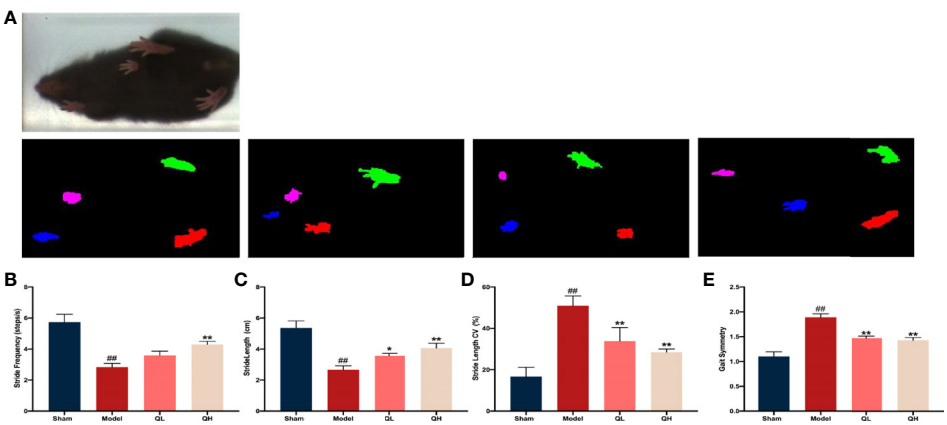

FIGURE 4 | Gait analysis in mice that underwent orchiectomy. **(A)** The full gait was recorded and segmented into independent gait cycles. Changes in gait characteristics: including the **(B)** stride length, **(C)** stride length CV, **(D)** stride frequency, and **(E)** gait symmetry. ##$p<0.01$ vs. sham group; *$p<0.05$, **$p<0.01$ vs. model group.

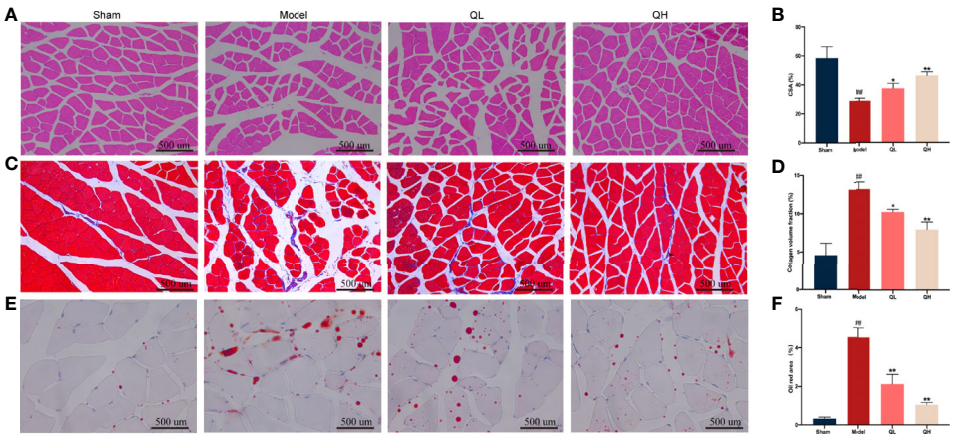

FIGURE 5 | Effects of quercetin on morphological changes in the gastrocnemius muscle of mice that underwent orchiectomy. **(A)** Morphological changes in the gastrocnemius, visualized by H&E staining, and **(B)** changes in the average cross-sectional area of myofibers (CSA). **(C)** Masson's staining of the gastrocnemius muscle, and **(D)** changes in the collagen fiber area. **(E)** Oil Red O staining of the gastrocnemius muscle, and **(F)** the changes in the area of the lipid droplet. ##p<0.01 vs. sham group; *p<0.05, **p<0.01 vs. model group.

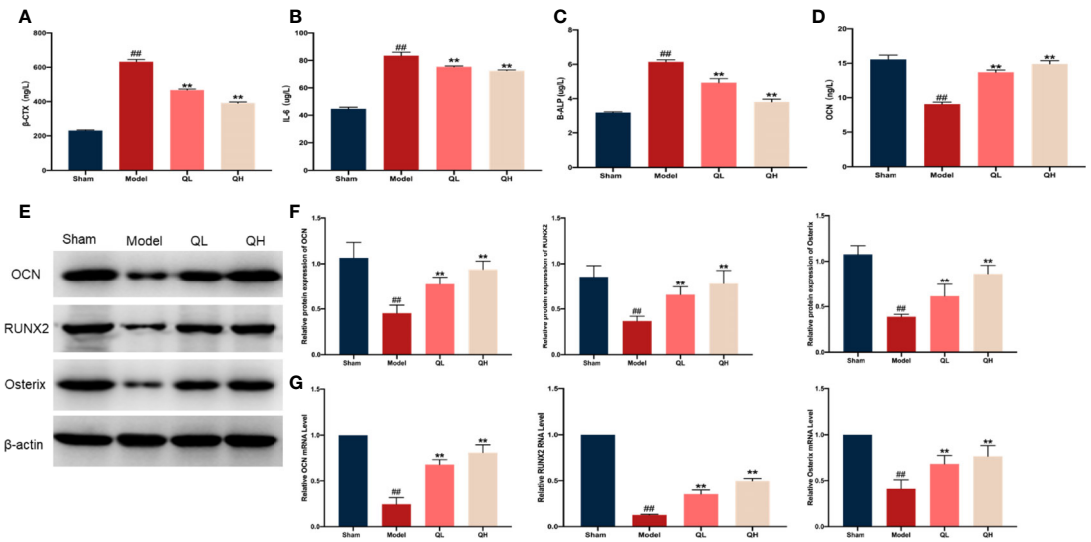

FIGURE 6 | Effects of quercetin on bone metabolism in mice that underwent orchiectomy. The serum levels of markers of bone resorption including **(A)** β-isomerized C-terminal telopeptides (β-CTX), **(B)** interleukin 6 (IL-6), **(C)** bone alkaline phosphatase (B-ALP), and **(D)** osteocalcin (OCN). **(E)** The expression of bone formation proteins in the tibia, including OCN, RUNX2, and Osterix. **(F)** Semi-quantification of OCN, RUNX2, and Osterix by Image J software. **(G)** The mRNA expression of OCN, RUNX2, and Osterix in tibia. ##p<0.01 vs. sham group; **p<0.01 vs. model group.

observed in the model group. Furthermore, the area of lipid droplets in the model group was markedly enlarged compared to that in the sham-operated group. However, hepatic steatosis was significantly attenuated, and the area of lipid droplets was smaller after quercetin intervention (**Figures 7B, C**). After orchiectomy, the serum levels of triglycerides, total cholesterol, LDL, and FFA were significantly increased in the model group (p<0.01), whereas HDL levels were decreased (p<0.01). However, following quercetin treatments, total cholesterol, triglycerides, LDL, and FFA were significantly decreased, whereas HDL was increased in the low- and high-quercetin groups (**Figures 7D–H**). The mild change in triglycerides and HDL in the low-quercetin group was not statistically significant (**Figures 7E, F**). We further examined the effects of quercetin on key proteins related to lipid metabolism, by analyzing the expression of Cebp/β and Ppar-γ. As shown in **Figure 8**, the protein levels of Cebp/β and Ppar-γ significantly decreased after 8 weeks of quercetin treatment. These results indicated that quercetin effectively alleviated hepatic steatosis and improved lipid metabolism.

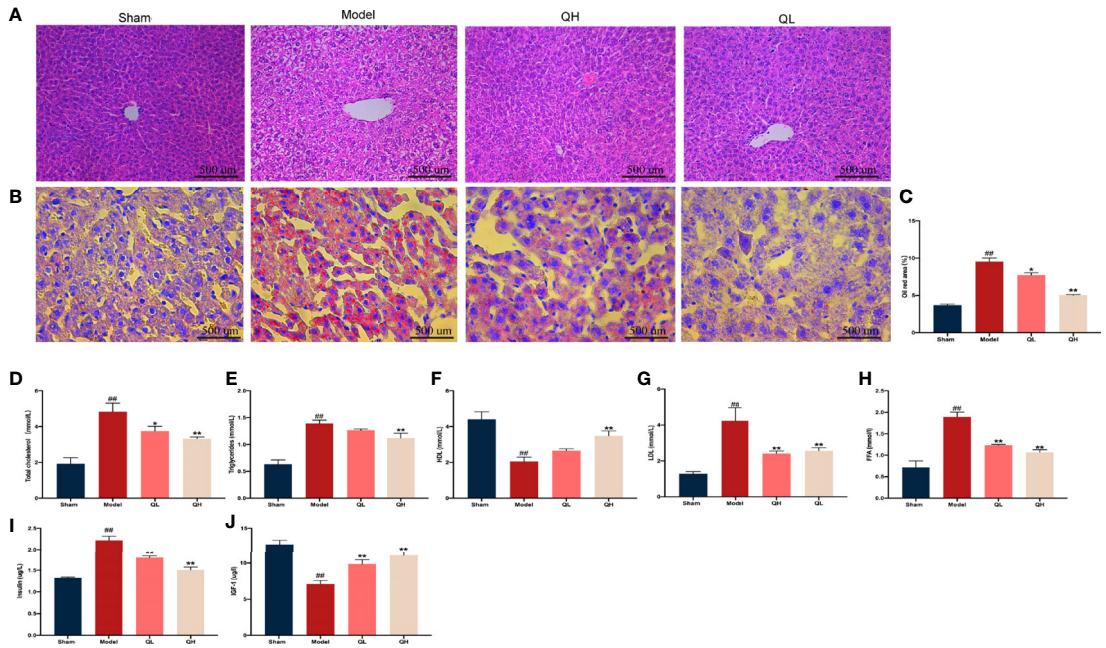

FIGURE 7 | Effects of quercetin on lipid and glucose metabolism in mice that underwent orchiectomy. **(A)** The effects of quercetin on liver tissue morphology, visualized by H&E staining. **(B)** Oil-Red O staining of the liver, and **(C)** the percentage of lipid droplet area analysis. The serum levels of markers of lipid metabolism including **(D)** total cholesterol, **(E)** triglycerides, **(F)** high-density lipoprotein (HDL), **(G)** low-density lipoprotein (LDL), and **(H)** free fatty acid (FFA). The serum levels of markers of glucose metabolism including **(I)** insulin, and **(J)** insulin-like growth factor-1 (IGF-1). ##p<0.01 vs. sham group; *p<0.05, **p<0.01 vs. model group.

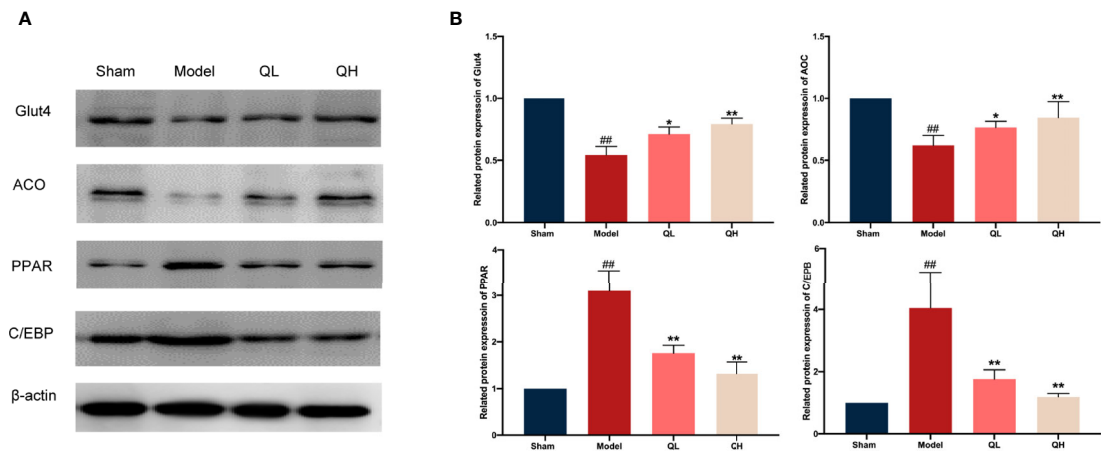

FIGURE 8 | Changes in lipid and glucose metabolism in mice that underwent orchiectomy after quercetin treatment. **(A)** Expression of lipid and glucose metabolism proteins in the liver, including Glut4, ACO, PPAR, and C/EBP. **(B)** Glut4, ACO, PPAR, and C/EBP were semi-quantified by Image J software ##p<0.01 vs. sham group; *p<0.05, **p<0.01 vs. model group.

Quercetin Improves Glucose Metabolism Upon Orchiectomy

In addition to lipid metabolism, we analyzed the corresponding glucose metabolism. After quercetin treatment, we observed a significant decrease in insulin and an increase in insulin-like growth factor-1 levels in the low- and high-quercetin groups (**Figures 7I, J**). Meanwhile, the expression of GLUT4 and ACO, which are major proteins related to glucose metabolism, as well as Cebp/β and Ppar-γ, key factors in lipid metabolism, was analyzed (**Figures 8A, B**). GLUT4 and ACO showed an increased expression upon quercetin treatment (p<0.05 for QL and p<0.01 for QH, **Figure 8B**). Protein levels of Cebp/β and

Ppar-γ significantly decreased after 8 weeks of quercetin treatment (p<0.01). These results indicated that quercetin effectively alleviated hepatic steatosis and improved both glucose and lipid metabolism.

Quercetin Modulates the GPRC6A/AMPK/mTOR Signaling Pathway

As an essential modulated regulator of metabolism, GPRC6A may play a critical role in osteoporosis. To further elucidate the possible mechanisms by which this occurs, the expression of GPRC6A in the liver and femur was analyzed. As shown in **Figure 9**, GPRC6A was broadly expressed in the liver and femur tissues, and its expression in both tissues decreased significantly after orchiectomy (p<0.01, **Figures 9A-D**). Following quercetin treatment, GPRC6A expression increased again (p<0.05 for QL and p<0.01 for QH, for both tissue types). Next, the downstream signaling of GPRC6A, including AMPK and mTOR, was examined in both the liver (**Figure 9E**) and femur (**Figure 9F**). We found that the phospho-AMPK/AMPK ratio was elevated in the low- and high-quercetin groups, whereas the phospho-mTOR/mTOR ratio was reduced. These results indicated that quercetin may promote AMPK phosphorylation and inhibit mTOR phosphorylation. Furthermore, quercetin may exert biological effects on osteoporosis with metabolic disorders and may be associated with the GPRC6A/AMPK/mTOR signaling pathway.

DISCUSSION

Among other symptoms, testosterone deficiency, due to either chronic illnesses or endocrine treatments, can result in bone mineral density (BMD) decline. Despite its beneficial effects on bone health, testosterone replacement therapy may cause other problems, including decreased sperm production and fertility, cardiovascular disease, and prostate cancer or hyperplasia. In this study we aimed to determine the bone-protective effects of quercetin in mouse model of testosterone deficiency-induced osteoporosis. In contrast to previous investigations on rats, where osteoporosis manifests at 12 weeks after orchiectomy (22), we found that it appears at 8 weeks after orchiectomy in mice. Due to testosterone deficiency, the mice that underwent orchiectomy not only exhibited decreased bone density, bone mass, and imbalance of bone metabolism, but also endocrine hormone disorders. These results are consistent with clinical presentations and may provide the foundation for subsequent studies.

The potential pharmacological effects of quercetin have been extensively explored as dietary constituents. Due to its antioxidative, anti-inflammatory, and anti-apoptotic effects, it has been clinically applied for the treatment of various diseases (11–15). In this study, we found that quercetin increased bone mass and improved bone strength in orchiectomy mice, indicating that quercetin has therapeutic effects on osteoporosis induced by testosterone deficiency. Furthermore, the effect of quercetin in musculoskeletal system has been described here for the first time. In this study,

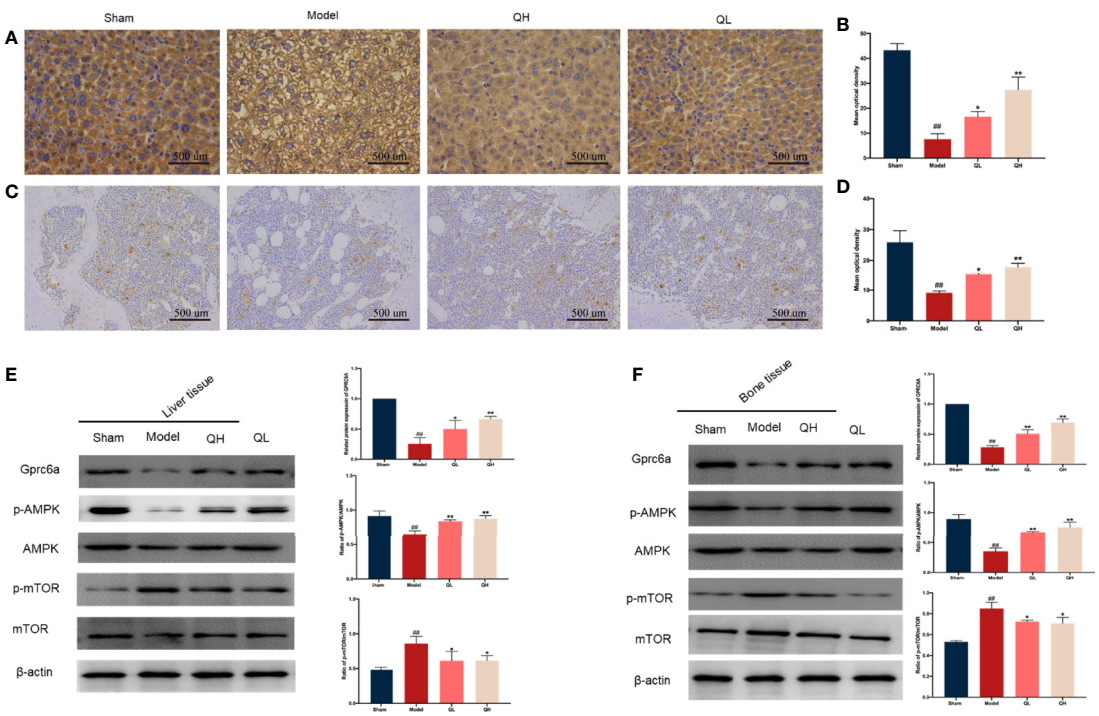

FIGURE 9 | Effects of quercetin on the GPRC6A/AMPK/mTOR signaling pathway in mice that underwent orchiectomy. Immunohistochemical staining for GPCR6A and staining quantification in liver **(A, B)** and **(C, D)**. Expression of GPCR6A in the liver **(E)** and bone **(F)** evaluated by western blotting assay (on the left) and semi-quantitative analysis (on the right). ##p<0.01 vs. sham group; *p<0.05, **p<0.01 vs. model group.

quercetin was confirmed to significantly promote histological changes by improving the cross-sectional area of the myofibers, decreasing collagen fiber area and lipid droplets in gastrocnemius muscle. In parallel, gait analysis results showed that quercetin could improve balance motion ability. These findings suggest that quercetin may have potential of reducing the fracture risk often experienced with osteoporosis.

Conventionally, testosterone affects bone mass and strength *via* its conversion to 5α-dihydrotestosterone in peripheral tissues. Then, 5α-dihydrotestosterone further promotes osteoblast proliferation and inhibits osteoblast apoptosis by interacting with the androgen receptor. When the androgen receptor signaling is blocked, the mice exhibits a series of abnormal musculoskeletal findings, including decreased bone volume and trabecular number (23). Previous studies have found that orchiectomy is often accompanied by decreased levels of testosterone and increased bone loss (24). Similarly, we found that markers for bone resorption, TRAP, β-CTX, and IL-1, were significantly elevated after orchiectomy. In addition, the correlated decrease in markers for bone resorption and the ratio of OCs/BS and N.OC/BS indicated that quercetin treatments alleviated trabecular bone loss in the distal femur after orchiectomy.

B-ALP is a ubiquitous metalloenzyme that catalyzes the hydrolysis of phosphate esters and generates an organic radical and inorganic phosphate. As a mature and active marker of osteoblasts, B-ALP is involved in bone formation and reflects osteocyte formation and activity status (25). As expected, the serum B-ALP levels increased gradually after orchiectomy. This suggests that testosterone deficiency impaired osteocyte function, and bone metabolism was in a high bone turnover state. The biochemical marker of bone turnover, OCN, principally reflects the bone formation produced by mature osteoblasts. In addition to being essential for mineralized bone matrix, OCN also stimulates testosterone biosynthesis *via* uOCN (26). Several researchers have found that $OCN^{-/-}$ mice exhibit severe hypergonadotropic hypogonadism, including small testes and impaired fertility (27). Additionally, a series of studies reported a close relationship among testosterone and OCN in patients with metabolic disorders (28–30). We found in this study that the levels of OCN and uOCN in serum decreased significantly following orchiectomy, which implies that the relationship between testosterone and OCN is not one-way but includes a network or coupling system. In the testes, 95% of testosterone is produced, with the remaining 5% secreted by the adrenal glands. Recent research has shown that the main mechanism by which quercetin increases testosterone is by promoting its synthesis in the Leydig cells (15). Notably, quercetin significantly increased the serum levels of testosterone, OCN, and uOCN after orchiectomy. On the one hand, the increase in testosterone suggests that quercetin does increase testosterone by promoting synthesis in the adrenal glands, whereas the increase in uOCN reflects, at least in part, that quercetin may also increase testosterone by promoting OCN synthesis.

As a cornerstone of treatment methods, orchiectomy has been widely applied and may be the most crucial cause of accelerated bone loss in prostate cancer (31). Previous studies have suggested that the level of serum testosterone is correlated with long-term survival rate in prostate cancer (32). Nevertheless, the decreasing serum levels of testosterone with orchiectomy were consistent with its clinical presentation after ADT, and quercetin increased testosterone levels in the serum. This may suggest that elevated serum testosterone levels might increase the possibility of recurrence in patients with prostate cancer. The importance of measuring changes in testosterone levels in patients undergoing ADT is undoubtedly important. However, a recent systematic review on the relationship between testosterone and prostate cancer reported that low serum levels of testosterone might enhance the risk of prostate cancer (33). These contradictions might have multiple explanations, including the fact that serum testosterone is not equivalent to intraprostatic testosterone, the indeterminate effects of androgen receptors, and the different testosterone measurement sites between serum and intraprostatic region (34). Furthermore, the contraindications for testosterone replacement in prostate cancer have been challenged. Several studies have suggested that the risk of exogenous testosterone replacement appears to be small and may reduce biochemical recurrence in prostate cancer following a prostatectomy (35–38). In addition, various studies have directly confirmed that intervention with 75–150 mg/kg of quercetin may inhibit tumor growth in mice with prostate cancer (39–42). This finding indicates that there is no additional risk of prostate cancer after quercetin treatment. Overall, based on the antitumor efficacy, quercetin could improve bone characteristics in osteoporosis due to testosterone deficiency.

As a main anabolic steroid hormone, testosterone exerts biological effects by regulating the energy balance to maintain glucose and lipid synthesis (43). Previous studies have shown that testosterone deficiency significantly alters glucose and lipid metabolism. In a prospective study of 177 patients who received ADT treatment for one year, total testosterone level decreased by 97.0%, but total cholesterol, LDL, and triglyceride levels increased by 10.6, 14.3, and 16.2%, respectively (44). In addition to alterations in triglyceride, cholesterol, LDL, and HDL levels, a decrease in FFA levels was also observed in our study. Consistently with previously reported data (45, 46), the elevation of circulating insulin level and lower serum level of IGF-1 indicates that orchiectomy induced insulin resistance. Testosterone deficiency often accounts for negative effects on lipid and glucose metabolism, and some bone and skeletal metabolism comorbidities may be associated with these changes. Abnormal bone metabolism can cause disturbed glucose metabolism by reducing the advanced glycation end product (AGE) (47). Aung and Lee found that inhibiting AGE and regulating glucose homeostasis may promote osteogenic differentiation of bone marrow mesenchymal stem cells (BMSCs) and improve bone metabolism and mass (47, 48). A recent study also found that orchiectomy could lead to lipid metabolism disorder, and decreased bone characteristics were improved after testosterone supplementation to decrease blood lipid levels. These findings show that glucose and lipid metabolic disturbances are risk factors for osteoporosis due to testosterone deficiency.

Consistently with computer simulations (19), except for increasing protein levels of molecules involved in glucose uptake (GLUT4) and decreasing proteins involved in lipid production (PPAR, C/EBP), quercetin significantly promoted the expression

level of GPRC6A in the liver. GPRC6A is activated by OCN and testosterone and performs an essential function in the modulation of testosterone and energy metabolism (18). Due to lack of OCN and testosterone, decreased expression of GPRC6A was simultaneously detected in orchiectomy mice. After knockout of GPRC6A in the hepatocytes, male mice exhibited several metabolic abnormalities, including abnormal glucose levels and increased serum FFA and cholesterol levels (49). Many of our findings are consistent with this study, which may indicate that GPRC6A is a potential therapeutic target for metabolic disorders in orchiectomy mice. To date, the downstream targets of quercetin-GPRC6A have not yet been identified. However, with intervention of quercetin, we found that the phospho-mTOR/mTOR ratio decreased gradually as the phospho-AMPK/AMPK ratio increased. The serine/threonine kinase, AMPK, that is phosphorylated in response to a decrease in AMP/ATP ratio, is an essential regulatory factor in glucose and lipid metabolism. Glut 1 and Glut 4 are the major insulin-sensitive glucose transporters, and they have been demonstrated to be stimulated by AMPK and promote glucose transfer into the cell (50). In addition, phosphorylated AMPK alleviates endoplasmic reticulum stress and increases hepatic autophagy to reduce the levels of hepatic cholesterol and triglycerides by inhibiting the phosphorylation levels of mTOR (51). These results indicate that quercetin regulates glucose metabolism and inhibits lipid metabolism *via* the GPRC6A/AMPK/mTOR signaling pathway.

Furthermore, PPAR and C/EBP were obviously downregulated, whereas RUNX2 and Osterix were markedly upregulated after quercetin treatment. Phosphorylated AMPK could significantly increase osteogenic differentiation by promoting RUNX2 expression and inhibiting PPAR expression, which is an indicator of differentiation from BMSCs to osteoblasts and adipocytes, respectively (52, 53). These findings initiated our further analysis of whether quercetin could regulate BMSC differentiation by regulating the GPRC6A/AMPK/mTOR signaling pathway. We found that GPRC6A was expressed in the bone tissues, and its expression decreased after orchiectomy. Furthermore, similar to its expression in the liver, changes in p-AMPK/AMPK and p-mTOR/mTOR ratios suggested that quercetin could inhibit adipogenic differentiation and promote osteogenic differentiation by directly regulating the GPRC6A/AMPK/mTOR signaling pathway. We found that GPRC6A was expressed in the bone tissues, and its expression decreased after orchiectomy. Furthermore, similar to its expression in the liver, changes in phospho-AMPK/AMPK and phospho-mTOR/mTOR ratios suggested that quercetin could inhibit adipogenic differentiation and promote osteogenic differentiation by directly regulating the GPRC6A/AMPK/mTOR signaling pathway.

CONCLUSION

In summary, we first verified the biological function of quercetin in testosterone deficiency-induced osteoporosis. We showed that 75 mg/kg/d and 150 mg/kg/d of quercetin partially improved bone quality through modulation of bone metabolism and bone microarchitecture in mice that had undergone orchiectomy. The beneficial effects of quercetin might be related to its ability to regulate glucose and lipid metabolism *via* the GPCR6A/AMPK/mTOR signaling pathway. These findings may act as a foundation for the further examination of quercetin as great potential drug for osteoporosis induced by testosterone deficiency.

DATA AVAILABILITY STATEMENT

The raw data supporting the conclusions of this article will be made available by the authors, without undue reservation. (NO. ACU170804).

ETHICS STATEMENT

The animal study was reviewed and approved by Experimental Animal Center of Nanjing University of Chinese Medicine.

AUTHOR CONTRIBUTIONS

JS and WD conceived and designed the experiment, analyzed the data and interpreted the results and developed the manuscript. YP, PT, CW, XL, and QH collaborated in the pharmacological experiments. YM and YG supervised the work and proofread the manuscript. All authors contributed to the article and approved the submitted version.

FUNDING

This work was supported by National Natural Science Foundation of China (No.81904229, 82074458, 81973881), Traditional Chinese and Western Medicine Clinical Medicine Brand Construction Project of Jiangsu Higher Education Institutions (Phase II)(2020PPZXL261), 2021 Future plans of Shanghai Municipal Hospital of Traditional Chinese Medicine (No.WLJH2021ZY-ZLZX001/GZS001/MZY034) and was also supported by the Postgraduate Research and Practice Innovation Program of Jiangsu Province (KYCX21_1646).

REFERENCES

1. Halpern JA, Brannigan RE. Testosterone Deficiency. *JAMA* (2019) 322:1116. doi: 10.1001/jama.2019.9290
2. Travison TG, Vesper HW, Orwoll E, Wu F, Kaufman JM, Wang Y, et al. Harmonized Reference Ranges for Circulating Testosterone Levels in Men of Four Cohort Studies in the United States and Europe. *J Clin Endocrinol Metab* (2017) 102:1161–73. doi: 10.1210/jc.2016-2935
3. Feldman HA, Longcope C, Derby CA, Johannes CB, Araujo AB, Coviello AD, et al. Age Trends in the Level of Serum Testosterone and Other Hormones in Middle-Aged Men: Longitudinal Results From the Massachusetts Male Aging Study. *J Clin Endocrinol Metab* (2002) 87:589–98. doi: 10.1210/jcem.87.2.8201
4. Kim DK, Lee HS, Park JY, Kim JW, Ahn HK, Ha JS, et al. Androgen-Deprivation Therapy and the Risk of Newly Developed Fractures in Patients With Prostate Cancer: A Nationwide Cohort Study in Korea. *Sci Rep* (2021) 11:10057. doi: 10.1038/s41598-021-89589-3

5. Qaseem A, Horwitch CA, Vijan S, Etxeandia-Ikobaltzeta I, Kansagara D, Forciea MA, et al. Testosterone Treatment in Adult Men With Age-Related Low Testosterone: A Clinical Guideline From the American College of Physicians. *Ann Intern Med* (2020) 172:126–33. doi: 10.7326/M19-0882
6. Snyder PJ, Bhasin S, Cunningham GR, Matsumoto AM, Stephens-Shields AJ, Cauley JA, et al. Lessons From the Testosterone Trials. *Endocr Rev* (2018) 39:369–86. doi: 10.1210/er.2017-00234
7. Ye J, Zhai X, Yang J, Zhu Z. Association Between Serum Testosterone Levels and Body Composition Among Men 20–59 Years of Age. *Int J Endocrinol* (2021) 2021:7523996. doi: 10.1155/2021/7523996
8. Meier C, Nguyen TV, Handelsman DJ, Schindler C, Kushnir MM, Rockwood AL, et al. Endogenous Sex Hormones and Incident Fracture Risk in Older Men: The Dubbo Osteoporosis Epidemiology Study. *Arch Intern Med* (2008) 168:47–54. doi: 10.1001/archinternmed.2007.2
9. Harman SM. Testosterone in Older Men After the Institute of Medicine Report: Where Do We Go From Here? *Climacteric* (2005) 8:124–35. doi: 10.1080/13697130500118001
10. Hosseini A, Razavi BM, Banach M, Hosseinzadeh H. Quercetin and Metabolic Syndrome: A Review. *Phytother Res* (2021) 35:5352–64. doi: 10.1002/ptr.7144
11. Li Y, Yao J, Han C, Yang J, Chaudhry MT, Wang S, et al. Quercetin, Inflammation and Immunity. *Nutrients* (2016) 8:167. doi: 10.3390/nu8030167
12. Vakili S, Zal F, Mostafavi-Pour Z, Savardashtaki A, Koohpeyma F. Quercetin and Vitamin E Alleviate Ovariectomy-Induced Osteoporosis by Modulating Autophagy and Apoptosis in Rat Bone Cells. *J Cell Physiol* (2021) 236:3495–509. doi: 10.1002/jcp.30087
13. Ojo OO, Olorunsogo OO. Quercetin and Vitamin E Attenuate Diabetes-Induced Testicular Anomaly in Wistar Rats *via* the Mitochondrial-Mediated Apoptotic Pathway. *Andrologia* (2021) 53:e14185. doi: 10.1111/and.14185
14. Wang N, Wang L, Yang J, Wang Z, Cheng L. Quercetin Promotes Osteogenic Differentiation and Antioxidant Responses of Mouse Bone Mesenchymal Stem Cells Through Activation of the AMPK/SIRT1 Signaling Pathway. *Phytother Res* (2021). doi: 10.1002/ptr.7010
15. Wang D, Li Y, Zhai QQ, Zhu YF, Liu BY, Xu Y. Quercetin Ameliorates Testosterone Secretion Disorder by Inhibiting Endoplasmic Reticulum Stress Through the miR-1306-5p/HSD17B7 Axis in Diabetic Rats. *Bosn J Basic Med Sci* (2021). doi: 10.17305/bjbms.2021.6299
16. Pi M, Kapoor K, Ye R, Nishimoto SK, Smith JC, Baudry J, et al. Evidence for Osteocalcin Binding and Activation of GPRC6A in β-Cells. *Endocrinology* (2016) 157:1866–80. doi: 10.1210/en.2015-2010
17. Pi M, Chen L, Huang MZ, Zhu W, Ringhofer B, Luo J, et al. GPRC6A Null Mice Exhibit Osteopenia, Feminization and Metabolic Syndrome. *PloS One* (2008) 3:e3858. doi: 10.1371/journal.pone.0003858
18. Pi M, Nishimoto SK, Quarles LD. GPRC6A: Jack of All Metabolism (or Master of None). *Mol Metab* (2017) 6:185–93. doi: 10.1016/j.molmet.2016.12.006
19. D'Arrigo G, Gianquinto E, Rossetti G, Cruciani G, Lorenzetti S, Spyrakis F. Binding of Androgen- and Estrogen-Like Flavonoids to Their Cognate (Non) nuclear Receptors: A Comparison by Computational Prediction. *Molecules* (2021) 26:1613. doi: 10.3390/molecules26061613
20. Straub B, Müller M, Schrader M, Heicappell R, Miller K. Osteoporosis and Mild Metabolic Acidosis in the Rat After Orchiectomy and Their Prevention: Should Prophylactic Therapy be Administered to Patients With Androgen Deprivation? *J Urol* (2001) 165:1783–9. doi: 10.1016/S0022-5347(05)66414-2
21. Wang L, Zheng S, Huang G, Sun J, Pan Y, Si Y, et al. Osthole-Loaded N-Octyl-O-Sulfonyl Chitosan Micelles (NSC-OST) Inhibits RANKL-Induced Osteoclastogenesis and Prevents Ovariectomy-Induced Bone Loss in Rats. *J Cell Mol Med* (2020) 24:4105–17. doi: 10.1111/jcmm.15064
22. Mohamad NV, Che Zulkepli MAA, May Theseira K, Zulkifli N, Shahrom NQ, Ridzuan NAM, et al. Establishing an Animal Model of Secondary Osteoporosis by Using a Gonadotropin-Releasing Hormone Agonist. *Int J Med Sci* (2018) 15:300–8. doi: 10.7150/ijms.22732
23. Ucer S, Iyer S, Bartell SM, Martin-Millan M, Han L, Kim HN, et al. The Effects of Androgens on Murine Cortical Bone Do Not Require AR or Erα Signaling in Osteoblasts and Osteoclasts. *J Bone Miner Res* (2015) 30:1138–49. doi: 10.1002/jbmr.2485
24. Mohamad NV, Soelaiman IN, Chin KY. A Concise Review of Testosterone and Bone Health. *Clin Interv Aging* (2016) 11:1317–24. doi: 10.2147/CIA.S115472
25. Migliorini F, Maffulli N, Spiezia F, Tingart M, Maria PG, Riccardo G. Biomarkers as Therapy Monitoring for Postmenopausal Osteoporosis: A Systematic Review. *J Orthop Surg Res* (2021) 16:318. doi: 10.1186/s13018-021-02474-7
26. Barbonetti A, D'Andrea S, Samavat J, Martorella A, Felzani G, Francavilla S, et al. Can the Positive Association of Osteocalcin With Testosterone Be Unmasked When the Preeminent Hypothalamic–Pituitary Regulation of Testosterone Production Is Impaired? The Model of Spinal Cord Injury. *J Endocrinol Invest* (2019) 42:167–73. doi: 10.1007/s40618-018-0897-x
27. Oury F, Sumara G, Sumara O, Ferron M, Chang H, Smith CE, et al. Endocrine Regulation of Male Fertility by the Skeleton. *Cell* (2011) 144:796–809. doi: 10.1016/j.cell.2011.02.004
28. Kirmani S, Atkinson EJ, Melton LJIII, Riggs BL, Amin S, Khosla S. Relationship of Testosterone and Osteocalcin Levels During Growth. *J Bone Miner Res* (2011) 26:2212–6. doi: 10.1002/jbmr.421
29. Jürimäe J, Lätt E, Remmel L, Purge P, Tillmann V. Longitudinal Changes in Bone-Testis Axis and Their Associations With Insulin Resistance in 11- to 12-Year-Old Boys. *Bone* (2018) 108:115–20. doi: 10.1016/j.bone.2018.01.005
30. Hannemann A, Breer S, Wallaschofski H, Nauck M, Baumeister SE, Barvencik F, et al. Osteocalcin Is Associated With Testosterone in the General Population and Selected Patients With Bone Disorders. *Andrology* (2013) 1:469–74. doi: 10.1111/j.2047-2927.2012.00044.x
31. Poulsen MH, Frost M, Abrahamsen B, Gerke O, Walter S, Lund L. Osteoporosis and Prostate Cancer; A 24-Month Prospective Observational Study During Androgen Deprivation Therapy. *Scand J Urol* (2019) 53:34–9. doi: 10.1080/21681805.2019.1570328
32. Lumbiganon S, Patcharatrakul S, Khongcharoensombat W, Sangkum P. Pre- and Post-Radical Prostatectomy Testosterone Levels in Prostate Cancer Patients. *Int J Impot Res* (2019) 31:145–9. doi: 10.1038/s41443-019-0116-0
33. Klap J, Schmid M, Loughlin KR. The Relationship Between Total Testosterone Levels and Prostate Cancer: A Review of the Continuing Controversy. *J Urol* (2015) 193:403–13. doi: 10.1016/j.juro.2014.07.123
34. Loughlin KR. The Testosterone Conundrum: The Putative Relationship Between Testosterone Levels and Prostate Cancer. *Urol Oncol* (2016) 34:482.e1–4. doi: 10.1016/j.urolonc.2016.05.023
35. Sarkar R, Parsons JK, Einck JP, Mundt AJ, Kader AK, Kane CJ, et al. Impact of Testosterone Replacement Therapy After Radical Prostatectomy on Prostate Cancer Outcomes. *JCO* (2019) 37:100. doi: 10.1200/JCO.2019.37.7_suppl.100
36. TE A, Huynh LM, Towe MM, See K, El Khatib F, Yafi FA. Is There a Role for Testosterone Replacement Therapy in Reducing Biochemical Recurrence Following Radical Prostatectomy? *JCO* (2019) 37:5085. doi: 10.1200/JCO.2019.37.15_suppl.5085
37. Santella C, Renoux C, Yin H, Yu OHY, Azoulay L. Testosterone Replacement Therapy and the Risk of Prostate Cancer in Men With Late-Onset Hypogonadism. *Am J Epidemiol* (2019) 188:1666–73. doi: 10.1093/aje/kwz138
38. Ahlering TE, My Huynh L, Towe M, See K, Tran J, Osann K, et al. Testosterone Replacement Therapy Reduces Biochemical Recurrence After Radical Prostatectomy. *BJU Int* (2020) 126:91–6. doi: 10.1111/bju.15042
39. Sun S, Gong F, Liu P, Miao Q. Metformin Combined With Quercetin Synergistically Repressed Prostate Cancer Cells *via* Inhibition of VEGF/PI3K/Akt Signaling Pathway. *Gene* (2018) 664:50–7. doi: 10.1016/j.gene.2018.04.045
40. Singh CK, Chhabra G, Ndiaye MA, Siddiqui IA, Panackal JE, Mintie CA, et al. Quercetin-Resveratrol Combination for Prostate Cancer Management in TRAMP Mice. *Cancers (Basel)* (2020) 12:E2141. doi: 10.3390/cancers12082141
41. Yang F, Jiang X, Song L, Wang H, Mei Z, Xu Z, et al. Quercetin Inhibits Angiogenesis Through Thrombospondin-1 Upregulation to Antagonize Human Prostate Cancer PC-3 Cell Growth *In Vitro* and *In Vivo*. *Oncol Rep* (2016) 35:1602–10. doi: 10.3892/or.2015.4481
42. Yang F, Song L, Wang H, Wang J, Xu Z, Xing N. Combination of Quercetin and 2-Methoxyestradiol Enhances Inhibition of Human Prostate Cancer LNCaP and PC-3 Cells Xenograft Tumor Growth. *PloS One* (2015) 10:e0128277. doi: 10.1371/journal.pone.0128277
43. Troncoso MF, Pavez M, Wilson C, Lagos D, Duran J, Ramos S, et al. Testosterone Activates Glucose Metabolism Through AMPK and Androgen Signaling in Cardiomyocyte Hypertrophy. *Biol Res* (2021) 54:3. doi: 10.1186/s40659-021-00328-4

44. Mitsuzuka K, Kyan A, Sato T, Orikasa K, Miyazato M, Aoki H, et al. Influence of 1 Year of Androgen Deprivation Therapy on Lipid and Glucose Metabolism and Fat Accumulation in Japanese Patients With Prostate Cancer. *Prostate Cancer Prostatic Dis* (2016) 19:57–62. doi: 10.1038/pcan.2015.50
45. Yawson EO, Akinola OB. Hippocampal Cellular Changes in Androgen Deprived Insulin Resistant Rats. *Metab Brain Dis* (2021) 36:1037–48. doi: 10.1007/s11011-021-00678-8
46. Doulamis IP, Tzani A, Konstantopoulos P, Daskalopoulou A, Spinos T, Bletsa E, et al. Experimental Hypogonadism: Insulin Resistance, Biochemical Changes and Effect of Testosterone Substitution. *J Basic Clin Physiol Pharmacol* (2019) 30. doi: 10.1515/jbcpp-2018-0118
47. Aung M, Amin S, Gulraiz A, Gandhi FR, Pena Escobar JAP, Malik BH. The Future of Metformin in the Prevention of Diabetes-Related Osteoporosis. *Cureus* (2020) 12:e10412. doi: 10.7759/cureus.10412
48. Lee SY, Long F. Notch Signaling Suppresses Glucose Metabolism in Mesenchymal Progenitors to Restrict Osteoblast Differentiation. *J Clin Invest* (2018) 128:5573–86. doi: 10.1172/JCI96221
49. Pi M, Xu F, Ye R, Nishimoto SK, Williams RW, Lu L, et al. Role of GPRC6A in Regulating Hepatic Energy Metabolism in Mice. *Sci Rep* (2020) 10:7216. doi: 10.1038/s41598-020-64384-8
50. Talagavadi V, Rapisarda P, Galvano F, Pelicci P, Giorgio M. Cyanidin-3-O-β-Glucoside and Protocatechuic Acid Activate AMPK/mTOR/S6K Pathway and Improve Glucose Homeostasis in Mice. *J Funct Foods* (2016) 21:338–48. doi: 10.1016/j.jff.2015.12.007
51. Rao X, Wang Y. Apolipoprotein A-I Improves Hepatic Autophagy Through the AMPK Pathway. *Biochimie* (2019) 165:210–8. doi: 10.1016/j.biochi.2019.08.001
52. Lee S, Le NH, Kang D. Melatonin Alleviates Oxidative Stress-Inhibited Osteogenesis of Human Bone Marrow-Derived Mesenchymal Stem Cells Through AMPK Activation. *Int J Med Sci* (2018) 15:1083–91. doi: 10.7150/ijms.26314
53. Gu H, Huang Z, Zhou K, Chen G, Bian C, Xu J, et al. Expression Profile Analysis of Long Non-Coding RNA in OVX Models-Derived BMSCs for Postmenopausal Osteoporosis by RNA Sequencing and Bioinformatics. *Front Cell Dev Biol* (2021) 9:719851. doi: 10.3389/fcell.2021.719851

Conflict of Interest: The authors declare that the research was conducted in the absence of any commercial or financial relationships that could be construed as a potential conflict of interest.

Publisher's Note: All claims expressed in this article are solely those of the authors and do not necessarily represent those of their affiliated organizations, or those of the publisher, the editors and the reviewers. Any product that may be evaluated in this article, or claim that may be made by its manufacturer, is not guaranteed or endorsed by the publisher.

frontiers | Frontiers in Endocrinology

ORIGINAL RESEARCH
published: 03 May 2022
doi: 10.3389/fendo.2022.878963

Zuo-Gui-Wan Aqueous Extract Ameliorates Glucocorticoid-Induced Spinal Osteoporosis of Rats by Regulating let-7f and Autophagy

Gengyang Shen[1,2,3†], Qi Shang[2,4†], Zhida Zhang[1,2†], Wenhua Zhao[2,4], Honglin Chen[2,4], Ibrayinjan Mijiti[5], Guifeng Chen[2,4], Xiang Yu[1,2], Fuyong Yu[2,4], Peng Zhang[2,4], Jiahui He[2,4], Xuelai Zhang[1,2], Jingjing Tang[1,2], Jianchao Cui[1,2], De Liang[1,2], Lingfeng Zeng[6], Hui Ren[1,2*] and Xiaobing Jiang[1,2*]*

[1] Department of Spinal Surgery, The First Affiliated Hospital of Guangzhou University of Chinese Medicine, Guangzhou, China, [2] Lingnan Medical Research Center of Guangzhou University of Chinese Medicine, Guangzhou, China, [3] Department of Spinal Surgery, Nanshan Hospital, The First Affiliated Hospital of Guangzhou University of Chinese Medicine, Shenzhen Nanshan Hospital of Chinese Medicine, Guangzhou, China, [4] The First Clinical College, Guangzhou University of Chinese Medicine, Guangzhou, China, [5] Department of Spinal Surgery, The First People's Hospital of Kashgar, Kashgar, China, [6] Department of Orthopedics, The 2nd Affiliated Hospital of Guangzhou University of Chinese Medicine, Guangzhou, China

Objective: This study proposes to explore the protective effect of Zuo-Gui-Wan (ZGW) aqueous extract on spinal glucocorticoid-induced osteoporosis (GIOP) *in vivo* and *in vitro*, and the underlying mechanisms of ZGW in GIOP and osteogenic differentiation of bone marrow-derived mesenchymal stem cells (BMSCs) were conducted.

Methods: *In vivo*, SD rats were randomly divided into three groups: control group (CON), dexamethasone (DEXM) group, and ZGW group, which were given vehicle, DEXM injection, and ZGW intragastric administration at the same time. Vertebral bone microarchitecture, biomechanics, histomorphology, serum AKP activity, and the autophagosome of osteoblasts were examined. The mRNA expressions of let-7f, autophagy-associated genes (mTORC1, Beclin-1, ATG12, ATG5, and LC3), Runx2, and CTSK were examined. *In vitro*, the let-7f overexpression/silencing vector was constructed and transfected to evaluate the osteogenic differentiation of BMSCs. Western blot was employed to detect the expression of autophagy-associated proteins (ULK2, ATG5, ATG12, Beclin-1, LC3).

Results: *In vivo*, ZGW promoted the bone quantity, quality, and strength; alleviated histological damage; increased the serum AKP activity; and reduced the autophagosome number in osteoblasts. Moreover, ZGW increased the let-7f, mTORC1, and Runx2 mRNA expressions and reduced the Beclin-1, ATG12, ATG5, LC3, and CTSK mRNA expressions. *In vitro*, bioinformatics prediction and dual luciferase reporter gene assay verified that let-7f targeted the binding to ULK2 and negatively regulated the ULK2 expression. Furthermore, by let-7f overexpression/silencing, ZGW may promote

OPEN ACCESS

Edited by:
Bo Liu,
Guangdong Provincial Hospital of Chinese Medicine, China

Reviewed by:
Yikai Li,
Southern Medical University, China
He Zhao,
Tsinghua University, China
Dezhi Tang,
Shanghai University of Traditional Chinese Medicine, China

***Correspondence:**
Xiaobing Jiang
spinedrjxb@sina.com
Hui Ren
renhuispine@163.com
Lingfeng Zeng
1347301175@qq.com

†These authors have contributed equally to this work

Specialty section:
This article was submitted to Bone Research, a section of the journal Frontiers in Endocrinology

Received: *18 February 2022*
Accepted: *11 March 2022*
Published: *03 May 2022*

Citation:
Shen G, Shang Q, Zhang Z, Zhao W, Chen H, Mijiti I, Chen G, Yu X, Yu F, Zhang P, He J, Zhang X, Tang J, Cui J, Liang D, Zeng L, Ren H and Jiang X (2022) Zuo-Gui-Wan Aqueous Extract Ameliorates Glucocorticoid-Induced Spinal Osteoporosis of Rats by Regulating let-7f and Autophagy. Front. Endocrinol. 13:878963. doi: 10.3389/fendo.2022.878963

osteoblast differentiation of BMSCs by regulating let-7f and autophagy as evidenced by Western blot (ULK2, ATG5, ATG12, Beclin-1, LC3).

Conclusions: ZGW may ameliorate GC-induced spinal osteoporosis by promoting osteoblast differentiation of BMSCs by activation of let-7f and suppression of autophagy.

Keywords: ZGW aqueous extract, GIOP, let-7f, autophagy, Chinese medicine

INTRODUCTION

Glucocorticoid-induced osteoporosis (GIOP) is the most common secondary osteoporosis, which is characterized by decreased bone mass and deteriorated bone microarchitecture and affects as many as 50% of patients who receive therapy with chronic glucocorticoid (GCs), the commonly used anti-inflammatory drugs (1). More and more pharmacological treatments, including calcium, vitamin D, bisphosphonates, teriparatide, and denosumab, have been recommended for treating osteoporosis, whereas GIOP is still clinically not well treated due to the side effects and "drug holidays" of existing management (1, 2). Therefore, a new drug therapy against GIOP is still supposed to be developed.

Traditional Chinese medicine (TCM) has fought against bone metabolism-associated diseases for more than 1,000 years and has accumulated a wealth of herbal compounds and clinical practice experience (3–5). As a well-known TCM for treating GIOP, Zuo-Gui-Wan (ZGW) comprises eight herbal medicines: Radix Rehmanniae, Semen Cuscutae, Radix Achyranthis Bidentatae, Carapax et Plastrum Testudinis, Cornu Cervi Pantotrichum, Rhizoma Dioscoreae, Fructus Corni, and Fructus Lycii. Recent research has found that ZGW can treat ovariectomy-induced osteopenia by regulating the Th17/Treg or RANKL/OPG signal transduction pathway (6–9). Moreover, our previous studies have demonstrated that extracts from plastrum testudinis, one of the major active ingredients of ZGW, may ameliorate GIOP *via* regulating OPG, Runx2, and CTSK expressions (10, 11). However, the pharmacological effect and mechanism of ZGW treating GIOP are still uncomprehensive and unclear.

MicroRNAs (miRNAs) consist of 19–25 nucleotides and regulate gene expressions at the posttranscriptional level by binding to 3′UTRs of target mRNAs (12). Accumulating evidence points to an intimate connection between miRNAs and bone metabolism, keeping balanced by osteoblastic bone formation and osteoclastic bone resorption (12, 13). However, the studies about the action mechanisms of miRNAs on GIOP are still limited. Our previous study has demonstrated that miRNA let-7f mimics could ameliorate GIOP (14), but the underlying mechanisms are still not elucidated. Therefore, the alterations in miRNA expression levels are associated with the pathogenesis of GIOP, but the underlying signaling mechanisms are still not well characterized and further studies are required.

Autophagy is characterized by the formation of autophagosomes by cell membrane encapsulation of part of the cytoplasm and organelles and fusion with lysosomes to form autophagolysosomes to degrade the encapsulated contents to achieve cellular metabolic homeostasis (15). Intriguingly, autophagy is of vital importance in bone metabolism involving osteoblast-dominated bone formation, osteoclast-dominated bone resorption, and osteocyte-mediated bone matrix formation (13, 15). Defective autophagy in osteoblasts resulted in endoplasmic reticulum stress and induced significant bone loss, and GC treatment led to a decrease of LC3 (typical markers of autophagy)-positive osteoblasts (16, 17). In addition, activation of autophagy by Beclin-1 overexpression induced osteoclast differentiation and conditional ablation of ATG7 and treatment with chloroquine, an autophagy inhibitor, ameliorated GC-induced bone loss *via* inhibiting osteoclastogenesis (18). Besides, recent studies indicated that GC can induce bone fragility and reduce osteocyte numbers by suppressing autophagy (19). Therefore, the maladjustment of autophagy may have a relationship with the occurrence and progression of GIOP, but related studies are still insufficient.

In the present study, we provide evidence that ZGW aqueous extract may ameliorate GIOP *via* targeting let-7f and autophagy-associated genes (mTORC1, Beclin-1, ATG12, ATG5, and LC3). There was a possibility that both let-7f and autophagy might be involved in GIOP and were utilized as the therapeutic targets for ZGW aqueous extract in experimental GIOP rats.

MATERIALS AND METHODS

Ethical Approval

The approvals of the animals and experimental procedures obtained access to the Ethics Committee of the First Affiliated Hospital of Guangzhou University of Chinese Medicine (GZUCM) (approval number: 20130425). Rats were fed in specific pathogen-free standard conditions which conform to the Guide for the Care and Use of Laboratory Animals, published by Institute of Laboratory Animal Resources (U.S.).

ZGW Preparation

ZGW was purchased from the Beijing Tongrentang Pharmaceutical Factory (State Food and Drug Administration approval number: Z11020735). It comprised eight herbal medicines: Radix Rehmanniae (24 g), Semen Cuscutae (12 g), Radix Achyranthis Bidentatae (9 g), Carapax et Plastrum Testudinis (12 g), Cornu Cervi Pantotrichum (12g), Rhizoma Dioscoreae (12 g), Fructus Corni (12 g), and Fructus Lycii (12 g). Before the experiment, the drug was dissolved in normal saline, and a magnetic stirrer was stirred to help in dissolving. After dissolution, it was used for the animal experiment. For the

cellexperiment, ZGW solutions were filtered and sterilized at a 0.22-μm pore size for later use.

Animals and Drug Administration

Three-month-old female Sprague-Dawley rats (n = 54) were obtained from the animal experiment center of Southern Medical University (Guangzhou, China), housed in the First Affiliated Hospital of GZUCM (SYXK [Yue] 2018-0092). The weight of rats at baseline was 220 ± 30 g. During the entire experiment, the rats were provided with food and water adequately.

After 1 week of adaptive feeding, the rats were randomly divided into three groups: the control group (CON) received vehicle intervention to eliminate systematic deviations caused by intervention factors; the dexamethasone (DEXA) group received subcutaneous injection of dexamethasone 0.6 mg/kg body weight twice a week for 3 consecutive months; and the ZGW group (ZGW) received oral administration of ZGW (1.62 g/kg), once a day for 3 consecutive months. The dose selection of ZGW was based on the recommended daily dose for humans (18 g/kg), and the equivalent conversion between animals and humans was based on the body surface area. This method of calculating the rat oral administration dose is similar to previous studies (9, 20).

Sample Preparation

Rats in the CON, DEXA, and ZGW groups underwent euthanasia for the next experimental analysis at the end of the fourth week (M1, N = 6/group), eighth week (M2, N = 6/group), and twelfth week (M3, N = 6/group). Lumbar 2 (L2) specimens were separated for microcomputed tomography (micro-CT) and biomechanical analysis. L4 specimens were fixed with 4% paraformaldehyde for the next HE staining. Before assessing the AKP activity, blood samples were collected, centrifuged for serum, and stored at -80°C. Transmission electron microscopy was employed to detect autophagolysosomes from osteoblast L5 specimens. L6 specimens were stored at -80°C for real-time qPCR.

Bone Microarchitecture

The software (μCT80 Evaluation Program v. 6.5-1; Scanco Medical, Brüttisellen, Switzerland) provided by the micro-CT system was employed to quantify the three-dimensional image and parameters of the L2 vertebral bodies, which was similar to previous studies (21, 22). The scanning conditions were 55 kV and 80 μA, and the spatial resolution was 14 μm. Vertebral cancellous bone was selected as the volume of interest. The microstructural parameters of cancellous bone were analyzed using micro-CT analysis software to determine the relative bone volume (BV/TV, %), structural model index (SMI), trabecular number (Tb. N), thickness (Tb. Th), and separation (Tb.Sp), and volumetric bone mineral density (vBMD). Three-dimensional images are obtained by reconstruction analysis.

Bone Biomechanics Analysis

A material testing machine (ElectroPuls E1000 Testing System; Instron Corp., Norwood, MA) was employed for bone biomechanics analysis. Both end plates of vertebral bodies and their appendages were excised to form a central cylinder with parallel planes at both ends. The vertebrae were then examined along the longitudinal axis in this machine at a speed of 1 mm/min. Then the bone biomechanics parameters, including compressive stiffness, strength, and displacement as well as energy absorption capacity, were analyzed.

Histological Analysis

L4 vertebral bodies were fixed with 4% paraformaldehyde for 48 h and then decalcified with 10% EDTA for 21–28 days. The samples were dehydrated with graded alcohol, embedded in paraffin, and then cut into 5-μm slices along the coronal plane using a paraffin microtome. Sections were stained with HE and observed under a microscope (BX53, Olympus Corporation, Tokyo, Japan).

Alkaline Phosphatase Activity Assay

Rat serum AKP activity was analyzed using a kit (Nanjing Jiancheng Biological Products Co., Ltd., Nanjing, China). The serum alkaline phosphatase (AKP) levels in rats were determined using a visible spectrophotometer (Thermo Fisher, Waltham, MA, USA).

Autophagolysosome Detection

The L5 samples were fixed with 0.2% glutaraldehyde at room temperature for 2 h, in 1% osmium tetroxide water for 1 h, and then stained in 2% uranyl acetate water for 1 h in the dark place. After dehydration through an alcohol gradient, the samples were embedded and sliced into 80-nm slices. The sections were stained with uranyl acetate and lead citrate and then observed with a transmission electron microscope (Philips CM, Amsterdam, Netherlands).

Real-Time qPCR

The expression levels of let-7f, autophagy-associated genes (mTORC1, Beclin-1, ATG12, ATG5, and LC3), Runx2, and Cathepsin K (CTSK) were evaluated by RT-qPCR. Total RNA was extracted from L6 vertebrae or BMSCs using the TRIzol Reagent (Thermo, USA). The PrimeScript™ RT Master Mix Kit (Takara, Shiga, Japan) was used to reverse transcribe RNA to cDNA. Quantitative analysis was performed under a Bio-Rad qPCR instrument using the SYBR Premix Ex Taq™ II Kit (Takara, Japan). Actin or U6 was used as the internal standard for mRNA and miRNA, respectively. The relative expression of each gene was quantified using the $2^{-\Delta\Delta Ct}$ method. The primer sequences are shown in **Supplementary Table 1**.

BMSC Culture, Osteogenic Differentiation, and ZGW Intervention

For osteoblast formation, we used rat bone marrow-derived mesenchymal stem cells (BMSCs). The separation and culture of rat BMSCs were performed as previously described (4). Briefly, we selected 7-day-old mice, dissected the femur in a sterile manner, and used a syringe needle to flush out bone marrow solutions. After centrifugation, the cell solutions were resuspended in α-MEM containing 10% fetal bovine serum (all from Gibco, Grand Island, NY, USA). The cells were cultured at 37°C in an incubator containing 5% CO_2. Osteogenic differentiation was induced in rat BMSC osteogenic

differentiation medium (Cyagen Biosciences, Santa Clara, CA, USA). After 7 days' osteogenic induction, osteoblasts were fixed with 4% paraformaldehyde and stained using an BCIP/NBT Alkaline Phosphatase (ALP) kit (Beyotime, Shanghai, China).

Luciferase Activity Assay

A PMIR-Report luciferase vector containing a let-7f binding site in the ULK2 3′-UTR was constructed. A mutant plasmid was used to measure binding specificity. Next, pGL3 luciferase reporter vectors were inserted into the let-7f promoter containing the ULK2 binding site. Then, we transfected luciferase vectors into osteoblasts. Luciferase activity was examined using the Luciferase Reporter Assay Kit (Promega, Madison, WI, USA).

Western Blotting

BMSCs were lysed with RIPA lysis buffer (Beyotime) containing 1% protease inhibitor and 1% PMSF phenylmethanesulfonyl fluoride (PMSF) for 30 min to inhibit protein degradation and centrifuged at 12,000 rpm for 10 min, and the supernatant was transferred to a new tube. The BCA Protein Assay Kit (Beyotime) was used to determine the protein concentration; the Gel Preparation Kit (Beyotime) was used to perform SDS-PAGE. The separated proteins were transferred to polyvinylidene fluoride (PVDF) membranes (Millipore) and blocked with QuickBlock™ Western Primary Dilution antibodies (Beyotime) overnight at 4°C temperature. Anti-β-actin primary antibody (1:5,000, mouse, ab6276, Abcam, Cambridge, MA, USA), ULK2 (1:1,000; Rabbit; DF9890; Affinity, Cincinnati, OH, USA), ATG5 (1:1,000, rabbit, #12994, Cell Signaling Technology (CST), Danvers, MA, USA), ATG12 (1:1,000, rabbit, #4180, CST), Beclin1 (1:1000, rabbit, #3495, CST), and LC3 (1:1000, rabbit, #4108, CST) were used as the primary antibodies following incubation with the membranes for 12 h at 4°C. After washing the membranes with TBST sufficiently, the membranes were incubated with the corresponding secondary antibody for 2 h at room temperature and then washed three times with TBST. The protein level was determined by BeyoECL Moon enhanced chemiluminescence (Beyotime).

Statistical Analysis

The data were analyzed with SPSS 19.0 software. For quantitative analysis, all results are expressed as mean ± standard deviations (SD). Statistical significance was evaluated by one-way analysis of variance (ANOVA) with the Student–Newman–Keuls (SNK) test for *post-hoc* analysis. Two-sided p-values < 0.05 were considered statistically significant.

RESULTS

ZGW Improves Bone Quality of GIOP Rats

Micro-CT showed that there was a small amount of trabecular bone thinning and damage in the DEXA group at each time point, while the ZGW group had more trabecular bone and more dense distribution of trabecular bone (**Figure 1A**). Microarchitecture data of L2 cancellous bone of vertebrae examined by micro-CT displayed that the DEXA group showed low BV/TV, Tb.N, Tb.Th, and vBMD and significantly high SMI and Tb.Sp at all the time points compared to those in the CON group. Compared with the DEXA group, the ZGW group displayed increased BV/TV, Tb.N, Tb.Th, and vBMD at each time point and decreased SMI and Tb.Sp at each time point (**Figure 1B**).

ZGW Increases Bone Strength of GIOP Rats

Compressive strength, compressive stiffness, compressive displacement, and energy absorption capacity were employed to evaluate the bone strength of GIOP rats. Compared to the CON group, the DEXA group displayed reductions in compressive strength at each time point and energy absorption capacity at M2 and M3. Meanwhile, the DEXA group (compared to the CON group) showed a decreased trend in compressive stiffness and compressive displacement at all the time points, although no significant differences were observed. Compared with the DEXA group, the ZGW group exhibited significantly increased compressive strength at each time point, high compressive stiffness, and energy absorption capacity at M3. Simultaneously, compared to the DEXA group, ZGW showed an increased trend in compressive stiffness at M1 and M2, compressive displacement at all the time points, and energy absorption capacity at M1 and M2, although the differences were not significant (**Figure 2**).

ZGW Mitigates Histological Damage of GIOP Rats

HE staining was employed to assess the morphological changes in the L4 trabeculae of the various groups. At each time point, the DEXA group displayed increased trabecular spacing, trabecular absorption, perforation, fracture, and poor trabecular continuity compared to the CON group. Compared with the DEXA group, the ZGW group manifested improvements in vertebral trabecular bone (**Figure 3**).

ZGW Increases Blood Serum AKP Activity of GIOP Rats

ELISA was employed to detect the blood serum AKP activity of each group at different time points. Compared to the CON group, the DEXA group exhibited significantly decreased serum levels of AKP at M2 and M3. Compared with the DEXA group, the ZGW group manifested significantly increased serum levels of AKP at M2 and M3 (**Figure 4**).

ZGW Decreases the Number of Osteoblast Autophagosomes

By transmission electron microscopic observation, at each time point, the DEXA group exhibited more cytosolic autophagosomes, which were abundant in the osteoblasts, than in the CON group. Compared with the DEXA group, the ZGW group showed a significantly opposite trend in autophagic characteristics (**Figure 5**).

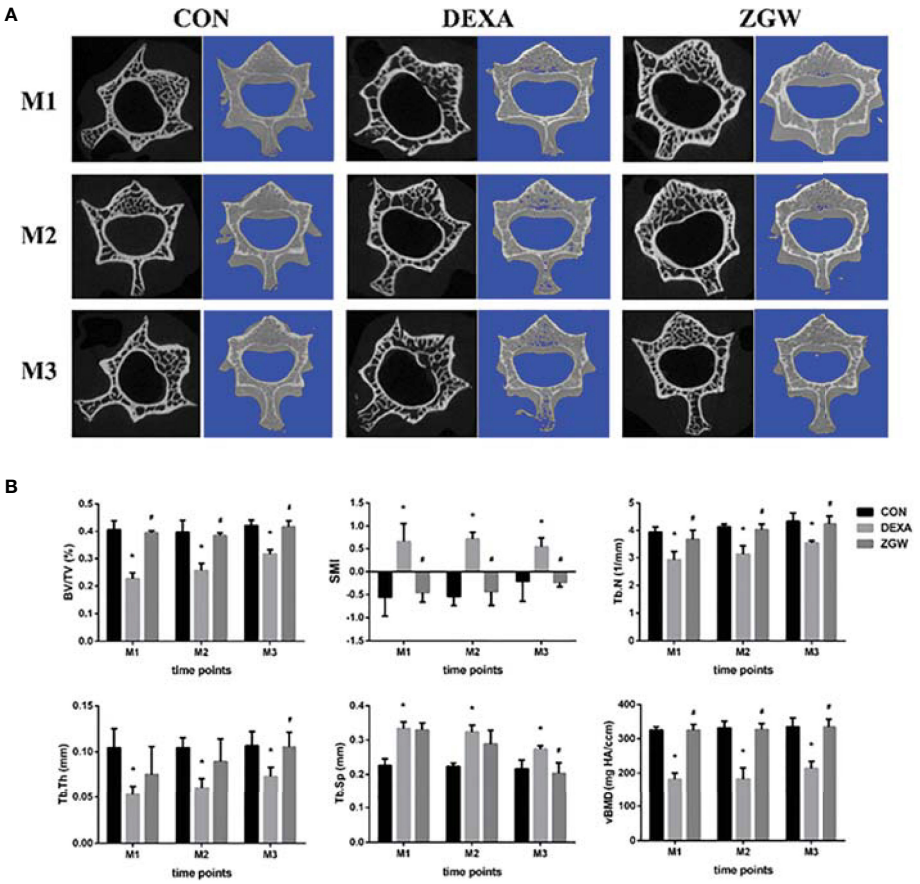

FIGURE 1 | Effects of ZGW on bone microarchitecture and parameters determined by micro-CT. **(A)** Representative 2D and 3D micro-CT images. **(B)** Bone microarchitecture and parameters BV/TV, SMI, Tb.Th, Tb.N, Tb.Sp, and vBMD were calculated based on micro-CT results. Values are the means ± SD. $^{*}p < 0.05$ vs. CON group; $^{\#}p < 0.05$ vs. DEXA group.

ZGW Promotes let-7f and Runx2 mRNA Expression, Increases Autophagy-Associated Negative Regulatory Gene mTORC1 Expression, and Reduces Autophagy-Associated Positive Genes (Beclin-1, ATG12, ATG5, and LC3) and CTSK mRNA Expressions

The expressions of let-7f, autophagy-associated genes (mTORC1, Beclin-1, ATG12, ATG5, and LC3), Runx2, and CTSK were detected at the mRNA level to explore how ZGW might function. After DEXA intervention, let-7f expression was downregulated at M2 and M3. Furthermore, the DEXA group exhibited a significantly downregulated mTORC1 (a negative autophagy regulatory gene) mRNA expression at all the time points, significantly upregulated Beclin-1, ATG5, and LC3 mRNA expressions at all the time points, and ATG12 mRNA expression at M2 and M3. Meanwhile, bone formation-related gene Runx2 expression was downregulated at M3, whereas bone resorption-related gene CTSK mRNA expression was significantly upregulated at M2 and M3 (**Figure 6**).

After ZGW intervention, let-7f expression was significantly upregulated at M2 and M3 and was upregulated to some extent at M1 but did not differ significantly from that of the DEXA group. Compared to the DEXA group, the ZGW group exhibited a significantly downregulated ATG5 expression at all the time points, Beclin-1 expression at M2 and M3, ATG12 mRNA expression at M2, and LC3 mRNA expression at M3. Simultaneously, Runx2 expression was significantly upregulated at M3, whereas CTSK expression was significantly decreased at M3 (**Figure 6**).

ZGW Partially Reverses the Decline of Osteogenic Differentiation Induced by let-7f Silencing

To explore the regulatory effect of ZGW on let-7f in osteogenic differentiation of BMSCs, we conducted gain-and-loss-of-function experiments by transfecting let-7f mimics of the inhibitor into BMSCs. The effect of overexpression or silencing was verified by qPCR (**Supplementary Figure 1A**). CCK8 was utilized to evaluate the effect of ZGW on BMSC proliferation. 10 μg/ml was the maximum concentration that did not affect BMSC proliferation, so we used 10 μg/

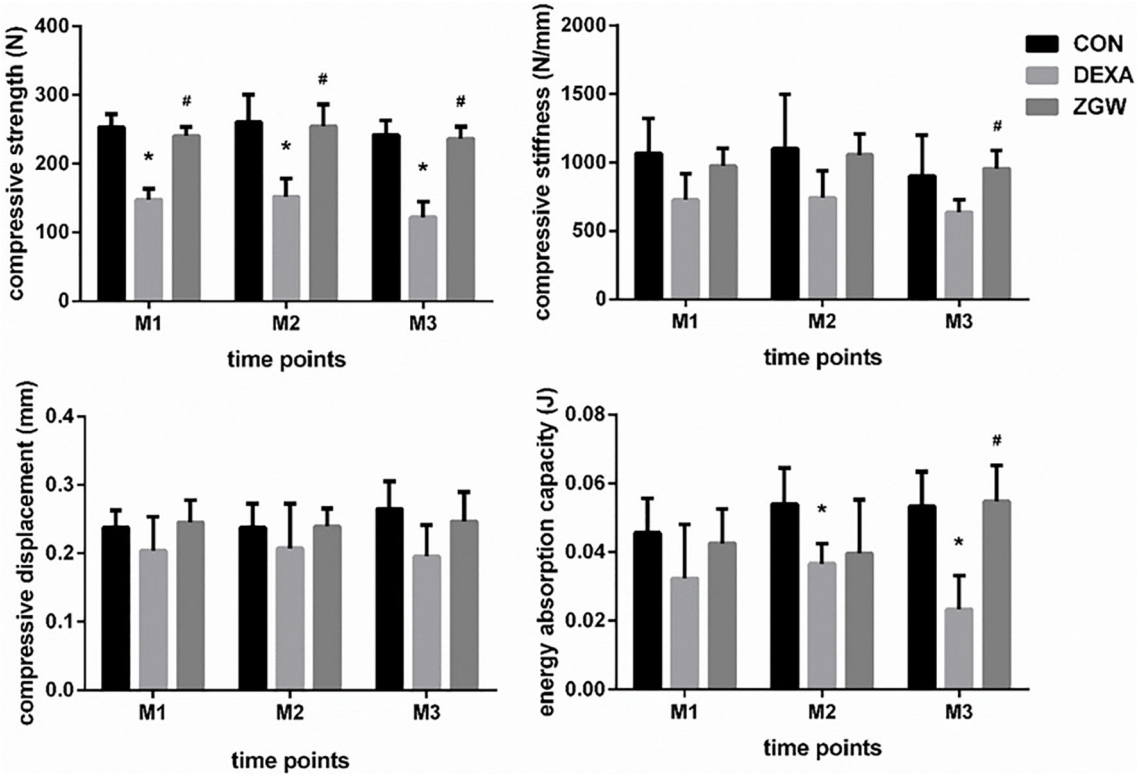

FIGURE 2 | Results of biomechanical analysis of L2. Data are the means ± SD. *$p < 0.05$ vs. CON group; #$p < 0.05$ vs. DEXA group.

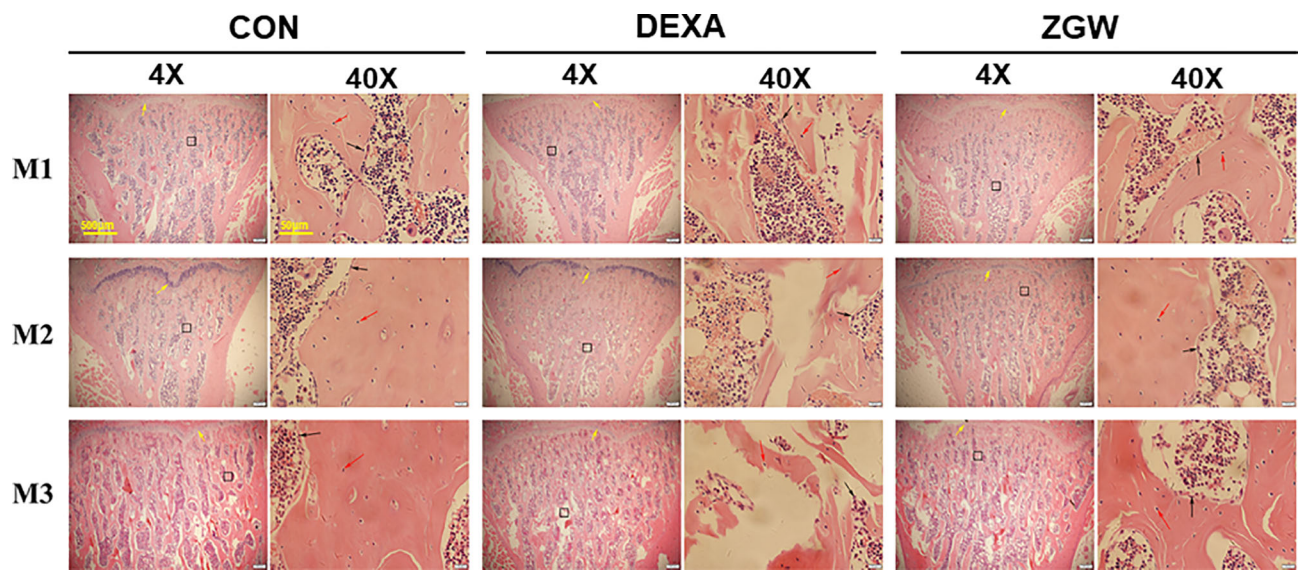

FIGURE 3 | Changes of bone histomorphology examined by H&E staining in the L4 bone trabecula of rats in each group. Scale bars and magnifications are displayed on the images. The red arrows represent osteocytes; the black arrows represent osteoblasts.

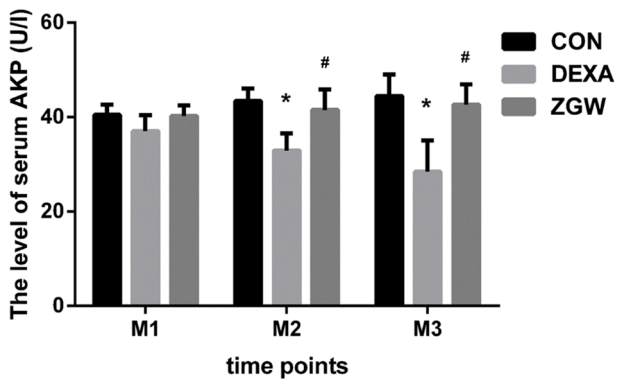

FIGURE 4 | The levels of serum AKP. Data are the means ± SD. $^{*}p < 0.05$ vs. CON group; $^{\#}p < 0.05$ vs. DEXA group.

ml ZGW as the optimum concentration in the next experiment (**Supplementary Figure 1B**). By ALP staining, we indicated that let-7f mimics could promote BMSC osteogenic differentiation, whereas the let-7f inhibitor suppressed BMSC osteogenic differentiation. After ZGW intervention, ZGW partially reversed the decline in osteogenic differentiation induced *via* let-7f silencing (**Figure 7**).

let-7f Targets Autophagy Key Gene ULK2

To examine whether let-7f binds to the 3′UTR of ULK2 (a positive autophagy regulatory gene), we conducted luciferase reporter assays by establishing a whole length of the ULK2 3′ UTR, which was considered as the ULK2 wild-type (WT) 3′UTR. The ULK2 mutant (Mut) 3′UTR was established by binding sequence mutation. Following let-7f mimic transfection into BMSCs, the ULK2 relative luciferase activity was suppressed compared with that in WT (**Figure 8**). However, in the mutant (Mut) groups, the activity of ULK2 relative luciferase has no significant differences among the different groups. These data indicated let-7f in the regulation of ULK2 3′UTR (**Figure 8**).

ZGW Suppresses let-7f Silencing-Induced Increased Autophagy

To further examine the effect of ZGW on let-7f in osteoblast differentiation of BMSCs, we employed Western blot to verify the relationship among let-7f, autophagy, and ZGW. We indicated that let-7f mimics could repress the autophagy-positive

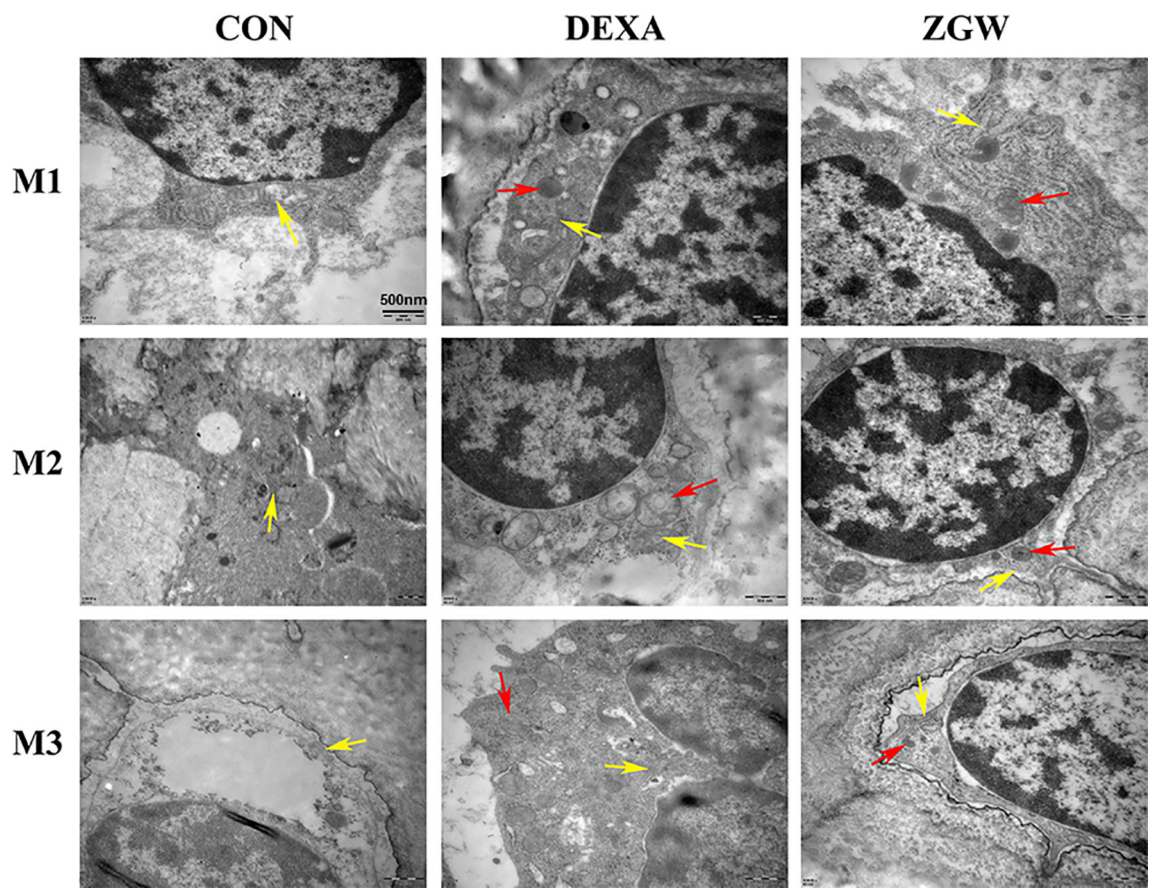

FIGURE 5 | Transmission electron microscopic observation. The yellow arrows indicate mitochondria, and the red arrows indicate autophagosomes.

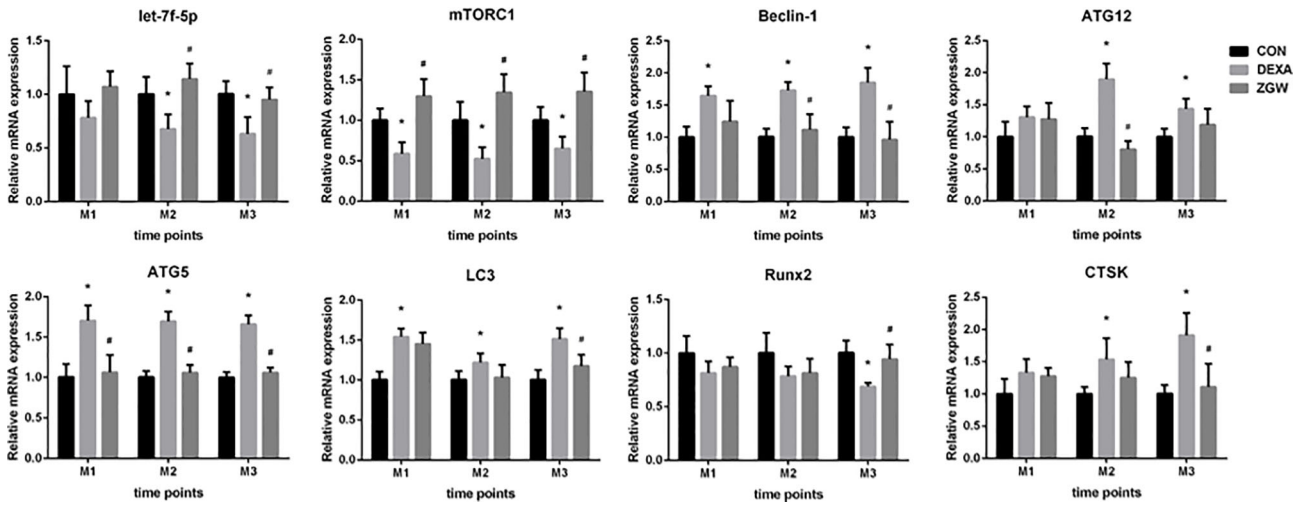

FIGURE 6 | The mRNA expression levels of let-7f, autophagy-associated genes (mTORC1, Beclin-1, ATG12, ATG5, and LC3), Runx2, and CTSK. Data are the means ± SD. $^{*}p < 0.05$ vs. CON group; $^{\#}p < 0.05$ vs. DEXA group.

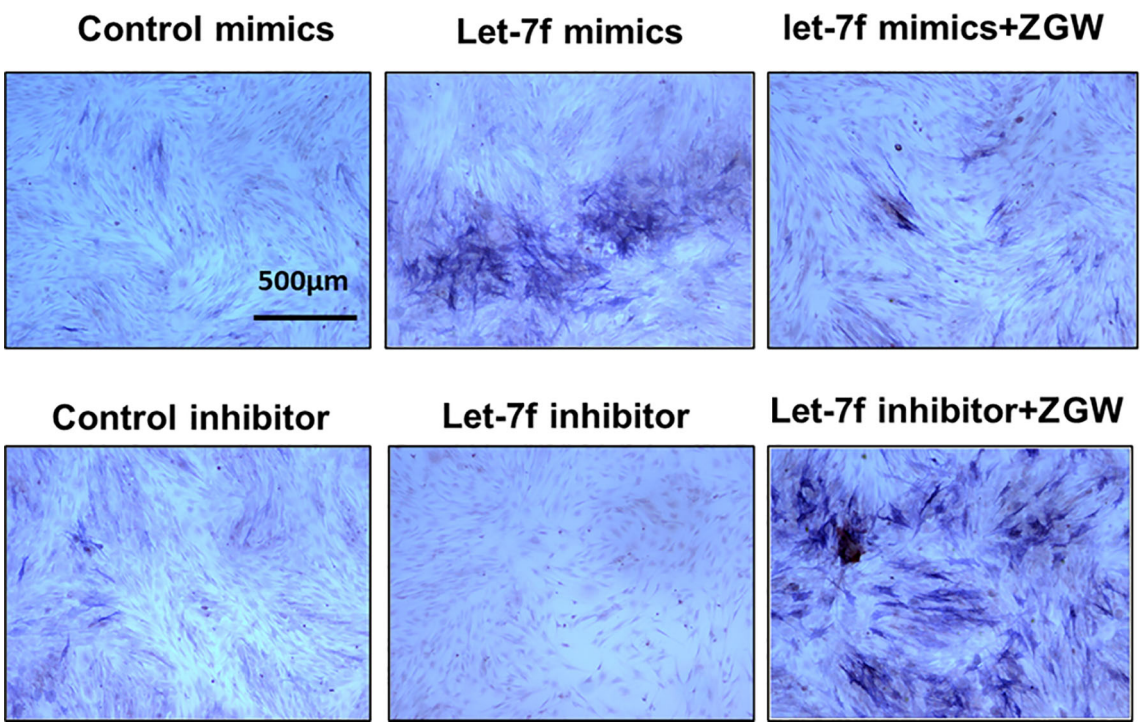

FIGURE 7 | The osteoblast differentiation ability of BMSCs was evaluated by ALP staining. Scale bars are displayed on the images. Magnifications: ×4.

regulatory proteins (ULK2, ATG5, ATG12, Beclin1, and LC3) compared with the control mimic group. The let-7f inhibitor could increase the autophagy proteins, especially ATG12, Beclin1, and LC3, compared to the control inhibitor group; however, ZGW partially reversed let-7f silencing-induced increased autophagy (**Figure 9**).

DISCUSSION

The main pathological cause of GIOP is an imbalance of bone homeostasis between osteoblastic bone formation and osteoclastic bone resorption (23). Previous studies indicated that GCs resulted in bone impairment by reducing osteoblast

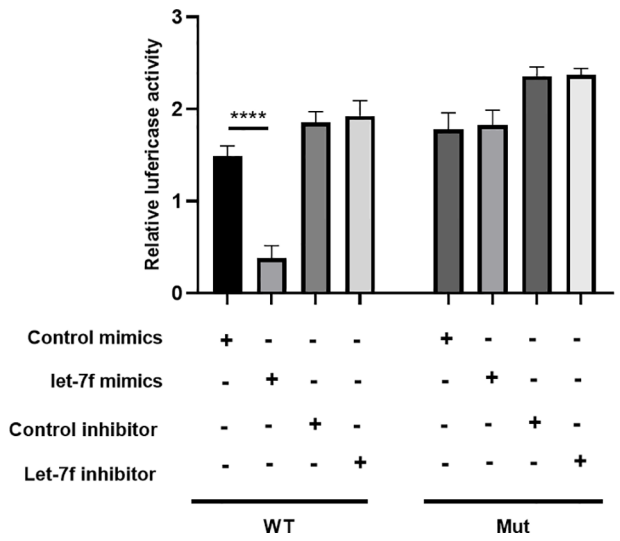

FIGURE 8 | Luciferase reporter assay was evaluated the target relationship between let-7f and ULK2. ****$p < 0.0001$.

differentiation, promoting the apoptosis of osteoblasts and osteocytes, and prolonging the life span of osteoclasts (2, 23). Furthermore, GCs can affect bone metabolism by regulating canonical Wnt-β-catenin and OPG/RANKL/RANK signaling, respectively (24). However, the precise pathogenesis of GIOP is not yet available and offering efficient therapy remains a challenge.

In the present study, we demonstrated that DEXA can result in severe bone damage, which was consistent with our previous studies (11, 25), indicating a success of the GIOP rat model. Simultaneously, our data showed that DEXA weakened serum AKP activity, which is recognized as an important marker of bone formation (26). We also verified that DEXA could increase CTSK expression, which is most abundant in osteoclasts (27), and decrease the expression of Runx2, an important osteoblast transcription factor, which was a benefit for bone formation (28), in GIOP rats. Moreover, DEXA induced the formation of autophagosomes in osteoblasts, suggesting that DEXA-induced excessive autophagy may be the key molecular mechanism of GIOP.

Intriguingly, ZGW, as an effective drug, had an ameliorative effect on GC-induced spinal osteoporosis of rats. Previously, some studies have indicated that ZGW was a promising prescription in the treatment of ovariectomy-induced bone loss (6, 9, 29). However, according to the authors' current knowledge, the effect of ZGW on GIOP has not been reported. The effect of this Chinese herbal compound prescription was not only its ability to inhibit the expression of CTSK and impede bone resorption but also its ability to stimulate the expression of Runx2 and accelerate bone formation. Furthermore, the underlying mechanism of inhibiting bone resorption and accelerating bone formation with the ZGW aqueous extract was mediated, at least partially, through the activation of let-7f and regulation of autophagy-associated genes. Overall, ZGW may be a promising drug to prevent and treat GIOP.

Autophagy is characterized by the formation of autophagosomes by cell membrane encapsulation of part of the cytoplasm and organelles and fusion with lysosomes to form autophagolysosomes to degrade the encapsulated contents to achieve cellular metabolic homeostasis (13, 15). Autophagy promoters, such as GC, starvation, and rapamycin, can promote the formation of the ULK1/2 complex and increase the activity of the Beclin1–vps34 complex by promoting the

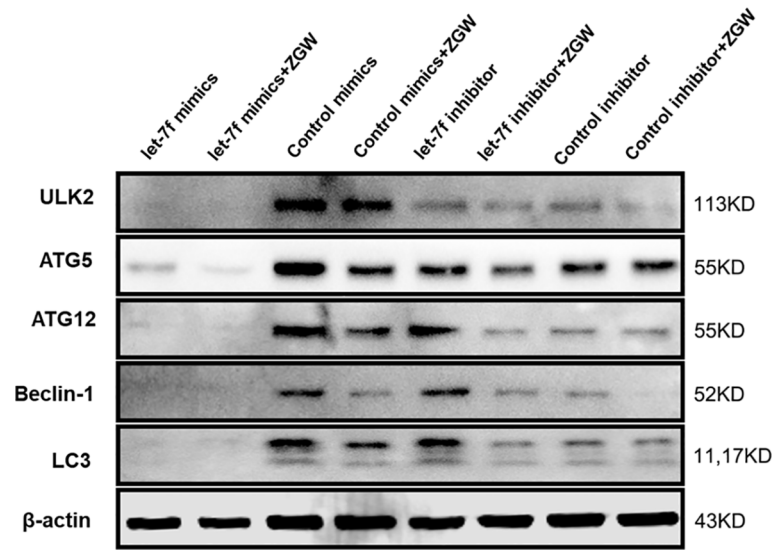

FIGURE 9 | Changes in autophagy-related protein expressions (ULK2, ATG12, ATG5, Beclin-1, and LC3).

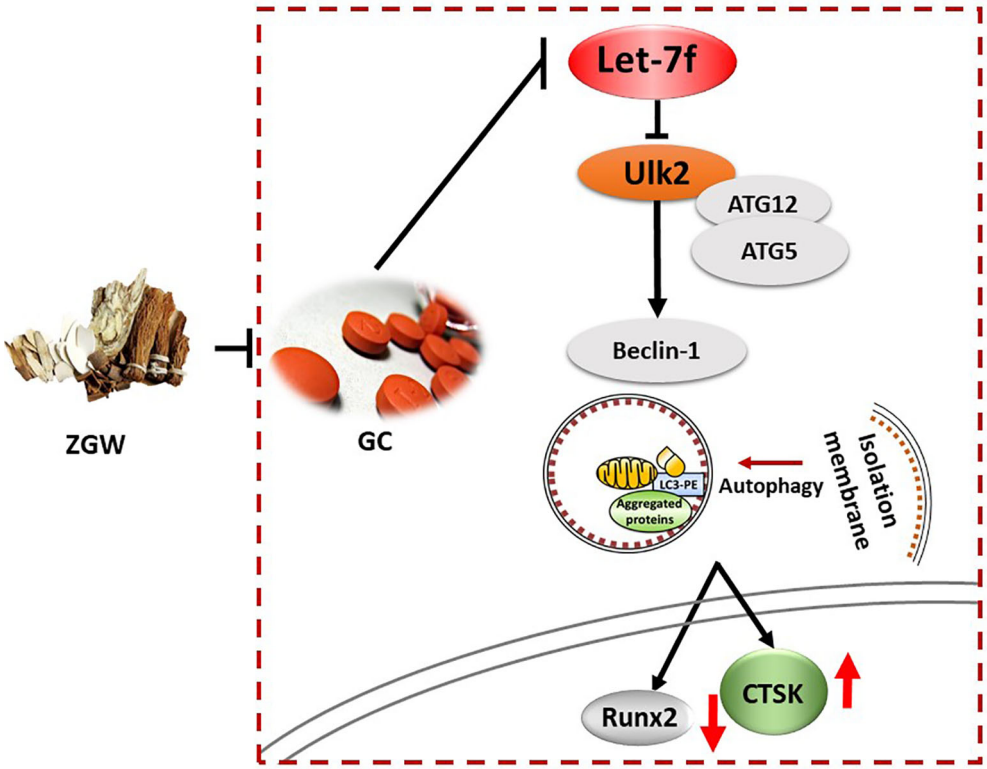

FIGURE 10 | Mechanism graphic of the study.

phosphorylation of Ambra1 and Beclin1 (30, 31). Autophagosome elongation is mediated by two conjugated systems, LC3 and ATG12–ATG5–ATG16L, which are formed by the combined action of ATG7 and ATG10 (32, 33). In our work, *in vivo*, the expressions of Beclin-1, ATG12, ATG5, and LC3 were increased, while those of let-7f and mTORC1 were reduced in GIOP rats compared to those of the CON group. The aberrant expression levels of autophagy-related genes returned to the control value in the ZGW-supplemented GIOP rats. *In vitro*, we indicated that ZGW partially reversed the decline in osteogenic differentiation induced by let-7f silencing, the mechanism of which may be closely related to the activation of let-7f and suppression of autophagy. Therefore, we have reason to believe that ZGW could significantly ameliorate bone deteriorations in GIOP rats and promote BMSC osteogenic differentiation through activation of let-7f and suppression of autophagy (**Figure 10**).

CONCLUSIONS

To our knowledge, for the first time, let-7f was selected to elaborate the pharmacological mechanisms for ZGW in experimental GIOP rats. Therefore, we have reason to believe that the ZGW aqueous extract could significantly ameliorate bone deteriorations in GIOP rats, and the underlying mechanism was mediated, at least partially, through activation of let-7f and suppression of autophagy. Our study provides an experimental basis for the clinical treatment of GIOP with traditional Chinese medicine. Moreover, it is beneficial to develop new drugs for treating GIOP concerning ZGW, let-7f, and autophagy-related targets. However, there are also some limitations in our study. First, the knockout and knock-in animals of let-7f are still necessary to further elucidate the mechanisms of ZGW in the treatment of GIOP. Besides, the efficacy of ZGW in the treatment of GIOP still needs to be confirmed by multicenter, double-blind, and randomized controlled clinical studies.

DATA AVAILABILITY STATEMENT

The original contributions presented in the study are included in the article/**Supplementary Material**. Further inquiries can be directed to the corresponding authors.

ETHICS STATEMENT

The animal study was reviewed and approved by the First Affiliated Hospital of Guangzhou University of Chinese Medicine (approval number: 20130425).

AUTHOR CONTRIBUTIONS

Study design: GS, X,J and HR. Study conduct: GS, HR, QS, ZZ, HC, WZ, GC, XY, FY, PZ, JH, XZ, and LZ. Data collection and analysis: IM, JT, JC, and DL. Manuscript draft: GS, HR, QS. Manuscript revision: XJ. All authors contributed to the article and approved the submitted version.

FUNDING

This research was funded by the National Natural Science Foundation of China (81904225 and 81774338), Innovation Team project of Guangdong Education Department (2021KCXTD017), Guangdong Natural Science Foundation (2020A1515110322 and 2021A1515011247), High-Level University Collaborative Innovation Team of GZUCM (2021xk57), and Natural Science Foundation of Xinjiang Autonomous Region (2019D01C013). The funding institutions had not any role in study design, data collection, data analysis, interpretation, or writing of the report in this study.

SUPPLEMENTARY MATERIAL

The Supplementary Material for this article can be found online at: https://www.frontiersin.org/articles/10.3389/fendo.2022.878963/full#supplementary-material

REFERENCES

1. Fleseriu M, Auchus R, Bancos I, Ben-Shlomo A, Bertherat J, Biermasz NR, et al. Consensus on Diagnosis and Management of Cushing's Disease: A Guideline Update. *Lancet Diabetes Endocrinol* (2021) 9(12):847–75. doi: 10.1016/S2213-8587(21)00235-7
2. Chotiyarnwong P, McCloskey EV. Pathogenesis of Glucocorticoid-Induced Osteoporosis and Options for Treatment. *Nat Rev Endocrinol* (2020) 16 (8):437–47. doi: 10.1038/s41574-020-0341-0
3. Shang Q, Zhao W, Shen G, Yu X, Zhang Z, Huang X, et al. Jingui Shenqi Pills Regulate Bone-Fat Balance in Murine Ovariectomy-Induced Osteoporosis With Kidney Yang Deficiency. *Evid Based Complement Alternat Med* (2020) 2020:1517596. doi: 10.1155/2020/1517596
4. Shang Q, Yu X, Ren H, Shen G, Zhao W, Zhang Z, et al. Effect of Plastrum Testudinis Extracts on the Proliferation and Osteogenic Differentiation of Rbmscs by Regulating P38 Mapk-Related Genes. *Evid Based Complement Alternat Med* (2019) 2019:6815620. doi: 10.1155/2019/6815620
5. Lin WL, Lin PY, Hung YC, Hsueh TP. Benefits of Herbal Medicine on Bone Mineral Density in Osteoporosis: A Meta-Analysis of Randomized Controlled Trials. *Am J Chin Med* (2020) 48(8):1749–68. doi: 10.1142/S0192415X20500871
6. Lai N, Zhang Z, Wang B, Miao X, Guo Y, Yao C, et al. Regulatory Effect of Traditional Chinese Medicinal Formula Zuo-Gui-Wan on the Th17/Treg Paradigm in Mice With Bone Loss Induced by Estrogen Deficiency. *J Ethnopharmacol* (2015) 166:228–39. doi: 10.1016/j.jep.2015.03.011
7. Zhang JH, Xin J, Fan LX, Yin H. [Intervention Effects of Zuoguiwan Containing Serum on Osteoblast Through Erk1/2 and Wnt/Beta-Catenin Signaling Pathway in Models With Kidney-Yang-Deficiency, Kidney-Yin-Deficiency Osteoporosis Syndromes]. *Zhongguo Zhong Yao Za Zhi* (2017) 42 (20):3983–9. doi: 10.19540/j.cnki.cjcmm.20170907.002
8. Li W, Liu Z, Liu L, Yang F, Li W, Zhang K, et al. Effect of Zuogui Pill and Yougui Pill on Osteoporosis: A Randomized Controlled Trial. *J Tradit Chin Med* (2018) 38(1):33–42. doi: 10.1016/j.jtcm.2018.01.005
9. Liu F, Tan F, Tong W, Fan Q, Ye S, Lu S, et al. Effect of Zuoguiwan on Osteoporosis in Ovariectomized Rats Through Rankl/Opg Pathway Mediated by Beta2ar. *BioMed Pharmacother* (2018) 103:1052–60. doi: 10.1016/j.biopha.2018.04.102
10. Liang D, Ren H, Qiu T, Shen G, Xie B, Wei Q, et al. Extracts From Plastrum Testudinis Reverse Glucocorticoid-Induced Spinal Osteoporosis of Rats *Via* Targeting Osteoblastic and Osteoclastic Markers. *BioMed Pharmacother* (2016) 82:151–60. doi: 10.1016/j.biopha.2016.04.068
11. Ren H, Shen G, Tang J, Qiu T, Zhang Z, Zhao W, et al. Promotion Effect of Extracts From Plastrum Testudinis on Alendronate Against Glucocorticoid-Induced Osteoporosis in Rat Spine. *Sci Rep* (2017) 7(1):10617. doi: 10.1038/s41598-017-10614-5
12. Shang Q, Shen G, Chen G, Zhang Z, Yu X, Zhao W, et al. The Emerging Role of Mir-128 in Musculoskeletal Diseases. *J Cell Physiol* (2021) 236(6):4231–43. doi: 10.1002/jcp.30179
13. Shen G, Ren H, Qiu T, Liang D, Xie B, Zhang Z, et al. Implications of the Interaction Between Mirnas and Autophagy in Osteoporosis. *Calcif Tissue Int* (2016) 99(1):1–12. doi: 10.1007/s00223-016-0122-x
14. Shen GY, Ren H, Shang Q, Zhao WH, Zhang ZD, Yu X, et al. Let-7f-5p Regulates Tgfbr1 in Glucocorticoid-Inhibited Osteoblast Differentiation and Ameliorates Glucocorticoid-Induced Bone Loss. *Int J Biol Sci* (2019) 15 (10):2182–97. doi: 10.7150/ijbs.33490
15. Shen G, Ren H, Shang Q, Qiu T, Yu X, Zhang Z, et al. Autophagy as a Target for Glucocorticoid-Induced Osteoporosis Therapy. *Cell Mol Life Sci* (2018) 75 (15):2683–93. doi: 10.1007/s00018-018-2776-1
16. Wang L, Heckmann BL, Yang X, Long H. Osteoblast Autophagy in Glucocorticoid-Induced Osteoporosis. *J Cell Physiol* (2019) 234(4):3207–15. doi: 10.1002/jcp.27335
17. Li H, Li D, Ma Z, Qian Z, Kang X, Jin X, et al. Defective Autophagy in Osteoblasts Induces Endoplasmic Reticulum Stress and Causes Remarkable Bone Loss. *Autophagy* (2018) 14(10):1726–41. doi: 10.1080/15548627.2018.1483807
18. Lin NY, Chen CW, Kagwiria R, Liang R, Beyer C, Distler A, et al. Inactivation of Autophagy Ameliorates Glucocorticoid-Induced and Ovariectomy-Induced Bone Loss. *Ann Rheum Dis* (2016) 75(6):1203–10. doi: 10.1136/annrheumdis-2015-207240
19. Xu K, Lu C, Ren X, Wang J, Xu P, Zhang Y. Overexpression of Hif-1alpha Enhances the Protective Effect of Mitophagy on Steroid-Induced Osteocytes Apoptosis. *Environ Toxicol* (2021) 36(11):2123–37. doi: 10.1002/tox.23327
20. Blanchard OL, Smoliga JM. Translating Dosages From Animal Models to Human Clinical Trials–Revisiting Body Surface Area Scaling. *FASEB J* (2015) 29(5):1629–34. doi: 10.1096/fj.14-269043
21. Shen G, Ren H, Shang Q, Zhao W, Zhang Z, Yu X, et al. Foxf1 Knockdown Promotes Bmsc Osteogenesis in Part by Activating the Wnt/Beta-Catenin Signalling Pathway and Prevents Ovariectomy-Induced Bone Loss. *EBioMedicine* (2020) 52:102626. doi: 10.1016/j.ebiom.2020.102626
22. Deng P, Yuan Q, Cheng Y, Li J, Liu Z, Liu Y, et al. Loss of Kdm4b Exacerbates Bone-Fat Imbalance and Mesenchymal Stromal Cell Exhaustion in Skeletal Aging. *Cell Stem Cell* (2021) 28(6):1057–73.e7. doi: 10.1016/j.stem.2021.01.010
23. Lee S, Kruger BT, Ignatius A, Tuckermann J. Distinct Glucocorticoid Receptor Actions in Bone Homeostasis and Bone Diseases. *Front Endocrinol (Lausanne)* (2021) 12:815386. doi: 10.3389/fendo.2021.815386
24. Fassio A, Rossini M, Viapiana O, Idolazzi L, Vantaggiato E, Benini C, et al. New Strategies for the Prevention and Treatment of Systemic and Local Bone Loss; From Pathophysiology to Clinical Application. *Curr Pharm Des* (2017) 23(41):6241–50. doi: 10.2174/1381612823666170713104431
25. Ren H, Liang D, Jiang X, Tang J, Cui J, Wei Q, et al. Variance of Spinal Osteoporosis Induced by Dexamethasone and Methylprednisolone and Its Associated Mechanism. *Steroids* (2015) 102:65–75. doi: 10.1016/j.steroids.2015.07.006
26. Li H, He D, Xiao X, Yu G, Hu G, Zhang W, et al. Nitrogen-Doped Multiwalled Carbon Nanotubes Enhance Bone Remodeling Through Immunomodulatory Functions. *ACS Appl Mater Interf* (2021) 13(21):25290–305. doi: 10.1021/acsami.1c05437

27. Xie H, Cui Z, Wang L, Xia Z, Hu Y, Xian L, et al. Pdgf-Bb Secreted by Preosteoclasts Induces Angiogenesis During Coupling With Osteogenesis. *Nat Med* (2014) 20(11):1270–8. doi: 10.1038/nm.3668
28. Wei J, Shimazu J, Makinistoglu MP, Maurizi A, Kajimura D, Zong H, et al. Glucose Uptake and Runx2 Synergize to Orchestrate Osteoblast Differentiation and Bone Formation. *Cell* (2015) 161(7):1576–91. doi: 10.1016/j.cell.2015.05.029
29. Liu FX, Tan F, Fan QL, Tong WW, Teng ZL, Ye SM, et al. Zuogui Wan Improves Trabecular Bone Microarchitecture in Ovariectomy-Induced Osteoporosis Rats by Regulating Orexin-A and Orexin Receptor. *J Tradit Chin Med* (2021) 41(6):927–34. doi: 10.19852/j.cnki.jtcm.20210903.001
30. Bodemann BO, Orvedahl A, Cheng T, Ram RR, Ou YH, Formstecher E, et al. Ralb and the Exocyst Mediate the Cellular Starvation Response by Direct Activation of Autophagosome Assembly. *Cell* (2011) 144(2):253–67. doi: 10.1016/j.cell.2010.12.018
31. Seidel T, Fiegle DJ, Baur TJ, Ritzer A, Nay S, Heim C, et al. Glucocorticoids Preserve the T-Tubular System in Ventricular Cardiomyocytes by Upregulation of Autophagic Flux. *Basic Res Cardiol* (2019) 114(6):47. doi: 10.1007/s00395-019-0758-6
32. Radoshevich L, Murrow L, Chen N, Fernandez E, Roy S, Fung C, et al. Atg12 Conjugation to Atg3 Regulates Mitochondrial Homeostasis and Cell Death. *Cell* (2010) 142(4):590–600. doi: 10.1016/j.cell.2010.07.018
33. Hill SM, Wrobel L, Ashkenazi A, Fernandez-Estevez M, Tan K, Burli RW, et al. Vcp/P97 Regulates Beclin-1-Dependent Autophagy Initiation. *Nat Chem Biol* (2021) 17(4):448–55. doi: 10.1038/s41589-020-00726-x

Conflict of Interest: The authors declare that the research was conducted in the absence of any commercial or financial relationships that could be construed as a potential conflict of interest.

frontiers | Frontiers in Endocrinology

REVIEW
published: 16 May 2022
doi: 10.3389/fendo.2022.901545

Evolving Roles of Natural Terpenoids From Traditional Chinese Medicine in the Treatment of Osteoporosis

Yue Zhuo[1†], Meng Li[2†], Qiyao Jiang[1], Hanzhong Ke[3], Qingchun Liang[4], Ling-Feng Zeng[5*] and Jiansong Fang[1*]*

[1] Science and Technology Innovation Center, Guangzhou University of Chinese Medicine, Guangzhou, China, [2] Guangdong Provincial Key Laboratory of Research in Structural Birth Defect Disease, Women and Children's Medical Center, Department of Pediatric Surgery, Guangzhou Institute of Pediatrics, Guangzhou Guangzhou Medical University, Guangzhou, China, [3] Department of Cancer Immunology and Virology, Dana-Farber Cancer Institute, Harvard Medical School, Boston, MA, United States, [4] The Third Affiliated Hospital of Southern Medical University, Guangzhou, China, [5] The 2nd Affiliated Hospital of Guangzhou University of Chinese Medicine, Guangzhou, China

OPEN ACCESS

Edited by:
Bo Liu,
Guangdong Provincial Hospital of Chinese Medicine, China

Reviewed by:
Xiao-Jia Chen,
University of Macau, China
Jinhua Wang,
Chinese Academy of Medical Sciences and Peking Union Medical College, China
Huajun Wang,
Jinan University, China

***Correspondence:**
Yue Zhuo
zhuoyue@gzucm.edu.cn
Ling-Feng Zeng
zenglf6778@163.com
Jiansong Fang
fangjs@gzucm.edu.cn

[†]These authors have contributed equally to this work

Specialty section:
This article was submitted to Bone Research, a section of the journal Frontiers in Endocrinology

Received: *22 March 2022*
Accepted: *13 April 2022*
Published: *16 May 2022*

Citation:
Zhuo Y, Li M, Jiang Q, Ke H, Liang Q, Zeng L-F and Fang J (2022) Evolving Roles of Natural Terpenoids From Traditional Chinese Medicine in the Treatment of Osteoporosis. Front. Endocrinol. 13:901545. doi: 10.3389/fendo.2022.901545

Osteoporosis (OP) is a systemic metabolic skeletal disease which can lead to reduction in bone mass and increased risk of bone fracture due to the microstructural degradation. Traditional Chinese medicine (TCM) has been applied in the prevention and treatment of osteoporosis for a long time. Terpenoids, a class of natural products that are rich in TCM, have been widely studied for their therapeutic efficacy on bone resorption, osteogenesis, and concomitant inflammation. Terpenoids can be classified in four categories by structures, monoterpenoids, sesquiterpenoids, diterpenoids, and triterpenoids. In this review, we comprehensively summarize all the currently known TCM-derived terpenoids in the treatment of OP. In addition, we discuss the possible mechanistic-of-actions of all four category terpenoids in anti-OP and assess their therapeutic potential for OP treatment.

Keywords: osteoporosis, traditional Chinese medicine, terpenoids, osteoblast, osteoclast

INTRODUCTION

As a systemic skeletal disease, Osteoporosis (OP) is characterized by increased risk of bone fragility, chronic pain, and even disability, leading to decreased life quality. Especially, OP strongly affects postmenopausal women and elderly population. About 30-50% of women and those who are more than 70 years old suffer from OP-induced fractures throughout their lives (1–3). In health condition, osteoblasts (OBs, bone-forming cells) and osteoclasts (OCs, bone-resorbing cells) form a balance for bone homeostasis. The lack of OB function or over-activated OC status will disturb the balance and induce OP.

In recent years, there has been a growing interest in traditional Chinese medicine (TCM) for the treatment of OP, such as Liu-Wei-Di-Huang Wan (formula), Morindae Officinalis Radix (herb), Longspur epimedium glycoside (natural product) (4). TCM has accumulated extensive experience for thousands of years and owns fewer adverse effects during a long-term usage comparing to some chemically synthesized medicines (5). Chinese herbal medicines usually play their therapeutic roles through a "multi-components, multi-targets, multi-pathway" mode, which is compatible with the multifactorial nature of OP. Plenty of evidence suggest that targeting OCs with TCM is an efficient strategy for the treatment of OP (6–8).

According to the theory of TCM on the pathogenesis and symptoms of OP, the kidney stores essence, turns it into bone marrow, nourishes bones to strengthen the skeleton, and promotes bone growth and repair. Therefore, 'kidney deficiency' is regarded as the underlying cause of all skeletal pathologies (9, 10). Many classic and empirical formulas of TCM used to tonify the kidney are clinically applied in OP treatment, TCMs like Liu Wei Di Huang Wan, Qing E Wan, Jiawei Yanghe Decoction, Er Zhi Wan, Qiangji Jianli Yin, Zuo Gui Wan, Rongjin Tablets, and You Gui Wan showed excellent anti-OP efficacy through reinforcing the kidney (8). Modern pharmacological studies have shown that these classic formulas significantly inhibited OC formation and bone resorption, and promoted bone formation to increase bone mineral density (BMD) (8, 9). Moreover, many individual herbs that make up the formulas of TCM are beneficial for bone formation since they are bone-specific drugs for the treatment of bone fractures and bone loss diseases (11). *Rehmanniae Radix* has been clinically used for more than 3,000 years in Chinese medicine, which has an anti-OP effect through modulating the kidney and liver functions and improving blood circulation (12). Over 140 individual compounds have been isolated from *Rehmanniae Radix*, and iridoid glycosides (a kind of monoterpenoids) are vital for the anti-OP activity of *Rehmanniae Radix* (6).

Terpenoids are structurally diverse and may represent the most diverse source of essential chemotherapeutic drugs. They are isoprene units (C_5H_8)n-based nature products and are classified into monoterpenes, sesquiterpenes, diterpenes, triterpenes, and tetraterpenes. To date, more than 40,000 different terpenoids have been obtained in nature (13, 14). Terpenoids are also reported to have anti-inflammatory, anti-cancer, and neuroprotective effects, with beneficial effects on human health. Although the treatment of OP using TCM has a long history and natural terpenoids have been extensively studied for their therapeutic activities against bone resorption (15), less attention has been given to the whole series of terpenoids in the treatment of OP. Therefore, we here summarize anti-OP advances and molecular mechanisms of terpenoids isolated from TCM.

NATURAL TERPENOIDS AGAINST OP

Terpenoids are classified as monoter-, sesquiter-, diter-, triter-, and tetra-penoids according to different structures (**Figures 1** and **2**). Although few natural terpenoids exhibit genotoxicity or carcinogenicity based on epigenetic mechanism, most are beneficial to humans (15). Natural terpenoids from TCM have been reported to regulate OBs and OCs *via* different signaling pathways (concluded in **Figure 3** and **Table 1**), such as nuclear factor-κB (NF-κB), Wnt/β-catenin, mitogen-activated protein kinases (MAPK), and receptor activator of nuclear factor-κB ligand (RANKL)/receptor activator of nuclear factor-κB (RANK). We will provide a comprehensive review of natural terpenoids from TCM and their potential in OP therapy.

Monoterpenoids

Sweroside, an iridoid glycoside obtained from *Cornus officinalis* Sieb. et Zucc. (Shan Zhu Yu in Chinese), is commonly used in TCM for treating OP in postmenopausal women or elderly men (93). Emerging evidences demonstrated that sweroside increased the proliferation and suppressed the apoptosis of human MG-63 cells and rat OBs (17). Yan et al. observed that sweroside effectively promoted OB differentiation in bone marrow mesenchymal stem cells (BMSCs) through hyperactivating the mechanistic target of rapamycin complex 1 (mTORC1)/pS6 signaling pathway (19). Additionally, sweroside treatment induced the mineralization of bone matrix *via* modulating the expression of bone morphogenetic protein (BMP)-2/core binding factor alpha 1 (CBFA1)-mediated molecules in postmenopausal OP. Meanwhile, sweroside promoted the mineralization of MC3T3-E1 cells by activating p38 signaling pathway (16, 18). Swertiamarin, a structural analog of sweroside, is a secoiridoid glycoside extracted from *Enicostemma axillere* subsp. axillere (Gentianaceae) (94). It was evidenced that swertiamarin could promote OB differentiation and exhibit anti-inflammatory activity by regulating NF-κB/inhibitor of κB (IκB) and Janus kinase 2 (JAK2)/signal transducer and activator of transcription 3 (STAT3) signaling pathways. In addition, swertiamarin treatment markedly reduced RANKL/RANK expression and elevated osteoprotegerin (OPG) level, showing an excellent anti-osteoclastogenic activity (20–22).

Morinda officinalis HOW (Ba Ji Tian in Chinese) has been continuously used for more than 2,000 years in China as a tonic to nourish the kidney, strengthen bones, and enhance immune function in the treatment of OP (95, 96). It has been reported that the root extracts of *Morinda officinalis* showed therapeutic effect by suppressing bone resorption and enhancing bone formation on OP rat model induced by sciatic neurectomy and ovariectomy (97). He et al. observed that monotropein, a natural iridoid glycoside in the root extracts of *Morinda officinalis*, effectively attenuated lipopolysaccharide (LPS)- and ovariectomy-induced bone loss, and reduced inflammatory responses in MC3T3-E1 cells *via* inhibiting the activation of NF-κB (23). Furthermore, monotropein showed anti-osteoporotic effect by increasing bone mineral content (BMC), BMD, bone volume fraction (BVF), and decreasing the levels of interleukin (IL)-1, IL-6 and soluble RANKL in the serum of ovariectomized (OVX) mice (25). Meanwhile, monotropein treatment attenuated oxidative stress and increased the proliferation of OBs (24, 25).

Catalpol, the major bioactive iridoid glycoside isolated from *Rehmannia glutinosa* (Gaertn.) Libosch. ex Fisch. et C. A. Mey. Root (Dihuang in Chinese), is clinically used for OP treatment in China (6). Meng et al. showed that catapol suppressed RANKL-induced bone resorption in bone marrow-derived macrophages (BMMs) and RAW264.7 cells by reducing the ubiquitination of phosphatase and tensin homolog (PTEN), which subsequently inhibited the activations of NF-κB and protein kinase B (Akt) (26). Other reports also proved that catalpol treatment promoted the osteogenic ability of BMSCs and BMSC-dependent angiogenesis, partly *via* activation of JAK2/STAT3 axis and

Monoterpenoids

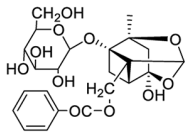

Paeoniflorin

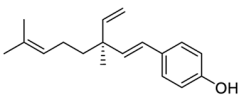

Bakuchiol

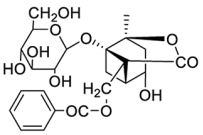

Albiflorin

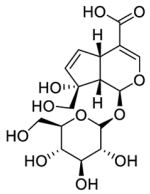

Monotropein

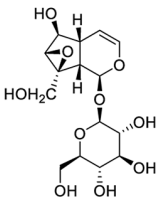

Catalpol

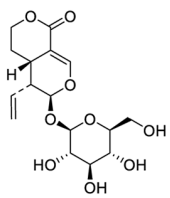

Sweroside

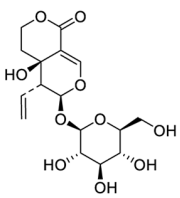

Swertiamarin

Sesquiterpenoids

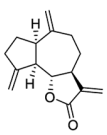

Dehydrocostus Lactone

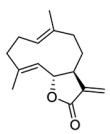

Costunolide

Diterpenoids

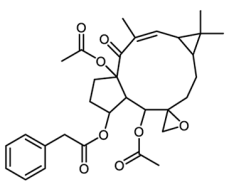

Euphorbia Factor L1

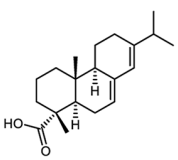

Abietic Acid

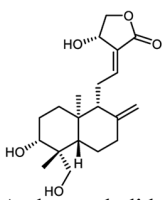

Andrographolide

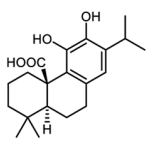

Carnosic Acid

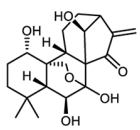

Oridonin

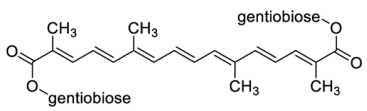

Crocin

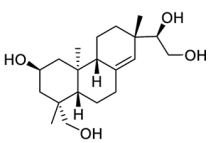

Kirenol

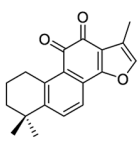

Tanshinone IIA

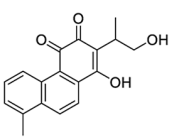

Tanshinone VI

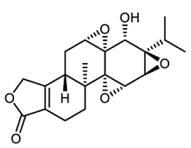

Triptolide

FIGURE 1 | Chemical structures of natural monoterpenoids, sesquiterpenoids and diterpenoids from TCM.

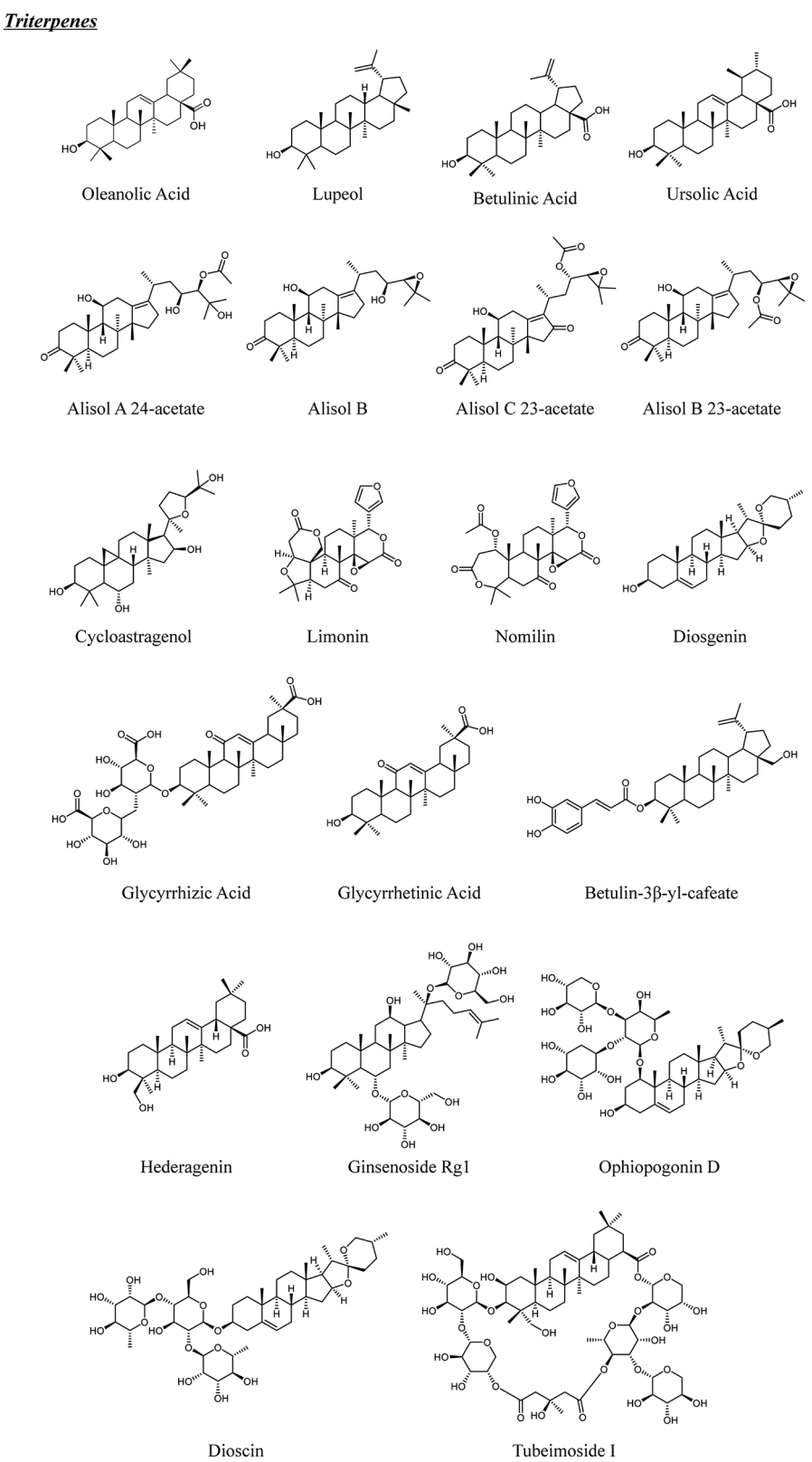

FIGURE 2 | Chemical structures of natural triterpenes from TCM.

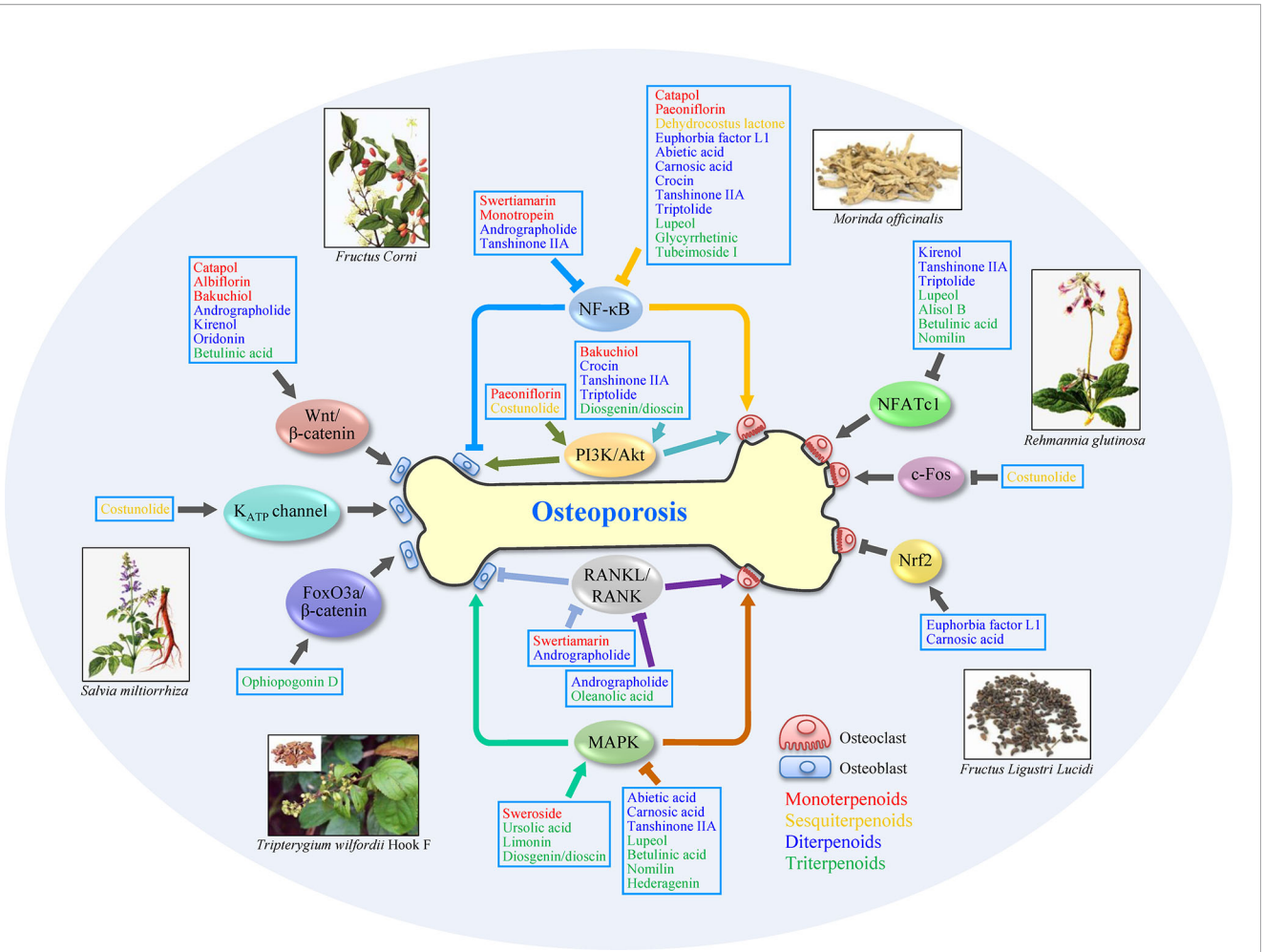

FIGURE 3 | Schematic of anti-osteoporosis mechanisms of terpenoid on osteoblasts and osteoclasts. The activation of MAPK, PI3K/Akt, Wnt/β-catenin signaling pathways and so on, or inhibition of NF-κB and RANKL/RANK signaling pathways, can promote cell proliferation or differentiation in osteoblasts, which benefits osteoporosis treatment. Meanwhile, the inhibition of MAPK, NF-κB, RANKL/RANK, and NFATc1 signaling pathways, or activation of PI3K/Akt and Nrf2 signaling pathways, also exerts potential therapeutic efficacy *via* regulating osteoclasts. Some terpenoids, such as andrographolide and tanshinone IIA, show anti-osteoporosis effect by modifying multi-targets. Arrows (↓) indicate activation of a factor or positive effect on indicated cell type, while inverted T marks (⊥) indicate inhibition or negative effect. Subclass of terpenoids is distinguished with different colors: monoterpenoids (red), sesquiterpenoids (yellow), diterpenoids (blue), and triterpenoids (green).

Wnt/β-catenin pathway (27, 28). Furthermore, Zhao et al. observed that catalpol could protect diabetic OP induced by high glucose treatment in MC3T3-E1 cells through regulating the migration and differentiation of OBs (29).

As a water-soluble monoterpene glucoside, paeoniflorin is the major bioactive components extracted from the root of *Paeonia lactifloral* Pall (98).. In antimycin A treated osteoblastic MC3T3-E1 cells, paeoniflorin attenuated cytotoxicity *via* improving the mitochondrial function. In addition, paeoniflorin also increased the differentiation of MC3T3-E1 cells and inhibited oxidative stress induced by methylglyoxal in the same cell model (30, 33, 98). In rats fed on high-carbohydrate/high-fat (HCHF) diet, paeoniflorin exhibited multiple pharmacological activities to prevent hyperlipidemia-induced OP. Intriguingly, paeoniflorin increased the trabecular and cortical parameters, as well as width and length of femur. Simultaneously, paeoniflorin rescued OB differentiation and the proliferation activities of bone turnover markers (99). Xu et al. reported that paeoniflorin suppressed bone destruction in collagen-induced arthritis (CIA) and decreased OC differentiation *in vitro* by down-regulating the activation of NF-κB (31). Wang et al. demonstrated that paeoniflorin suppressed OC generation and promoted OB formation *via* regulating NF-κB signaling pathway in BMMs and OVX mice (32).

Albiflorin, a monoterpene glycoside isolated from the roots of *Paeonia lactifloral* Pall., owns the ability to increase the differentiation of osteoblastic MC3T3-E1 cells (98). Kwang et al. found that albiflorin maintained mitochondrial function by reducing cytochrome c loss and cardiolipin peroxidation in MC3T3-E1 cells, which contributed to the inhibition of antimycin A-induced oxidative stress and toxicity (34). Another study showed that albiflorin treatment promoted the

TABLE 1 | Summary of studies for the antiosteoporotic effects of natural terpenoids from natural Chinese medicine.

Category	Compound	TCM	Cells/*in vivo* model	Mechanism	Reference
Monoterpenoids	Sweroside	*Cornus officinalis*	Human osteosarcoma cell line (SaOS-2); OVX mice	Induced the mineralization of bone matrix *via* promoting BMP2/CBFA1	(16)
			Human MG-63 cells; Rat OBs	Promoted differentiation and inhibited apoptosis	(17)
			MC3T3-E1 cells	Activated p38 signaling pathway	(18)
			BMSCs; OVX mouse	Hyperactivated the mTORC1/PS6 signaling pathway	(19)
	Swertiamarin	*Enicostema axillare*	Rat fibroblast-like synoviocytes (FLS)	Inhibited caspase 3, TNFa, IL-6, PGE2, COX-2, iNOS, MMPs, p38 MAPKa and modulated RANKL	(20)
			RAW 264.7 macrophage cells	Inhibited NF-κB/IκB and JAK2/STAT3 signaling	(21)
			C57/BL6J BMCs; Sprague Dawley rat neonates OBs; Freund's Complete Adjuvant induced rat arthritis	Inhibited RANKL/RANK; promoted OPG signaling	(22)
	Monotropein	*Morinda officinalis*	MC3T3-E1 cell line; Female osteoporotic C57/BL6 mice	Blocked NF-κB pathway; Enhanced bone formation and blocked increased secretion of inflammatory cytokines	(23)
			Primary OBs	Prevented Akt/mTOR signaling pathway	(24)
			MC3T3-E1 cells; OVX C57/BL6 mice	Inhibited sRANKL signaling	(25)
	Catalpol	*Rehmannia glutinosa*	BMMs; RAW264.7 cells; C57BL/6 mice	Suppressed NF-κB and AKT signaling pathways	(26)
			BMSCs; Male Sprague-Dawley rats	Activated Wnt/β-catenin pathway.	(27)
			BMSCs; SD female rats	Activated JAK2/STAT3 axis	(28)
			MC3T3-E1 cells; Male ICR mice	Inhibited bone resorption *via* the OPG/RANKL pathway; enhanced bone formation by regulating IGF-1/PI3K/mTOR pathways	(29)
	Paeoniflorin	*Paeonia lactifloral*	MC3T3-E1 cells	Enhanced glyoxalase system and inhibited the glycation	(30)
			Mice BM cells; Mice OC; RAW 264.7 cells; Male DBA/1 mice; Male C57/BL6 mice	Suppressed NF-κB signaling pathway	(31)
			Mouse BMMs; OVX C57BL/6 mice	Inhibited NF-κB signaling pathway	(32)
			Murine osteoblastic MC3T3-E1 cells	Activated PI3K signaling pathway	(33)
	Albiflorin		MC3T3-E1 cells	Suppressed oxidative damage through protecting cytochrome c and cardiolipin	(34)
			MC3T3-E1 cells; Sprague Dawley rats femoral fractures	Activated BMP-2/Smad and Wnt/β-catenin pathway	(35)
	Bakuchiol	*Psoralea corylifolia*	Primary human OBs; OVX rats Sprague-Dawley rats	Up-regulated the Wnt signalling pathway	(36)
			MCF-7 cells; OVX Sprague–Dawley rats	Increased alkaline phosphatase, Ca concentrations, serum E2 concentration and bone mineral density, and decreased the inorganic P level	(37)
			Primary mouse OC precursor cells; Bone marrow cells	Inhibited AKT and AP-1 pathways	(38)
Sesquiterpenoid	Costunolide	*Saussurea lappa*	Murine OB MC3T3-E1 cells	Activated PI3K signaling pathway	(39)
			Mice BMCs	Suppressed RANKL-mediated c-Fos transcriptional activity	(40)
	Dehydrocostus lactone		Mice BMMs, BMSCs, RAW264.7 cells; OVX C57BL/6J mice	Suppressed NF-κB and NFAT signaling pathways	(41)
			Mice BMMs; Male C57BL/6 mice	Modulated NF-κB signalling pathway	(42)
			RAW264.7 cells, Mice BMMs (C57BL/6 male mice)	Inhibiting NF-κB and AP-1 pathways	(43)
			Mice BMMs; OVX C57BL/6 female mice	Down-regulated the integrin b3, PKC-b, and Atg5 expression	(44)
Diterpenoids	Euphorbia factor L1	*Euphorbia lathyris*	Mouse BMMs; C57BL/6 male mice	Attenuated c-Fos expression and NF-κB activation; activated Nrf2 signaling pathway	(45)
	Abietic acid	*Pimenta racemosa*	RAW 264.7 cell line; Mice BMMs; C57/BL6 male mice	Inhibited NF-KB and MAPK signaling	(46)
	Andrographolide	*Andrographis paniculata*	BMSC; SD rat	Activated wnt/β-catenin signaling pathway	(47)
			Mouse BMMs; RAW 264.7 cells; OVX C57BL/6 mice	Suppressed RANKL signaling pathways	(48)
			MC3T3-E1 cell; OVX Sprague Dawley rats	Up-regulated the OPG/RANKL signaling pathway	(49)

(Continued)

TABLE 1 | Continued

Category	Compound	TCM	Cells/*in vivo* model	Mechanism	Reference
			Mouse BMSCs; OVX Sprague Dawley rats	Inhibited the NF-kB signaling pathway	(50)
			Mouse BMM Cells; C57/BL6 mice	Attenuated NF-κB and ERK/MAPK signalling pathways	(51)
	Carnosic acid	*Salvia officinalis*	RAW 264.7 cells; Mouse BMMs; C57BL/6 male mice	Activated the Nrf2 and suppressed the NF-κB pathways	(52)
			RAW 264.7 cells; Mouse BMMs; Female C57BJ/6L mice	Dual-targeting of sterol regulatory element-binding protein 2 and ERRα	(53)
	Crocin	*Crocus sativus*	RAW264.7 cells	Regulated glyoxalase, oxidative stress, and mitochondrial function	(54)
			Mice BMMs; Murine macrophage cell line; RAW264.7 cells	Suppressed NF- B signaling pathway	(55)
	Kirenol	*Siegesbeckia orientalis*	Mouse BMMs; OVX C57BL/6 mice	Inhibited Cav-1, NFATc1 and the related NF-κB/MAPKs/c-Fos signaling pathways	(56)
			MC3T3-E1 cells	Activated the BMP and Wnt/β-catenin signaling pathways	(57)
	Tanshinone IIA	*Salvia miltiorrhiza*	Human embryonic kidney (HEK) 293 cells; C57BL/6 mice	Inhibited renin activity	(58)
			Mice osteoblasts; Female $Wnt1^{sw/sw}$ mice	Up-regulated the NF-κB signaling pathway	(55)
	Tanshinone VI		Mice BMMCs; RAW-264.7 cells; C57BL/6 mice	Suppresed the NF-κB, PI3-kinase/Akt, and MAPK pathways, as well as the transcription factor NFATc1	(59)
			Mice bone marrow cells; Male ICR mice.	Inhibited the expression of c-Fos and NFATc1	(60)
			OCs	Inhibited RANKL expression and NFkB induction	(61)
	Triptolide	*Tripterygium wilfordii*	Male Sprague-Dawley rats	Down-regulated RANKL and up-regulated OPG	(62)
			RAW 264.7 (mouse macrophage)	Inhibited NF-kB activation, inhibited IkBa kinase activation, IkBa phosphorylation, and IkBa degradation	(63)
			RAW 264.7 cells; Mice BMMCs; Female C57BL/6 mice	Inhibited PI3K-AKT-NFATc1 pathway	(64)
	Oridonin	*Rabdosia rubescens*	Mouse BMMs; MC3T3-E1 cells; Female C57BL/J6 mice (OVX mice)	Inhibited IκB phosphorylation and Ifrd1 degradation	(65)
			Mouse BMSCs; Mouse BMMs; SD rats	Activated Wnt/β-catenin signaling pathway, down-regulated RANKL and up-regulated OPG expression *in vitro*	(66)
Triterpenoids	Lupeol	*Bombax ciba*	UMR-106 cell; Female Wistar albino rats	Inhibited MAPK, NF- κB, NFATc1, and c-Fos	(67)
	Alisol B 24-acetate	*Alismatis rhizoma*	Mast cells; Balb/c mice, ICR mice	Released Syk-mediated down-stream signals including PLC, ERK, and p38 MAPK, NF-κB, $cPLA_2$, COX-2, and Ca^{2+},	(68)
	Alisol B		OBs; Bone marrow cells; ddY mice; C57BL/6J (B6) (wild-type) mice	Inhibit NFATc1 and c-Fos signaling pathway	(69)
	Alisol C 23-acetate		Calvaria osteoblastic cell; OCs; OVX rat	Inhibited RANKL-induced osteoclast differentiation and function	(70)
	Alisol A 24-acetate		Mouse BMCs; BMMs	Downregulated NFATc1	(71)
	Oleanolic acid	*Ligustri lucidi*	Cell Counting Kit-8 (CCK-8); Mouse BMMs; OVX C57BL/6 mice	Inhibited the expression of NFATc1 and suppressed the expression of MMP9, Ctsk, TRAP and Car2	(72)
			RAW264.7 cells	Inhibited RANKL-induced osteoclastogenesis *via* ERα/miR-503/RANK signaling pathway	(73)
	Ursolic acid	*Ligustri lucidi*	Mouse osteoblastic MC3T3-E1 subclone 4 cells	Activated MAP kinases and NF-κB signaling pathway	(74)
	Glycyrrhizic acid	*Glycyrrhiza glabra*	Male Sprague–Dawley rats	Inhibited the 11β-hydroxysteroid dehydrogenase type 1 enzyme (11β-HSD1)	(7)
			RAW264.7 cell; Mouse BMMs; C57BL/6/Bkl mice (OVX mouse)	Suppressed NF-κB, ERK, and JNK pathway	(75)
			RAW264.7 cells; Mouse BMMs;OVX C57BL/6J mice	Inactivated NF-κB signaling.	(76)
			Male CSF1r-eGFP-KI mice and their wild type strain C57BL/6	Diminished the size of inflammatory osteolysis *via* the number of CXCR4+OCPs and TRAP+osteoclasts, decreased the senescence-	(77)

(Continued)

TABLE 1 | Continued

Category	Compound	TCM	Cells/*in vivo* model	Mechanism	Reference
				associated secretory phenotype markers, and elevated the senescence-protective markers	
	Glycyrrhetinic Acid		Mouse BMMs; RAW264.7 cells; OVX C57BL/6 female mice	Inhibited NF-κB and MAPK signaling pathways.	(78)
	Ginsenoside Rg1	*Panax ginseng*	Human dental pulp stem cells (hDPSCs); BMSCs; OCs	Promoted the proliferation and differentiation of DPSCs into odontoblast-like cells by promoted the expression of anti-osteoporosis related genes	(79)
	Betulinic Acid	*Betula pubescens*	Mouse BMMs; Female C57BL/6 mice; OVX mice	Inhibited MAPK and NFATc1 signaling pathways	(80)
			MC3T3-E1 OBs	Activated BMP/Smad/Runx2 and β-catenin signal pathways	(81)
	Limonin	*Evodia rutaecarpa*	OC-like cell model	Inhibited bone resorption and reduced the number of multinucleated cells	(82)
			MC3T3-E1 cell line	Promoted the p38-MAPK signaling	(83)
	Nomilin	*Citrus junos*	Mouse BMMs; Mouse RAW 264.7	Suppressed NFATc1 and MAPK signaling pathways	(84)
	Diosgenin	*Dioscorea nipponica*	OVX rats	Decreased the RANKL/OPG ratio	(85)
	Dioscin		Mouse BMMs cells; RAW264.7 cells; LPS- induced bone loss mouse	inhibiting the Akt signaling pathway	(86)
			MC3T3-E1 cells and MG-63 cells	Promoted osteoblasts proliferation and differentiation *via* Lrp5 and ER pathway	(87)
	Ophiopogonin D	*Ophiopogon japonicus*	OBs MC3T3-E1 cell; RAW264.7 cells; OVX mouse	Reducted oxidative stress *via* the FoxO3a-β-catenin signaling pathway	(88)
			Endothelium-specific Klf3 knockout mice	Inhibited Krüppel-like factor 3 (KLF3)	(89)
	Cycloastragenol	*Astragalus membranaceus*	MC3T3-E1 cells	Activated telomerase	(90)
	Hederagenin	*Hedera helix*	Mice BMMs; OVX mice	Inhibited RANKL-induced bone resorption and OC generation, activated MAPK signaling pathway (ERK and p38)	(91)
	Tubeimoside I	*Bolbostemma paniculatum*	Mice BMMs; RAW 264.7 cells; Male SD rats	Down-regulated NF-κB signaling pathway	(92)

generation of OBs and expression of runt-related transcription factor 2 (RUNX2) through activating BMP-2/Smad and Wnt/β-catenin signaling pathways (35). Meanwhile, albiflorin up-regulated the levels of various osteogenic genes, such as osteocalcin (OCN), osteopontin (OPN), osteonectin (OSN), bone sialoprotein (BSP), and AP. In femur fracture rat model, albiflorin stimulated the expression of osteogenic genes in femoral tissue and promoted callus formation at the early stage during fracture recovery. Additionally, albiflorin could increase the expression of bone-related genes (35). This finding suggested that albiflorin motivated bone calcification, osteogenesis and bone formation, resulting in improving the fracture healing.

Bakuchiol is a prenylated phenolic monoterpene in the fruit of *Psoralea corylifolia* (L.) Medik (37, 100). And *Psoralea corylifolia* was used in TCM formulas to treat osteoporosis for a long history time (101). Recent researches indicated that *Psoralea corylifolia* and its major active ingredient bakuchiol possessed anti-OP activity (100, 102). Bakuchiol treatment significantly inhibited bone resorption and OC differentiation *via* the inhibition of Akt phosphorylation and c-jun nuclear translocation induced by macrophage colony stimulating factor (M-CSF) plus RANKL (38). In OVX Sprague-Dawley (SD) rats, bakuchiol treatment reduced bone loss through increasing Ca^{2+} and serum E2 concentrations, AP activity, and BMD, along with reduced inorganic P level (37). Li et al. found that bakuchiol significantly stimulated OB proliferation and differentiation (103). In addition, bakuchiol treatment prevented bone loss in OVX rats induced by estrogen deficiency and induced OB differentiation by up-regulating the Wnt signaling pathway (36).

Collectively, monoterpenoids can protect bone from erosion *via* targeting different signaling pathways. In OBs, catapol, albiflorin, and bakuchiol can activate Wnt/β-catenin signaling pathway; paeoniflorin and sweroside stimulate PI3K/Akt and MAPK signaling pathways respectively; swertiamarin inhibits RANKL/RANK signaling pathway; monotropein and swertiamarin suppress NF-κB signaling pathway. In OCs, catapol and paeoniflorin depress NF-κB signaling pathway; bakuchiol enhances PI3K/Akt signaling pathway.

Sesquiterpenoids

Costunolide is sesquiterpene lactones derived from *Saussurea lappa* C.B. Clarke roots. A recent research showed that costunolide markedly induced bone mineralization and differentiation and increased cell growth, AP activity, and collagen synthesis in osteoblastic MC3T3-E1 cells *via* targeting diverse key proteins, such as estrogen receptor (ER), phosphoinositide 3-kinase (PI3K), extracellular signal-regulated kinase (ERK), protein kinase C (PKC), mitochondrial ATP-sensitive K^+ channel, p38, and c-Jun N-terminal kinase (JNK) (39). Moreover, Cheon et al. observed that costunolide

suppressed RANKL-induced OC differentiation *via* suppressing c-Fos transcriptional activity without affecting c-Fos expression (40).

Saussurea lappa C.B. Clarke has been used in clinic for decades as a TCM (104). Sesquiterpenes and sesquiterpene lactones are main bioactive constituent of this herb. As a member of sesquiterpene lactones, dehydrocostus lactone is extracted from the roots of *Saussurea lappa* and has been reported to exert various pharmacological activities including anti-ulcer, anti-tumor, anti-inflammatory, and immunomodulation (42, 105). In mouse BMMs, dehydrocostus lactone attenuated the RANKL-dependent OC differentiation through modulating IκB kinase (IKK), JNK, nuclear factor of activated T cell cytoplasmic 1 (NFATc1), and nuclear factor-erythroid 2-related factor 2 (Nrf2). Moreover, it suppressed the activation of OCs through down-regulating the expression of integrin β_3, PKC-β, and autophagy related 5 (43, 44). Besides, dehydrocostus lactone reduced RANKL-induced OC formation and differentiation *via* modulating NF-κB signaling pathway both *in vitro* and *in vivo* (41, 42).

Therefore, costunolide owns the ability to increase bone formation by modulating K_{ATP} channel and activating PI3K/Akt signaling pathway in OBs, and dehydrocostus lactone can decrease OC differentiation *via* inhibiting NF-κB signaling pathway.

Diterpenoids

Euphorbia factor L1 (EFL1) is an active diterpenoid composition extracted from the seed oil of Chinese herb *Euphorbia lathyrism* L. (Qian Jin Zi in Chinese) (106). EFL1 inhibited RANKL-induced osteoclastogenesis by inhibiting c-Fos expression and NF-κB activation. Meanwhile, apoptosis induced by EFL1 in differentiated OCs resulted from caspase activation and enhanced Fas ligand expression. In mice, EFL1 ameliorated bone destruction induced by inflammation and ovariectomy. These findings demonstrated that EFL1 can block OC differentiation through modulating inflammatory responses and trigger Fas-regulated apoptosis, which offers the potential to treat OP caused by excessive Ocs (45).

Abietic acid is a bioactive diterpene isolated from *Pimenta racemosa* var. *grissea* which exhibits anti-obesity and anti-inflammatory activities (107). In RAW264.7 cells and mouse BMMs, abietic acid inhibited RANKL-induced OC formation *via* suppressing NF-κB and MAPK signaling pathways. It also decreased the expression of osteoclastic genes, such as NFATc1, tartrate-resistant acid phosphatase (TRAP), dendritic cell specific transmembrane protein (DC-STAMP), and c-Fos. In C57/BL6 male mice of osteolysis model induced by LPS, abietic acid significantly reduced the number of Ocs and the levels of inflammatory cytokines, including tumor necrosis factor (TNF)-α and IL-6 (46).

As a bicyclic diterpenoid lactone, andrographolide can be isolated from the leaves of traditional herb *Andrographis aniculate* (Burm. F.) Wall. Ex Nees in Wallich (Chuan Xin Lian). According to previous study, andrographolide has extensive pharmacological activities, such as anti-inflammation, anti-oxidation, anti-platelet aggregation, immunomodulation, and potential antineoplastic properties partly by targeting NF-κB (108–111). Andrographolide showed the capacity to protect breast cancer-induced bone loss (112) and inflammatory osteolysis (51, 113). Furthermore, andrographolide depressed osteoclastogenesis in BMMs by decreasing the expression of OC-related genes induced by RANKL and inhibiting bone loss and inflammation in OVX mice (48, 51). In addition, andrographolide promoted osteogenesis of mouse and rat BMSCs and blocked the inhibitory effect of TNF-α on OB formation and mineralization (47, 50). Other study indicated that andrographolide increased OPG expression and suppressed OC differentiation in MC3T3-E1 cells. It also stimulated the differentiation and survival of OBs, which increased bone deposition. Meanwhile, the study confirmed that andrographolide prevented bone loss and improved bone turnover rate in OVX rat model (49).

Carnosic acid, an abietane diterpenoid extracted from *Rosmarinus officinalis* (rosemary) and *Salvia officinalis* (common sage), displayed anti-angiogenic, anti-neoplastic, anti-oxidant and anti-HIV activities (114). Recent study had suggested the protective effect of rosemary against OP through effectively mitigated bone loss induced by calcium deficiency (115). Both in RAW 264.7 cells and mouse BMMs, carnosic acid decreased the osteoclastogenesis and reactive oxygen species (ROS) generation *via* activating Nrf2 and suppressing NF-κB and MAPK signaling pathways. The same results were also detected in C57BL/6 male mice of LPS-induced OP (52). Furthermore, Zheng et al. found that carnosic acid played a dual role *via* targeting sterol regulatory element-binding protein 2 (SREBP2) and estrogen-related receptor alpha (ERRα) to suppress RANKL-mediated osteoclastogenesis and restrained bone loss induced by ovariectomy (53).

Crocin, a diterpenoid glycoside carotenoid component of *Crocus sativus* L., shows various pharmacological activities (116, 117). It was observed that crocin treatment mitigated bone loss in metabolic syndrome-induced OP rat model (118). Meanwhile, this research showed anti-inflammatory and anti-oxidative activities of crocin which significantly decreased the production of IL-6, TNF-α, reduced glutathione (GSH), and superoxide dismutase (SOD). In RAW264.7 cells, crocin attenuated the dysfunction of OCs induced by methylglyoxal *via* modulating glyoxalase I, oxidative stress, and mitochondrial function (54). Moreover, Fatemeh et al. observed that crocin could effectively improve the differentiation of BMSCs, by inhibiting NF-κB signaling pathway activation, crocin treatment suppressed RANKL-induced bone resorption and OC formation (55, 119).

Kirenol is a bioactive diterpenoid compound derived from *Siegesbeckia orientalis* L. that was used as an anti-rheumatic TCM (120, 121). Kim et al. demonstrated that kirenol stimulated OB differentiation *via* activation of BMP and Wnt/β-catenin signaling pathways in MC3T3-E1 cells, which increased the levels of AP, OPN, type I collagen, and OB differentiation markers, as well as the OPG/RANKL ratio (57). Furthermore, kirenol treatment suppressed RANKL-induced OC formation and the NFATc1/Cav-1 signaling pathway in BMMs and OVX rats, consequently preventing ovariectomy-induced OP (56).

Tanshinone IIA is an abietane diterpenoid isolated from *Salvia miltiorrhiza* Bunge (Danshen) that is used for the

treatment of trauma and fractures in clinical according to the dispelling stasis theory of TCM (122). 36 clinical trials used *Salvia miltiorrhiza* to treat different kinds of osteoporosis displayed high efficacy and low toxicity (123). Modern pharmacological studies showed that the ethanol extract of *Salvia miltiorrhiza* could inhibit trabecular bone loss by restraining bone resorption both in OVX and naturally menopaused mice (124). Tanshinone IIA blocked dexamethasone induced OB apoptosis through the suppression on NADPH oxidase (Nox) 4-derived ROS production. In addition, it blocked RANKL-mediated OC differentiation by decreasing the expression of c-Fos and NFATc1 (60). Tanshinone IIA could attenuate the formation of OCs by depressing the NF-κB, PI3K/Akt, and MAPK signaling pathways in OVX mice model (59). Zhu et al. found that tanshinone IIA administration prevented the harmfulness of oxidative stress and promoted the activity and functions of OBs in genetic OP model, $Wnt1^{sw/sw}$ mice, through regulating the NF−κB signaling pathway (125). Recently, in streptozotocin (STZ)-induced C57BL/6 diabetic mice, tanshinone IIA treatment restrained the activity of renin that resulted in protecting OP (58). As another abietane diterpenoid constituent obtained from *Salvia miltiorrhiza*, tanshinone VI significantly suppressed the differentiation of OCs and bone resorption *via* down-regulating the expression of RANKL and activation of NF−κB (61).

Triptolide, the major active diterpenoid component isolated from *Tripterygium wilfordii* Hook F, has been used in TCM for hundreds of years to treat cancer and bone loss (126, 127). A recent study suggested that triptolide effectively suppressed the activation of NF-κB induced by RANKL, as well as tumor cell- and RANKL-induced OC formation (63). Triptolide showed the protective effects on bone loss both in old male rats and OVX C57BL/6 mice (62, 64). Triptolide could suppress RANKL-induced OC formation and prevented the bone resorption of OCs in BMSCs and RAW264.7 cells, resulting from inhibiting PI3K/Akt/NFATc1 signaling pathway.

Oridonin is an ent-kaurane diterpenoid extracted from the TCM herb *Rabdosia rubescens* (Hemsl.) Hara (128). As a plant metabolite, oridonin acts as an anti-tumor agent, angiogenesis inhibitor, apoptosis inducer, anti-asthmatic agent, and anti-bacterial agent (129, 130). Recent studies demonstrated that oridonin could maintain bone homeostasis (65, 66). In ovariectomy-induced OP mouse model, oridonin could protect bone loss *via* inhibiting osteoclastogenesis and enhancing osteogenesis by inhibiting interferon-related development regulator 1 (Ifrd1) and IκBα-mediated p65 nuclear translocation. Simultaneously, *in vitro* study revealed that oridonin motivated osteogenesis by Wnt/β-catenin signaling pathway and suppressed RANKL-induced OC formation in BMSCs.

In conclusion, diterpenoids are mostly investigated terpenoids that exert superior anti-OP efficacy by affecting various signaling pathways. In OBs, andrographolide, kirenol, and oridonim activate Wnt/β-catenin signaling pathway; andrographolide inhibits RANKL/RANK and NF-κB signaling pathways; tanshinone IIA blocks NF-κB signaling pathway. In OCs, euphorbia factor L1, abietic acid, carnosic acid, crocin, tanshinone IIA, and triptolide depress NF-κB signaling pathway; crocin, tanshinone IIA, and triptolide activate PI3K/Akt signaling pathway; andrographolide inhibits RANKL/RANK signaling pathway; abietic acid, carnosic acid, and tanshinone IIA inhibit MAPK signaling pathway; kirenol, tanshinone IIA, and triptolide depress NFATc1 signaling pathway; euphorbia factor L1 and carnosic acid promote Nrf2 signaling pathway.

Triterpenoids

Lupeol is a major active lupine-type pentacyclic triterpenoid of *Sorbus commixta* Hedlund and *Celastrus orbiculatus* Thunb (131). Recently, lupeol has attracted the attention of researchers for its osteogenic activity. On one hand, lupeol significantly suppressed OC differentiation and bone resorption mediated by 1α, 25-$(OH)_2D_3$ and prostaglandin E2 (PGE2) *via* inhibiting the activities of MAPK and transcription factors (NF-κB, NFATc1, and c-Fos). On another hand, lupeol decreased hypercalcemic mediated bone loss in C57BL/6 mice (67). In addition, lupeol in *bombax ceiba* contributed to relieve bone fragility and fracture (132).

Alismatis Rhizoma is a famous traditional Chinese herb, which has been used for hepatoprotective, diuretic, hypolipidemic, anti-tumor, anti-inflammatory and anti-diabetic treatments for more than ten centuries (133, 134). More and more researches reported that the terpenoids constituents of this herb, such as the protostane triterpenes compounds Alisol B (69), Alisol A 24-acetate (71, 135), Alisol B 23-acetate (68), and Alisol C 23-acetate (70), own the protective activity against bone loss. Alisol A 24-acetate suppressed OC differentiation mediated by RANKL through downregulating NFATc1 and restraining the DC-STAMP and cathepsin K expression in mouse BMMs (71). Moreover, in OVX mice, alisol A 24-acetate and alisol C 23-acetate could effectively protect bone loss (70, 135). Alisol B suppressed the RANKL-induced osteoclastogenesis in mouse BMMs and stopped bone loss in 2-methylene-19-nor-(20S)-1a,25$(OH)_2D_3$ (2MD)-induced hypercalcemia mouse model (69).

As a member of the pentacyclic triterpenoids, oleanolic acid is a free acid or triterpenoid saponins in many Chinese herbs, such as Nvzhenzi (*Ligustri lucidi* W. T. Aiton), Baihuasheshecao (*Hedyotis diffusa*), Renshen (*Panax ginseng C. A. Meyer*), and Sanqi (*Panax Notoginseng (Burk.) F.H.Chen*). Nvzhenzi has been clinically applied in the treatment of OP for over 1,000 years (136). Chen et al. summarized more than 150 articles and reviews on the anti-osteoporosis activity of *Ligustri lucidi*. In TCM, *Ligustri lucidi* is believed to have anti-osteoporosis effects, improve liver and kidney deficiency and reduce lower back pain. Pharmacological experiments showed *Ligustri lucidi* improved bone metabolism and bone quality in OVX, growing, aged and diabetic rats *via* regulating PTH/FGF-23/1,25-(OH) 2D3/CaSR, Nox4/ROS/NF-κB, and OPG/RANKL/cathepsin K signaling pathways (137) Oleanolic acid could suppress RANKL-mediated osteoclastogenesis in BMMs, and attenuate bone loss through decreasing the quantity of OC in C57BL/6 OVX mouse model (72). Furthermore, it has been proved that oleanolic acid modulated the ER alpha/miR-503/RANK signaling pathway to inhibit RANKL-induced osteoclastogenesis in

RAW264.7 cells (138). In aged female rats and mature OVX mice, oleanolic acid regulated vitamin D metabolism to exhibit osteoprotective effect (73). The investigation with high-throughput metabolomics showed that oleanolic acid ameliorated the disordered metabolism state in glucocorticoid-induced OP rats (139). In addition, five oleanolic acid glycosides of *Achyranthes bidentata* also exerted inhibitory effect on the formation of OC-like multinucleated cells (OCLs) induced by 1α, 25-$(OH)_2D_3$ (140).

Ursolic acid, as the isomer of oleanolic acid, is a ubiquitous active triterpenoids constituent in traditional Chinese medicinal herbs, such as *Salvia miltiorrhiza* (141, 142), *Fructus ligustri lucidi* (143), and *Eriobotrya japonica* (144, 145). Ursolic acid exhibited multiple pharmacological activities, including anti-cancer, anti-inflammation, anti-anaphylaxis, and anti-aging (146–148). In recent years, ursolic acid has attracted the attention of researchers for its osteogenic activity. Lee et al. proved that ursolic acid induced the expression of OB-specific genes by activating NF-κB, MAPK, and activator protein-1. Moreover, they demonstrated the osteogenic activity of ursolic acid in a mouse calvarial bone model (74). As the two most abundant ingredients in *Fructus ligustri lucidi*, both ursolic acid and oleanolic acid regulated the expression of bone turnover markers and calcium balance in mature OVX rats. In addition, the combination of these two compounds significantly improved bone properties and vitamin D metabolism in aged female rats (143, 149). Tan et al. observed that ursolic acid prevents OC differentiation induced by RANKL in RAW 264.7 cells through targeting XPO5 (150).

Glycyrrhizic acid, as well as glycyrrhetinic acid, are extracted from the root of *Glycyrrhiza glabra* L., and glycyrrhizic acid is formed by the combination of pentacyclic triterpenoid glycoside and glycyrrhetinic acid (151). Both of them showed protective effects on glucocorticoid-induced OP (152). Glycyrrhizic acid and glycyrrhetinic acid could act as the ligands for glucocorticoid receptor (GR), which further modulated glucocorticoid resistance and ameliorated inflammatory responses by disrupting the GR-heat shock protein 90 (HSP90) (76, 153). Glycyrrhizic acid prevented glucocorticoid-induced OP in male SD rats through inhibiting the 11β-hydroxysteroid dehydrogenase type 1 enzyme (11β-HSD1) (75). Furthermore, Yamada et al. found that in an aging mouse model of periprosthetic osteolysis, glycyrrhizic acid alleviated inflammatory bone loss and increased senescence-protective sirtuins expression (77). In OVX mice model, glycyrrhizic acid treatment improved bone metabolism and suppressed OC differentiation *via* modulating NF-κB, ERK, and JNK signaling pathways (7, 154). Glycyrrhetinic acid inhibited osteoclastogenesis *via* decreasing RANKL-mediated association of RANK and TNF receptor associated factor 6 (TRAF6), and consequently inactivating the NF-κB and MAPK signaling pathways *in vitro* (BMMs and RAW264.7 cells) and *in vivo* (OVX C57BL/6 mice) (78).

Betulinic acid is a pentacyclic lupane-type triterpene derivative of *Betula pubescens* Ehrh., exhibiting multiple biological effects including osteogenic activity. Betulinic acid could enhance the proliferation, differentiation, and mineralization of osteoblastic MC3T3-E1 through regulating the BMP/Smad/Runx2 and β-catenin signal pathways (81). Furthermore, betulinic acid reduced RANKL-associated osteoclastogenesis *via* suppressing the MAPK and NFATc1 signaling pathways in BMMs isolated from C57BL/6 mice. In the osteoporotic C57/BL6 mice, betulinic acid prevented ovariectomy-induced bone loss (80).

Ginsenoside Rg1, a tetracyclic triterpenoid, is an active compound in *Panax ginseng* C. A. Meyer and *Panax japonicus* (T. Nees) C. A. Meyer, which acts as a neuroprotective agent and pro-angiogenic agent. Ginsenoside Rg1 promoted the proliferation and odontogenic/osteogenic differentiation of human dental pulp stem cells (hDPSCs), stimulated the proliferation of BMSCs, and suppressed the maturation and differentiation of OCs (79). Zishen Jiangtang Pill (ZJP) is a formula of Chinese medicine, which regulated bone metabolism in diabetic OP (DOP) and consequently exhibited a protective effect. As the primary active ingredient of ZJP, Ginsenoside Rg1 improved the ultrastructure and histomorphology of bone and islets in DOP rats (155).

Limonin is a tetracyclic triterpenoid of various TCM and fruits, such as *Evodia rutaecarpa*, *Coptidis rhizoma*, *Cortex chinensis phellodendri*, *bergamot*, *Aurantii fructus immaturus*, *Citri reticulatae pericarpium*, and citrus fruits (156). Early study showed that limonin significantly inhibited bone resorption and reduced the number of multinucleated cells with TRAP-positive nature in OC-like cell model (82). Otherwise, limonin treatment modulated the ERK and p38-MAPK signaling in osteoblastic MC3T3-E1 cell line to induce osteogenic differentiation (83).

Nomilin, a furan-containing triterpenoid isolated from medicinal citrus, showed inhibitory effects on RANKL-stimulated OC differentiation and bone resorption in RAW 246.7 cells and mouse BMMs cells, resulting from the inhibition of-NFATc1 and MAPK signaling pathways (84).

Diosgenin and dioscin are steroid sapogenin triterpenoids, which are extracted from *Dioscorea nipponica* Makino (157).. It was reported that diosgenin could suppress osteoclastogenesis and bone resorption. Meanwhile, it enhanced the osteogenic activity of OBs that contributed to increased bone formation *in vitro*, and anti-osteoporotic effect *in vivo* (85, 158–162). Diosgenin ameliorated bone loss by decreasing the RANKL/OPG ratio in OVX rats (85, 163) and retinoic acid-induced OP rats (164). Similarly, dioscin enhanced osteoblastogenesis and inhibited osteoclastogenesis to prevent ovariectomy-induced bone loss (165). In addition, dioscin blocked OC differentiation and bone resorption *via* inhibiting the activation of Akt signaling pathway (86). In human and mouse OB-like cell lines, dioscin promoted the proliferation and differentiation of OBs *via* Lrp5 and ER pathway (87).

Ophiopogonin D is a saposins triterpenoid extracted from the TCM *Ophiopogon japonicus* (L. f.) Ker-Gawl. and has been applied in clinical use for a long time. Ophiopogonin D suppressed ROS generation to exert anti-OP effects *via* the FoxO3a/β-catenin signaling pathway in both RAW264.7 and MC3T3-E1 cells. In RAW264.7 cells, ophiopogonin D decreased the expression of Osteoclastic genes and the activity of CTX1 and

TRAP, which are bone degradation markers in serum. In MC3T3-E1 cells, ophiopogonin D significantly promoted cell proliferation and increased the gene levels of some osteogenic markers (88). Furthermore, Yang et al. highlighted that ophiopogonin D owned the ability to inhibit Krüppel-like factor 3 (KLF3), resulting in increased abundance of vessels in the bone tissue for bone formation (89).

As a pentacyclic triterpenoid compound, cycloastragenol is the aglycone derivative of astragaloside IV isolated from the root of *Astragalus membranaceus* (Fisch.) Bunge, which is a TCM used for thousands of years (166). Recent study reported that cycloastragenol might be a candidate drug to treat glucocorticoid-induced OP (GIOP) through alleviating the inhibition of osteogenic differentiation induced by dexamethasone (90). Yu et al. also observed that cycloastragenol treatment could improve bone formation, protect bone microstructure from degradation, reduce OC number, and augment bone biomechanical properties in both bone loss models induced by aging and D-galactose. Furthermore, cycloastragenol promoted the differentiation, viability, and mineralization of osteoblastic MC3T3-E1 cells. Cycloastragenol could also alleviate bone loss through increasing osteoactivin expression (167).

Hederagenin is a pentacyclic triterpenoid sapogenin extracted from *Hedera helix* (common ivy). In BMM cell model, hederagenin depressed the formation and bone (hydroxyapatite) resorption of OC induced by RANKL. Mechanism study revealed that hederagenin reduced the production of intracellular reactive oxygen species (ROS) and the activation of MAPK signaling pathway (ERK and p38), causing decreased induction of c-Fos and NFATc1. Similar to the *in vitro* effects, hederagenin treatment significantly prevented bone loss in OVX mice *via* inhibiting RANKL-induced bone resorption and OC generation (91). Meanwhile, hederagenin 3-*O*-(2-*O*-acetyl)-α-L-arabinopyranoside remarkably elevated the protein levels of BSP and osteocalcin and augmented AP activity (168).

Tubeimoside I, isolated from the Chinese medicinal herb *Bolbostemma paniculatum* (Maxim) Franquet (Cucurbitaceae), is a natural pentacyclic triterpenoid, and traditionally used for the treatment of snake venoms and inflammation. Recently, it was reported that tubeimoside I could inhibit the formation and function of OCs, as well as type 2 diabetes-induced decrease of bone mass in SD rats, resulting from down-regulating IκBα degradation which subsequently suppressed NF-κB transcriptional activity (92).

In summary, triterpenoids are potential anti-OP candidates with multi-target characteristics. In OBs, betulinic acid can activate Wnt/β-catenin signaling pathway; ophiopogonin D stimulates FoxO3a/β-catenin signaling pathway; ursolic acid, limonin, diosgenin, and dioscin promote MAPK signaling pathway. In OCs, diosgenin and dioscin enhance PI3K/Akt signaling pathway; lupeol, glycyrrhetinic, and tubeimoside I inhibit NF-κB signaling pathway; oleanolic acid inhibits RANKL/RANK signaling pathway; lupeol, betulinic acid, nomilin, and hederagenin depress MAPK signaling pathway; lupeol, alisol B, betulinic acid, and nomilin block NFATc1 signaling pathway.

CONCLUSION AND PROSPECTS

TCM has been widely used around the world for thousands of years to treat various diseases. These *in vivo* and *in vitro* findings discussed above demonstrate that terpenoids in natural Chinese medicine own the potential ability to provide therapeutic benefits for OP treatment.

Although terpenoids are beneficial for OP treatment, some terpenoids have been reported to be toxic. Cantharidin, a monoterpene obtained from *Mylabris phalerata* showed nephrotoxicity by suppressing the lactate dehydrogenase expression and intracellular release (169). Diterpene compound Pekinenin C and pekinenal also exhibited serious cytotoxicity intestinal toxicity (170). Thus, modification of their structures for lower toxicity and stronger efficacy are needed. For example, the quinoxaline derivative of oleanolic acid, QOA-8a, could not only inhibit bone resorption but also stimulate bone formation, playing dual roles in anti-OP (171). Meanwhile, the addition of quinoxaline contributed to lower cytotoxicity (172). Comparing with andrographolide itself, its derivative 14-deoxy-11,12-didehydroandrographolide showed stronger anti-osteoclastogenesis effect with significantly reduced cytotoxicity (173, 174). Therefore, structure modification will be an optional strategy for anti-OP drug development based on natural terpenoids. In addition, other problems, such as poor water solubility, short half-life, poor stability, and low bioavailability, severely limit the development and clinical use of TCM. The application of modern technologies (nanotechnology and co-crystallization) can overcome these short comings (175–177). Hence, for those terpenoids with perfect anti-OP efficacy but poor water solubility, we can apply nanoparticles in the drug delivery.

Nowadays, though a massive of studies reveal the anti-OP effects and molecular mechanisms of terpenoids, most of their direct targets as well as regulation mechanisms have not been illustrated. Several advanced technologies, such as proteomics (178) and systems pharmacology-based approaches (179, 180), have offered effective tools to identify potential targets of natural terpenoids. Proteomics and systems pharmacology-based approaches could perform the large-scale study of proteins and the major targets of most compounds. On the one hand, it is helpful to explain the exact pharmacological mechanism for pre-clinical drug development. On the other hand, the screening of terpenoids targeted proteins in OP treatment benefits researchers for understanding the pathogenesis of osteoporosis.

Moreover, TCM not only exerted anti-OP functions alone through diverse signaling pathways, but also showed enhancing effects *via* combining with clinically used hormones (estrogen or growth hormone) to prevent bone loss (181). This combination can avoid possible toxic side-effects and improve clinical efficacy (182). In the future, more in-depth and high-quality clinical researches are essential to ensure the safety, efficacy, and

specificity of the terpenoids, which will provide more evidence for the candidates in efficiently anti-osteoporotic applications.

AUTHOR CONTRIBUTIONS

JF and YZ: conceptualization. YZ and ML: writing — original draft preparation. QJ, HK, QL, and L-FZ: editing, and revising. JF: supervision. All authors contributed to the article and approved the submitted version.

FUNDING

The work was supported by the National Natural Science Foundation of China (No.82074278), the Guangdong Basic and Applied Basic Research Foundation (No. 2021A1515110584), Special Foundation of Guandong Educational Committe (No. 2021ZDZX2001), and Guangdong Province Science and Technology Plan International Cooperation Project (No. 2020A0505100052).

REFERENCES

1. Qadir A, Liang S, Wu Z, Chen Z, Hu L, Qian A. Senile Osteoporosis: The Involvement of Differentiation and Senescence of Bone Marrow Stromal Cells. *Int J Mol Sci* (2020) 21:349. doi: 10.3390/ijms21010349
2. An J, Yang H, Zhang Q, Liu C, Zhao J, Zhang L, et al. Natural Products for Treatment of Osteoporosis: The Effects and Mechanisms on Promoting Osteoblast-Mediated Bone Formation. *Life Sci* (2016) 147:46–58. doi: 10.1016/j.lfs.2016.01.024
3. Melton LJ3rd. How Many Women Have Osteoporosis Now? *J Bone Miner Res* (1995) 10:175–7. doi: 10.1002/jbmr.5650100202
4. Liu Y, Liu JP, Xia Y. Chinese Herbal Medicines for Treating Osteoporosis. *Cochrane Database Syst Rev* (2014) 3:CD005467. doi: 10.1002/14651858.CD005467.pub2
5. Bu L, Dai O, Zhou F, Liu F, Chen JF, Peng C, et al. Traditional Chinese Medicine Formulas, Extracts, and Compounds Promote Angiogenesis. *BioMed Pharmacother* (2020) 132:110855. doi: 10.1016/j.biopha.2020.110855
6. Liu C, Ma R, Wang L, Zhu R, Liu H, Guo Y, et al. Rehmanniae Radix in Osteoporosis: A Review of Traditional Chinese Medicinal Uses, Phytochemistry, Pharmacokinetics and Pharmacology. *J Ethnopharmacol* (2017) 198:351–62. doi: 10.1016/j.jep.2017.01.021
7. Yin Z, Zhu W, Wu Q, Zhang Q, Guo S, Liu T, et al. Glycyrrhizic Acid Suppresses Osteoclast Differentiation and Postmenopausal Osteoporosis by Modulating the Nf-Kappab, Erk, and Jnk Signaling Pathways. *Eur J Pharmacol* (2019) 859:172550. doi: 10.1016/j.ejphar.2019.172550
8. Zhang ND, Han T, Huang BK, Rahman K, Jiang YP, Xu HT, et al. Traditional Chinese Medicine Formulas for the Treatment of Osteoporosis: Implication for Antiosteoporotic Drug Discovery. *J Ethnopharmacol* (2016) 189:61–80. doi: 10.1016/j.jep.2016.05.025
9. Wang SJ, Yue W, Rahman K, Xin HL, Zhang QY, Qin LP, et al. Mechanism of Treatment of Kidney Deficiency and Osteoporosis Is Similar by Traditional Chinese Medicine. *Curr Pharm Des* (2016) 22:312–20. doi: 10.2174/1381612822666151112150346
10. Gao Z, Lu Y, Halmurat U, Jing J, Xu D. Study of Osteoporosis Treatment Principles Used Historically by Ancient Physicians in Chinese Medicine. *Chin J Integr Med* (2013) 19:862–8. doi: 10.1007/s11655-013-1328-z
11. He J, Li X, Wang Z, Bennett S, Chen K, Xiao Z, et al. Therapeutic Anabolic and Anticatabolic Benefits of Natural Chinese Medicines for the Treatment of Osteoporosis. *Front Pharmacol* (2019) 10:1344. doi: 10.3389/fphar.2019.01344
12. Tan W, Yu KQ, Liu YY, Ouyang MZ, Yan MH, Luo R, et al. Anti-Fatigue Activity of Polysaccharides Extract From Radix Rehmanniae Preparata. *Int J Biol Macromol* (2012) 50:59–62. doi: 10.1016/j.ijbiomac.2011.09.019
13. Withers ST, Keasling JD. Biosynthesis and Engineering of Isoprenoid Small Molecules. *Appl Microbiol Biotechnol* (2007) 73:980–90. doi: 10.1007/s00253-006-0593-1
14. Ateba SB, Mvondo MA, Ngeu ST, Tchoumtchoua J, Awounfack CF, Njamen D, et al. Natural Terpenoids Against Female Breast Cancer: A 5-Year Recent Research. *Curr Med Chem* (2018) 25:3162–213. doi: 10.2174/0929867325666180214110932
15. Bellavia D, Caradonna F, Dimarco E, Costa V, Carina V, De Luca A, et al. Terpenoid Treatment in Osteoporosis: This Is Where We Have Come in Research. *Trends Endocrinol Metab* (2021) 32:846–61. doi: 10.1016/j.tem.2021.07.011
16. Choi Y, Kim MH, Yang WM. Promotion of Osteogenesis by Sweroside *Via* Bmp2-Involved Signaling in Postmenopausal Osteoporosis. *Phytother Res* (2021) 35:7050–63. doi: 10.1002/ptr.7336
17. Sun H, Li L, Zhang A, Zhang N, Lv H, Sun W, et al. Protective Effects of Sweroside on Human Mg-63 Cells and Rat Osteoblasts. *Fitoterapia* (2013) 84:174–9. doi: 10.1016/j.fitote.2012.11.010
18. Wu QC, Tang XY, Dai ZQ, Dai Y, Xiao HH, Yao XS. Sweroside Promotes Osteoblastic Differentiation and Mineralization *Via* Interaction of Membrane Estrogen Receptor-Alpha and Gpr30 Mediated P38 Signalling Pathway on Mc3t3-E1 Cells. *Phytomedicine* (2020) 68:153146. doi: 10.1016/j.phymed.2019.153146
19. Ding Y, Jiang H, Meng B, Zhu B, Yu X, Xiang G. Sweroside-Mediated Mtorc1 Hyperactivation in Bone Marrow Mesenchymal Stem Cells Promotes Osteogenic Differentiation. *J Cell Biochem* (2019) 120:16025–36. doi: 10.1002/jcb.28882
20. Saravanan S, Islam VI, Thirugnanasambantham K, Pazhanivel N, Raghuraman N, Paulraj MG, et al. Swertiamarin Ameliorates Inflammation and Osteoclastogenesis Intermediates in Il-1beta Induced Rat Fibroblast-Like Synoviocytes. *Inflammation Res* (2014) 63:451–62. doi: 10.1007/s00011-014-0717-5
21. Saravanan S, Islam VI, Babu NP, Pandikumar P, Thirugnanasambantham K, Chellappandian M, et al. Swertiamarin Attenuates Inflammation Mediators *Via* Modulating Nf-Kappab/I Kappab and Jak2/Stat3 Transcription Factors in Adjuvant Induced Arthritis. *Eur J Pharm Sci* (2014) 56:70–86. doi: 10.1016/j.ejps.2014.02.005
22. Hairul-Islam MI, Saravanan S, Thirugnanasambantham K, Chellappandian M, Simon Durai Raj C, Karikalan K, et al. Swertiamarin, a Natural Steroid, Prevent Bone Erosion by Modulating Rankl/Rank/Opg Signaling. *Int Immunopharmacol* (2017) 53:114–24. doi: 10.1016/j.intimp.2017.10.022
23. He YQ, Yang H, Shen Y, Zhang JH, Zhang ZG, Liu LL, et al. Monotropein Attenuates Ovariectomy and Lps-Induced Bone Loss in Mice and Decreases Inflammatory Impairment on Osteoblast Through Blocking Activation of Nf-Kappab Pathway. *Chem Biol Interact* (2018) 291:128–36. doi: 10.1016/j.cbi.2018.06.015
24. Shi Y, Liu XY, Jiang YP, Zhang JB, Zhang QY, Wang NN, et al. Monotropein Attenuates Oxidative Stress *Via* Akt/Mtor-Mediated Autophagy in Osteoblast Cells. *BioMed Pharmacother* (2020) 121:109566. doi: 10.1016/j.biopha.2019.109566
25. Zhang Z, Zhang Q, Yang H, Liu W, Zhang N, Qin L, et al. Monotropein Isolated From the Roots of Morinda Officinalis Increases Osteoblastic Bone Formation and Prevents Bone Loss in Ovariectomized Mice. *Fitoterapia* (2016) 110:166–72. doi: 10.1016/j.fitote.2016.03.013
26. Meng J, Zhang W, Wang C, Zhang W, Zhou C, Jiang G, et al. Catalpol Suppresses Osteoclastogenesis and Attenuates Osteoclast-Derived Bone Resorption by Modulating Pten Activity. *Biochem Pharmacol* (2020) 171:113715. doi: 10.1016/j.bcp.2019.113715
27. Zhu Y, Wang Y, Jia Y, Xu J, Chai Y. Catalpol Promotes the Osteogenic Differentiation of Bone Marrow Mesenchymal Stem Cells *Via* the Wnt/Beta-Catenin Pathway. *Stem Cell Res Ther* (2019) 10:37. doi: 10.1186/s13287-019-1143-y
28. Chen L, Zhang RY, Xie J, Yang JY, Fang KH, Hong CX, et al. Stat3 Activation by Catalpol Promotes Osteogenesis-Angiogenesis Coupling, Thus Accelerating Osteoporotic Bone Repair. *Stem Cell Res Ther* (2021) 12:108. doi: 10.1186/s13287-021-02178-z
29. Zhao L, Du W, Zhao D, Ji X, Huang Y, Pang Y, et al. Catalpol Protects Against High Glucose-Induced Bone Loss by Regulating Osteoblast Function. *Front Pharmacol* (2021) 12:626621. doi: 10.3389/fphar.2021.626621
30. Choi EM, Suh KS, Rhee SY, Kim YS. Inhibitory Effect of Paeoniflorin on Methylglyoxal-Mediated Oxidative Stress in Osteoblastic Mc3t3-E1 Cells. *Phytomedicine* (2014) 21:1170–7. doi: 10.1016/j.phymed.2014.05.008

31. Xu H, Cai L, Zhang L, Wang G, Xie R, Jiang Y, et al. Paeoniflorin Ameliorates Collagen-Induced Arthritis *Via* Suppressing Nuclear Factor-Kb Signalling Pathway in Osteoclast Differentiation. *Immunology* (2018) 154:593–603. doi: 10.1111/imm.12907
32. Wang Y, Dai J, Zhu Y, Zhong W, Lu S, Chen H, et al. Paeoniflorin Regulates Osteoclastogenesis and Osteoblastogenesis *Via* Manipulating Nf-Kb Signaling Pathway Both *In Vitro* and *In Vivo*. *Oncotarget* (2018) 9:7372. doi: 10.18632/oncotarget.23677
33. Choi EM, Lee YS. Paeoniflorin Isolated From Paeonia Lactiflora Attenuates Osteoblast Cytotoxicity Induced by Antimycin A. *Food Funct* (2013) 4:1332–8. doi: 10.1039/c3fo60147a
34. Suh KS, Choi EM, Lee YS, Kim YS. Protective Effect of Albiflorin Against Oxidative-Stress-Mediated Toxicity in Osteoblast-Like Mc3t3-E1 Cells. *Fitoterapia* (2013) 89:33–41. doi: 10.1016/j.fitote.2013.05.016
35. Kim JH, Kim M, Hong S, Kim EY, Lee H, Jung HS, et al. Albiflorin Promotes Osteoblast Differentiation and Healing of Rat Femoral Fractures Through Enhancing Bmp-2/Smad and Wnt/Beta-Catenin Signaling. *Front Pharmacol* (2021) 12:690113. doi: 10.3389/fphar.2021.690113
36. Weng ZB, Gao QQ, Wang F, Zhao GH, Yin FZ, Cai BC, et al. Positive Skeletal Effect of Two Ingredients of Psoralea Corylifolia L. On Estrogen Deficiency-Induced Osteoporosis and the Possible Mechanisms of Action. *Mol Cell Endocrinol* (2015) 417:103–13. doi: 10.1016/j.mce.2015.09.025
37. Lim SH, Ha TY, Kim SR, Ahn J, Park HJ, Kim S. Ethanol Extract of Psoralea Corylifolia L. And Its Main Constituent, Bakuchiol, Reduce Bone Loss in Ovariectomised Sprague-Dawley Rats. *Br J Nutr* (2009) 101:1031–9. doi: 10.1017/S0007114508066750
38. Chai L, Zhou K, Wang S, Zhang H, Fan N, Li J, et al. Psoralen and Bakuchiol Ameliorate M-Csf Plus Rankl-Induced Osteoclast Differentiation and Bone Resorption *Via* Inhibition of Akt and Ap-1 Pathways in Vitro. *Cell Physiol Biochem* (2018) 48:2123–33. doi: 10.1159/000492554
39. Lee YS, Choi EM. Costunolide Stimulates the Function of Osteoblastic Mc3t3-E1 Cells. *Int Immunopharmacol* (2011) 11:712–8. doi: 10.1016/j.intimp.2011.01.018
40. Cheon YH, Song MJ, Kim JY, Kwak SC, Park JH, Lee CH, et al. Costunolide Inhibits Osteoclast Differentiation by Suppressing C-Fos Transcriptional Activity. *Phytother Res* (2014) 28:586–92. doi: 10.1002/ptr.5034
41. Li Z, Yuan G, Lin X, Liu Q, Xu J, Lian Z, et al. Dehydrocostus Lactone (Dhc) Suppresses Estrogen Deficiency-Induced Osteoporosis. *Biochem Pharmacol* (2019) 163:279–89. doi: 10.1016/j.bcp.2019.02.002
42. Hu B, Wu F, Shi Z, He B, Zhao X, Wu H, et al. Dehydrocostus Lactone Attenuates Osteoclastogenesis and Osteoclast-Induced Bone Loss by Modulating Nf-Kappab Signalling Pathway. *J Cell Mol Med* (2019) 23:5762–70. doi: 10.1111/jcmm.14492
43. Lee HI, Lee GR, Lee J, Kim N, Kwon M, Kim HJ, et al. Dehydrocostus Lactone Inhibits Nfatc1 *Via* Regulation of Ikk, Jnk, and Nrf2, Thereby Attenuating Osteoclastogenesis. *BMB Rep* (2020) 53:218–22. doi: 10.5483/BMBRep.2020.53.4.220
44. Lee HI, Lee J, Hwang D, Lee GR, Kim N, Kwon M, et al. Dehydrocostus Lactone Suppresses Osteoclast Differentiation by Regulating Nfatc1 and Inhibits Osteoclast Activation Through Modulating Migration and Lysosome Function. *FASEB J* (2019) 33:9685–94. doi: 10.1096/fj.201900862R
45. Hong SE, Lee J, Seo DH, In Lee H, Ri Park D, Lee GR, et al. Euphorbia Factor L1 Inhibits Osteoclastogenesis by Regulating Cellular Redox Status and Induces Fas-Mediated Apoptosis in Osteoclast. *Free Radic Biol Med* (2017) 112:191–9. doi: 10.1016/j.freeradbiomed.2017.07.030
46. Thummuri D, Guntuku L, Challa VS, Ramavat RN, Naidu VGM. Abietic Acid Attenuates Rankl Induced Osteoclastogenesis and Inflammation Associated Osteolysis by Inhibiting the Nf-Kb and Mapk Signaling. *J Cell Physiol* (2018) 234:443–53. doi: 10.1002/jcp.26575
47. Jiang T, Zhou B, Huang L, Wu H, Huang J, Liang T, et al. Andrographolide Exerts Pro-Osteogenic Effect by Activation of Wnt/Beta-Catenin Signaling Pathway in Vitro. *Cell Physiol Biochem* (2015) 36:2327–39. doi: 10.1159/000430196
48. Wang T, Liu Q, Zhou L, Yuan JB, Lin X, Zeng R, et al. Andrographolide Inhibits Ovariectomy-Induced Bone Loss *Via* the Suppression of Rankl Signaling Pathways. *Int J Mol Sci* (2015) 16:27470–81. doi: 10.3390/ijms161126039
49. Tantikanlayaporn D, Wichit P, Suksen K, Suksamrarn A, Piyachaturawat P. Andrographolide Modulates Opg/Rankl Axis to Promote Osteoblastic Differentiation in Mc3t3-E1 Cells and Protects Bone Loss During Estrogen Deficiency in Rats. *BioMed Pharmacother* (2020) 131:110763. doi: 10.1016/j.biopha.2020.110763
50. Yongyun C, Jingwei Z, Zhiqing L, Wenxiang C, Huiwu L. Andrographolide Stimulates Osteoblastogenesis and Bone Formation by Inhibiting Nuclear Factor Kappa-Beta Signaling Both *In Vivo* and *In Vitro*. *J Orthop Translat* (2019) 19:47–57. doi: 10.1016/j.jot.2019.02.001
51. Zhai ZJ, Li HW, Liu GW, Qu XH, Tian B, Yan W, et al. Andrographolide Suppresses Rankl-Induced Osteoclastogenesis *In Vitro* and Prevents Inflammatory Bone Loss *In Vivo*. *Br J Pharmacol* (2014) 171:663–75. doi: 10.1111/bph.12463
52. Thummuri D, Naidu VGM, Chaudhari P. Carnosic Acid Attenuates Rankl-Induced Oxidative Stress and Osteoclastogenesis *Via* Induction of Nrf2 and Suppression of Nf-Kappab and Mapk Signalling. *J Mol Med (Berl)* (2017) 95:1065–76. doi: 10.1007/s00109-017-1553-1
53. Zheng ZG, Cheng HM, Zhou YP, Zhu ST, Thu PM, Li HJ, et al. Dual Targeting of Srebp2 and Erralpha by Carnosic Acid Suppresses Rankl-Mediated Osteoclastogenesis and Prevents Ovariectomy-Induced Bone Loss. *Cell Death Differ* (2020) 27:2048–65. doi: 10.1038/s41418-019-0484-5
54. Suh KS, Chon S, Jung WW, Choi EM. Crocin Attenuates Methylglyoxal-Induced Osteoclast Dysfunction by Regulating Glyoxalase, Oxidative Stress, and Mitochondrial Function. *Food Chem Toxicol* (2019) 124:367–73. doi: 10.1016/j.fct.2018.12.031
55. Fu L, Pan F, Jiao Y. Crocin Inhibits Rankl-Induced Osteoclast Formation and Bone Resorption by Suppressing Nf-Kappab Signaling Pathway Activation. *Immunobiology* (2017) 222:597–603. doi: 10.1016/j.imbio.2016.11.009
56. Zou B, Zheng J, Deng W, Tan Y, Jie L, Qu Y, et al. Kirenol Inhibits Rankl-Induced Osteoclastogenesis and Prevents Ovariectomized-Induced Osteoporosis *Via* Suppressing the Ca(2+)-Nfatc1 and Cav-1 Signaling Pathways. *Phytomedicine* (2021) 80:153377. doi: 10.1016/j.phymed.2020.153377
57. Kim MB, Song Y, Hwang JK. Kirenol Stimulates Osteoblast Differentiation Through Activation of the Bmp and Wnt/Beta-Catenin Signaling Pathways in Mc3t3-E1 Cells. *Fitoterapia* (2014) 98:59–65. doi: 10.1016/j.fitote.2014.07.013
58. Zhang J, Cai Z, Yang M, Tong L, Zhang Y. Inhibition of Tanshinone Iia on Renin Activity Protected Against Osteoporosis in Diabetic Mice. *Pharm Biol* (2020) 58:219–24. doi: 10.1080/13880209.2020.1738502
59. Cheng L, Zhou S, Zhao Y, Sun Y, Xu Z, Yuan B, et al. Tanshinone Iia Attenuates Osteoclastogenesis in Ovariectomized Mice by Inactivating Nf-Kb and Akt Signaling Pathways. *Am J Transl Res* (2018) 10:1457–68.
60. Kwak HB, Yang D, Ha H, Lee JH, Kim HN, Woo ER, et al. Tanshinone Iia Inhibits Osteoclast Differentiation Through Down-Regulation of C-Fos and Nfatc1. *Exp Mol Med* (2006) 38:256–64. doi: 10.1038/emm.2006.31
61. Nicolin V, Dal Piaz F, Nori SL, Narducci P, De Tommasi N. Inhibition of Bone Resorption by Tanshinone Vi Isolated From Salvia Miltiorrhiza Bunge. *Eur J Histochem* (2010) 54:e21. doi: 10.4081/ejh.2010.e21
62. Luo D, Ren H, Zhang H, Zhang P, Huang Z, Xian H, et al. The Protective Effects of Triptolide on Age-Related Bone Loss in Old Male Rats. *BioMed Pharmacother* (2018) 98:280–5. doi: 10.1016/j.biopha.2017.12.072
63. Park B. Triptolide, a Diterpene, Inhibits Osteoclastogenesis, Induced by Rankl Signaling and Human Cancer Cells. *Biochimie* (2014) 105:129–36. doi: 10.1016/j.biochi.2014.07.003
64. Cui J, Li X, Wang S, Su Y, Chen X, Cao L, et al. Triptolide Prevents Bone Loss *Via* Suppressing Osteoclastogenesis Through Inhibiting Pi3k-Akt-Nfatc1 Pathway. *J Cell Mol Med* (2020) 24:6149–61. doi: 10.1111/jcmm.15229
65. Xie Z, Yu H, Sun X, Tang P, Jie Z, Chen S, et al. A Novel Diterpenoid Suppresses Osteoclastogenesis and Promotes Osteogenesis by Inhibiting Ifrd1-Mediated and Ikappabalpha-Mediated P65 Nuclear Translocation. *J Bone Miner Res* (2018) 33:667–78. doi: 10.1002/jbmr.3334
66. Zhou L, Huang Y, Zhao J, Yang H, Kuai F. Oridonin Promotes Osteogenesis Through Wnt/Beta-Catenin Pathway and Inhibits Rankl-Induced Osteoclastogenesis in Vitro. *Life Sci* (2020) 262:118563. doi: 10.1016/j.lfs.2020.118563
67. Im NK, Lee DS, Lee SR, Jeong GS. Lupeol Isolated From Sorbus Commixta Suppresses 1alpha,25-(Oh)2d3-Mediated Osteoclast Differentiation and Bone Loss *In Vitro* and *In Vivo*. *J Nat Prod* (2016) 79:412–20. doi: 10.1021/acs.jnatprod.5b01088
68. Shao C, Fu B, Ji N, Pan S, Zhao X, Zhang Z, et al. Alisol B 23-Acetate Inhibits Ige/Ag-Mediated Mast Cell Activation and Allergic Reaction. *Int J Mol Sci* (2018) 19:4092. doi: 10.3390/ijms19124092

69. Lee JW, Kobayashi Y, Nakamichi Y, Udagawa N, Takahashi N, Im NK, et al. Alisol-B, A Novel Phyto-Steroid, Suppresses the Rankl-Induced Osteoclast Formation and Prevents Bone Loss in Mice. *Biochem Pharmacol* (2010) 80:352–61. doi: 10.1016/j.bcp.2010.04.014
70. Jia X, Zhu H, Li G, Lan M, Li X, Huang M, et al. Anti-Osteoporotic Effects of Alisol C 23-Acetate *Via* Osteoclastogenesis Inhibition. *BioMed Pharmacother* (2021) 137:111321. doi: 10.1016/j.biopha.2021.111321
71. Kim KJ, Leutou AS, Yeon JT, Choi SW, Kim SH, Yee ST, et al. The Inhibitory Effect of Alisol a 24-Acetate From Alisma Canaliculatum on Osteoclastogenesis. *Int J Endocrinol* (2015) 2015:132436. doi: 10.1155/2015/132436
72. Zhao D, Li X, Zhao Y, Qiao P, Tang D, Chen Y, et al. Oleanolic Acid Exerts Bone Protective Effects in Ovariectomized Mice by Inhibiting Osteoclastogenesis. *J Pharmacol Sci* (2018) 137:76–85. doi: 10.1016/j.jphs.2018.03.007
73. Cao S, Dong XL, Ho MX, Yu WX, Wong KC, Yao XS, et al. Oleanolic Acid Exerts Osteoprotective Effects and Modulates Vitamin D Metabolism. *Nutrients* (2018) 10:247. doi: 10.3390/nu10020247
74. Lee SU, Park SJ, Kwak HB, Oh J, Min YK, Kim SH. Anabolic Activity of Ursolic Acid in Bone: Stimulating Osteoblast Differentiation in Vitro and Inducing New Bone Formation in Vivo. *Pharmacol Res* (2008) 58:290–6. doi: 10.1016/j.phrs.2008.08.008
75. Ramli ES, Suhaimi F, Asri SF, Ahmad F, Soelaiman IN. Glycyrrhizic Acid (Gca) as 11beta-Hydroxysteroid Dehydrogenase Inhibitor Exerts Protective Effect Against Glucocorticoid-Induced Osteoporosis. *J Bone Miner Metab* (2013) 31:262–73. doi: 10.1007/s00774-012-0413-x
76. Kao TC, Shyu MH, Yen GC. Glycyrrhizic Acid and 18beta-Glycyrrhetinic Acid Inhibit Inflammation *Via* Pi3k/Akt/Gsk3beta Signaling and Glucocorticoid Receptor Activation. *J Agric Food Chem* (2010) 58:8623–9. doi: 10.1021/jf101841r
77. Yamada C, Ho A, Akkaoui J, Garcia C, Duarte C, Movila A. Glycyrrhizin Mitigates Inflammatory Bone Loss and Promotes Expression of Senescence-Protective Sirtuins in an Aging Mouse Model of Periprosthetic Osteolysis. *BioMed Pharmacother* (2021) 138:111503. doi: 10.1016/j.biopha.2021.111503
78. Chen X, Zhi X, Yin Z, Li X, Qin L, Qiu Z, et al. 18beta-Glycyrrhetinic Acid Inhibits Osteoclastogenesis in Vivo and in Vitro by Blocking Rankl-Mediated Rank-Traf6 Interactions and Nf-Kappab and Mapk Signaling Pathways. *Front Pharmacol* (2018) 9:647. doi: 10.3389/fphar.2018.00647
79. Wang P, Wei X, Zhang F, Yang K, Qu C, Luo H, et al. Ginsenoside Rg1 of Panax Ginseng Stimulates the Proliferation, Odontogenic/Osteogenic Differentiation and Gene Expression Profiles of Human Dental Pulp Stem Cells. *Phytomedicine* (2014) 21:177–83. doi: 10.1016/j.phymed.2013.08.021
80. Wei J, Li Y, Liu Q, Lan Y, Wei C, Tian K, et al. Betulinic Acid Protects From Bone Loss in Ovariectomized Mice and Suppresses Rankl-Associated Osteoclastogenesis by Inhibiting the Mapk and Nfatc1 Pathways. *Front Pharmacol* (2020) 11:1025. doi: 10.3389/fphar.2020.01025
81. Lo YC, Chang YH, Wei BL, Huang YL, Chiou WF. Betulinic Acid Stimulates the Differentiation and Mineralization of Osteoblastic Mc3t3-E1 Cells: Involvement of Bmp/Runx2 and Beta-Catenin Signals. *J Agric Food Chem* (2010) 58:6643–9. doi: 10.1021/jf904158k
82. Li H, Miyahara T, Tezuka Y, Namba T, Nemoto N, Tonami S, et al. The Effect of Kampo Formulae on Bone Resorption in Vitro and in Vivo. I. Active Constituents of Tsu-Kan-Gan. *Biol Pharm Bull* (1998) 21:1322–6. doi: 10.1248/bpb.21.1322
83. Dahye L, Eunjoo J, Jiyun A, Jintaek H, Jinyoung H, Taeyoul H, et al. Limonin Enhances Osteoblastogenesis and Prevents Ovariectomy-Induced Bone Loss. *J Funct Foods* (2016) 23:105–14. doi: 10.1016/j.jff.2016.02.008
84. Kimira Y, Taniuchi Y, Nakatani S, Sekiguchi Y, Kim HJ, Shimizu J, et al. Citrus Limonoid Nomilin Inhibits Osteoclastogenesis in Vitro by Suppression of Nfatc1 and Mapk Signaling Pathways. *Phytomedicine* (2015) 22:1120–4. doi: 10.1016/j.phymed.2015.08.013
85. Zhang Z, Song C, Fu X, Liu M, Li Y, Pan J, et al. High-Dose Diosgenin Reduces Bone Loss in Ovariectomized Rats *Via* Attenuation of the Rankl/Opg Ratio. *Int J Mol Sci* (2014) 15:17130–47. doi: 10.3390/ijms150917130
86. Qu X, Zhai Z, Liu X, Li H, Ouyang Z, Wu C, et al. Dioscin Inhibits Osteoclast Differentiation and Bone Resorption Though Down-Regulating the Akt Signaling Cascades. *Biochem Biophys Res Commun* (2014) 443:658–65. doi: 10.1016/j.bbrc.2013.12.029
87. Zhang C, Peng J, Wu S, Jin Y, Xia F, Wang C, et al. Dioscin Promotes Osteoblastic Proliferation and Differentiation *Via* Lrp5 and Er Pathway in Mouse and Human Osteoblast-Like Cell Lines. *J BioMed Sci* (2014) 21:30. doi: 10.1186/1423-0127-21-30
88. Huang Q, Gao B, Wang L, Zhang HY, Li XJ, Shi J, et al. Ophiopogonin D: A New Herbal Agent Against Osteoporosis. *Bone* (2015) 74:18–28. doi: 10.1016/j.bone.2015.01.002
89. Yang M, Guo Q, Peng H, Xiao YZ, Xiao Y, Huang Y, et al. Kruppel-Like Factor 3 Inhibition by Mutated Lncrna Reg1cp Results in Human High Bone Mass Syndrome. *J Exp Med* (2019) 216:1944–64. doi: 10.1084/jem.20181554
90. Wu J, Zeng Z, Li Y, Qin H, Zuo C, Zhou C, et al. Cycloastragenol Protects Against Glucocorticoid-Induced Osteogenic Differentiation Inhibition by Activating Telomerase. *Phytother Res* (2021) 35:2034–44. doi: 10.1002/ptr.6946
91. Tian K, Su Y, Ding J, Wang D, Zhan Y, Li Y, et al. Hederagenin Protects Mice Against Ovariectomy-Induced Bone Loss by Inhibiting Rankl-Induced Osteoclastogenesis and Bone Resorption. *Life Sci* (2020) 244:117336. doi: 10.1016/j.lfs.2020.117336
92. Yang M, Xie J, Lei X, Song Z, Gong Y, Liu H, et al. Tubeimoside I Suppresses Diabetes-Induced Bone Loss in Rats, Osteoclast Formation, and Rankl-Induced Nuclear Factor-Kappab Pathway. *Int Immunopharmacol* (2020) 80:106202. doi: 10.1016/j.intimp.2020.106202
93. Wang SF, Chen XG, Hu ZD, Ju Y. Analysis of Three Effective Components in Fructus Corni and Its Preparations by Micellar Electrokinetic Capillary Chromatography. *BioMed Chromatogr* (2003) 17:306–11. doi: 10.1002/bmc.247
94. Magora HB, Rahman M, Gray AI, Cole MD. Swertiamarin From Enicostemma Axillare Subsp. Axillare (Gentianaceae). *Biochem Systematics Ecol* (2003) 31:553–5. doi: 10.1016/S0305-1978(02)00200-4
95. Heffels P, Muller L, Schieber A, Weber F. Profiling of Iridoid Glycosides in Vaccinium Species by Uhplc-Ms. *Food Res Int* (2017) 100:462–8. doi: 10.1016/j.foodres.2016.11.018
96. Seo BI, Ku SK, Cha EM, Park JH, Kim JD, Choi HY, et al. Effect of Mornidae Radix Extracts on Experimental Osteoporosis in Sciatic Neurectomized Mice. *Phytother Res* (2005) 19:231–8. doi: 10.1002/ptr.1683
97. Li N, Qin LP, Han T, Wu YB, Zhang QY, Zhang H. Inhibitory Effects of Morinda Officinalis Extract on Bone Loss in Ovariectomized Rats. *Molecules* (2009) 14:2049–61. doi: 10.3390/molecules14062049
98. Yen PH, Van Kiem P, Nhiem NX, Tung NH, Quang TH, Van Minh C, et al. A New Monoterpene Glycoside From the Roots of Paeonia Lacti-Flora Increases the Differentiation of Osteoblastic Mc3t3-E1 Cells. *Arch Pharm Res* (2007) 30:1179–85. doi: 10.1007/BF02980258
99. Wang Y, Zhu Y, Lu S, Hu C, Zhong W, Chai Y. Beneficial Effects of Paeoniflorin on Osteoporosis Induced by High-Carbohydrate, High-Fat Diet-Associated Hyperlipidemia in Vivo. *Biochem Biophys Res Commun* (2018) 498:981–7. doi: 10.1016/j.bbrc.2018.03.093
100. Xin Z, Wu X, Ji T, Xu B, Han Y, Sun M, et al. Bakuchiol: A Newly Discovered Warrior Against Organ Damage. *Pharmacol Res* (2019) 141:208–13. doi: 10.1016/j.phrs.2019.01.001
101. Zhang X, Zhao W, Wang Y, Lu J, Chen X. The Chemical Constituents and Bioactivities of Psoralea Corylifolia Linn.: A Review. *Am J Chin Med* (2016) 44:35–60. doi: 10.1142/S0192415X16500038
102. Zhang CZ, Wang SX, Zhang Y, Chen JP, Liang XM. *In Vitro* Estrogenic Activities of Chinese Medicinal Plants Traditionally Used for the Management of Menopausal Symptoms. *J Ethnopharmacol* (2005) 98:295–300. doi: 10.1016/j.jep.2005.01.033
103. Li WD, Yan CP, Wu Y, Weng ZB, Yin FZ, Yang GM, et al. Osteoblasts Proliferation and Differentiation Stimulating Activities of the Main Components of Fructus Psoraleae Corylifoliae. *Phytomedicine* (2014) 21:400–5. doi: 10.1016/j.phymed.2013.09.015
104. Jeong SJ, Itokawa T, Shibuya M, Kuwano M, Ono M, Higuchi R, et al. Costunolide, a Sesquiterpene Lactone From Saussurea Lappa, Inhibits the Vegfr Kdr/Flk-1 Signaling Pathway. *Cancer Lett* (2002) 187:129–33. doi: 10.1016/s0304-3835(02)00361-0
105. Lee HK, Song HE, Lee HB, Kim CS, Koketsu M, Ngan LT, et al. Growth Inhibitory, Bactericidal, and Morphostructural Effects of Dehydrocostus Lactone From Magnolia Sieboldii Leaves on Antibiotic-Susceptible and -Resistant Strains of Helicobacter Pylori. *PloS One* (2014) 9:e95530. doi: 10.1371/journal.pone.0095530

106. Bicchi C, Appendino G, Cordero C, Rubiolo P, Ortelli D, Veuthey JL. Hplc-Uv and Hplc-Positive-Esi-Ms Analysis of the Diterpenoid Fraction From Caper Spurge (Euphorbia Lathyris) Seed Oil. *Phytochem Anal* (2001) 12:255–62. doi: 10.1002/pca.592
107. Gao Y, Zhaoyu L, Xiangming F, Chunyi L, Jiayu P, Lu S, et al. Abietic Acid Attenuates Allergic Airway Inflammation in a Mouse Allergic Asthma Model. *Int Immunopharmacol* (2016) 38:261–6. doi: 10.1016/j.intimp.2016.05.029
108. Zhao J, Yang G, Liu H, Wang D, Song X, Chen Y. Determination of Andrographolide, Deoxyandrographolide and Neoandrographolide in the Chinese Herb Andrographis Paniculata by Micellar Electrokinetic Capillary Chromatography. *Phytochem Anal* (2002) 13:222–7. doi: 10.1002/pca.644
109. Abu-Ghefreh AA, Canatan H, Ezeamuzie CI. *In Vitro* and in Vivo Anti-Inflammatory Effects of Andrographolide. *Int Immunopharmacol* (2009) 9:313–8. doi: 10.1016/j.intimp.2008.12.002
110. Liu J, Jiang T, He M, Fang D, Shen C, Le Y, et al. Andrographolide Prevents Human Nucleus Pulposus Cells Against Degeneration by Inhibiting the Nf-Kappab Pathway. *J Cell Physiol* (2019) 234:9631–9. doi: 10.1002/jcp.27650
111. Reabroi S, Chairoungdua A, Saeeng R, Kasemsuk T, Saengsawang W, Zhu W, et al. A Silyl Andrographolide Analogue Suppresses Wnt/Beta-Catenin Signaling Pathway in Colon Cancer. *BioMed Pharmacother* (2018) 101:414–21. doi: 10.1016/j.biopha.2018.02.119
112. Zhai Z, Qu X, Yan W, Li H, Liu G, Liu X, et al. Andrographolide Prevents Human Breast Cancer-Induced Osteoclastic Bone Loss *Via* Attenuated Rankl Signaling. *Breast Cancer Res Treat* (2014) 144:33–45. doi: 10.1007/s10549-014-2844-7
113. Al Batran R, Al-Bayaty FH, Al-Obaidi MM. *In-Vivo* Effect of Andrographolide on Alveolar Bone Resorption Induced by Porphyromonas Gingivalis and Its Relation With Antioxidant Enzymes. *BioMed Res Int* (2013) 2013:276329. doi: 10.1155/2013/276329
114. Birtic S, Dussort P, Pierre FX, Bily AC, Roller M. Carnosic Acid. *Phytochemistry* (2015) 115:9–19. doi: 10.1016/j.phytochem.2014.12.026
115. Elbahnasawy AS, Valeeva ER, El-Sayed EM, Rakhimov II. The Impact of Thyme and Rosemary on Prevention of Osteoporosis in Rats. *J Nutr Metab* (2019) 2019:1431384. doi: 10.1155/2019/1431384
116. Bukhari SI, Manzoor M, Dhar MK. A Comprehensive Review of the Pharmacological Potential of Crocus Sativus and Its Bioactive Apocarotenoids. *BioMed Pharmacother* (2018) 98:733–45. doi: 10.1016/j.biopha.2017.12.090
117. Hosseinzadeh H, Nassiri-Asl M. Avicenna's (Ibn Sina) the Canon of Medicine and Saffron (Crocus Sativus): A Review. *Phytother Res* (2013) 27:475–83. doi: 10.1002/ptr.4784
118. Algandaby MM. Crocin Attenuates Metabolic Syndrome-Induced Osteoporosis in Rats. *J Food Biochem* (2019) 43:e12895. doi: 10.1111/jfbc.12895
119. Kalalinia F, Ghasim H, Amel Farzad S, Pishavar E, Ramezani M, Hashemi M. Comparison of the Effect of Crocin and Crocetin, Two Major Compounds Extracted From Saffron, on Osteogenic Differentiation of Mesenchymal Stem Cells. *Life Sci* (2018) 208:262–7. doi: 10.1016/j.lfs.2018.07.043
120. Wu B, Huang XY, Li L, Fan XH, Li PC, Huang CQ, et al. Attenuation of Diabetic Cardiomyopathy by Relying on Kirenol to Suppress Inflammation in a Diabetic Rat Model. *J Cell Mol Med* (2019) 23:7651–63. doi: 10.1111/jcmm.14638
121. Lu Y, Xiao J, Wu ZW, Wang ZM, Hu J, Fu HZ, et al. Kirenol Exerts a Potent Anti-Arthritic Effect in Collagen-Induced Arthritis by Modifying the T Cells Balance. *Phytomedicine* (2012) 19:882–9. doi: 10.1016/j.phymed.2012.04.010
122. Chin A, Yang Y, Chai L, Wong RW, Rabie AB. Effects of Medicinal Herb Salvia Miltiorrhiza on Osteoblastic Cells in Vitro. *J Orthop Res* (2011) 29:1059–63. doi: 10.1002/jor.21376
123. Guo Y, Li Y, Xue L, Severino RP, Gao S, Niu J, et al. Salvia Miltiorrhiza: An Ancient Chinese Herbal Medicine as a Source for Anti-Osteoporotic Drugs. *J Ethnopharmacol* (2014) 155:1401–16. doi: 10.1016/j.jep.2014.07.058
124. Lee SR, Jeon H, Kwon JE, Suh H, Kim BH, Yun MK, et al. Anti-Osteoporotic Effects of Salvia Miltiorrhiza Bunge Etoh Extract Both in Ovariectomized and Naturally Menopausal Mouse Models. *J Ethnopharmacol* (2020) 258:112874. doi: 10.1016/j.jep.2020.112874
125. Zhu S, Wei W, Liu Z, Yang Y, Jia H. Tanshinoneiia Attenuates the Deleterious Effects of Oxidative Stress in Osteoporosis Through the Nfkappab Signaling Pathway. *Mol Med Rep* (2018) 17:6969–76. doi: 10.3892/mmr.2018.8741
126. Tao X, Younger J, Fan FZ, Wang B, Lipsky PE. Benefit of an Extract of Tripterygium Wilfordii Hook F in Patients With Rheumatoid Arthritis: A Double-Blind, Placebo-Controlled Study. *Arthritis Rheum* (2002) 46:1735–43. doi: 10.1002/art.10411
127. Wang Y, Wang B, Yang X. The Study of Cellular Mechanism of Triptolide in the Treatment of Cancer, Bone Loss and Cardiovascular Disease and Triptolide's Toxicity. *Curr Stem Cell Res Ther* (2020) 15:18–23. doi: 10.2174/1574888X14666190301155810
128. Li D, Han T, Liao J, Hu X, Xu S, Tian K, et al. Oridonin, a Promising Ent-Kaurane Diterpenoid Lead Compound. *Int J Mol Sci* (2016) 17:1395. doi: 10.3390/ijms17091395
129. Hsieh TC, Wijeratne EK, Liang JY, Gunatilaka AL, Wu JM. Differential Control of Growth, Cell Cycle Progression, and Expression of Nf-Kappab in Human Breast Cancer Cells Mcf-7, Mcf-10a, and Mda-Mb-231 by Ponicidin and Oridonin, Diterpenoids From the Chinese Herb Rabdosia Rubescens. *Biochem Biophys Res Commun* (2005) 337:224–31. doi: 10.1016/j.bbrc.2005.09.040
130. Ku CM, Lin JY. Anti-Inflammatory Effects of 27 Selected Terpenoid Compounds Tested Through Modulating Th1/Th2 Cytokine Secretion Profiles Using Murine Primary Splenocytes. *Food Chem* (2013) 141:1104–13. doi: 10.1016/j.foodchem.2013.04.044
131. Vu TO, Tran PT, Seo W, Lee JH, Min BS, Kim JA. Triterpenoids From Celastrus Orbiculatus Thunb. Inhibit Rankl-Induced Osteoclast Formation and Bone Resorption *Via* C-Fos Signaling. *J Nat Med* (2021) 75:56–65. doi: 10.1007/s11418-020-01444-3
132. Chauhan S, Sharma A, Upadhyay NK, Singh G, Lal UR, Goyal R. *In-Vitro* Osteoblast Proliferation and in-Vivo Anti-Osteoporotic Activity of Bombax Ceiba With Quantification of Lupeol, Gallic Acid and Beta-Sitosterol by Hptlc and Hplc. *BMC Complement Altern Med* (2018) 18:233. doi: 10.1186/s12906-018-2299-1
133. Xiu RJ. Microcirculation and Traditional Chinese Medicine. *JAMA* (1988) 260:1755–7. doi: 10.1001/jama.260.12.1755
134. Zhang LL, Xu W, Xu YL, Chen X, Huang M, Lu JJ. Therapeutic Potential of Rhizoma Alismatis: A Review on Ethnomedicinal Application, Phytochemistry, Pharmacology, and Toxicology. *Ann N Y Acad Sci* (2017) 1401:90–101. doi: 10.1111/nyas.13381
135. Hwang YH, Kang KY, Lee SJ, Nam SJ, Son YJ, Yee ST. The Protective Effects of Alisol a 24-Acetate From Alisma Canaliculatum on Ovariectomy Induced Bone Loss in Vivo. *Molecules* (2016) 21:74. doi: 10.3390/molecules21010074
136. Pang Z, Zhi-yan Z, Wang W, Ma Y, Feng-ju N, Zhang X, et al. The Advances in Research on the Pharmacological Effects of Fructus Ligustri Lucidi. *BioMed Res Int* (2015) 2015:281873. doi: 10.1155/2015/281873
137. Chen B, Wang L, Li L, Zhu R, Liu H, Liu C, et al. Fructus Ligustri Lucidi in Osteoporosis: A Review of Its Pharmacology, Phytochemistry, Pharmacokinetics and Safety. *Molecules* (2017) 22:1469. doi: 10.3390/molecules22091469
138. Xie BP, Shi LY, Li JP, Zeng Y, Liu W, Tang SY, et al. Oleanolic Acid Inhibits Rankl-Induced Osteoclastogenesis *Via* Er Alpha/Mir-503/Rank Signaling Pathway in Raw264.7 Cells. *BioMed Pharmacother* (2019) 117:109045. doi: 10.1016/j.biopha.2019.109045
139. Xu Y, Chen S, Yu T, Qiao J, Sun G. High-Throughput Metabolomics Investigates Anti-Osteoporosis Activity of Oleanolic Acid *Via* Regulating Metabolic Networks Using Ultra-Performance Liquid Chromatography Coupled With Mass Spectrometry. *Phytomedicine* (2018) 51:68–76. doi: 10.1016/j.phymed.2018.09.235
140. Li JX, Hareyama T, Tezuka Y, Zhang Y, Miyahara T, Kadota S. Five New Oleanolic Acid Glycosides From Achyranthes Bidentata With Inhibitory Activity on Osteoclast Formation. *Planta Med* (2005) 71:673–9. doi: 10.1055/s-2005-871275
141. Orgah JO, He S, Wang Y, Jiang M, Wang Y, Orgah EA, et al. Pharmacological Potential of the Combination of Salvia Miltiorrhiza (Danshen) and Carthamus Tinctorius (Honghua) for Diabetes Mellitus and Its Cardiovascular Complications. *Pharmacol Res* (2020) 153:104654. doi: 10.1016/j.phrs.2020.104654
142. Steinkamp-Fenske K, Bollinger L, Voller N, Xu H, Yao Y, Bauer R, et al. Ursolic Acid From the Chinese Herb Danshen (Salvia Miltiorrhiza L.) Upregulates Enos and Downregulates Nox4 Expression in Human

Endothelial Cells. *Atherosclerosis* (2007) 195:e104–11. doi: 10.1016/j.atherosclerosis.2007.03.028
143. Cao S, Wastney ME, Lachcik PJ, Xiao HH, Weaver CM, Wong MS. Both Oleanolic Acid and a Mixture of Oleanolic and Ursolic Acids Mimic the Effects of Fructus Ligustri Lucidi on Bone Properties and Circulating 1,25-Dihydroxycholecalciferol in Ovariectomized Rats. *J Nutr* (2018) 148:1895–902. doi: 10.1093/jn/nxy242
144. Tan H, Furuta S, Nagata T, Ohnuki K, Akasaka T, Shirouchi B, et al. Inhibitory Effects of the Leaves of Loquat (Eriobotrya Japonica) on Bone Mineral Density Loss in Ovariectomized Mice and Osteoclast Differentiation. *J Agric Food Chem* (2014) 62:836–41. doi: 10.1021/jf402735u
145. Tan H, Ashour A, Katakura Y, Shimizu K. A Structure-Activity Relationship Study on Antiosteoclastogenesis Effect of Triterpenoids from the Leaves of Loquat (Eriobotrya Japonica). *Phytomedicine* (2015) 22:498–503. doi: 10.1016/j.phymed.2015.03.002
146. Pitaloka DAE, Cooper AM, Artarini AA, Damayanti S, Sukandar EY. Regulation of Mitogen-Activated Protein Kinase Signaling Pathway and Proinflammatory Cytokines by Ursolic Acid in Murine Macrophages Infected With Mycobacterium Avium. *Infect Dis Rep* (2020) 12:8717. doi: 10.4081/idr.2020.8717
147. Tohme MJ, Gimenez MC, Peralta A, Colombo MI, Delgui LR. Ursolic Acid: A Novel Antiviral Compound Inhibiting Rotavirus Infection *In Vitro*. *Int J Antimicrob Agents* (2019) 54:601–9. doi: 10.1016/j.ijantimicag.2019.07.015
148. Tan H, Sonam T, Shimizu K. The Potential of Triterpenoids From Loquat Leaves (Eriobotrya Japonica) for Prevention and Treatment of Skin Disorder. *Int J Mol Sci* (2017) 18:1030. doi: 10.3390/ijms18051030
149. Cao S, Tian XL, Yu WX, Zhou LP, Dong XL, Favus MJ, et al. Oleanolic Acid and Ursolic Acid Improve Bone Properties and Calcium Balance and Modulate Vitamin D Metabolism in Aged Female Rats. *Front Pharmacol* (2018) 9:1435. doi: 10.3389/fphar.2018.01435
150. Tan H, Zhao C, Zhu Q, Katakura Y, Tanaka H, Ohnuki K, et al. Ursolic Acid Isolated From the Leaves of Loquat (Eriobotrya Japonica) Inhibited Osteoclast Differentiation Through Targeting Exportin 5. *J Agric Food Chem* (2019) 67:3333–40. doi: 10.1021/acs.jafc.8b06954
151. Kiratipaiboon C, Tengamnuay P, Chanvorachote P. Glycyrrhizic Acid Attenuates Stem Cell-Like Phenotypes of Human Dermal Papilla Cells. *Phytomedicine* (2015) 22:1269–78. doi: 10.1016/j.phymed.2015.11.002
152. Zhang L, Li X, Ying T, Wang T, Fu F. The Use of Herbal Medicines for the Prevention of Glucocorticoid-Induced Osteoporosis. *Front Endocrinol (Lausanne)* (2021) 12:744647. doi: 10.3389/fendo.2021.744647
153. Kao TC, Wu CH, Yen GC. Glycyrrhizic Acid and 18beta-Glycyrrhetinic Acid Recover Glucocorticoid Resistance *Via* Pi3k-Induced Ap1, Cre and Nfat Activation. *Phytomedicine* (2013) 20:295–302. doi: 10.1016/j.phymed.2012.10.013
154. Tang Y, Lv XL, Bao YZ, Wang JR. Glycyrrhizin Improves Bone Metabolism in Ovariectomized Mice *Via* Inactivating Nf-Kappab Signaling. *Climacteric* (2021) 24:253–60. doi: 10.1080/13697137.2020.1828853
155. Chu S, Liu D, Zhao H, Shao M, Liu X, Qu X, et al. Effects and Mechanism of Zishen Jiangtang Pill on Diabetic Osteoporosis Rats Based on Proteomic Analysis. *Evid Based Complement Alternat Med* (2021) 2021:7383062. doi: 10.1155/2021/7383062
156. Fan S, Zhang C, Luo T, Wang J, Tang Y, Chen Z, et al. Limonin: A Review of Its Pharmacology, Toxicity, and Pharmacokinetics. *Molecules* (2019) 24:3679. doi: 10.3390/molecules24203679
157. Son IS, Kim JH, Sohn HY, Son KH, Kim JS, Kwon CS. Antioxidative and Hypolipidemic Effects of Diosgenin, a Steroidal Saponin of Yam (Dioscorea Spp.), on High-Cholesterol Fed Rats. *Biosci Biotechnol Biochem* (2007) 71:3063–71. doi: 10.1271/bbb.70472
158. Folwarczna J, Zych M, Nowinska B, Pytlik M, Bialik M, Jagusiak A, et al. Effect of Diosgenin, a Steroidal Sapogenin, on the Rat Skeletal System. *Acta Biochim Pol* (2016) 63:287–95. doi: 10.18388/abp.2015_1095
159. Shishodia S, Aggarwal BB. Diosgenin Inhibits Osteoclastogenesis, Invasion, and Proliferation Through the Downregulation of Akt, I Kappa B Kinase Activation and Nf-Kappa B-Regulated Gene Expression. *Oncogene* (2006) 25:1463–73. doi: 10.1038/sj.onc.1209194
160. Alcantara EH, Shin MY, Sohn HY, Park YM, Kim T, Lim JH, et al. Diosgenin Stimulates Osteogenic Activity by Increasing Bone Matrix Protein Synthesis and Bone-Specific Transcription Factor Runx2 in Osteoblastic Mc3t3-E1 Cells. *J Nutr Biochem* (2011) 22:1055–63. doi: 10.1016/j.jnutbio.2010.09.003
161. Zhang Z, Chen Y, Xiang L, Wang Z, Xiao GG, Ju D. Diosgenin Protects Against Alveolar Bone Loss in Ovariectomized Rats *Via* Regulating Long Non-Coding Rnas. *Exp Ther Med* (2018) 16:3939–50. doi: 10.3892/etm.2018.6681
162. Yen ML, Su JL, Chien CL, Tseng KW, Yang CY, Chen WF, et al. Diosgenin Induces Hypoxia-Inducible Factor-1 Activation and Angiogenesis Through Estrogen Receptor-Related Phosphatidylinositol 3-Kinase/Akt and P38 Mitogen-Activated Protein Kinase Pathways in Osteoblasts. *Mol Pharmacol* (2005) 68:1061–73. doi: 10.1124/mol.104.010082
163. Chiang SS, Chang SP, Pan TM. Osteoprotective Effect of Monascus-Fermented Dioscorea in Ovariectomized Rat Model of Postmenopausal Osteoporosis. *J Agric Food Chem* (2011) 59:9150–7. doi: 10.1021/jf201640j
164. Zhao S, Niu F, Xu CY, Liu Y, Ye L, Bi GB, et al. Diosgenin Prevents Bone Loss on Retinoic Acid-Induced Osteoporosis in Rats. *Ir J Med Sci* (2016) 185:581–7. doi: 10.1007/s11845-015-1309-2
165. Tao X, Qi Y, Xu L, Yin L, Han X, Xu Y, et al. Dioscin Reduces Ovariectomy-Induced Bone Loss by Enhancing Osteoblastogenesis and Inhibiting Osteoclastogenesis. *Pharmacol Res* (2016) 108:90–101. doi: 10.1016/j.phrs.2016.05.003
166. Li L, Hou X, Xu R, Liu C, Tu M. Research Review on the Pharmacological Effects of Astragaloside Iv. *Fundam Clin Pharmacol* (2017) 31:17–36. doi: 10.1111/fcp.12232
167. Yu Y, Wu J, Li J, Liu Y, Zheng X, Du M, et al. Cycloastragenol Prevents Age-Related Bone Loss: Evidence in D-Galactose-Treated and Aged Rats. *BioMed Pharmacother* (2020) 128:110304. doi: 10.1016/j.biopha.2020.110304
168. Kim BS, Kim YC, Zadeh H, Park YJ, Pi SH, Shin HS, et al. Effects of the Dichloromethane Fraction of Dipsaci Radix on the Osteoblastic Differentiation of Human Alveolar Bone Marrow-Derived Mesenchymal Stem Cells. *Biosci Biotechnol Biochem* (2011) 75:13–9. doi: 10.1271/bbb.100379
169. Xiang JY, Chi YY, Han JX, Xiang H, Xie Q. The Toxicity and Attenuation Methods of Toxic Chinese Materia Medica for Its Reasonable Application: A Review. *Am J Chin Med* (2021) 49:41–67. doi: 10.1142/S0192415X21500038
170. Cao Y, Cheng F, Yao W, Bao B, Zhang K, Zhang L, et al. Toxicity of Pekinenin C From Euphorbia Pekinensis Radix on Rat Small Intestinal Crypt Epithelial Cell and Its Apoptotic Mechanism. *Int J Mol Sci* (2016) 17:850. doi: 10.3390/ijms17060850
171. Wu J, Shen Q, Cui W, Zhao Y, Huai Y, Zhang YC, et al. Dual Roles of Qoa-8a in Antiosteoporosis: A Combination of Bone Anabolic and Anti-Resorptive Effects. *Acta Pharmacol Sin* (2018) 39:230–42. doi: 10.1038/aps.2017.63
172. Zhao Y, Huai Y, Jin J, Geng M, Li JX. Quinoxaline Derivative of Oleanolic Acid Inhibits Osteoclastic Bone Resorption and Prevents Ovariectomy-Induced Bone Loss. *Menopause* (2011) 18:690–7. doi: 10.1097/gme.0b013e3181fd7f4b
173. Zhang S, Zhang Y, Fang Y, Chen H, Hao M, Tan Q, et al. Synthesis and Evaluation of Andrographolide Derivatives as Potent Anti-Osteoporosis Agents in Vitro and in Vivo. *Eur J Med Chem* (2021) 213:113185. doi: 10.1016/j.ejmech.2021.113185
174. Zhao C, Huang D, Li R, Xu Y, Su S, Gu Q, et al. Identifying Novel Anti-Osteoporosis Leads With a Chemotype-Assembly Approach. *J Med Chem* (2019) 62:5885–900. doi: 10.1021/acs.jmedchem.9b00517
175. Smith AJ, Kavuru P, Wojtas L, Zaworotko MJ, Shytle RD. Cocrystals of Quercetin With Improved Solubility and Oral Bioavailability. *Mol Pharm* (2011) 8:1867–76. doi: 10.1021/mp200209j
176. Wang R, Han J, Jiang A, Huang R, Fu T, Wang L, et al. Involvement of Metabolism-Permeability in Enhancing the Oral Bioavailability of Curcumin in Excipient-Free Solid Dispersions Co-Formed With Piperine. *Int J Pharm* (2019) 561:9–18. doi: 10.1016/j.ijpharm.2019.02.027
177. Zuo W, Qu W, Li N, Yu R, Hou Y, Liu Y, et al. Fabrication of Multicomponent Amorphous Bufadienolides Nanosuspension With Wet Milling Improves Dissolution and Stability. *Artif Cells Nanomed Biotechnol* (2018) 46:1513–22. doi: 10.1080/21691401.2017.1375938
178. Zhuo Y, Zhang Y, Li M, Wu H, Gong S, Hu X, et al. Hepatotoxic Evaluation of Toosendanin *Via* Biomarker Quantification and Pathway Mapping of Large-Scale Chemical Proteomics. *Food Chem Toxicol* (2021) 153:112257. doi: 10.1016/j.fct.2021.112257
179. Gao L, Cao M, Li JQ, Qin XM, Fang J. Traditional Chinese Medicine Network Pharmacology in Cardiovascular Precision Medicine. *Curr Pharm Des* (2021) 27:2925–33. doi: 10.2174/1381612826666201112142408

180. Fang J, Liu C, Wang Q, Lin P, Cheng F. In Silico Polypharmacology of Natural Products. *Brief Bioinform* (2018) 19:1153–71. doi: 10.1093/bib/bbx045
181. Audran M. Drug Combination Strategies for Osteoporosis. *Joint Bone Spine* (2006) 73:374–8. doi: 10.1016/j.jbspin.2006.02.004
182. Zou H, Ye H, Kamaraj R, Zhang T, Zhang J, Pavek P. A Review on Pharmacological Activities and Synergistic Effect of Quercetin with Small Molecule Agents. *Phytomedicine* (2021) 92:153736. doi: 10.1016/j.phymed.2021.153736

Conflict of Interest: The authors declare that the research was conducted in the absence of any commercial or financial relationships that could be construed as a potential conflict of interest.

Publisher's Note: All claims expressed in this article are solely those of the authors and do not necessarily represent those of their affiliated organizations, or those of the publisher, the editors and the reviewers. Any product that may be evaluated in this article, or claim that may be made by its manufacturer, is not guaranteed or endorsed by the publisher.

Advantages of publishing in Frontiers

OPEN ACCESS
Articles are free to read for greatest visibility and readership

FAST PUBLICATION
Around 90 days from submission to decision

HIGH QUALITY PEER-REVIEW
Rigorous, collaborative, and constructive peer-review

TRANSPARENT PEER-REVIEW
Editors and reviewers acknowledged by name on published articles

Frontiers
Avenue du Tribunal-Fédéral 34
1005 Lausanne | Switzerland

Visit us: www.frontiersin.org
Contact us: frontiersin.org/about/contact

REPRODUCIBILITY OF RESEARCH
Support open data and methods to enhance research reproducibility

DIGITAL PUBLISHING
Articles designed for optimal readership across devices

FOLLOW US
@frontiersin

IMPACT METRICS
Advanced article metrics track visibility across digital media

EXTENSIVE PROMOTION
Marketing and promotion of impactful research

LOOP RESEARCH NETWORK
Our network increases your article's readership